

UNIVERSITY OF CALGARY

A Novel Measure of In-Vivo Knee Joint Laxity

by

Jessica Küpper

A THESIS

SUBMITTED TO THE FACULTY OF GRADUATE STUDIES
IN PARTIAL FULFILMENT OF THE REQUIREMENTS FOR THE
DEGREE OF MASTER OF SCIENCE

DEPARTMENT OF MECHANICAL AND MANUFACTURING ENGINEERING

CALGARY, ALBERTA

January, 2008

© Jessica Küpper 2008

UNIVERSITY OF CALGARY
FACULTY OF GRADUATE STUDIES

The undersigned certify that they have read, and recommend to the Faculty of Graduate Studies for acceptance, a thesis entitled "A Novel Measure of In-Vivo Knee Joint Laxity" submitted by Jessica Küpper in partial fulfilment of the requirements of the degree of Master of Science.

*Supervisor, Dr. J. Ronsky, Department of Mechanical and
Manufacturing Engineering*

*Dr. L. Sudak, Department of Mechanical and
Manufacturing Engineering*

*Dr. D. Hart, Departments of Surgery, Microbiology and
Infectious Diseases, and Medicine*

*Dr. R. Frayne, Departments of Radiology and Clinical
Neuroscience*

Date

Abstract

Current measures of knee joint laxity, such as those found clinically using the KT-2000 arthrometer, are not highly repeatable or reliable (Huber et al, 1997). In this study, a non-invasive *in-vivo* Magnetic Resonance imaging-based measure of laxity, the Knee Loading Apparatus (KLA), was designed and evaluated with five normal subjects (repeatability study, n=3). Effects of total body water content, hormones, and muscle guarding were considered. When compared to the KT-2000, the KLA was found to be less variable (± 0.58 mm vs. ± 1.47 mm). Future KLA design iterations should aim to control the initial positioning of the subject, a finding that may shed light on the low reliability of the KT-2000. The KLA enabled quantification of both *in-vivo* knee joint stress relaxation and ACL (ligament specific) laxity for the first time. The KLA shows promise as an accurate and reliable tool for measuring *in-vivo* joint and ligament laxity, and viscoelastic behavior.

Acknowledgements

I would like to acknowledge and thank...

My supervisor, Dr. Janet Ronsky: for her guidance, knowledge, and support. Thank you for helping me, and for cheering me on and inspiring me with your enthusiasm when I felt overwhelmed. I cannot thank you enough for the opportunities you have given me to delve into biomechanics and learn at every level.

Dr. Gail Thornton: without whom I would never have pursued this degree. Thank you for giving me my first chance to try biomechanics, and for being an amazing mentor.

Ion Robu: for the vast amount of help and support that you gave. I learned so much from you, from intelligent and practical designs to the inner workings of the universe.

Dr. Barbara Loitz-Ramage: for her wisdom, experience, and help with data collection.

Dr. Richard Frayne, Dr. David Corr, S.K. Park, and the members of the CIHR NET grant: for going out of their way to provide me with valuable feedback and help with all manner of topics from data collection to ligament mechanics.

Dr. Houman Mahalti and Dr. Tak Shing Fung: for your invaluable help with anatomy in MR images and statistics, respectively.

My fantastic group mates and officemates: for providing daily support and suggestions, particularly Ingrid Fjeld, Bryan Donnelly, Kim Connolly, Brady Anderson, Matt Gotch, Cindy Samaan, Steve Andrews, Lindsey Westover, Rita Cheng, and Steve Thannhauser.

My family and friends: Cynthia and Gerry, Michelle, João e Angela, Suzana, Lisa, Liz, and Larissa. Your love and support are a blessing.

My husband Arthur: who stands beside me, and whose love is all that I ever need.

To my parents
for inspiring my love for health care and construction
which sort of works out to biomechanics
and To my husband
for bringing me dinner when I was writing,
and a million other wonderful things

Table of Contents

Approval Page.....	ii
Abstract.....	iii
Acknowledgements.....	iv
Table of Contents.....	vi
List of Tables	ix
LIST OF FIGURES AND ILLUSTRATIONS.....	X
List of Symbols, Abbreviations and Nomenclature.....	xv
CHAPTER ONE: INTRODUCTION.....	1
1.1 Introduction.....	1
1.2 Background.....	1
1.3 Objectives and Specific Aims.....	9
1.4 Thesis Outline.....	10
CHAPTER TWO: LITERATURE REVIEW.....	12
2.1 Introduction.....	12
2.2 Terminology.....	12
2.3 Tendon and Ligament Mechanics.....	13
2.3.1 Modelling Stress Relaxation.....	15
2.4 Joint Laxity	17
2.5 Measuring Laxity in Females	20
2.5.1 Total Body Water	21
2.6 Current Measures of Laxity	22
2.6.1 Traditional Measurement Systems	23
2.6.1.1 KT-2000.....	23
2.6.1.2 Genucom.....	25
2.6.1.3 Rolimeter	26
2.6.1.4 Stryker Ligament Tester	27
2.6.1.5 System Outputs.....	28
2.6.2 Alternate Measurement Systems	34
2.6.2.1 Planar Stress Radiography and RSA	34
2.6.2.2 MR Imaging.....	35
2.7 Criteria for a Measure of Joint Laxity	36
2.7.1 Joint Position, Applied Force, and Motion Constraints	36
2.7.2 Muscle Activity	37
2.8 Theoretical Models	39
2.8.1 Contact Models.....	40
2.8.2 Lumped Parameter Models.....	44
2.8.3 Finite Element Models	48
2.8.4 Theoretical Modelling Summary.....	50
2.9 Summary.....	51
CHAPTER THREE: LOADING APPARATUS DESIGN	54
3.1 Design Criteria.....	54

3.2 Final Design.....	56
3.2.1 Design Components.....	57
3.2.2 System Cost.....	60
3.3 Design Rationale.....	61
3.3.1 Positioning.....	61
3.3.2 External Applied Force.....	62
3.3.3 Free Body Diagrams.....	64
3.4 Design Evaluation.....	69
3.4.1 Pilot Study.....	71
3.5 Summary.....	72
CHAPTER FOUR: METHODS.....	74
4.1 Study Participants.....	75
4.2 General Protocol.....	76
4.2.1 Hormonal Effects.....	76
4.2.2 Total Body Water.....	77
4.3 MR Imaging.....	78
4.4 Image Registration.....	81
4.4.1 Image Digitization.....	82
4.4.2 Coordinate System Definition.....	84
4.4.2.1 Femoral Local Coordinate System.....	85
4.4.2.2 Tibial Local Coordinate System.....	88
4.4.3 Surface Reconstruction.....	91
4.4.4 Registration Technique.....	93
4.5 Coordinate Transformations to obtain Gross Joint Displacement.....	95
4.5.1 Verification of Transformation Matrices Calculations.....	99
4.6 ACL Insertion Point Displacement.....	100
4.7 Load Data Processing.....	103
4.8 KT-2000 Testing.....	106
4.8.1 Data Processing.....	108
4.9 Electromyography.....	110
4.9.1 Data Processing.....	114
4.10 Statistics.....	115
CHAPTER FIVE: RESULTS.....	117
5.1 Introduction.....	117
5.2 Total Body Water.....	117
5.3 Knee Loading Apparatus.....	118
5.3.1 Repeatability of Force Application.....	118
5.3.2 Repeatability of Positioning.....	120
5.3.3 Force-Displacement.....	122
5.3.4 Sources of Error.....	127
5.4 KT-2000.....	131
5.4.1 Displacement.....	135
5.4.2 Compliance Index.....	136
5.4.3 Stiffness.....	137
5.5 Electromyography.....	138

5.5.1 Maximum Signal	139
5.5.2 Average Signal	141
5.6 Stress Relaxation.....	141
CHAPTER SIX: DISCUSSION AND FUTURE WORK.....	145
6.1 KLA Design.....	146
6.1.1 KLA Subject Positioning.....	147
6.1.2 Force Application	151
6.2 Three Dimensional Joint Motion and ACL Insertion Point Distance.....	153
6.2.1 Joint Displacement	156
6.2.2 ACL insertion	159
6.3 Comparison to a Clinical Arthrometer.....	164
6.3.1 Muscle Guarding	168
6.3.2 Stress Relaxation	171
6.4 Summary and Future Work.....	174
REFERENCES	177
APPENDIX A: KÜPPER ET AL 2006	190
A.1. Publisher’s Permission to Include Publication in Thesis.....	190
A.2. Co-Authors’ Permission to Include Publication in Thesis.....	192
A.3. Breakdown of Contributions by Section.....	193
A.4. Küpper, J.C., Loitz-Ramage, B., Corr, D.T., Hart, D.A., Ronsky, J.L. Measuring Knee Joint Laxity: A Review of Applicable Models and the need for New Approaches to Minimize Variability. Clinical Biomechanics, 22(1):1-13, 2007	193
APPENDIX B: ETHICS.....	207

List of Tables

Table 2-1: Accuracy and Repeatability of Current Laxity Measurement Devices	32
Table 3-1: Importance Level for Design Criteria	56
Table 3-2: Cost Summary for KLA	60
Table 3-3: Subject Specific Anthropometric values	67
Table 3-4: Design Components relating to Design Criteria.....	70
Table 4-1: Menstrual Cycle and Test Dates.....	77
Table 5-1: Cronbach's Alpha for reliability of force application with the KLA	119
Table 5-2: Force Levels at which significant differences in Anterior Tibial Position may be detectable at $p \leq 0.05$ with a sample size of $n > 5$	124
Table 5-3: Force Levels at which significant differences in Internal Tibial Rotation angle may be detectable at $p < 0.05$ with a sample size of $n > 5$	125
Table 5-4: Instances of Movement during MR Scanning.....	131
Table 5-5: Cronbach's Alpha Method Reliability for KLA and KT-2000	136

List of Figures and Illustrations

Figure 1-1: The Knee Joint (a) Sagittal view (b) Anterior view (Gray, 1918)	2
Figure 1-2: Muscles of the Thigh (a) Anterior view (b) Posterior view (Gray, 1918)	3
Figure 1-3: Schematic of variables that affect stability	4
Figure 2-1: Anatomical planes of the body from SEER Program (2007).....	13
Figure 2-2: The hierarchical organization of tendon structure: from collagen fibrils to the entire tendon (Jozsa, 1997)	14
Figure 2-3: Spectrum of Laxity.....	18
Figure 2-4: (a) Positioning of subject for testing with the KT-2000 arthrometer. (b) A typical force-displacement curve resulting from testing with the KT-2000 arthrometer; “A” and “B” denote peak posterior and anterior displacement respectively. Stiffness is calculated as $\Delta L/\Delta D$	25
Figure 2-5: Number of Publications per year that include the KT-1000/2000, Genucom, Stryker Ligament Tester, or Rolimeter arthrometers from 1985 to 2006.....	31
Figure 2-6: Exemplary free body diagram of the knee joint including external (ext) forces, forces due to compression (comp), muscle force [gastrocnemius (gast), hamstring (ham), quadriceps femoris (quad)], femoral mass (fem), tibial and fibular mass (tib/fib), and forces through the ACL, PCL, LCL, and PT	45
Figure 3-1: Borehole Dimensions	55
Figure 3-2: KLA System Components including a positioning apparatus [A], hydraulic system [B], and software interface [C]	57
Figure 3-3: Labelled positioning apparatus: (a) base plate, (b) thigh support, (c) hinge, (d) foot plate, (e) hinge, (f) tibial platform	57
Figure 3-4: 3D Solidworks (Solidworks Corp., Concord, MA, USA) model of the positioning apparatus with force applied at the proximal end of the tibia (a)	59
Figure 3-5: Figure 1 from Maitland et al. (1995) showing a representative force- displacement curve from an uninjured subject; modified to show the five load levels chosen to characterize the force-displacement curve. “The initial steep rise in curve is due to the weight of the leg (a). Middle region (b). The inflection point (c) is assumed to be due to the onset of the primary restraints to anterior displacement of the tibia, and by definition results in the x intercept of the second derivative. The cut –off point (d) was chosen at an anterior applied force of 134 N.”	63

Figure 3-6: Applied Force during MR scanning for one subject	64
Figure 3-7: Free Body Diagram of the determinate force system for the KLA calibration. Forces include the applied force from the hydraulic force system (F_a), calibration weight force (F_p), the counteractive mass (F_w), the KLA mass (F_m), and the reaction forces at the hinge (F_f , F_n).	65
Figure 3-8: Force-Voltage relationship from calibration of KLA	66
Figure 3-9: Free Body Diagram of the indeterminate force system for the KLA during testing. Forces include the applied force from the hydraulic force system (F_a), the reaction forces and moments at the knee (F_{ry} , F_{rx} , M_r), the counteractive mass (F_w), the KLA mass (F_m), and the reaction forces at the hinge (F_f , F_n).	67
Figure 3-10: Axial view of femoral contact area on tibia at a) the neutral position and b) 70 N applied load.....	72
Figure 4-1: Flowchart for Methods to obtain a measure of laxity with the KLA	74
Figure 4-2: Goniometer.....	79
Figure 4-3: MR Imaging test setup (a) prior to and (b) after adding the flex coil	80
Figure 4-4: Flow Chart depicting the image data analysis process through digitization to obtain local joint coordinate systems (Fjeld, 2007), thin plate spline mappings of joint surfaces, registration to match surfaces (Cheng, 2006), combined to find anterior joint displacement.....	82
Figure 4-5: Image Digitization for (a) LCS and (b) Joint Image Registration	83
Figure 4-6: Digitization of ACL insertion point on (a) femur and (b) tibia	84
Figure 4-7: fLCS definition: (a) outline of a sagittal slice through a femoral condyle with region selected for facet circle fit, (b) axial view from the distal end of the femur with the resulting z axis through the centres of the facet circles, (c) fLCS displayed within the femur, x' axis shown as longitudinal axis of femur shaft, origin located at projection of x' axis on the z axis used with permission from Fjeld (2007).....	87
Figure 4-8: (a) Centroid (red) of a slice of the tibial shaft (axial view) based on an elliptical fit resulting in (b) a line of centroids in 3D.....	88
Figure 4-9: Demonstration of misalignment of long axis based on proximal tibial geometry (a) an exemplary sagittal tibial radiograph (www.fighttimes.com) and (b) an exemplary MR image with either a cylinder fit or ellipse fit	89
Figure 4-10: (a) Medial/Lateral z-axis definition (red) based on the PTCL using a 5 th order polynomial (green) and (b) the tLCS.....	90

Figure 4-11: TPS Surfaces for high resolution (a) femur and (b) tibia.....	91
Figure 4-12: ‘Coplanarity condition describes the correspondence between a point in S1 and a patch in S2 after performing 3D similarity transformation’ used with permission from Cheng (2006)	94
Figure 4-13: Transformation matrices for conversion from low resolution images (applied load) to high resolution images (T_l2hfem, T_l2htib) to LCS (T_bonefem, T_bonetib). Cumulative transformation matrices from low resolution images to LCS (T_fem, T_tib) are used to obtain relative motion between tibia and femur.....	98
Figure 4-14: (a) Test object as it is (b) shifted (from blue to red) to simulate relative bone displacement and rotation.....	100
Figure 4-15: Digitized Points for (a) tibial and (b) femoral insertion points with insertion point shown in red.....	101
Figure 4-16: Ellipse fit to (a) Tibial and (b) Femoral ACL insertion data points with insertion point shown in red.....	102
Figure 4-17: TPS Surface of the femoral groove for registration between axial and sagittal high resolution images.....	103
Figure 4-18: Applied force during MR scanning for one subject.....	103
Figure 4-19: Normal Probability Plot for Sample Load Data.....	104
Figure 4-20: KT-2000 Testing	107
Figure 4-21: Power Spectrum for (a) force and (b) displacement KT-2000 data.....	108
Figure 4-22: Exemplary plot of KT-2000 force-displacement curve including raw data, 5th order polynomial fit, and first (stiffness) and second (change in stiffness) derivatives. Inflection points are indicated with the dashed lines, separating the curve into 3 sections: initial rise, middle, and linear regions.	110
Figure 4-23: Electrode placement for EMG	111
Figure 4-24: EMG collected at a neutral position outside of the KLA.....	112
Figure 4-25: Maximum voluntary contraction tests for (a) the quadriceps and (b) the hamstring muscle groups	112
Figure 4-26: Maximum voluntary contraction test for the gastrocnemius muscle group.....	113
Figure 4-27: Power spectrum for lower limb muscle signals	114
Figure 5-1: Average Total Body Water	118

Figure 5-2: Actual force compared to target force using the KLA across days (n=3). ^ indicates significant correlation (high reliability) of loading across days (where D1 = Day 1, D2 = Day 2, and D3 = Day 3)	119
Figure 5-3: Initial anterior position of the tibia with respect to the femur, and ACL insertion point distance, averaged over 3 test days.....	120
Figure 5-4: Relationship between the initial anterior tibial position and initial internal rotation angle	121
Figure 5-5: Knee flexion angle for all subjects and test days, where D1 = Day 1, D2 = Day 2, and D3 = Day 3	122
Figure 5-6: KLA Anterior Force-Displacement (S01) showing force ascending (open symbols) and descending (closed symbols).....	123
Figure 5-7: KLA Anterior Force-Displacement (S02) showing force ascending (open symbols) and descending (closed symbols) over three test days (D1, D2, D3).....	124
Figure 5-8: KLA Anterior Force-Displacement (S03) showing force ascending (open symbols) and descending (closed symbols) over three test days (D1, D2, D3).....	125
Figure 5-9: KLA Anterior Force-Displacement (S04) showing force ascending (open symbols) and descending (closed symbols).....	125
Figure 5-10: KLA Anterior Force-Displacement (S05) showing force ascending (open symbols) and descending (closed symbols) over three test days (D1, D2, D3).....	126
Figure 5-11: Exemplary plot of ACL insertion point distance (S05) across three test days (D1, D2, D3).....	126
Figure 5-12: Exemplary plot of internal tibial rotation angle (S05) across three test days (D1, D2, D3).....	127
Figure 5-13: Error in rotation parameters due to mapping low to high resolution images and possible subject movement at the reference position.....	128
Figure 5-14: Error in translation parameters due to mapping low to high resolution images and possible subject movement at the reference position.....	128
Figure 5-15: Exemplary plot of tibial and femoral translation in the anterior direction of the ICS for S01, normalized to the reference position (Nu refers to ‘Newtons of force on the ascending curve’ and Nd refers to ‘Newtons of force on the descending curve’)	129
Figure 5-16: Variability of ACL insertion point location for the Tibia in the tLCS	130
Figure 5-17: Variability of ACL insertion point location for the Femur in the fLCS	130

Figure 5-18: KT-2000 Force-Displacement (S01) showing filtered raw data (grey) and the 5 th order polynomial fit (black)	132
Figure 5-19: KT-2000 Force-Displacement (S02) showing filtered raw data across three days (D1, D2, D3)	132
Figure 5-20: KT-2000 Force-Displacement (S03) showing filtered raw data across three days (D1, D2, D3)	133
Figure 5-21: KT-2000 Force-Displacement (S04) showing filtered raw data across three trials on one day (T1, T2, T3). A typical shift of data over trials was observed (red). For all subjects, the first full curve (T1) is used to assess KT-2000 data, shifted to 0 mm.	133
Figure 5-22: KT-2000 Force-Displacement (S05) showing filtered raw data across three days (D1, D2, D3)	134
Figure 5-23: Mean displacement at each load level for the KLA and KT-2000 (n=5) ..	135
Figure 5-24: KT-2000 Compliance Index.....	137
Figure 5-25: KT-2000 average Stiffness for the three regions of the force-displacement curve.....	138
Figure 5-26: EMG signal as % of MVC for all muscles (VM, VL, RF, BF, ST, GL, GM) for all subjects (n=5). The X-axis crosses the Y-axis at 5%	140
Figure 5-27: Exemplary Stress Relaxation Curve showing G(t) (fitted curve, red) and the raw data (blue)	142
Figure 5-28: Distribution of time constants indicates no correlation with anterior force	143
Figure 5-29: Variability in force over 1 minute scan length shows a general increase with anterior force during ascending loading	143
Figure 5-30: Stress relaxation time constants for all subjects across days (D1, D2, D3)	144

List of Symbols, Abbreviations and Nomenclature

Symbol	Definition
ACL	Anterior Cruciate Ligament
PCL	Posterior Cruciate Ligament
PT	Patellar Tendon
MCL	Medial Collateral Ligament
LCL	Lateral Collateral Ligament
RF	Rectus Femoris
VL	Vastus Lateralis
VI	Vastus Intermedius
VM	Vastus Medialis
BF	Biceps Femoris
ST	Semitendinosus
GM	Gastrocnemius Medialis
GL	Gastrocnemius Lateralis
EMG	Electromyography
3D	Three Dimensional
MR	Magnetic Resonance
KLA	Knee Loading Apparatus
TPS	Thin Plate Spline
LVDT	Linear Variable Differential Transducer
QLV	Quasilinear Viscoelastic Theory
OC	Oral Contraceptives
RSA	Roentgen Stereophotogrammetric Analysis
FE	Finite Element
DC	Design Criteria
FBD	Free Body Diagram
F_p	Calibration weight force
F_w	Counteractive mass
F_m	KLA mass
F_a	Applied force
F_f	Reaction force 1
F_n	Reaction force 2
F_{ry}	Anterior reaction force at the knee
F_t	Lower limb weight
COM	Center of Mass
M_s	Lower Limb mass
M_r	Moment reaction at the knee
F_{rx}	Axial reaction at the knee
BMI	Body Mass Index
TBW	Total Body Water
FOV	Field of View
ICS	Image Coordinate System
LCS	Local Coordinate System
fLCS	Femoral Coordinate System

tLCS	Tibial Coordinate System
RMS	Root Mean Square
PTCL	Posterior Tibial Condylar Line
S ₁	Surface 1 (registration)
S ₂	Reference Surface (registration)
XT	Transformation parameter X (registration)
YT	Transformation parameter Y (registration)
ZT	Transformation parameter Z (registration)
ω	Transformation Rotation (X) (registration)
ϕ	Transformation Rotation (Y) (registration)
S	Scaling Factor (registration)
SVD	Singular Value Decomposition
PCS	Plane Coordinate System
CI	Compliance Index
MVC	Maximum Voluntary Contraction
α_c	Cronbach's Alpha
D1/D2/D3	Day 1/2/3
T1/T2/T3	Trial 1/2/3
AM	Anteromedial
PL	Posterolateral

Chapter One: Introduction

1.1 Introduction

The components of the knee joint function as an integrated system, and loss of integrity to any one component may jeopardize the long-term function and health of the system. The high incidence of knee joint injuries, pain, and degeneration can result in substantial increases in morbidity, functional loss, and health care expenditures (Gupta, et al., 2005; Lohmander, et al., 2007). Knee joint laxity can result from soft tissue injury, such as a ligament tear, or from genetic factors such as joint hypermobility syndrome and various forms of Ehlers–Danlos Syndrome. As a result of the laxity, patients may experience instability, recurrent dislocations or subluxations, or low-grade inflammatory arthritis (Lewkonia, 1993). Current techniques available for non-invasive quantification of joint laxity (arising from either ligament laxity or deficiency) based on a 1D force-displacement measurement device (e.g. KT-2000) are inadequate and inaccurate (Kupper, et al., 2007a). Additionally, the role that ligament laxity plays to help maintain joint stability is not well understood. This research aims to develop and evaluate a novel measurement tool to better quantify knee joint laxity.

1.2 Background

The knee is a complex synovial joint. It is capable of motion in all six degrees of freedom (three rotations and three translations about orthogonal coordinate axes), as seen when the articulating surfaces glide and roll as the knee flexes and extends. The knee is composed of quasi-passive components including bone and soft tissues, and active

muscular components that provide dynamic force control. The femur, tibia, and patella form the bony components of the knee (Figure 1-1a), lined with low friction cartilage on the articulating surfaces. These are attached with intra-articular ligaments including the anterior and posterior cruciate ligaments (ACL, PCL), and the menisci (Figure 1-1b). Ligaments are referred to as quasi-passive as they have been shown to have hormone and mechanoreceptors (Dragoo, et al., 2003; Liu, et al., 1996; Schultz, et al., 1984; Zimny and Wink, 1991). The capsule surrounds the knee joint and synovial fluid, and functions to seal the joint space and provide added stability (Ralphs and Benjamin, 1994). It is strengthened by the extracapsular structures, including the ligamentum patelle/patellar tendon (PT), and tibial/medial and fibular/lateral collateral ligaments (MCL, LCL).

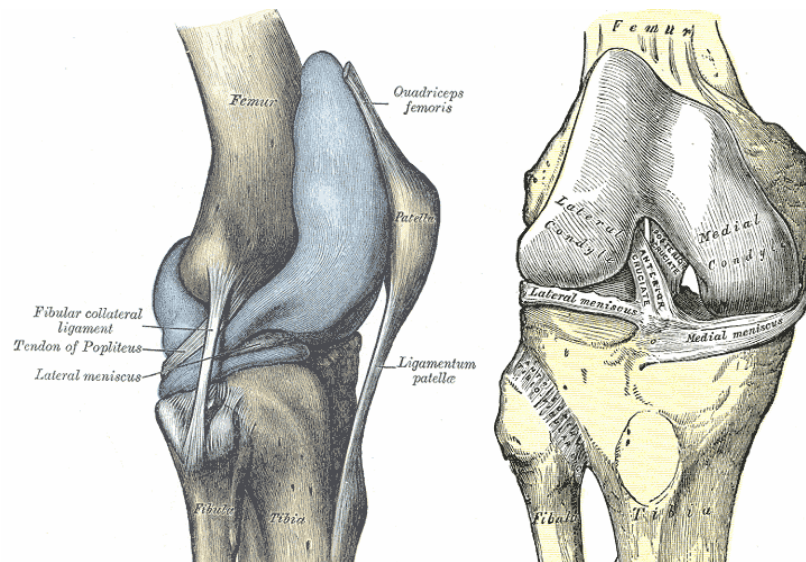


Figure 1-1: The Knee Joint (a) Sagittal view (b) Anterior view (Gray, 1918)

The largest leg extensor muscle is the quadriceps femoris, which includes the rectus femoris (RF), and vastus lateralis (VL), intermedius (VI), and medialis (VM) (Figure

1-2a). They originate proximally from the anterior inferior iliac spine, greater trochanter, intertrochanteric line, and anterior/lateral surfaces of the femur, respectively. All three muscles end distally at the quadriceps tendon, which attaches to the base of the patella and by PT to the tibial tuberosity.

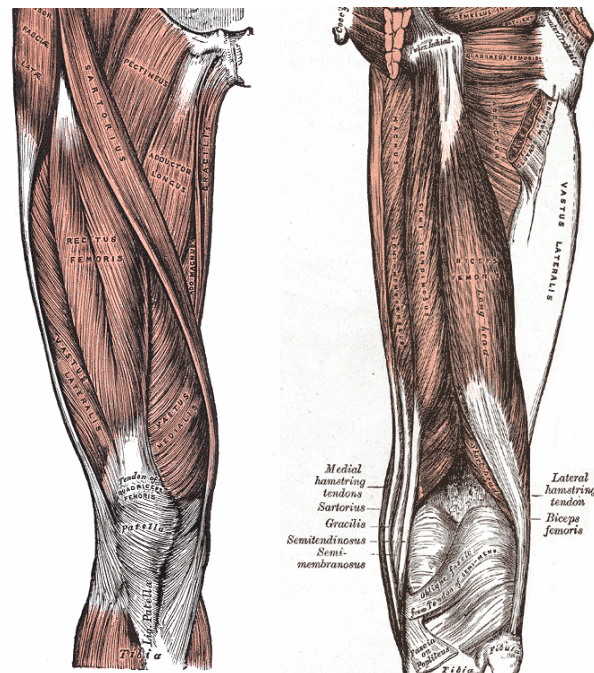


Figure 1-2: Muscles of the Thigh (a) Anterior view (b) Posterior view (Gray, 1918)

Knee flexors in the thigh include the hamstrings which are comprised of the long head of the biceps femoris (BF), the semimembranosus, and semitendinosus (ST) muscles (Figure 1-2b). They attach proximally from the ischial tuberosity and insert into the lateral side of the fibular head, the posterior side of the medial tibial condyle, and the medial surface of the superior part of the tibia, respectively. The gastrocnemius is the knee flexor of the lower leg, and can be separated into medial (GM) and lateral (GL) heads. The medial

head attaches proximally from the surface of the femur, superior to the medial condyle, and the lateral head attaches to the lateral condyle of the femur. They distally attach at the posterior surface of the calcaneus.

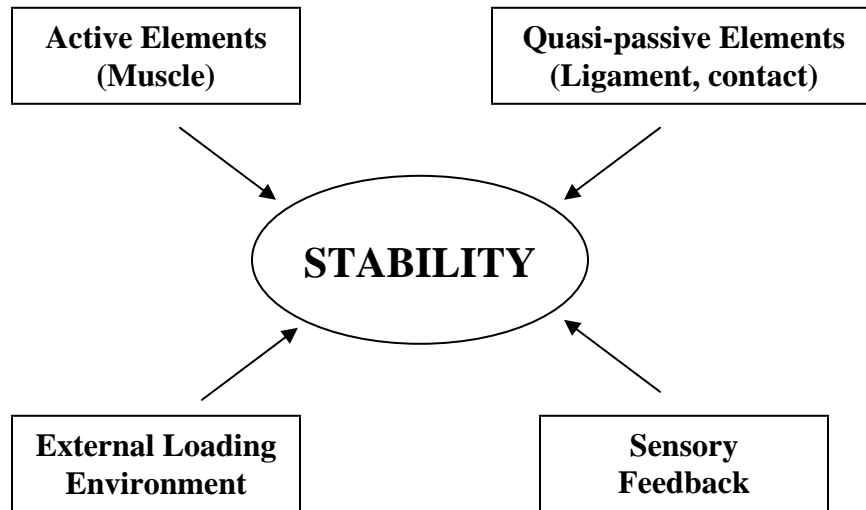


Figure 1-3: Schematic of variables that affect stability

The components of the knee work in synergy to provide a stable, functional joint. Functionally, this implies interplay between four main components: sensory systems such as visual, vestibular, and somatosensory, the external loading environment, active elements such as muscle, and quasi-passive elements such as tendons, ligaments, or cartilage contact (Figure 1-3). Sensory feedback provides the connection between the external environment and the reaction of the system to maintain stability. During a dynamic task, forces are modulated within the knee joint due to the load sharing of quasi-passive knee structures and the muscle forces that oppose external forces and moments.

Simultaneous contraction of major stabilizing knee flexor and extensor muscles, or co-contraction, provides added dynamic stability to the joint (Aalbersberg, et al., 2005a). In a healthy joint, the soft tissue structures such as the tendons (joining muscle to bone) and ligaments (joining bone to bone) provide a quasi-passive restraint to knee motion while enabling joint mobility. Tendon, as part of the musculotendinous unit, directly interfaces with the active muscular components. In particular, the ACL, comprised of the anteromedial (AM) and posterolateral (PL) bands, is the main structure opposing anterior translation and internal rotation of the tibia (Butler, et al., 1980). Any damage to the soft tissue structures or loss of integrity compromises joint stability. The quantitative relationship between the modulation of forces through the quasi-passive structures and joint stability and function remains unclear. One contributing factor to this lack of clarity may be the limitations of current measures for joint structure integrity.

The primary measure of joint structure integrity is joint displacement or laxity. It is important to distinguish passive laxity from functional or active laxity. In biomechanical terms, passive laxity is a measure of joint movement within the constraints of ligaments, capsule, and cartilage (Cross, 1996) when an external force is applied to the joint during a state of muscular relaxation. Laxity depends on the shape of the involved bony surfaces, the mechanical behavior of the joint's soft tissue structures, such as the joint capsule and ligaments, and contributions from other supporting structures, such as menisci, that may improve the bony fit between relatively incongruent joint surfaces. In typical joint laxity testing, an anterior force is applied to the tibia, thereby testing the ACL in the primary direction of resistance. Functional or active laxity describes the joint motion that occurs

during functional activities. The forces applied through the joint arise from muscle contraction or external loads related to movement, such as inertial or ground reaction forces. Muscle contraction or co-contraction (Aalbersberg et al., 2005a) that is well-timed and of an appropriate magnitude may play a role in controlling dynamic joint function by preventing excessive joint laxity from limiting function or increasing joint injury risk. This distinction is clinically important because some patients with passive laxity do not demonstrate functional laxity (Snyder-Mackler et al., 1997). This highlights the complex interaction between quasi-passive joint structures and the active muscle element, as well as the importance of distinguishing passive laxity from functional laxity. A systematic approach must be used to first quantify the quasi-passive structure behavior reliably before applying muscle force to include dynamic behavior.

In passive tests, muscle activity must be minimized. Typical methods used to reduce muscle activation include verbal instruction to relax along with muscle palpation, or administration of general or spinal anaesthetics (Sernert, et al., 2001). Both practicality (cost, time) and a modest potential for side effects when using anaesthetics eliminates this method for non-surgical clinical use (Derrington and Smith, 1987; Grathwohl, 2007; Williams, et al., 2000). Alternatively, surface electromyography (EMG) is a non-invasive measure of muscle activity that uses skin electrodes to measure the electrical signal produced by muscle activity (Cram, 2003; Merletti, et al., 2001). EMG provides a way to measure muscle activity and to ensure that subjects are relaxing during a passive knee laxity test.

Traditionally, passive tests rather than dynamic tests have been used to assess knee laxity in patients. This is primarily due to the reduced complexity of a laxity test by removing factors such as muscle contraction. These measures include the Lachman test, the anterior/posterior drawer test, the pivot shift test, the quadriceps active test, and the varus/valgus stress test (Malanga, et al., 2003). The primary structures being tested are the ACL, PCL, MCL, and LCL. These clinical measures can be effective for an experienced physician, and have been useful for determining treatment protocol. However, they do not allow for quantitative comparison between subjects or testers since the results are qualitative and primarily used for diagnosis (Malanga, et al., 2003).

In response to this need, instrumented devices such as the KT-2000 arthrometer (predecessor by the KT-1000) (MedMetric, San Diego, CA, USA), the Genucom Knee Analysis System (Faro Medical Technologies, Champlain, NY, USA), the Rolimeter (Aircast, Summit, NJ, USA), and the Stryker Ligament Tester (Stryker, Kalamazoo, MI, USA) were developed to quantify laxity. These devices use displacement transducers and/or digitized bony landmark positions to measure tibial translation with respect to the patella under an applied load. Current measures of laxity have been found to have low repeatability (Cannon, 2002; Highgenboten, et al., 1989; Huber, et al., 1997), and were found to overestimate the laxity values when compared to a 'gold standard' (Jorn, et al., 1998). The KT-1000, for example, was found to have an intertester reliability of ± 2.95 mm and ± 3.74 mm for posterior and anterior translation, respectively (Huber, et al., 1997). Given that a right-left difference of 3 mm or more is taken as an indication of increased laxity (Cannon, 2002), poor intertester reliability may result in false negative

tests because the difference between examiners is greater than the patient's interlimb difference. Possible reasons for variability include improper anterior/posterior alignment due to user dependence, muscle contraction, and a lack of size adjustment for a variety of limb lengths and sizes. There is a need for a repeatable measure of knee joint laxity. The link between instability and laxity may be further understood if laxity can be reliably and accurately quantified.

In-vitro joint laxity has also been measured in cadaveric specimens with high accuracy (Darcy, et al., 2006; Pearsall, et al., 1996). Typically either load cells in combination with a linear variable differential transducer (LVDT) or a robotic system are used to apply anterior loads and measure the resulting displacement. It has been reported that the LVDT displacement accuracy is ± 0.1 mm. The repeatability of the robotic system at the University of Pittsburgh is ± 0.02 mm and 0.2 N (Rudy, et al., 2000). In this thesis, a novel method of measuring passive joint laxity *in-vivo* is proposed. Based on the results for *in-vitro* testing, it is expected that *in-vivo* testing can be measured within the same order of magnitude, given a controlled force application and high resolution imaging (\pm pixel size).

This thesis presents a novel method of measuring passive knee joint laxity *in-vivo*. An *in-vivo*, non invasive measure of laxity with an improved accuracy and repeatability over other laxity measures would be useful both clinically and in the research sector. Detailed *in-vivo* three dimensional (3D) geometry of the joint can be obtained with Magnetic Resonance (MR) imaging. Using this geometry in combination with a known applied

force and a model of the summation of forces on the knee joint, the force-displacement characteristics of the knee can be obtained. To our knowledge there are no current methods or published research that specifically measure passive *in-vivo* knee joint laxity using MR imaging under an externally applied anterior load. Furthermore, the potential to consider the contribution of individual joint structures to gross joint laxity makes this a novel measurement tool.

1.3 Objectives and Specific Aims

The long term research goal is to advance understanding of the relationships between joint mechanics and joint health, and between joint structure and dynamic joint function. The objective of this research project is to develop and evaluate a novel measurement tool to quantify non-invasive, *in-vivo* knee joint laxity.

Hypotheses: The novel MR-based measure of laxity and incorporated knee model will be tested on normal subjects through the following hypotheses:

H1: The loading apparatus will have repeatable positioning and load application.

H2: Joint and ACL insertion point displacement will be repeatable (± 0.5 mm) for a given applied load. The force-displacement curves will show increasing displacement with increasing force.

H3: Force-displacement curves found using novel technique will be less variable and differ from those using the KT-2000.

H4: Subjects will be capable of muscle relaxation in the loading apparatus such that the electromyography (EMG) signal will be less than 5% of manual maximum contraction in all muscles.

This will be achieved through the following specific aims:

Specific Aim 1: Design an MR compatible loading apparatus that applies an anterior load to the knee (H1).

Specific Aim 2: Apply a registration technique to MR images to observe 3D joint motion and change in ACL insertion point location (H2).

Specific Aim 3: Measure *in-vivo* joint response (displacement and time-dependent phenomena) to applied stepped forces. (H2, H4).

Specific Aim 4: Investigate repeatability of force-displacement curves in normal subjects (n=3) over 3 trials (H2, H3).

Specific Aim 5: Use EMG to evaluate the ability of subjects to avoid muscle activation during knee joint loading (H4).

1.4 Thesis Outline

The goal for this thesis is to develop a tool to measure laxity that improves upon current methods. The novel measure will be used to quantify knee joint laxity in normal subjects, and to investigate the repeatability of the method. In the long term, improving the methodology for measuring knee laxity may lead to a better understanding of the

effect of passive laxity on joint stability. In addition, it may improve the reliability for detecting differences in knee laxity between various injured populations.

Chapter One provides an introduction to the research topic. Chapter Two reviews the literature, spanning topics such as current laxity measurement techniques and variables that affect joint laxity. A portion of this chapter was published as a review article in *Clinical Biomechanics* (Kupper, et al., 2007a). Chapter Three presents the design of the novel measurement of joint laxity. Chapter Four describes the methods and equipment used to test normal subjects for a measure of gross knee joint laxity and the repeatability of this measure. Chapter Five outlines the results including EMG data that show minimal effects of muscle guarding, and the force-displacement curves for normal knees under anterior loading as measured with both the KT-2000, and the MR images with loading apparatus. Chapter Six concludes the thesis with a full discussion of the findings and recommendations for future research.

This research has been presented at a number of conferences including the 3rd Annual Schulich School of Engineering Graduate Student Research Conference (Johnson, 2006), and the Canadian Arthritis Network's 2006 Annual Scientific Conference and Satellite Workshop (Kupper, et al., 2006a; Kupper, et al., 2006b). This research was most recently presented at the 2007 ASME Summer Bioengineering Conference in Keystone, Colorado, and awarded an Honorable Mention in the Student Paper Competition (Kupper, et al., 2007b).

Chapter Two: Literature Review

2.1 Introduction

This chapter presents background information that forms the basis of the motivation and objectives for this thesis project. Tendon and ligament mechanics are reviewed to frame the effects of applying load to the viscoelastic knee joint. Concepts of joint laxity are introduced, followed by a review of the effects of hormone fluctuation and oral contraceptives on laxity. Current methods of measuring laxity are reviewed including traditional and alternate systems. Studies that have evaluated these devices will be considered. Criteria for a measure of laxity are defined and reviewed. Finally, theoretical models are discussed to frame the selection of a contact model to quantify gross joint displacement. Portions of the literature review have been published as a review article in *Clinical Biomechanics* (Kupper, et al., 2007a). Appendix A includes a copy of this paper along with a guideline of the division of work done by each author, and permission from the publisher and co-authors to use this paper as a portion of this thesis.

2.2 Terminology

The human body is typically described in anatomical planes and directions (Figure 2-1). Anterior and posterior axes are oriented to the front and back of the body. The medial direction is closer to the midline of the body (axis of symmetry) and lateral is away from the midline. The superior axis is directed towards the head and the inferior axis points towards the feet.

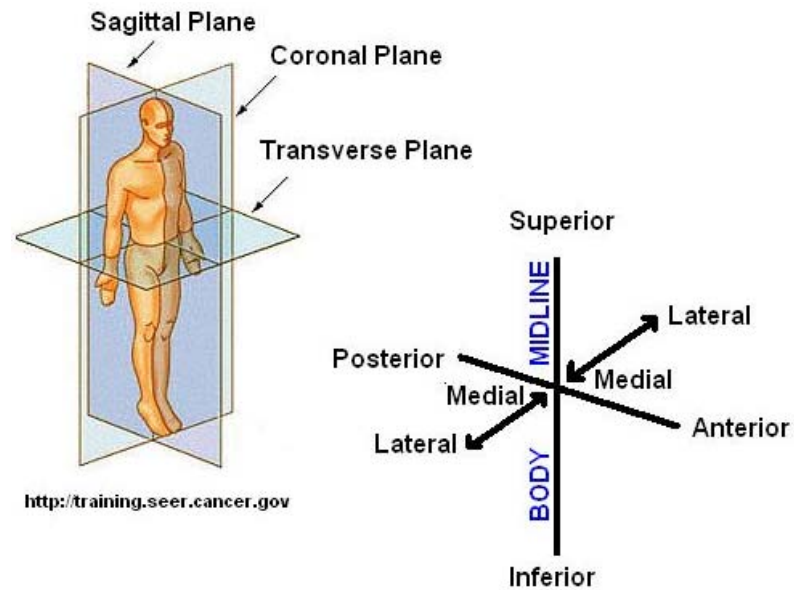


Figure 2-1: Anatomical planes of the body from SEER Program (2007)

Knee flexion is measured as the angle between the long axis of the femur and the long axis of the tibia in the sagittal plane. Full extension (straight leg) is roughly equal to 0° of knee flexion.

2.3 Tendon and Ligament Mechanics

Tendons and ligaments are connective tissue made of proteins (collagen and elastin) and polysaccharides (proteoglycans). Collagen fibrils group into fibres that form subfascicular units that group together in fascicles (Figure 2-2). Collagen fibres are aligned axially along the length of the anisotropic material. This structural organization provides stiffness in the direction of the axial tensile forces that are the principal loading state of tendons and ligaments (Netti, et al., 1996).

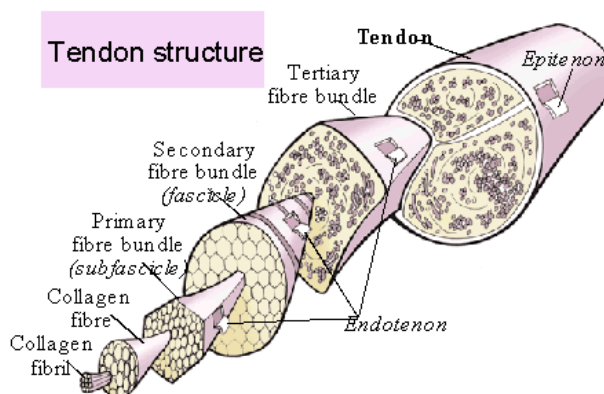


Figure 2-2: The hierarchical organization of tendon structure: from collagen fibrils to the entire tendon (Jozsa, 1997)

Tendons and ligaments are viscoelastic, showing time-dependent behavior (Woo, et al., 1999). This characteristic is often demonstrated through *in-vitro* creep and stress relaxation testing (Thornton, et al., 1997). Stress relaxation is the stress response of a system under constant strain. Creep is the strain response of a system under constant stress. Recently creep has been identified as an important parameter, as it is thought that excessive creep could result in joint laxity (Bray, et al., 2005). However, both types of tests are conducted as there is currently no conclusive evidence and no consensus about whether ligaments are strain or stress modulated structures (Thornton, et al., 1997).

Mechanical testing of ligaments *in-vitro* has been widely studied (Hingorani, et al., 2004; Netti, et al., 1996; Provenzano, et al., 2001; Thornton, et al., 1997; Thornton, et al., 2001; Woo, et al., 1999). Quantifying the viscoelastic properties of ligaments is thought to play an important role in understanding normal joint mechanics, and altered joint mechanics due to ligament injury or other pathologies (Hingorani, et al., 2004). However, to the

author's knowledge, no studies have tested stress relaxation in the human knee joint *in-vivo*. A study by Duong et al. (2001) measured stress relaxation in the ankle joint by applying a fixed dorsiflexion angle for 20 minutes to 8 normal subjects, and continuously measuring the resulting torque. Understandably, testing joint viscoelastic properties can be more precisely controlled *in-vitro* than *in-vivo*, and faces many methodological challenges (Woo, et al., 1999). However, much insight into knee joint mechanics has been gained in other areas by testing the knee-joint *in-vivo* through techniques such as gait analysis and imaging (DeFrate, et al., 2004; Fjeld, 2007). Quantifying stress relaxation *in-vivo* could be an important step in gaining insight about normal and pathological joint mechanics.

2.3.1 Modelling Stress Relaxation

A typical model for ligament behavior is the Quasilinear Viscoelastic Theory (QLV), originally proposed by Fung (1972) and applied extensively by Woo (1982). It assumes the stress relaxation function to be described by:

$$\sigma[\varepsilon(t);t] = G(t) * \sigma^e(\varepsilon) \quad (2.1)$$

where σ^e is the elastic response and $G(t)$ is the reduced relaxation function.

For a continuous spectrum of relaxation, Fung proposed the following $G(t)$:

$$G(t) = \frac{1 + C[E_1(t/\tau_2) - E_1(t/\tau_1)]}{1 + C \ln(\tau_2/\tau_1)} \quad (2.2)$$

where $E_1(y) = \int_y^\infty e^{-z} / z dz$ is the exponential integral and C , τ_1 , and τ_2 are material

constants.

Based on Lanczos (1956), a relaxation curve fit can be described by:

$$G(t) = Ae^{\frac{-t}{\tau_1}} + Be^{\frac{-t}{\tau_2}} \quad (2.3)$$

where A and B are constants. By fitting a sum of exponentials to the stress relaxation curve normalized to initial (peak) stress, the constants A, B, τ_1 , and τ_2 can be solved for. Thus, τ_1 describes the time constant for the instantaneous response and τ_2 describes the time constant for the time-dependent response. The exponential shape of the stress relaxation curve is typically thought to be due to changes at the collagen level as they reorient in a viscoelastic matrix (Provenzano, et al., 2001). However, a study by Purslow et al. (1998) using X ray diffraction showed that collagen fibers in rat semitendinosis perimysium did not change orientation during stress relaxation. It was speculated that time-dependent reorganization could occur with respect to collagen crimp without changing the collagen orientation. The authors also suggested was the possibly that stress relaxation was occurring 1) at the fiber level, 2) within the matrix, or 3) at fibril connections to the matrix.

For stepped loading, Sarver et al (2003) proposed an alternate form of normalizing the stress relaxation curve. The stress is normalized to the peak stress, and each stress value divided by the difference between the peak stress and the final stress. This removes the strain-dependence that is seen with the typical method, although strain independence is an inherent assumption of the QLV theory.

2.4 Joint Laxity

Theoretically, laxity can be measured at any joint, although some joints are inherently very stable, such as the sacroiliac joints between the two halves of the pelvis and the centrally located sacrum. In these cases, laxity is not typically assessed by quantifying the motion of the joint, but by whether passive motion produces pain or other symptoms. The human shoulder is a good example of a lax joint that relies entirely upon ligaments for passive stability because the capsule is very loose and the bony anatomy provides minimal contributions to joint stability. In this case, the benefit of having a lax joint is a considerable increase in the total range of joint motion, allowing humans to reach overhead with relative ease. Therefore, a measure of laxity must be interpreted contextually, including the function of the joint (weightbearing support versus functional reach or grasping).

Increased joint laxity can result from a local soft tissue injury such as a ligament tear or from genetic factors such as joint hypermobility syndrome and the various forms of Ehlers–Danlos Syndrome. Excessive joint laxity predisposes the joint to instability including recurrent dislocations and subluxations, and low grade inflammatory arthritis (Lewkonia, 1993). However, the link between instability and laxity is not fully understood (Maffulli, 1998; Patel, et al., 2003). Knee joint laxity is of particular interest, and has been studied extensively, in part, due to the high incidence of knee injuries, knee joint pain, and degeneration that account for substantial morbidity, functional loss, and health care expenditures.

The knee joint exhibits a wide spectrum of laxity, from inherently stable joints at one end, to excessively lax joints at the other (Figure 2-3). The causes of abnormal laxity are numerous and complex. Individuals with high joint laxity, such as those with ACL tears, are more likely to incur subsequent knee injuries. Interestingly, even the normal, uninjured population displays a wide range of knee laxity. For example, young, fit military recruits, who are otherwise healthy, have exhibited laxity at the high end of the spectrum, without any prior injury or existing pathology (Uhorchak, et al., 2003). This normal range of laxity is further complicated in sexually mature females where, at least in a subpopulation, changes in joint laxity have been reported to occur during the menstrual cycle (Deie, et al., 2002; Shultz, et al., 2006; Shultz, et al., 2004; Wojtys, et al., 2002). However, this point is still controversial (Belanger, et al., 2004), and it is not clear whether there are biologically different populations, or subtle differences in methodology that are confounding the findings.



Figure 2-3: Spectrum of Laxity

In the ACL deficient knee, laxity values lie at the far end of the spectrum. ACL deficient subjects are often subdivided into copers, who functionally adjust to the injury, and noncopers, who experience increased instability, including recurrent subluxations (Eastlack, et al., 1999). Noncopers are often candidates for ACL reconstruction, where the torn ligament is commonly replaced by either the central third of the patellar tendon

or the gracilis/semitendinosus tendon (Herrington, et al., 2005). After reconstruction, laxity is reduced but typically the joint does not return to normal function (Almekinders, et al., 2004; Ejerhed, et al., 2003).

Another factor affecting joint laxity is an individual's genetic predisposition for pathologies such as Marfan's syndrome, Ehlers–Danlos syndrome, and joint hypermobility syndrome. This latter disorder appears to affect connective tissue matrix proteins, thereby altering the mechanical properties of the soft tissues and creating an inherent joint laxity (Hakim and Grahame, 2003). The majority of individuals with joint hypermobility syndrome are female (Acasuso Diaz, et al., 1993; Baum and Larsson, 2000; Bridges, et al., 1992), with the incidence reported to vary from 5% of the Caucasian population to roughly 30% of females of Middle Eastern descent (Al-Rawi, et al., 1985; Bridges, et al., 1992; Fitzcharles, 2000). These subjects are more lax than normal. This group is uniquely different from an injured population because the musculoskeletal laxity is something they have matured with rather than having to adjust to a sudden change in joint laxity following an acute injury. Those with joint hypermobility syndrome are also unique because the laxity may not be restricted to a particular joint. Some patients with joint hypermobility syndrome demonstrate laxity throughout all joints, while others may experience laxity in only upper extremity or solely lower extremity joints. Regardless of the underlying cause or number of affected joints, at a certain threshold along the spectrum a patient will be at risk for joint injury.

2.5 Measuring Laxity in Females

ACL injuries occur at a higher rate in females than in males (Arendt, et al., 1999). Additionally, females have been demonstrated to have greater knee laxity than males (Rozzi, et al., 1999). Consequently, measuring joint laxity in females may be one important factor in understanding the causes for the higher injury incidence. Although the linkages amongst knee laxity, injury incidence, and mechanism are not clear, the differences between males and females are thought to be caused by numerous factors (Davis, et al., 2007). These factors include structural differences such as a larger Q-angle (Moul, 1998), a smaller ACL (Chandrashekar, et al., 2005), and a combination of biomechanical and neuromuscular differences that affect dynamic performance such as strategies for movement (Landry, et al., 2007). Interestingly, the timing of ACL injury in females is reportedly not evenly distributed over the course of the menstrual cycle (Slauterbeck, et al., 2002). Across multiple studies, there is no agreement with regards to the time during the cycle when injury rate increases, if at all (Arendt, et al., 1999; Slauterbeck, et al., 2002; Wojtys, et al., 2002). As a potential explanation of this potential phenomenon, sex hormones are speculated to alter the mechanical properties of the ACL (Slauterbeck, et al., 1999). It is unknown what the timing effects are of hormones on ACL mechanical properties (Zazulak, et al., 2006). Receptors have been identified on the ACL for estrogen, progesterone, and relaxin (Dragoo, et al., 2003; Liu, et al., 1996). While this evidence has motivated several studies investigating the effect of hormones on knee laxity, in general, no conclusive result has emerged regarding changes in laxity over the hormonal cycle (Zazulak, et al., 2006).

The use of oral contraceptives (OC) has been shown to reduce the rate of traumatic injury in female athletes (Moller-Nielsen and Hammar, 1989). In a study by Martineau, et al. (2004), knee joint laxity measured with the KT-1000 showed a significant decrease in subjects taking an OC compared to non-users. It has been postulated that OC use may help to inhibit or stabilize the potential variability phase to phase hormonal level, expressed as a reduction in knee joint laxity in OC users compared to normals (Martineau, et al., 2004). This suggests that testing female subjects who are OC users may be more appropriate for repeatability testing of knee joint laxity, as the variability introduced by hormone fluctuation may be reduced.

2.5.1 Total Body Water

Evidence suggests that fluid retention may change with hormone levels. Bioelectric impedance measures have shown changes in total body water over the menstrual cycle. In women taking one-phase oral contraceptives, changes in skin thickness thought to be caused by increased fluid retention were not present. Increases in skin thickness were seen in women on three-phase oral contraceptives during mid-cycle when taking a high dose of estradiol. The same was observed in women with a normal spontaneous menstrual cycle during days 12-22 when estradiol levels typically peak and remain high (Eisenbeiss, et al., 1998). A small number of studies have investigated the effect of water content on ligament behavior. In the human patellar tendon *in-vitro*, it was found that increased water content caused increased load relaxation, and increased stiffness at the 50% per second strain rate (Haut and Haut, 1997). Increased water content has been shown to have *in-vitro* effects on pre-stress, creep, and viscoelastic behavior in the rabbit

MCL (Chimich, et al., 1992; Thornton, et al., 2001). To the knowledge of this author, there have not been any studies that measure or control for water content during laxity testing.

Total body water may be one method of accounting for water content *in-vivo* in subject populations (Himmelfarb, et al., 2002). Bioelectrical impedance analysis is considered to be a gold standard measure of total body water (Chertow, et al., 1997). However more accessible methods in the form of predictive equations have been developed, including the Watson (Watson, et al., 1980), Hume-Weyer (Hume and Weyers, 1971), Chertow (Chertow, et al., 1997), and physiologic (Himmelfarb, et al., 2002) techniques. These equations are based on age (years), sex (M=1, F=0), height (cm) and weight (kg), and in one case may also account for presence of diabetes (Y=1, N=0). The Chertow and physiologic techniques have been found to be closest to predicting the bioelectrical impedance analysis results (Chertow, et al., 1997; Himmelfarb, et al., 2002).

2.6 Current Measures of Laxity

The devices that have been and are currently used to measure joint laxity can be categorized into traditional and alternative systems. The traditional systems, including the KT-2000 arthrometer (<http://www.medmetric.com>, MedMetric, San Diego, CA, USA), the Genucom Knee Analysis System (<http://www.faro.com/>, Faro Medical Technologies, Champlain, NY, USA), the Rolimeter (<http://www.rolimeter.com>, Aircast, Summit, NJ, USA), and the Stryker Ligament Tester (<http://www.stryker.com>, Stryker, Kalamazoo, MI, USA) have been used in research and clinical settings. Each system has

features that have contributed towards establishing the standard for measuring knee laxity. Cannon (2002) noted that arthrometers allow experienced clinicians to detect ACL injuries that may have otherwise been missed. Alternate systems, such as planar stress radiography, Roentgen Stereophotogrammetric Analysis (RSA), and MR imaging, have been primarily employed in research to obtain more accurate measures of displacement under a known applied force or task (DeFrate, et al., 2004; Fleming, et al., 2002). In the current study, MR imaging will be applied to measure joint displacement under applied loading.

2.6.1 Traditional Measurement Systems

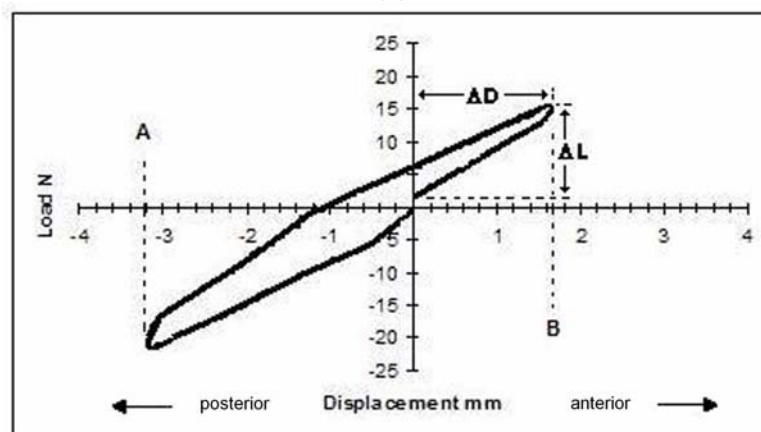
2.6.1.1 KT-2000

The most commonly used arthrometer in both biomechanical research and clinics is the KT-2000, which measures anterior–posterior knee laxity during the drawer test. The subject lies supine in slight hip flexion ($\sim 30^\circ$) and with a knee flexion angle between 20° and 35° (Figure 2-4a). The knee must be flexed adequately to engage the patella in the femoral groove. If the flexion is inadequate, the patella will not provide a stable base from which tibial displacement can be measured. External hip rotation is restricted by a Velcro strap placed midthigh and tibial position is maintained by placing the subject's feet between two vertical supports that prevent the feet from rolling outward. The arthrometer is secured to the anterior tibia with Velcro straps, with a proximal bar contacting the anterior patella surface, the motion axis oriented over the joint line, and the force plunger positioned over the tibial tubercle.

With the subject relaxed, a dial on the front of the machine is adjusted to a neutral starting position of the tibia with respect to the patella. The examiner then passively translates the tibia posteriorly and anteriorly, with a goal of establishing the same neutral starting position with each cycle. This pre-test also helps the subject to completely relax because it allows them to become accustomed to the motion. If the initial starting position changes between cycles, it is likely that the subject is either protecting the joint by contracting the thigh muscles, or the patellar reference pad is moving. If the starting position is stable, anteriorly and posteriorly directed passive loads of 67 N and 178 N (Myrer, et al., 1996) are then applied through the force handle of the arthrometer.



(a)



(b)

Figure 2-4: (a) Positioning of subject for testing with the KT-2000 arthrometer. (b) A typical force-displacement curve resulting from testing with the KT-2000 arthrometer; “A” and “B” denote peak posterior and anterior displacement respectively. Stiffness is calculated as $\Delta L/\Delta D$.

2.6.1.2 Genucom

The Genucom is also used to measure anterior–posterior knee laxity, however, it is also capable of measuring motion in several planes simultaneously (Cannon, 2002). This includes measuring varus-valgus, pivot shift, and recurvatum (Highgenboten, et al., 1989). The testing procedure for measuring anterior–posterior knee laxity with this device, as summarized here, was originally described in Highgenboten et al. (1989). The

Genucom system includes a computer that is used to record the subject's data file. The subject is positioned with the knee flexed to 20° . The thigh is secured with restraints, and an electrogoniometer is attached to the thigh and shank. Anatomical landmarks including the tibial tubercle, tibial crest, medial and lateral femoral condyles, and the patella are marked and digitized. These landmarks are used to obtain a segment coordinate system and to record the relative displacement at the knee joint, and the distance between markers is documented. Consequently, this system is sensitive to soft tissue motion as with any skin based markers, although this effect is minimized by locating them on bony landmarks. To account for motion within the Genucom, a soft tissue compensation test can be performed in three planes while maintaining the same distance between the markers. Furthermore, as with the KT-2000, the patella should be engaged in the femoral groove. The anterior–posterior drawer test is completed at the system's required force magnitude of 21 lbs (93.45 N). Data is collected continuously at a rate of 8 Hz (Andersen and Jorgensen, 1998), and is stored electronically.

2.6.1.3 Rolimeter

The Rolimeter is used to measure anterior–posterior laxity for Lachman, anterior drawer, and 'step off' tests. The subject is positioned supine, with knees flexed to 25° for the Lachman test, 80° for the anterior drawer test, and an unspecified angle for the 'step off' test. The knee is supported by a pillow for the Lachman test. Unlike the KT-2000, the only specification for foot position is for the anterior drawer test, where the tester sits on the subject's foot. A proximal convex pad rests over the patella, and a distal pad is fixed to the tibia with a rubber strap (Papandreou, et al., 2005). The two pads are connected

approximately 5cm above the limb by a calibrated steel bar. The stylus is an additional arm that projects down from the steel bar onto the tibial tuberosity. As described in Muellner et al. (2001), the patella can either be stabilized with the thumb, or with the technique used for the KT-1000. Similarly for the KT-2000, the quadriceps muscles must be relaxed. The knee is preconditioned with three applications of a posterior force to the tibia. The tester must ensure that the stylus foot is in contact with the tibial tuberosity, and the white indicator, a movable plastic ring, is against the adjustment knob. The white indicator displaces when the tibia is manually pulled anteriorly. The displacement is measured in increments of 2 mm. For both the Lachman and anterior drawer tests, a manual maximum anterior force is applied three times, and the three maximal anterior translations are measured and averaged. For the 'step off' or side-to-side difference test, the Rolimeter is calibrated by applying it to the injured leg while applying a posterior force, ensuring that the stylus is in contact with the tibial tuberosity. It is then applied to the uninjured leg, and the side to side difference can be recorded. The benefit of the Rolimeter is that it is small, portable, and autoclavable. However, it neither records data nor tests at a variety of force levels. Furthermore, the displacements are measured at the endpoint of tibial motion with relatively low resolution (± 2 mm).

2.6.1.4 Stryker Ligament Tester

The Stryker Ligament Tester has a patient positioning seat, force applicator, and a displacement transducer. Like both the KT-2000 and the Rolimeter, this device uses the patella and the tibial tuberosity as reference points to measure displacement. One disadvantage of using the patella as a reference point is that it is not firmly attached to the

femur, and therefore must be well-seated in the femoral groove to reduce the relative motion. Unlike the Genucom, which can account for out of plane motion, the Stryker Ligament Tester assumes that there is only anterior–posterior displacement. As Cannon (2002) describes, the ankle is secured with a strap, and the flexion angle is set between 0° and 90° , although 25° – 30° is typical. The calibrated ruler is positioned horizontally, and the proximal tibial bracket is placed on the tibial tubercle. The distal bracket is positioned above the ankle, with an external rotation to align it with the tibia. Three straps secure the device at the proximal and distal ends of the tibia, and at the thigh just above the patella. The measuring gauge is positioned over the patella with the button at the midpoint. The patient leans back and relaxes while the examiner stabilizes the thigh with their non dominant hand. Simultaneously, the tester applies a load with the force applicator, which is positioned over the crest of the tibia for a posterior load and behind the proximal calf for an anterior load. The resulting displacement at the endpoint of tibial displacement is measured to the nearest 0.5 mm.

2.6.1.5 System Outputs

For the arthrometers that are capable of measuring continuously during the anterior–posterior drawer test, including the KT-2000 and the Genucom, force and displacement of the tibial sensor are recorded throughout the posterior and anterior motions, and can result in a plot (Figure 2-4b). Traditionally, laxity is measured from these cycles as the peak displacement with respect to the starting zero point at a given load. A compliance index (Daniel, et al., 1985a) is also computed from the force–displacement curve as the slope of a line connecting the points corresponding to zero displacement and the peak

anterior or posterior displacement. Both knees of the subject are tested and an interlimb difference is computed. Interlimb differences normalize the subject's involved knee to the uninjured, thereby accounting for the subject's specific, total body laxity. Interestingly, this compliance index can also be obtained by arthrometers that only measure the displacement at the endpoint of tibial motion, including the Rolimeter and the Stryker Ligament Tester. An interlimb peak displacement difference greater than 3 mm is considered indicative of anterior cruciate ligament insufficiency.

Efforts to characterize the entire nonlinear force-displacement curve have been implemented based on quantifying the first (stiffness) and second (change in stiffness) derivatives (Maitland, et al., 1995). These values differ from the compliance index, as calculating the instantaneous slope at each discrete point along the force-displacement curve, giving true stiffness, rather than an average displacement based on the change in displacements. By accounting for the entire nonlinear response, this method is able to identify significant material behaviors that could not be detected by an average linear stiffness. Quantifying the entire force-displacement curve highlights an increasing slope as the ACL works to restrain the knee after tibial weight is overcome. In this study, the authors showed that low values of stiffness and change in stiffness were typical for ACLD subjects in the upper region of the force-displacement curve, where the ACL is believed to be the primary restraint. In comparison, control subjects showed higher stiffness and change in stiffness over this range. These results highlight the value in quantifying stiffness along the curve, as individual sections of the curve (toe region, linear portion, upper region) can be analyzed and used to differentiate injured from

control populations. It is particularly important to quantify the low load behavior during the toe region of the force–displacement curve as it spans the normal operating range of the knee.

The relative rate of use of these arthrometers has changed over time. The KT-2000 system continues to be the most popular device for measuring joint laxity, while other units such as the Genucom appear to be used less frequently in recent years based on literature reports. This conclusion is highlighted in Figure 2-5, which shows the number of papers per year in which each type of arthrometer is referenced. Searches were done using the National Center for Biotechnology Information PubMed database (from 1966 to June 2006) using the search terms “KT 1000” or “KT-1000” or “KT 2000” or “KT-2000”, “Genucom”, “Stryker Ligament Tester” or “Stryker Knee Laxity Tester” or “Stryker Laxity Tester”, and “Rolimeter”. There are many possible reasons why the KT-2000 appears to be the preferred laxity measurement system. Some factors could include cost, availability, or the suitability of the system to the application. Complex systems that allow a greater range of measurements such as the Genucom may be better suited to a research environment, however, using the KT-2000 in a research study allows for comparison of data to a large body of published work. The KT-2000 is smaller and thus more easily portable than the Genucom, making it amenable to the clinical setting. The Rolimeter and the Stryker Ligament Tester are also small lightweight systems, making them easily transportable and straightforward to use. However, the KT-2000 has a digital output rather than analog, and thus can generate real-time force–displacement

graphs. It seems that the KT-2000 may fit a niche due to the balance of convenience and simplicity with descriptive output measures.

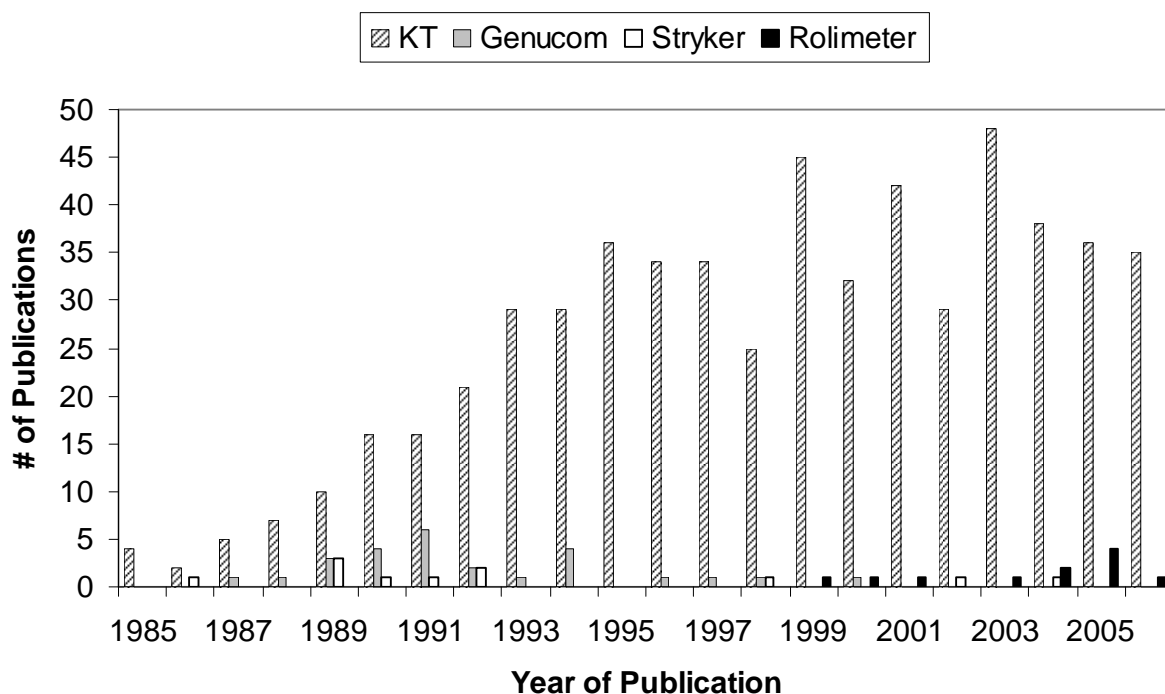


Figure 2-5: Number of Publications per year that include the KT-1000/2000, Genucom, Stryker Ligament Tester, or Rolimeter arthrometers from 1985 to 2006

One limitation of the majority of these devices is that they only measure translational displacement, which is assumed to be solely in the anterior/posterior direction, thereby neglecting the entire range of laxity as the knee moves with six degrees of freedom.

Passive laxity tests with the KT-2000 have been reported to correlate poorly to functional outcome after ACL injury (Snyder-Mackler, et al., 1997). The accuracy and reliability of these devices (Table 2-1) has been assessed extensively (Anderson and Lipscomb, 1989; Anderson, et al., 1992; Cannon, 2002; Highgenboten, et al., 1989; Huber, et al., 1997; Papandreou, et al., 2005). Most of these studies rely on comparisons between

arthrometers or repeatability studies for validation, rather than determining accuracy with respect to a ‘gold standard’ measurement device. It is important to note that the importance of studying accuracy is to determine how closely an arthrometer can measure the correct value. Conversely, repeatability describes how closely a device can obtain the same value over multiple measurements, regardless of whether this value is correct or not. Thus, assessing accuracy is equally important for evaluation of a laxity measurement device as repeatability.

Table 2-1: Accuracy and Repeatability of Current Laxity Measurement Devices

Device	Repeatability/Reliability	References
KT-1000 or KT-2000	* Anterior: ± 3.99 mm, ± 3.89 mm, ± 3.74 mm Posterior: ± 2.95 mm, ± 2.53 mm, ± 3.27 mm ^ Anterior: 0.87 Posterior: 0.79 † 0%, 82% † 0%, 75%	Huber et al., 1997 Highgenboten et al., 1989 Anderson et al., 1992 Anderson and Lipscomb, 1989
Genucom	^ Anterior: 0.96 Posterior: 0.86 † 23%, 76% † 10%, 70%	Highgenboten et al., 1989 Anderson et al., 1992 Anderson and Lipscomb, 1989
Rolimeter	^ Anterior between 3 testers: $r(P1 \text{ vs } P2) = 0.96$ $r(P1 \text{ vs } P3) = 0.55$ $r(P2 \text{ vs } P3) = 0.57$	Papandreou et al., 2005
Stryker Ligament Tester	^ Anterior: 0.74 Posterior: 0.87 Anterior/Posterior: 0.83 † 0%, 82% † 10%, 75% ** 4.4 mm, 8.0 mm	Highgenboten et al., 1989 Jorn et al., 1998 Anderson et al., 1992 Anderson and Lipscomb, 1989 Jorn et al., 1998

* 95% CI for novice, experienced, and intertester respectively

^ r value

† percentage of 50 subjects diagnosed with false positives for ACL deficiency, percentage of 50 subjects diagnosed with true positives for ACL deficiency

** mean difference from known value at 90 N and 180 N respectively

One of the biggest limitations of these devices is variability between testers (Cannon, 2002). The KT-1000, for example, had an intertester reliability of ± 2.95 mm and ± 3.74 mm for posterior and anterior translation, respectively (Huber, et al., 1997). Given that a right-left difference of 3 mm or more is considered an indication of increased laxity (Cannon, 2002), poor intertester reliability may result in false negative tests because the difference between examiners is greater than the patient's interlimb difference.

Highgenboten et al. (1989) compared the KT-1000, Genucom, and Stryker Ligament Tester devices. The Genucom reportedly produced significantly higher anterior laxity values than the other devices, indicating that the results are device specific. These studies have shown that although the current laxity devices have made methodological advances for quantifying laxity, poor inter-tester reliability continues to plague current devices.

Few studies have been conducted to determine the accuracy of arthrometers. Jorn et al. (1998), found anterior tibial translation to be overestimated with the Stryker Ligament Tester compared to measurements based on RSA. The error was attributed to soft tissue displacement. Thus, there is clearly a need for both a measure of laxity that is less variable and improved methodology for clinical assessment of joint laxity in a defined manner. This is of particular importance to understanding the mechanisms involved with, and the efficacy of, interventions developed to negate the impact of excessive or variable laxity on joint function and minimize risk for loss of joint health.

2.6.2 Alternate Measurement Systems

Various medical imaging techniques have been used to quantify relative tibial-femoral motion, including planar stress radiography, RSA, and MR imaging. These imaging techniques have shown promise in measuring displacement, especially as the quality of images improves with technology. Images of the knee can also be reconstructed or quantified in three dimensions, thereby allowing calculation of the entire 3D tibial displacement, rather than simply in the anterior/posterior direction.

2.6.2.1 Planar Stress Radiography and RSA

Planar stress radiography uses a series of lateral radiographs to quantify the displacement of the tibial condyles with respect to the femoral condyles (Fleming, et al., 2002). It is noninvasive, with a reported reproducibility of ± 0.5 mm (Staubli, et al., 1992). RSA measures motion in three dimensions by spatial reconstruction of tantalum beads implanted into the cortices of the bones of interest, with reported translational and rotational accuracies of 10–250 μm and 0.03° – 0.6° respectively (Karrholm, 1989; Selvik, 1989). Although this technique provides the most accurate measure of laxity, the implantation of tantalum beads is highly invasive, and thus, cannot be readily applied to every subject group. Despite the benefits of both planar stress radiography and RSA, a major drawback to each is that patient exposure to radiation is required. The current standard for the recommended use of radiation is to minimize subject exposure, based on the understanding that any dose of radiation can have harmful effects (Picano, 2004). Furthermore, while radiography provides very clear images of bone, it does not image soft tissues well. This is an important limitation, as the majority of the passive restraints

of the knee are soft tissues. Thus, a very clear view of joint laxity can be gained through bone-bone displacement, however, the behaviors of joint's soft tissues cannot be well observed, and thus the underlying reasons for the laxity may not be appreciated.

2.6.2.2 MR Imaging

MR imaging shows promise as a noninvasive, accurate modality for measuring displacement. Our group has applied methods from Geomatics engineering to improve surface registration of MR images, and have obtained results with an average normal distance (a measure of how well two superimposed or registered images fit together) of 0.201 mm (Cheng, et al., 2005). Employing imaging techniques to measure laxity would provide an improvement over knee arthrometer measurements because arthrometers require that the patella be well seated in the femoral groove, as the patella is used to obtain an indication of the position of the femur relative to the tibia. Conversely, imaging modalities allow a direct measurement of the femoral position rather than the patellar position. Additionally, the detailed geometry attained with imaging techniques allows for additional measures to be made. For example, the location of the tibiofemoral cartilage contact area can be found as an alternative measure of relative position.

Alternatively, the change in total length of the ACL resulting from an applied load can be quantified. MR Imaging has the additional benefit over other imaging modalities of being able to visualize soft tissues without requiring the subjects to be exposed to radiation.

Thus, the entire joint, including the soft tissue structures, can be imaged in a radiation-free, non-invasive fashion. The best image quality can be achieved with a closed bore MR imaging compared to open bore or dynamic MR imaging (Wacker, et al., 2005).

Closed bore MR imaging is also more widely available and is appropriate for the positioning typically used to measure knee joint laxity (eg: 30° knee flexion). However, closed bore MR imaging limits the range of motion that can be tested because of bore hole constraints, and requires the patient to lie supine.

2.7 Criteria for a Measure of Joint Laxity

A measure of laxity must be applicable to a wide range of pathological and physiological conditions, including normal (normal males and hormonally cycling females), ACLD, ACLR, and joint hypermobility syndrome. Experimental protocols and theoretical models must therefore be designed to account for these conditions, and appreciate their differences amongst various patient populations. Daniel and Stone (1990) identified six variables upon which a measure of laxity will depend: measurement system, initial joint position, motion constraints of the test system, applied force, muscle activity, and passive motion constraints. All of these variables must be controlled or accounted for if laxity is to be accurately and precisely measured. The measure of laxity should also be accessible, *in-vivo*, non-invasive, safe, accurate, and repeatable to be applied successfully to either a clinical or research population (Daniel and Stone, 1990).

2.7.1 Joint Position, Applied Force, and Motion Constraints

Laxity has typically been assessed statically with the subject lying supine and the knee flexed at angles between full extension and 90° of flexion (Malanga, et al., 2003).

Anterior translation is most commonly assessed at a flexion angle of 30°, since this angle is believed to represent the slack-taut transition for the ACL (Sheehan and Rebmann,

2003). A limitation of testing in a supine position is that physiological loads of the knee cannot be obtained. To overcome this limitation, a method was developed in which the subject can either apply a load (10%–15% of maximum) to a foot pedal or to resist a plantar force applied to the foot (Ronsky, 1994). This increases the patello-femoral contact area, confirming that external or resistive loading does affect knee contact mechanics (Gold, et al., 2004; Ronsky, 1994). The external force must be applied uniformly to the tibia to ensure that the displacement is solely in the anterior direction. Laxity measures appear to be sensitive to the location of a point load because of the resulting internal/external moment applied to the tibia (Rudy, et al., 2000). Forces are typically applied in the anterior–posterior direction, although some studies of laxity apply a torque to the tibia and measure torsional joint stiffness (Hsu, et al., 2006). The wide ranging methods used to measure laxity underscore the need for a systematic and universally accepted definition of joint laxity and a similarly accepted technique for applying the necessary loads. Before undertaking comprehensive studies of interventions aimed at influencing joint laxity, researchers and clinicians must adopt similar language and measuring tools to allow comparison between laboratories and across disciplines.

2.7.2 Muscle Activity

In measurements of laxity, methods are typically employed to minimize or exclude muscular contributions, such as quadriceps palpation to reduce muscle guarding during the anterior drawer test, and the administration of anaesthetics to induce muscle relaxation (Sernert, et al., 2001). Alternatively, muscle forces can be included in laxity measurements; however, they must be accurately quantified. Muscle force can be

measured directly, although these techniques are invasive, and typically reserved for animal models (Herzog and Leonard, 1996). To partially address this limitation, approaches that include noninvasive measures of muscular contributions, such as EMG have been introduced. Although EMG has been used to measure muscle force (Doorenbosch, et al., 2005), it is still a highly controversial method. Nigg (1999) notes that while there is a qualitative relation between muscle force and EMG signal, quantifying that relationship is affected by a number of variables. Firstly, electrodes must be mounted properly to achieve a clear signal. Secondly, an electromechanical delay exists between the onset of the EMG signal and the actual force production of the muscle. Although the delay can be quantified, it may be variable throughout the contraction due to the viscoelasticity in the muscle–tendon unit. Isometric quadriceps contraction as seen in laxity testing is the optimal case for relating EMG to muscle force because a one to one relationship exists (ie: a relatively constant signal related directly to a relatively constant force). Electromechanical delay will not change the result because there is no time dependence (ie: if the signal is delayed from onset, it doesn't interfere with describing a relationship between the force and the signal). However, deep muscle force cannot be measured from surface EMG, and thus the muscle force contribution assessed will be restricted to that of the superficial muscles. Therefore, using EMG to measure muscle force should be approached with caution. The strength of this method is in obtaining relative force contributions rather than absolute measures of muscle force. If EMG is used in a theoretical knee model, the model should be tested for sensitivity to muscle force.

EMG has a practical application for passive knee laxity tests as a confirmation that the subject is not contracting their lower limb muscles (muscle guarding). To the authors' knowledge, no studies have shown the EMG response of a subject tested with the KT-2000. A study by Feller, et al. (2000) used EMG feedback to encourage hamstring relaxation, and found that this did not significantly change the laxity measures for a subject. However, EMG values were not output to discern whether the subject was significantly contracting during the 'no feedback' trials. Studies have also shown that anterior laxity values are greater for subjects under anaesthetics than when conscious (Highgenboten, et al., 1992). The contribution of muscle guarding to passive knee joint laxity tests cannot be excluded, and should be assessed for any measure of knee joint laxity.

2.8 Theoretical Models

A theoretical model of joint laxity requires a set of measurable inputs, outputs, and known constraints regardless of the modeling method chosen. The inputs can include: the magnitude and direction of the applied force, knee flexion angle, detailed *in-vivo* knee geometry before and after load application, limb mass, and constraint of all degrees of freedom of the femur. Additional inputs that could be measured include: muscle force derived or based on EMG, and ground reaction force at the foot using a force transducer. The desired output of a theoretical model is a measure of joint laxity. Laxity can be viewed as the compliance of the joint, which is the reciprocal of joint stiffness. Therefore, an increase in joint compliance (laxity) will appear as a proportional decrease in joint stiffness. Stiffness is related to the quasi-passive structures of the knee joint,

which are intimately related to the joint function. Consequently, stiffness has been identified as a promising measure to study knee joint laxity (Maitland et al., 1995). If forces in the internal structures are plotted against their respective displacements, for given applied loading conditions, the stiffness of each structure can be determined as the slope of its force–displacement curve. Likewise, stiffness of the joint as a whole can be found from its total displacement under an applied load. Stiffness provides a measure well-suited to quantify the behavior of the joint and internal structures because it describes the resistance of a body to applied forces.

Extensive literature exists that describes theoretical knee modeling, and consequently only a portion of this literature most relevant to knee laxity was reviewed. Applicable knee models can be grouped into three main categories: contact, lumped parameter, and finite element models. The following discusses these categories of theoretical modeling, highlighting many of the advantages and limitations of each method.

2.8.1 Contact Models

Contact models use contact points or areas between cartilage layers or bone position to describe tibial translation with respect to the femur in the direction of applied force. A proximity algorithm is often used to determine the points of contact. This method is well-suited to a gross measure of laxity, since displacement of the whole joint can be quantified based on anatomical landmarks. However, the specific points of contact considered and how displacement of those points is quantified influence the findings and must be considered when interpreting the data.

DeFrate et al. (2004) measured tibial displacement as the perpendicular distance from a line, connecting the mid-points of the medial and lateral tibial plateaus to the contact point. The contact point was defined in two ways: the centroid of the area formed by the overlap of the tibial and femoral cartilage, and the shortest distance between the tibia and femur, perpendicular to the tibial plateau. Their results revealed a difference between the two contact point methods, highlighting the importance of using cartilage geometry rather than bony geometry in determining contact points (DeFrate et al., 2004).

Other landmarks have been used to define anterior–posterior motion in the sagittal plane. Logan et al. (2004a; 2004b) used the technique developed by Iwaki et al. (2000) in which the distance between the flexion facet center (the center of the posterior circular surfaces of the femoral condyles) and a line from the ipsilateral posterior tibial cortex is measured. Scarvell et al. (2004), calculated the distance between the center of the tibiofemoral contact area and the posterior tibial cortex. This choice was supported by the concept that these contact patterns describe motion that may affect articular cartilage degradation. Displacement in three dimensions was considered by Wretenberg et al. (2002) for contact areas on the medial and lateral condyles. They identified the most anterior, posterior, medial, and lateral contact point coordinates. These four points determined a contact area, from which the centroid points in all three planes were found. The benefit of considering a three dimensional measure is that it is speculated to provide more information about complex motion at the tibofemoral interface than a simple two dimensional measure.

In a contact model, the magnitude and direction of the applied forces, limb position, and opposing muscle forces are assumed to be consistent between tests and across subjects. However, in practice, while applied forces and positioning can be controlled by the tester, some variability is introduced by the muscle forces acting on the knee. Furthermore, the relative contribution of the involved muscles may differ between patient populations. For example, slight subjects may exhibit different muscular activation strategies than trained individuals with well developed musculature, such as athletes. This is particularly important since athletes comprise a large portion of the ACL-injured population for whom laxity measures may be most relevant. Therefore, it is critical to control muscle activation levels when applying contact models, to minimize variability and improve the accuracy of comparisons across and within subject populations. One manner in which variability can be reduced is to employ a muscle palpation method, such as that used in KT-2000 tests, to ensure that the subject is fully relaxed. As a result, the subject is maintained in a state of muscular relaxation, and the variability incurred by muscle activation will be minimized, or avoided entirely.

Theoretical models are driven by the clinical purpose or research questions being asked. To understand the link between laxity and dynamic function, contact models may be advantageous because they provide a measure of whole joint laxity. Laxity measured at the whole joint level may be more clinically relevant since, theoretically, two individual joints may have identical whole joint laxity regardless of differences in the dimensions or mechanical properties of the internal structures. Furthermore, a measure of joint laxity describes how the joint performs as a whole, in physiologic conditions. Since contact

models quantify relative joint position, they offer the theoretical model that most closely parallels current clinical laxity tests with potentially improved accuracy because displacement measurements are taken from accurate images of internal structures rather than external landmarks. Another benefit of contact models is that, in general, the model will not change among various subject populations. This is because the output measurements do not rely upon the material properties of the soft tissue, or the existence of specific structures other than the femur, tibia, and cartilage. For example, the model measurements do not depend on the existence of the ACL, and consequently, identical input and output variables are required when applying this model to a control population as for an ACLD population.

If the researcher or clinician desires to understand the underlying mechanisms of joint laxity, specifically within well-defined subject groups, a contact model will not be sufficient. Since the model does not include knowledge of the internal soft tissue structures, it is unable to evaluate their contributions to whole joint mechanics. The clinical importance of identifying how individual soft tissue structures affect the whole joint motion is an improved understanding of the underlying mechanisms of laxity. For example, comparing the stiffness of soft tissue structures in a normal knee to those in a knee with an MCL tear may aid in interpreting how and why the gross joint motion and functional ability of the patient differs from normal. Furthermore, if muscles are activated during a laxity test, these forces and their effects could be included to ensure consistency across tests. To account for these soft tissue effects, a specific lumped parameter model may be employed.

2.8.2 Lumped Parameter Models

Lumped parameter models use simple geometric shapes to characterize the arrangement of the underlying structures (e.g. muscles, tendons, and ligaments). The joint is modeled as a system of simplified geometries or mechanical constructs (e.g. two-force member) (Pandy and Shelburne, 1998; Shahar and Banks-Sills, 2004). The combined behavior of these elements produces a model that displays similar mechanical behavior to the joint. These models provide an appropriate model of joint laxity provided the goal is to determine a gross value of stiffness for each soft tissue element that is individually included. Tendons and ligaments are assumed to behave as two force members. Therefore, lumped parameter models typically assume that all tendon and ligament fibers are the same length, and shorten the same amount. Two dimensional geometrical arrangements are often assumed to simplify the model, although three dimensional models have been constructed (Shahar and Banks-Sills, 2004).

The underlying assumptions of a lumped parameter model have a direct impact on the resulting measure of laxity. The knee joint represents an indeterminate system where the number of unknown internal forces is greater than the available equations describing the system (Herzog and Binding, 1999) (Figure 2-6). The available equations include the four equations of static equilibrium (sum of forces and moments is zero), and the compatibility of deformations. These can be written for both the tibiofemoral and patellofemoral joints. The unknown internal forces include the forces in the ACL, PCL, LCL, MCL, patellar tendon, capsule, contacting cartilage, menisci, and muscle forces (either passive or active). The modeller must then make the indeterminate system

solvable. One solution method reduces the number of unknowns and/or increases the number of equations. The limitation of this approach is that relevant information about the contribution of a structure may be lost due to the simplification. Optimization is an alternative solution to the distribution problem that overcomes this issue. The system may be optimized to minimize a variable such as metabolic cost, total muscle force, or total muscle stress. These optimization techniques assume that the human body regulates forces in this manner, which is unlikely to be the true physiological mechanism. The clinical impact is that the model being used to treat and assess may be based on faulty assumptions. This could affect the accuracy of the outcome measures, and provide the clinician with incorrect values. Any or all of these methods may be employed to obtain a solvable model.

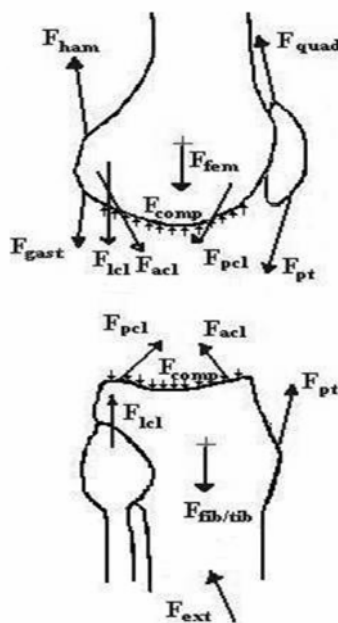


Figure 2-6: Exemplary free body diagram of the knee joint including external (ext) forces, forces due to compression (comp), muscle force [gastrocnemius (gast), hamstring (ham), quadriceps femoris (quad)], femoral mass (fem), tibial and fibular mass (tib/fib), and forces through the ACL, PCL, LCL, and PT

Lumped parameter models have been applied in a variety of ways to solve for the internal forces in the knee. Shahar and Banks-Sills (2004) included the femur, tibia, and patella, the hip joint reaction force, ground reaction force, muscle forces acting on the femur, and the collateral and cruciate ligaments of the knee in a three dimensional quasistatic model of the canine knee joint. They neglected hind limb weight, menisci, friction between joint surfaces, extensibility of the patellar ligament, and out of sagittal plane rotation of the patella. This model was applied to a simulated slow walk to observe ligament forces during stance phase in both an intact knee and a knee with a ruptured cranial cruciate ligament. This study provided an excellent illustration of how a lumped parameter model can be developed to solve for ligament forces during a task and altered to consider other scenarios such as the effect of removing a structure.

Some studies consider various methods for determining the lines of actions of the force bearing structures (Aalbersberg et al., 2005b; Lu and O'Connor, 1996) or the muscle moment arms (Arnold et al., 2000). These types of studies often address parameter accuracy, and model sensitivity to each parameter (Toutoungi et al., 1997). This is an important step in the modeling process. The model output accuracy is highly dependent on the accuracy and relative weighting of the input values. If an input value is physiologically variable, difficult to measure accurately, or can be measured in a variety of ways, it is crucial to test the sensitivity of the model to that input. Sensitivity is indicated by the amount of change in the output as a result of a change in the input. Each researcher must determine what level of sensitivity is acceptable given the specific application of the model.

Lumped parameter models allow ligament and tendon forces to be estimated *in-vivo*.

This class of model is quite flexible because it can be a simple model such as a four bar linkage, or sufficiently complex to include additional structures such as the joint capsule (Pandy and Shelburne, 1998). This flexibility could be quite valuable clinically, as the model is adjustable to include subjects who have an incomplete or missing structure. The complexity of the model is determined by its purpose. As no assumptions are made with respect to material properties, a lumped parameter model would theoretically be equally applicable to a model where the joint laxity is due to ACL loss compared to whole joint laxity associated with joint hypermobility syndrome. The ACLD model would simply require one less unknown ligament force, and thus one less two-force member in the model. A model of knee joint laxity may help to determine how the muscle forces and the passive forces of the major supporting structures contribute to the overall joint stiffness.

The lumped parameter model has the potential to add more information to the clinician's assessment of laxity. This is achieved by identifying the mechanical contributions of individual soft tissue structures. These could be used to assess the mechanism of abnormal joint laxity and thus help to identify the appropriate treatment. Furthermore, coping strategies may be better understood if muscle forces and stiffness are determined. Lumped parameter models may provide a balance between increasing the understanding of how the soft tissue structures affect subject specific knee laxity and providing a level of detail that is appropriate for clinical application.

Nevertheless, the lumped parameter model can be quite sensitive to the assumptions that are made. As more structures are included, more constraints and assumptions must be included to solve the system. Furthermore, not all structures can be simply represented as a two force member, such as the capsule or the cartilage. To gain insight into the mechanical behavior of individual structures based on *in-situ* knee geometry rather than assuming idealized geometrical shapes, a finite element model can be used.

2.8.3 Finite Element Models

The finite element (FE) method is a modeling technique (numerical method) that discretizes a continuum into simple shapes called finite elements. Engineering concepts, including but not limited to beam theory, dynamical theory, or heat transfer theory, and constraints are applied to the elements to solve for the mechanical behavior of the entire structure. The advantage of an FE model is that complex three-dimensional geometry may be considered. Additionally, the mechanical contributions of the individual structures can be included. Stress and displacement solutions can be found for the entire structure at each discrete point. This is a more detailed result than a lumped parameter model, and may potentially reveal localized weak points in the components that comprise the structure. Furthermore, the ability to apply static, dynamic, and thermal analyses to a complex geometry makes the FE method well suited to biomechanical problems.

FE models have been applied to solve the indeterminate system of the knee (Bendjaballah et al., 1998; Li et al., 2002; Moglo and Shirazi-Adl, 2003). That is, since the model accounts for the mechanical contributions of the soft tissue structures individually, it

allows tests (simulations) to be conducted in which tissue parameters are altered in a controlled manner. FE models can investigate the sensitivity of joint function to the mechanics of the supporting structures, providing a unique experimental avenue that cannot be carried out *in-vivo*. These models can be employed to study the contributions of the musculature and quasi-passive tissue structures to knee joint function, such as the effect of quadriceps force when the ACL is removed, or partially torn (Li et al., 2002), the effect of quasi-passive tissue structure removal (Bendjaballah et al., 1998; Moglo and Shirazi-Adl, 2003), or reduced ligament stiffness on joint function (Li et al., 2002).

Modeling at this structural level allows FE models to evaluate the contributions of individual soft tissue structures to overall joint mechanics, as well as the sensitivity of the joint's function (e.g. range of motion, laxity) to changes in the individual soft tissue structures. However, since joint behavior is determined by the combined mechanical contributions of the substructure, the accuracy of FE models is only as good as the geometric representations and the material properties used to describe the soft tissue structures. One such mechanical property is Young's Modulus, which quantifies a material's ability to resist forces independent of geometry. It is not suited to a gross measure of laxity because there is no clear way to describe cross sectional area or a reference length for the entire knee joint; necessary quantities in the measurement of stress and strain. Young's Modulus could be used to describe each of the internal structures of the knee, such as the ACL, PCL, MCL, and LCL. However, difficulties arise in quantifying stress and strain because they vary along the length and throughout the tissue cross section (Fleming and Beynon, 2004). The assumption of linear

elasticity may not be highly representative of ligament properties. These properties are often obtained experimentally with cadaveric tissue (Quapp and Weiss, 1998). This may be a source of error for models of joint hypermobility syndrome, for example, in which connective tissue mechanical behavior differs from that of normal subjects. Further, the manner in which it differs is not well understood. FE models must converge to a repeatable solution regardless of how many finite elements the model is divided into (referred to as mesh size). Thus, substantial time and computer memory is typically required to handle refined meshes in complex models that cannot take advantage of symmetry and other model simplifications. The FE model is only as relevant as the material properties and geometric representation of the included structures. More importantly, FE modeling has a complexity that may not be appropriate for the level of detail required from a model of laxity. However, further work must be done to identify the necessary modeling detail required to differentiate between groups across the spectrum of laxity.

2.8.4 Theoretical Modelling Summary

A theoretical model of knee joint laxity can be as broad as a gross measure of displacement under a translational force or as specific as the complex three dimensional displacement or stress distribution of each structure within the joint. The main concern with any theoretical model is to determine whether it will provide information that cannot otherwise be obtained. The benefit of a gross model of laxity is that the displacement measurement does not require knowledge of the mechanics of the internal joint structures. Since a gross model describes joint laxity with a single measure, it may be

easier to make comparisons between subjects. Additionally, a gross measure may be easier to correlate to other subject variables like dynamic function or stability because it characterizes the behavior of the joint as a whole. However, if the relative contribution of the soft tissue structures to overall joint laxity is desired, a different modeling technique must be employed. It could be valuable to further describe differences between subjects by quantifying the laxity of each internal structure and identifying how those individual structures contribute to the increased laxity of the entire knee joint. This information would require more in-depth modeling, such as lumped parameter or finite element approaches. The advantage of quantifying laxity at the ligament level is that it could lead to improved clinical techniques (therapy or surgery), or further understanding regarding the underlying mechanisms of joint laxity.

2.9 Summary

There is a decisive gap between engineering models and clinical measures of laxity. One reason for this gap may be the disparity between clinical and engineering goals. For example, the clinician may be interested in the effect of acquired knowledge on treatment protocol, while the engineer may focus on measurement techniques such as accurately calculating the strain in the ACL. This review highlights the need for collaboration and the development of models that are appropriate for the desired level of detail. Integration of the two may require such developments as increased accessibility to MR imaging; however the primary hurdle is to fully validate an appropriate model and measurement technique. The lack of a clinical ‘gold standard’ measure of joint laxity leaves an open avenue for clinicians and engineers to move forward. The challenge is to develop an

experimental and theoretical method that provides insight into the mechanics of the many structures of the knee, while maintaining safety, ease of use, and clear data interpretation that is necessary for clinical evaluation.

Joint laxity is usually measured as anterior tibial translation under a known applied load, giving a gross measure of joint laxity. Only a few studies have used gold standards, such as RSA, to validate the existing arthrometers that are often used to quantify joint laxity in a clinical setting. In the study by Jorn et al. (1998), arthrometers were found to overestimate anterior tibial translation, which was attributed to soft tissue deformation. Otherwise, validations have been based on relative performance between arthrometers, or on repeatability. In a clinical setting, arthrometers are often used exclusively as a diagnostic tool. This may help to explain why the definition of quantified joint laxity and its relation to stability remain unclear.

Models, by nature, are driven by the questions being asked. This reality tends to lead toward more specialized rather than generalized models. Models are available to consider the joint at varying levels of detail, including contact models for a gross measure of joint laxity, lumped parameter models for further information about the contributions of the tissue structures that comprise the joint, and FE models for more detailed analysis of stress and strain in those structures, often based on experimental data. The modeling techniques described in this article are currently used to address a wide variety of research questions. Focusing on these proven techniques when building theoretical models of joint laxity could help to bridge the gap to clinical assessment.

The benefit of incorporating an engineering model into a clinical laxity assessment is that it could improve the manner in which laxity is measured and interpreted. Currently, the primary clinical concern is to identify injured versus non injured knee joint structures, and to determine the change in laxity before and after treatment such as pre- and post-ACL reconstruction. However, there is also potential to develop a diagnostic tool that provides further detail and is patient specific anatomically. For example, an internal image of the knee could be combined with a knee laxity test and a resultant model with predictive capabilities such as stiffness of key ligaments or contact forces. This is the focus of the current study, which will address the development and evaluation of a novel device for measuring knee joint laxity. Measuring laxity at the ligament level will be explored for the first time.

The ligament laxity measures could be used to help to identify candidates for ligament reconstruction or other treatments, determine an optimal tensioning force for a replacement ACL, simulate surgical results, identify the root cause of the laxity, or develop and evaluate clinical interventions such as exercise programs. The development of theoretical models that accurately represent joint behavior, as well as its supporting structures, in combination with more precise and repeatable clinical assessment of joint laxity, should ultimately lead to an improved understanding of joint laxity and the factors associated with acute injury and genetic pathologies that affect joint stability.

Chapter Three: Loading Apparatus Design

To achieve the first specific aim of this thesis, a Knee Loading Apparatus (KLA) was designed to apply an anterior force to the knee joint. This section details the design criteria, conceptual device design, device pilot testing, and final device design with components and specifications.

3.1 Design Criteria

Daniel and Stone (1990) identified six variables upon which a measure of laxity depends: measurement system, initial joint position, motion constraints of the test system, applied force, muscle activity, and quasi-passive motion constraints. All of these variables must be controlled or accounted for if laxity is to be accurately and precisely measured. For successful application to either a clinical or research population, the measure of laxity should also be accessible, *in-vivo*, non-invasive, safe, accurate, and repeatable (Daniel and Stone, 1990). These standards form the basis for the design criteria of the proposed KLA.

The first set of design criteria (DC) are related to the MR compatibility of the KLA.

DC1: The KLA should be made of non ferro-magnetic material, so as not to induce electromagnetic fields, currents, or heat. This prevents injury to the subject, and interference with the MR images.

DC2: The KLA should fit within the MR scanner borehole dimensions (Figure 3-1).

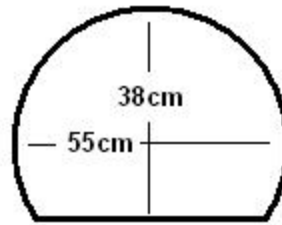


Figure 3-1: Borehole Dimensions

DC3: The force must be applied from the MR control room such that the tester can control the force applied to the subject's knee.

DC4: The subject must lie supine, as this is the orientation of the MR scanner.

The second set of design criteria are related to the mechanical function of the KLA.

DC5: Friction effects should be minimized to reduce the error in the force measurement.

DC6: The net force direction should be known and constant, to allow for consistency across tests.

DC7: The thigh motion must be constrained so that the desired knee angle, and direction of loading is maintained as the knee is anteriorly loaded.

Lastly, a number of criteria are related to size, practicality, and cost of the design.

DC8: The KLA should be size adjustable, and fit a range of subject sizes to allow for consistency of fit and loading across subjects.

DC9: The system should be easily transportable, lightweight, and compact.

DC10: The system should be easy to use. The set up should not be time consuming, and the software interfaces and force application should be user friendly.

DC11: The system should be safe and comfortable for the subjects.

DC12: The system should be inexpensive in relation to commercially available systems such as the KT-2000 (\$7700 USD), the Genucom (\$49000 USD), the Rolimeter (\$850 USD), or the Stryker Ligament Tester (\$900 USD) (Aircast, 2007; Highgenboten, et al., 1989; MEDmetric-Corporation, 2007).

The design criteria were subdivided qualitatively into three groups based on level of importance: Tier I (essential), Tier II (highly desirable), and Tier III (desirable) (Table 3-1).

Table 3-1: Importance Level for Design Criteria

Tier	Importance	Design Criteria Number
I	Essential	1, 2, 3, 4, 11
II	Highly Desirable	5, 6, 7, 8
III	Desirable	9, 10, 12

The final design must satisfy all items in Tier I, and the maximum number of items in Tiers II and III possible.

3.2 Final Design

The basic design of the KLA is shown in Figure 3-2. It is physically divided into components in the scanner room and in the control room. The entire system consists of a positioning apparatus [A], a hydraulic system [B], and a software interface [C].

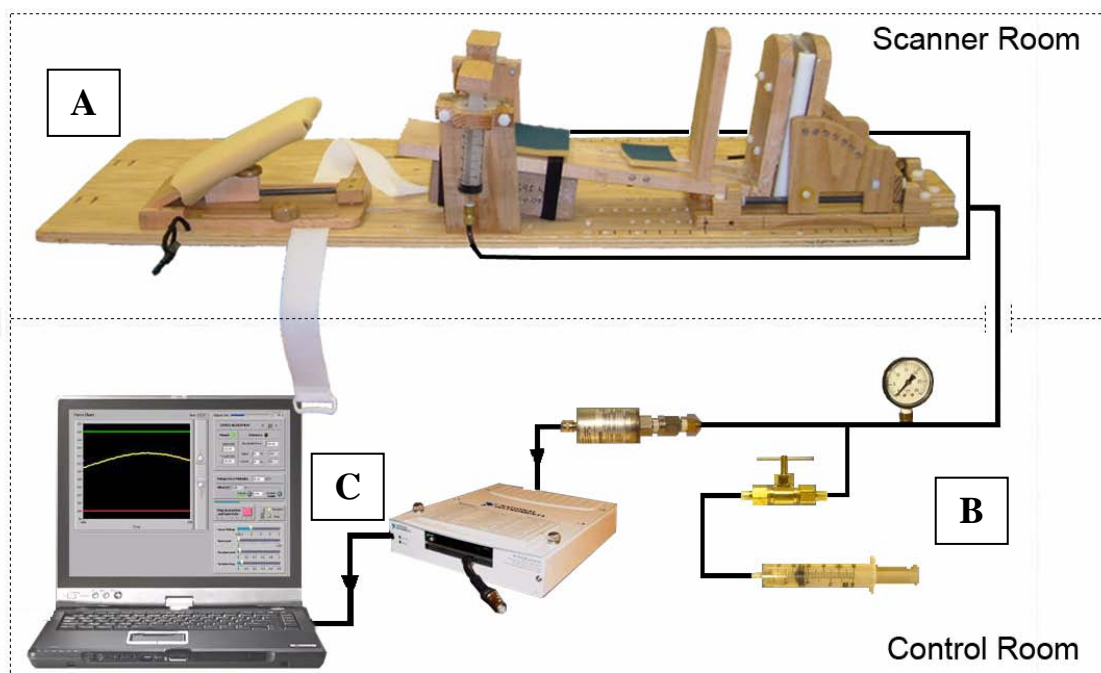


Figure 3-2: KLA System Components including a positioning apparatus [A], hydraulic system [B], and software interface [C]

3.2.1 Design Components

To achieve Specific Aim 1, a positioning apparatus was designed to constrain the applied force to an anterior direction and hold the joint and limbs in a consistent position (DC6, DC7). Subjects lie supine in the non-ferromagnetic knee flexion (DC1) device that was designed based on the criteria listed in Section 3.1.

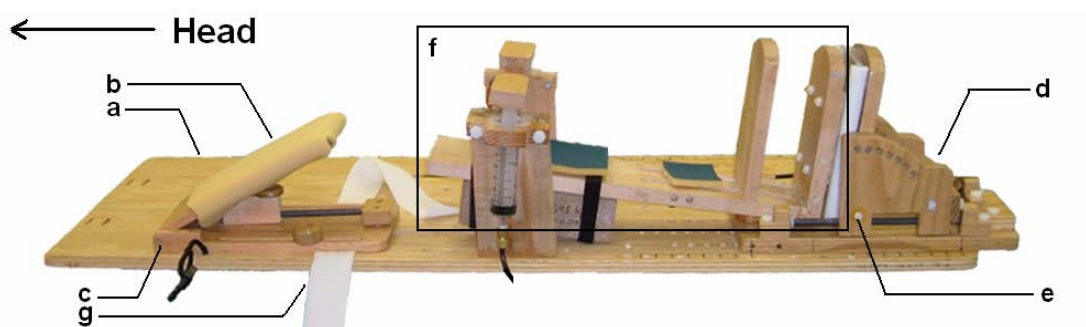


Figure 3-3: Labelled positioning apparatus: (a) base plate, (b) thigh support, (c) hinge, (d) foot plate, (e) hinge, (f) tibial platform

A portion of the positioning apparatus is an existing platform design used in our research group (DC2) (Robu, 2005). Components of the positioning apparatus (Figure 3-3) are mounted on the long base plate (a) with two main systems attached. The first is an adjustable thigh support (b) that rotates about a medial/lateral oriented hinge (c) to control knee angle (DC7). The second is a foot plate (d) that can slide in the superior/inferior direction, and rotate about a medial-lateral hinge (e) to control ankle angle.

The positioning apparatus of the KLA was made by adding a tibial platform (f) to the existing system. The tibial platform is rigidly mounted to the foot plate. The foot plate is secured such that it cannot slide in the superior/inferior direction, but can rotate freely about the medial/lateral axis at the inferior end (DC5). The tibial platform supports the tibia, and includes an adjustable foot support (DC8). The joint line of the subject is positioned just superior of the superior edge of the tibial platform. The adjustable foot support enables subjects of different tibial lengths to be tested. This feature allows the tibia to be loaded at a consistent location (DC7). The custom load cylinders were positioned to apply a load proximally with respect to the tibia (Figure 3-4). The most proximal edge of the tibial platform was positioned posterior to the tibial crest, several centimetres distal to the joint line. This is a similar technique to the KT-2000 protocol (Daniel, et al., 1985b).

The tibia is secured to the tibial platform, and the femur is secured to the thigh support with a custom attachment system. This system was comprised of velcro straps that were

tightened over semi-rigid plastic covers. This attachment system provides a distribution of the force from the straps over the anterior surface of the limb. The thigh strap is secured such that the patellar tendon is not tight (confirmed by palpation), and thus avoids loading the joint through tension in the patellar tendon. Both thigh and tibial straps were tightened to minimize motion while facilitating circulation and comfort (DC11). The thigh strap was located at the distal end of the thigh, closest to the knee joint.

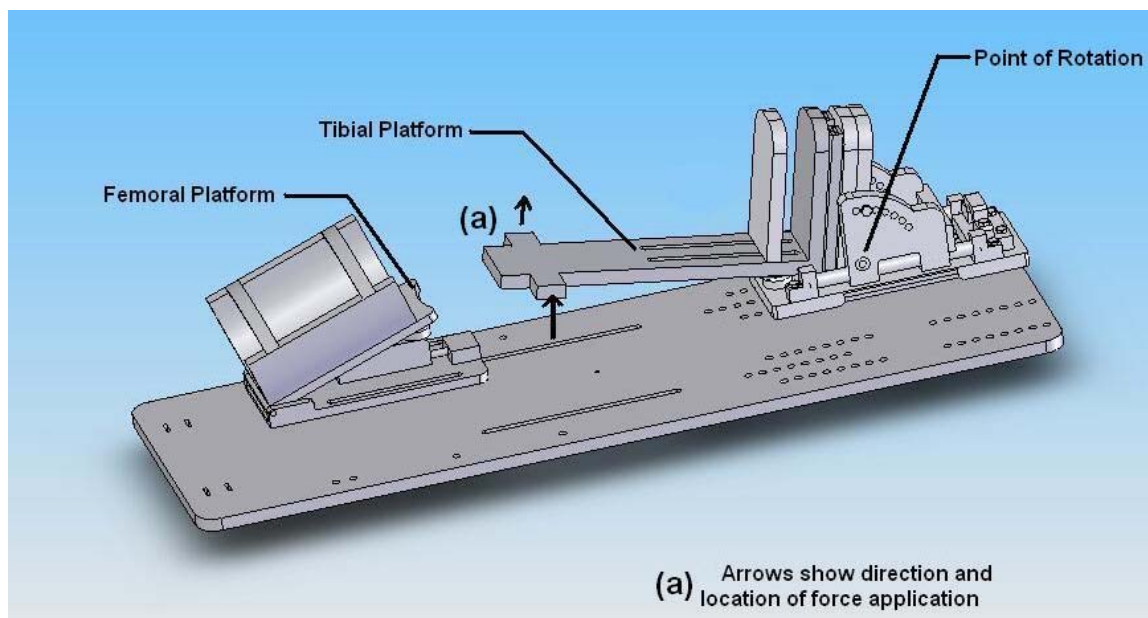


Figure 3-4: 3D Solidworks (Solidworks Corp., Concord, MA, USA) model of the positioning apparatus with force applied at the proximal end of the tibia (a)

The hydraulic system allows a force to be applied to the subject in the MR scanner from the control room (DC3). The piston of a custom load cylinder located in the control room is manually pushed, pressurizing the hydraulic line. This causes an extension of the load cylinder piston in the scanner room. The hydraulic portion of the design was developed

for applying compressive knee joint loads through the heel (Robu, 2005). For the specific loading configuration required for this application, the piston in the scanner room is secured to a support column that orients the piston perpendicular to the tibial platform. At a zero-pressure state, the tibial platform is at a 7° angle to the long base plate.

The system pressure is measured with a pressure transducer (PX 305, Omega Engineering Inc.) that links to a data acquisition box (DAQPad-6016, National Instruments Corp.). The pressure signal is converted into a voltage via the data acquisition box software. This voltage is output to a laptop computer with data acquisition Labview software (Labview 7.1, National Instruments Corp.) to interface with the user. By inputting a force-voltage relationship, the user can see a plot of the applied force over time (DC10).

3.2.2 System Cost

The total system cost was \$3950 (DC12). The itemized cost is detailed in Table 3-2. The cost does not include fees related to MR scanner use (\$550/hr).

Table 3-2: Cost Summary for KLA

Item	Cost (CAD)
Laptop	\$1500
National Instruments DAQ box	\$1200
Omega Pressure Transducer	\$350
Wood	\$100
Assembly Parts (screws, glue, valves, syringes, Velcro, etc)	\$800
TOTAL	\$3950

3.3 Design Rationale

The selections for joint position and loading were based on a review of literature, specifically related to soft tissue mechanical properties (Section 2.3). External loading is applied through the custom load cylinders (hydraulic system) in stepped loads to the tibia positioned at $30^\circ \pm 5^\circ$ of knee flexion. The anterior shear force at the knee is applied at 30 N, 40 N, 50 N, 100 N, and 180 N. Free Body Diagrams (FBD) of the loading apparatus and lower limb are used in combination with calibration weights to determine subject specific knee loads (Figure 3-7, Figure 3-9). This allows approximately equal force application between subjects.

3.3.1 Positioning

The subject is positioned supine and with a knee flexion angle of $30 \pm 5^\circ$. This angle was selected based on the notion that 30° is the slack-taught transition knee angle of the ACL (Fleming, et al., 1994). This is supported by a study by Zantop et al. (2007) that found maximum anterior tibial displacement at 30° compared to other knee angles. Placing the subject in this position causes the ACL to maximally engage in resisting the applied anterior loads in the linear region of the force-displacement curve. If the ACL is below the slack-taught transition, the anterior load will serve to take up slack or crimp in the ligament, but not test the ACL as the main supporting structure.

It was assumed that the motion of the tibial platform was in the anterior direction only. A calculation was done to assess the displacement error associated with the assumption that rotation about a far point (hinge) is roughly equivalent to a purely anterior displacement.

The maximum global tibial displacement observed during testing was 28 mm. This corresponds to a tibial platform rotation of 3.1° . The displacement error (arc length - measured distance) at this angle is 0.03 mm. Based on this small error value relative to the maximal displacement, the anterior assumption was determined to be valid.

3.3.2 External Applied Force

Externally applied anterior load values ($F_{ry} = 30 \text{ N}, 40 \text{ N}, 50 \text{ N}, 89 \text{ N}, \text{ and } 133 \text{ N}$) were chosen based on typical force displacement curves for the knee joint (Daniel and Stone, 1990; Maitland, et al., 1995). The primary objectives for selecting load values were to choose 1) load values that captured the general force-displacement plot, 2) fewer points at linear sections and more points where the slope was quickly changing, and 3) clinically relevant points (89 N, 133 N) such that the results could be compared to literature values (Daniel, et al., 1985a; Stratford, et al., 1991). Data from existing literature provided a best estimate of a force displacement curve. A modified plot from Maitland et al. (1995) shows the selection of points based on the primary objectives (Figure 3-5).

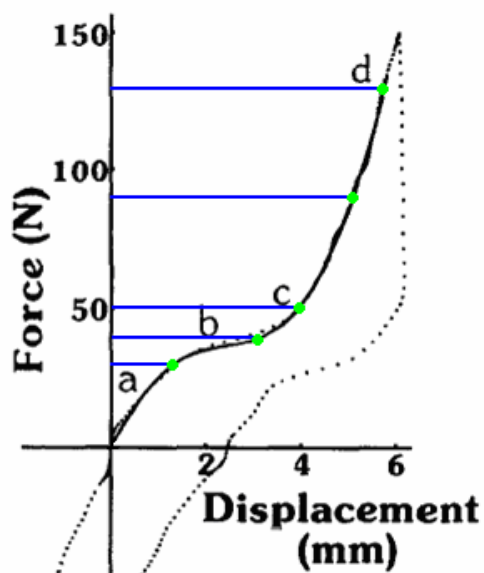


Figure 3-5: Figure 1 from Maitland et al. (1995) showing a representative force-displacement curve from an uninjured subject; modified to show the five load levels chosen to characterize the force-displacement curve. “The initial steep rise in curve is due to the weight of the leg (a). Middle region (b). The inflection point (c) is assumed to be due to the onset of the primary restraints to anterior displacement of the tibia, and by definition results in the x intercept of the second derivative. The cut –off point (d) was chosen at an anterior applied force of 134 N.”

The force-displacement curve (Figure 3-5) was described in three parts: 1) the initial rise as the weight of the leg is overcome, 2) the middle region as slack is taken up in the quasi-passive joint structures, and 3) the linear region where the onset of primary restraints to anterior displacement occurs (Maitland, et al., 1995). Typical force-displacement curves are constructed by applying instantaneous loading, and measuring the instantaneous displacement. MR imaging has the benefit of providing detailed joint geometry, but requires a finite time to obtain the joint image. Stepped loading, was required to apply MR imaging to capture the joint displacement while loaded. An exemplary plot shows the applied stepped loading during MR imaging (Figure 3-6). In the original study design, an anterior force of 0 N was planned to be tested. However,

inadvertently during actual testing, the image to correspond to the zero load (0 N) condition was obtained at the reference ‘neutral’ position. This typically resulted in an applied load of less than 0 N ($-51 \text{ N} \pm 7 \text{ N}$) for all subjects. The joint displacement at 0 N can be interpolated by fitting a 5th degree polynomial to the force-displacement curve (Maitland, et al., 1995).

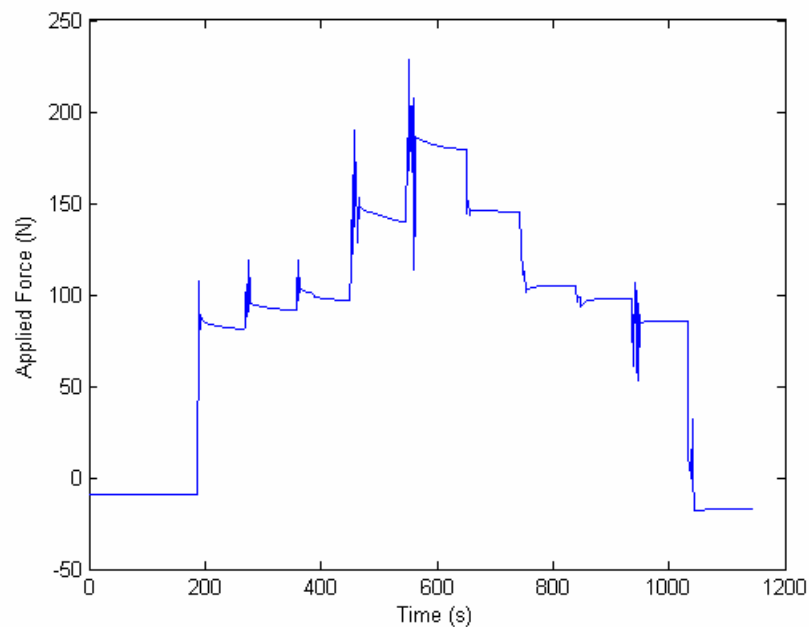


Figure 3-6: Applied Force during MR scanning for one subject

3.3.3 Free Body Diagrams

The KLA and hydraulic force system was calibrated with applied weights and a determinate force model system. The forces acting on the KLA during calibration can be divided into known and unknown quantities (Figure 3-7). The known forces were the calibration weight force (F_p), the counteractive mass (F_w), and the KLA mass (F_m). The unknown forces were the applied force from the hydraulic force system (F_a), and the

reaction forces at the hinge (F_f , F_n). The governing equations of static equilibrium resulted in the following system of equations:

$\rightarrow + \sum F_x$:

$$F_w \sin \theta + F_{p1/2} \sin \theta + F_m \sin \theta - F_n = 0 \quad (3.1)$$

$\uparrow + \sum F_y$:

$$F_a - F_{p1/2} \cos \theta - F_m \cos \theta - F_w \cos \theta - F_f = 0 \quad (3.2)$$

$\curvearrowright + \sum M_{aZ}$:

$$-F_a d_2 + F_w d_2 \cos \theta + F_{p1/2} d_{3/4} \cos \theta + F_m d_5 \cos \theta = 0 \quad (3.3)$$

where $F_w = 25.0 \text{ N}$

$F_{p1/2} = F_{p1}$ (at distance d_3) or F_{p2} (at distance d_4)

$F_m = 18.1 \text{ N}$

$d_1 = 55 \text{ cm}$

$d_2 = 45 \text{ cm}$

$d_{3/4} = d_3$ or d_4 (corresponding to F_{p1} or F_{p2})

$d_3 = 36 \text{ cm}$

$d_4 = 28 \text{ cm}$

$d_5 = 21 \text{ cm}$

$\theta = 7^\circ$

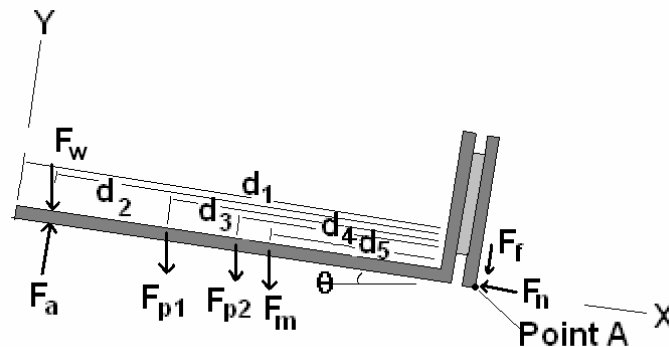


Figure 3-7: Free Body Diagram of the determinate force system for the KLA calibration. Forces include the applied force from the hydraulic force system (F_a), calibration weight force (F_p), the counteractive mass (F_w), the KLA mass (F_m), and the reaction forces at the hinge (F_f , F_n).

The system was calibrated by solving for F_a at a range of calibration weights [$F_{p1/2}=9.81 \text{ m/s}^2*(3, 4, 5, 10.25, 18.5 \text{ kg})$] and at 2 distances (d_3, d_4). For each calibration weight, average F_a was plotted against average output voltage at each load to determine the calibration parameters for the force-voltage relationship (Figure 3-8).

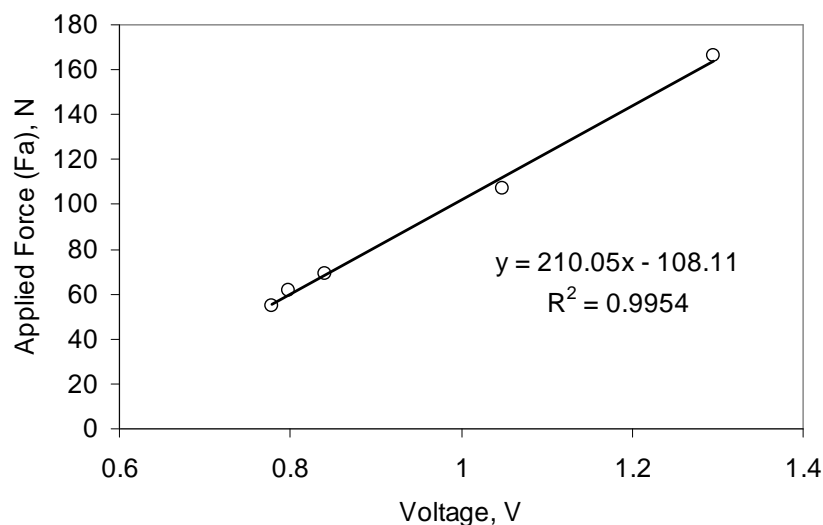


Figure 3-8: Force-Voltage relationship from calibration of KLA

The force-voltage relationship was applied to the test set-up. From the voltage at any given hydraulic pressure, the applied force F_a was output. To resolve the forces acting on the knee joint, an indeterminate force system was solved. An indeterminate system has more forces than equations that describe the system, and is a common biomechanics problem when studying the knee joint (Herzog and Binding, 1999). In this system, it was not the individual structures of the knee but rather the KLA in combination with net knee joint reaction forces that resulted in an indeterminate problem. The known forces were the desired anterior reaction force at the knee (F_{ry}), the lower limb weight (F_l), the counteractive mass (F_w), and the KLA mass (F_m). The counteractive mass served the

function of bringing the system back to equilibrium more quickly when the pressure in the hydraulic system was released. The lower limb mass (M_s) and center of mass location (COM) were calculated for each subject (Table 3-3) with classic anthropometric data (Winter, 1990), governed by the following equations:

$$M_s = 0.061M \quad (3.4)$$

$$COM = 0.394L \quad (3.5)$$

Where M = body mass

L = distance from femoral condyles to the medial malleolus.

Table 3-3: Subject Specific Anthropometric values

Subject	Lower Limb Mass (F_t) (kg)	COM to Pt A (d_g) (cm)
S01	3.29	29.85
S02	3.87	25.61
S03	3.67	26.22
S04	5.67	25.31
S05	3.97	23.79

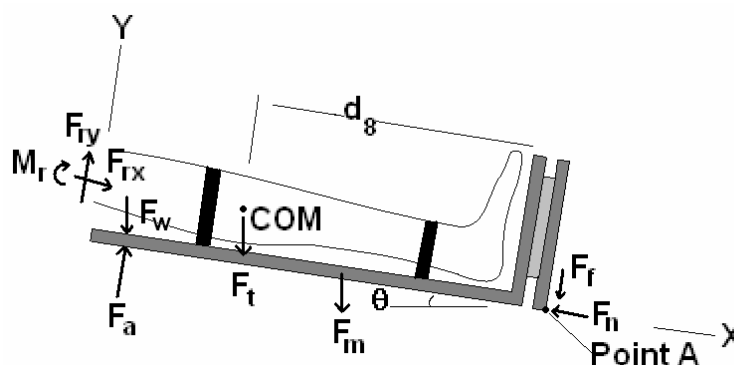


Figure 3-9: Free Body Diagram of the indeterminate force system for the KLA during testing. Forces include the applied force from the hydraulic force system (F_a), the reaction forces and moments at the knee (F_{ry} , F_{rx} , M_r), the counteractive mass (F_w), the KLA mass (F_m), and the reaction forces at the hinge (F_f , F_n).

The unknown forces were the required applied force (F_a), the moment and axial reaction forces acting at the knee joint (M_r , F_{rx}), and the two reaction forces at the hinge (F_f , F_n). To add two additional constraint equations, two main assumptions were made. First, that the axial force F_{rx} could be neglected since the primary direction and largest magnitude of force application was in the anterior (y) direction. In an FE model by Moglo and Shirazi-Adl (2003), a normal tibiofemoral joint was loaded at 100 N of posterior force to the femur. The contact forces (approximately axial) were ~ 75 N at 30° of flexion, summing the medial and lateral sides. The ACL force (approximately anterior) was ~ 160 N, resulting in an approximate axial to anterior load ratio of 1:2. This supports the assumption that the primary direction and largest magnitude of force is in the anterior direction. However, contact forces could be accounted for in future design iterations, as they are within an order of magnitude of the anterior forces, and may have a marked effect on a lumped parameter or FE model. Second, the ratio of F_n/F_f was assumed to be 0.37. The F_n/F_f ratio value was obtained from the calibration (0.37 ± 0.03), based on the average calculated ratio of F_n/F_f at a distance of d_4 . In the calibration, both F_n and F_f were known values and therefore the ratio could be directly calculated. The governing equations of static equilibrium were used to calculate the target applied force (F_a) required to reach the desired anterior knee force (F_{ry}):

$\rightarrow + \sum F_x:$

$$F_{rx} + F_w \sin \theta + F_t \sin \theta + F_m \sin \theta - F_n = 0 \quad (3.6)$$

$\uparrow + \sum F_y:$

$$F_{ry} + F_a - F_w \cos \theta - F_t \cos \theta - F_m \cos \theta - F_f = 0 \quad (3.7)$$

$$\curvearrowright^+ \sum M_a z$$

$$-M_r - F_{ry}d_1 + F_w d_2 \cos \theta - F_a d_2 + F_t d_8 \cos \theta + F_m d_5 \cos \theta = 0 \quad (3.8)$$

The added constraint equations are defined by:

$$F_n = 0.37F_f \quad (3.9)$$

$$F_{rx} = 0 \quad (3.10)$$

A sensitivity study investigated the effect of the F_n/F_f ratio on the calculated applied force F_a . For an increase of the F_n/F_f ratio of 0.1, the calculated force F_a increased linearly by 9 N. An increase of the F_n/F_f ratio by 0.1 corresponded to a shift in the location of the COM by approximately 10 cm (based on calibration values). After testing, it was found that the difference between d_4 and the subject specific COM locations was 1.5 ± 2.3 cm. The F_n/F_f ratio assumption may have introduced an average overestimation in the target applied force values of approximately 1 to 4 N. The anterior reaction force at the knee (F_w) applied during each scan was determined using a back-calculation (Eqn. 3.7) with the actual applied force F_a input.

3.4 Design Evaluation

The design components met the overall design criteria extremely well (Table 3-4). As specified, all five Tier I criteria were achieved. Of the remaining criteria, three were met and four were partially satisfied.

Table 3-4: Design Components relating to Design Criteria

DC	Description	Tier	DC Met	Design Component
1	Non ferromagnetic	I	√	+ Use of plastic, wood, and brass
2	Fit within borehole dimensions	I	√	+ KLA < borehole
3	Force operated in control room	I	√	+ Hydraulic System
4	Subject lies supine	I	√	+ Orientation of positioning apparatus
5	Reduced Friction in KLA	II	~	+ Hinged loading device - Friction in load cylinder (hydraulics)
6	Known force direction	II	√	+ Positioning apparatus
7	Thigh motion constrained	II	√	+ Thigh constraint
8	Size adjustable, fits range of subjects	II	~	+ adjustable foot plate (tibial length) + adjustable positioning apparatus (knee angles) - width of tibial platform suitable for average or underweight subjects only
9	Transportable, lightweight, compact	III	~	+ positioning apparatus can be disassembled to portable pieces + hydraulic system and software interface are transportable, lightweight, and compact - multiple pieces make it difficult for one tester to transport KLA without a cart or additional assistance
10	Easy to use	III	√	+ Computer interface + Straightforward setup
11	Safe and comfortable system	I	√	+ Loads applied are equal to clinical values + MR imaging does not expose the subject to harmful radiation + Use of non ferromagnetic materials prevents risk of injury due to heating or impact of objects + Subjects informally reported no pain or discomfort related to the KLA
12	Inexpensive	III	~	Total Cost: \$3950 < KT-2000 < Genucom > Stryker Ligament Tester > Rolimeter

√ Design Criteria met

X Design Criteria not met

~ Design Criteria partially met

+ Advantage

- Disadvantage

3.4.1 Pilot Study

A pilot study was done prior to full experimental implementation and subject testing to assess whether the device was operating as expected. At the time of the pilot study, a sliding mechanism rather than the hinge was in place at the distal end of the tibia. Otherwise, the test methods were equivalent. The subject was imaged at the neutral position and at 70 N of applied load. A contact model, described in detail in Connelly et al, (2006), enabled the contact areas of the femoral cartilage on the tibial cartilage to be tracked at each load level (Figure 3-10). The relative benefits of a modelling approaches including contact modelling are detailed in Section 2.8. In the contact model, the cartilage surfaces are modeled with thin plate splines (Section 4.4.3), and a proximity algorithm is applied to determine which portions of the cartilage surfaces are considered to be in contact (within a threshold value). The centroids of the contact areas can be found by integrating over the surface. In this pilot study the contact area centroids, mapped on the tibial plateau, moved posteriorly by 2.5 mm and 2.8 mm on the medial and lateral side, respectively. This was an indication that the KLA was effectively applying a load such that the tibia was moving in an anterior direction relative to the femur. As a result of this pilot testing, the sliding mechanism was removed because it did not allow higher loads to be reached, and did not achieve a low friction interface due to locking. A hinge mechanism was introduced in place of the slider. Further pilot tests showed the hinge system to reach higher loads and allow for smooth platform translation.

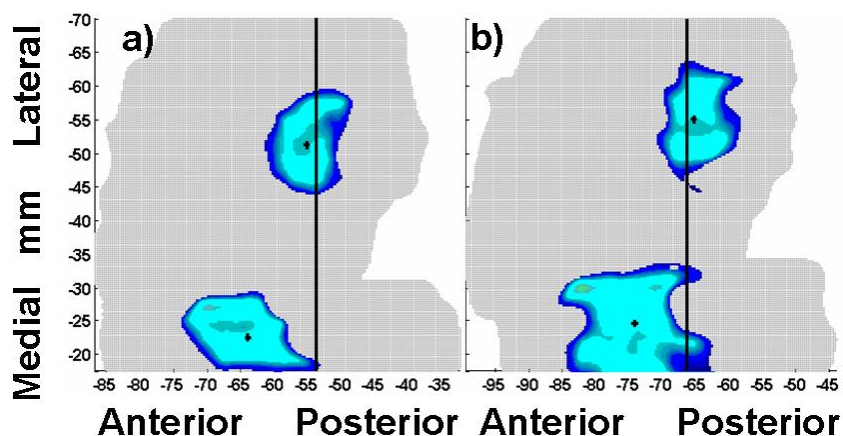


Figure 3-10: Axial view of femoral contact area on tibia at a) the neutral position and b) 70 N applied load

3.5 Summary

The KLA presented in Chapter Three is the first iteration of a novel device for measuring knee joint laxity. It is an MR compatible device that is designed to apply an anterior load to the tibia. Other tools to measure joint laxity (specifically joint displacement under an anterior force) have been designed previously (Daniel, et al., 1985a; Highgenboten, et al., 1989; Muellner, et al., 2001; Un, et al., 2001). Many suffer from poor inter-tester repeatability, and lack the detail required to investigate individual joint structures. To the author's knowledge, the novel combination of controlled, quantified loading, positioning with a device like the KLA, and images of internal joint structures has never been applied to measure joint laxity.

Existing systems from our research group were integrated into this design, including a hydraulic force application system, and a thigh support and foot plate mounted on a base plate. A novel tibial platform was designed and built to allow for repeatable subject positioning and consistent force application (direction and magnitude). The design successfully met all 12 design criteria either fully or partially.

One of the primary design criteria for the KLA specifies that the device be safe. Choices for safe load values are based on well documented anterior load levels used clinically and in research. Use of non-ferromagnetic materials ensured subject safety with respect to MR imaging. A pilot study indicates that the KLA is achieving the design goal of applying an anterior load that results in an anterior tibial displacement. Based on the success of the KLA in pilot testing and in meeting the primary design criteria, it was determined that the KLA was ready to be tested in a pilot population of normal subjects (n=5, Chapter Four). The application of the KLA design to a pilot subject population is the topic of Chapters Four, Five, and Six, where the methods, results, and discussion of the design evaluation are detailed.

Chapter Four: Methods

A combination of both novel and previously developed methods and technical approaches were used in this study with the ultimate goal of quantifying gross knee joint laxity (Figure 4-1). The KLA described in Chapter Three provided the positioning device and applied force to control force direction and magnitude applied to the knee joint. MR images were obtained in a 3.0 Tesla scanner to quantify the joint and ACL force-displacement curves. In addition, EMG was used prior to the MR testing to confirm that the subjects were not ‘muscle guarding’ (resisting the applied load by contracting their lower limb muscles) when the external load was applied and held. KT-2000 data was collected for comparison of the novel method with current clinical measures.

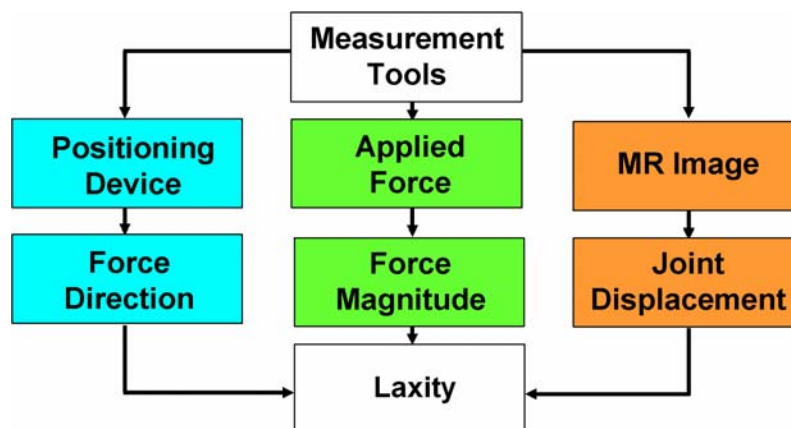


Figure 4-1: Flowchart for Methods to obtain a measure of laxity with the KLA

4.1 Study Participants

Five healthy female subjects with no history of lower limb pathology [aged 24 ± 1 years, height 167 ± 9 cm, weight 67 ± 15 kg, body mass index (BMI) 24 ± 5 kg/m²] were recruited for this study. The sample size is small for this study as it is exploratory and primarily intended to evaluate the KLA and allow for design improvements before conducting a larger study. A questionnaire (Appendix B) was given to all subjects to ensure that they met the study criteria. The subject was required to:

- Be female, aged 19 to 35
- Weigh less than 300 lbs and be no taller than 5'10" (to fit in the MR scanner)
- Have a BMI between 18.5 and 31
- Have no previous injury or surgeries to the knee
- Have no reported history of lower limb pathology or injury/pain in either knee for which treatment was sought or which interfered with function for more than one week within the last 12 months
- Not be pregnant currently or previously
- Not be claustrophobic
- Not have a serious medical condition (i.e. cancer)
- Not have inflammatory or post-infection arthritis of the knee
- Not be unable to speak or read English, or have any condition that limits informed consent
- Not have metallic implants or tattoos with magnetic properties
- Not have a history of welding or contact with metallic dust
- Be currently taking OC pills that allows a tracking of a 28 day menstrual cycle

Normal subjects were recruited via recruitment posters located on the University of Calgary campus. The University of Calgary Conjoint Health Research Ethics Committee approved all aspects of the experimental protocol, and all subjects gave their informed consent prior to testing. The ethics submission, approval letters, and the consent form are detailed in Appendix B.

4.2 General Protocol

The dominant limb of each subject was tested (n=5, right limb). A subset of subjects were tested for repeatability (n=3) of the KLA and KT-2000. The main input variable was the applied external anterior force. The main outcome variables were joint displacements, and rotations. A secondary outcome variable was the time constants related to stress relaxation. Several variables that may potentially affect joint laxity were controlled and documented, including hormonal effects and body water content.

4.2.1 Hormonal Effects

To control for possible hormonal effects, subjects were tested once each month for three months at the same time point within their menstrual cycle. All subjects were on four week cycles due to use of oral contraceptives. Table 4-1 below shows the test dates, corresponding cycle date, and type of oral contraceptive used. It is noted that subject S03 missed week 3 of pills between test days 1 and 2, however this was considered to introduce minor variability. Also of note is the KT-2000 test dates for subjects S01 and S04, which were delayed by 1 month as the KT-2000 malfunctioned on the test date 05-03-07. A replacement KT-2000 was used for the remainder of the tests.

Table 4-1: Menstrual Cycle and Test Dates

Subject	Brand of Oral Contraceptive	Dose	Menstrual Cycle Day*		
			MR test	KT test	EMG test
S01	Yasmin (28)	3 mg Drospirenone 0.03 mg Ethinyl Estradiol Oral Tablet	07-25,17	07-24,16	07-23,15
S02	Alesse (21)	100 µg Levonorgestrel 20 µg Ethinyl Estradiol Oral Tablet	04-05,19 05-04,19 06-01,19	03-08,18 04-04,18 05-31,18	04-04,18
S03	Alesse (28)	100 µg Levonorgestrel 20 µg Ethinyl Estradiol Oral Tablet	04-20,13 06-08,13 07-06,13	04-19,12 06-07,12 07-05,12	04-19,12
S04	Diane 35 (21)	35 µg Ethinyl Estradiol 2 mg Cyproterone Acetate	05-04,17	07-26,16	05-03,16
S05	Orthotricyclene (28)	Norgestimate, Ethinyl Estradiol 1-7 (0.18 mg, 0.035 mg) 2-14 (0.215 mg, 0.035 mg) 15-21 (0.25 mg, 0.035 mg)	05-28,8 06-25,8 07-24,9	05-29,9 06-26,9 07-25,10	05-25,5

* Test Date (month-day of 2007) followed by menstrual cycle day

4.2.2 Total Body Water

Estradiol is thought to be the hormone affecting body water content (Section 2.5.1). All subjects were taking oral contraceptives with a constant dosage (within brand) of ethinyl estradiol, the synthetic derivative of estradiol (Table 4-1). Total body water (TBW) calculations were based on age (years), sex (M=1, F=0), height (cm), presence of diabetes (Yes=1, No=0), and weight (kg) using four different techniques: Watson (Watson, et al., 1980), Hume-Weyer (Hume and Weyers, 1971), Chertow (Chertow, et al., 1997), and physiologic (Himmelfarb, et al., 2002). Four techniques were employed because, as there is no strong indication in the literature of the most definitive measure, agreement among methods would provide increased confidence that the TBW was controlled. These techniques are governed by the following equations:

Watson for Females:

$$TBW = -2.097 + 0.1069 * height + 0.2466 * weight \quad (4.1)$$

Hume-Weyer for Females:

$$TBW = 0.34454 * height + 0.183809 * weight - 35.270121 \quad (4.2)$$

Chertow:

$$\begin{aligned} TBW = & -0.07493713 * age - 1.01767992 * male + 0.12703384 * height \quad (4.3) \\ & - 0.04012056 * weight + 0.57894981 * diabetes - 0.00067247 * weight^2 \\ & - 0.03486146 * age * male + 0.11262857 * male * weight \\ & + 0.00104135 * age * weight + 0.00186104 * height * weight \end{aligned}$$

Physiologic for Females:

$$TBW = weight * 0.55 \quad (4.4)$$

Total body water was monitored for each test day using the above calculations. Efforts were made to schedule subjects at consistent times of day (early afternoon) to reduce effects of daytime-dependent influences and fluctuations.

4.3 MR Imaging

MR images of the knee joint were obtained using a 3 Tesla MR scanner (VH/I, General Electric Healthcare, General Electric Company, Fairfield, CT, USA) located at the Seaman's Family MR Research Centre at the Foothills Hospital in Calgary, Alberta, Canada. Trained MR technicians acquired all images. All parameters were developed to best image tendon and cartilage by experienced MR physicists and physicians, including Dr. Richard Frayne, Dr. Mohammad Sabati, and Dr. Houman Mahallati, with the aid of mechanical engineer Ion Robu. The primary criterion for the image sequences were to 1) provide sufficient contrast between bone, cartilage, tendon, and synovial fluid to delineate the individual structures, 2) minimize scan time length, and 3) allow a field of

view (FOV) sufficiently large to capture the tibia and femur from articulating surface to a portion of the bone shaft (Connolly, 2006).

The knee joint geometry was obtained at a knee angle of 30° (Frey, et al., 2006; Sakane, et al., 1999) at anterior load levels of 0, 30, 40, 50, 89, and 133 N. The load was applied with the KLA loading apparatus (Chapter Three). The subject's tibia and foot were placed on the tibial platform, with the footplate adjusted for tibial length such that the end of the tibial platform was just distal to the knee joint line. The thigh platform angle was adjusted as required to obtain 30° of knee flexion. This knee angle was confirmed prior to load application with a goniometer (Figure 4-2), a device that has an absolute mean error of measurement of $4 \pm 2^\circ$ (Jagodzinski, et al., 2000).

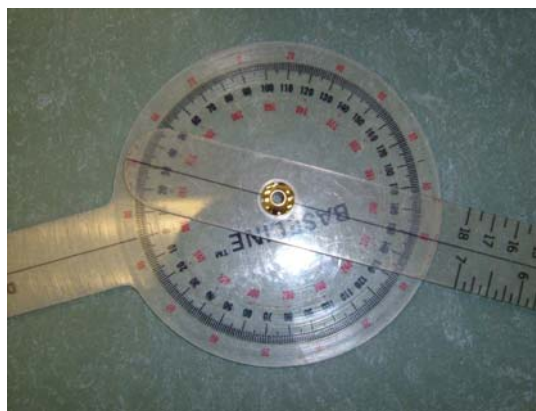


Figure 4-2: Goniometer

A protective shin pad was placed over the anterior shank to distribute the force from the distal strap. The proximal strap was secured just distal of the joint line, located approximately in line with the edge of the tibial platform. The thigh strap was tightened, with palpation of the patellar tendon to ensure that quadriceps muscles were relaxed, and

that the thigh restraint was not causing tightening of the patellar tendon. A general purpose flex coil (General Electric Medical Systems Corporation, Milwaukee WI, US) was fit around the knee joint loosely so as not to interfere with knee motion or the KLA. The purpose of this added local flex coil was to improve image signal to noise ratio and quality by intensifying the field and brightening the image around the knee joint.



(a) (b)
Figure 4-3: MR Imaging test setup (a) prior to and (b) after adding the flex coil

A non-ferromagnetic hydraulic system (Chapter Three) was used to apply the force at the proximal end of the tibia. The tester was able to modulate forces from the control room to the Scanner room via the hydraulic system. No active participation was required of the subject, they were required to lie still and relax.

A localizing scan was used to locate the image space. A fat-saturated steady-state free-precession imaging sequence was used to obtain high resolution sagittal and axial plane

images of the knee joint. The fat-saturation method is a fat-suppression technique that allows for better contrast between water and lipids (Hargreaves, et al., 2003). Collection of 3D image data allowed for image slices in any desired plane. The knee was in the reference position (hydraulic system not pressurized) at a resolution of 0.234 mm x 0.234 mm x 1.0 mm [FOV 14 cm x 14 cm, 512 x 512 matrix]. Low resolution sagittal images of the knee joint were obtained during loading, at a resolution of 0.547 mm x 0.547 mm x 3.0 mm (FOV 14 cm x 14 cm, 256 x 256 matrix) using a balanced steady-state free precession sequence. Steady-state free precession imaging is a rapid and efficient imaging method that provides good tissue contrast. The high resolution images provide more detailed joint geometry at the expense of longer scan times (2 minutes and 38 seconds). During joint loading, to reduce the effect stress relaxation over longer loading times, low resolution images were used to minimize scan time (1 minute and 3 seconds) at the cost of image quality. Registration techniques developed in Geomatics Engineering (Habib, et al., 2001) allowed the lower resolution images to be spatially matched to the higher resolutions images. The high resolution images were used to define accurate coordinate systems from bony landmarks that were then applied to the lower resolution images via the registration technique.

4.4 Image Registration

Image registration begins with digitization of both high and low resolution images to capture the 3D joint geometry. The high resolution geometry is used to define local coordinate systems for the femur and the tibia. Insertion points (location where the ligament inserts into the bone) of the ACL are captured in the high resolution axial

images. Reconstructed surfaces of the femur and tibia allow registration of high resolution scans to low resolution scans at each load level. This approach enabled the 3D joint motion of the femur with respect to the tibia under loading to be calculated, specifically anterior displacement of the tibia (Figure 4-4).

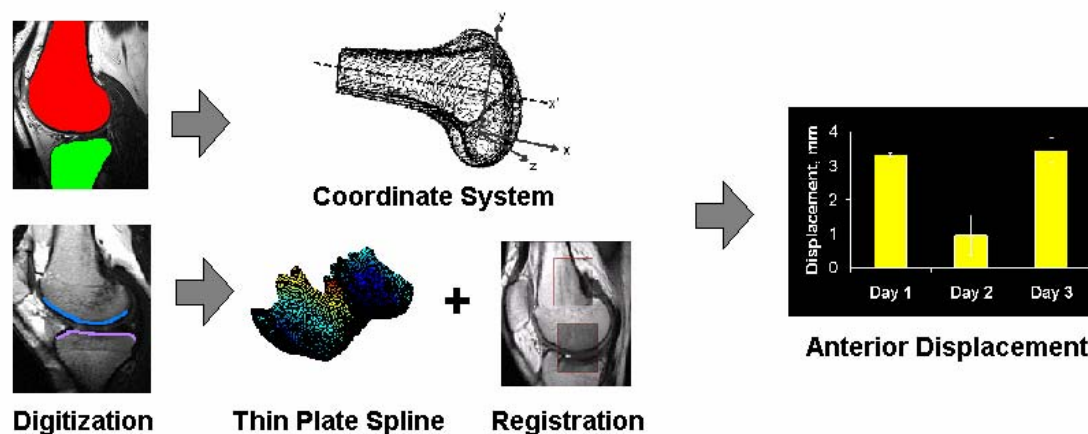
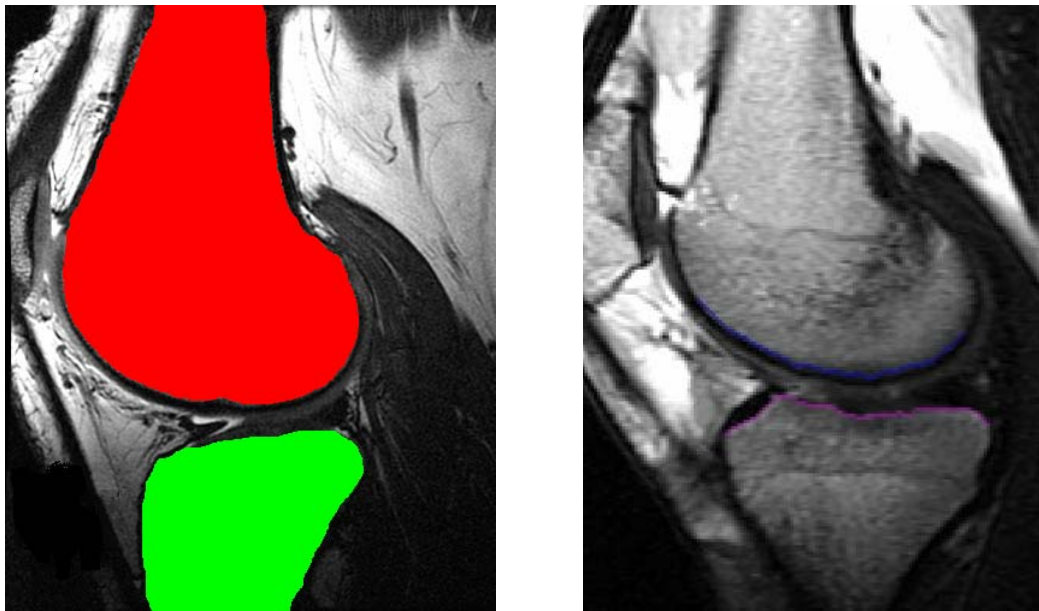


Figure 4-4: Flow Chart depicting the image data analysis process through digitization to obtain local joint coordinate systems (Fjeld, 2007), thin plate spline mappings of joint surfaces, registration to match surfaces (Cheng, 2006), combined to find anterior joint displacement

4.4.1 Image Digitization

MR images were digitized using SliceOmatic 4.2 software (Tomovision, Montreal, CA, USA). The digitization technique was manual, as a previous study within the research group found the available semi-automated edge detection algorithm (Baker, 2002; Moss, 2001) to have large errors, increased time due to error correction, and a less user-friendly interface (Connolly, 2006).

For coordinate system definition, the areas of femur and tibia of each sagittal HR image slice were digitized, using the trabecular/cortical bone interface as the perimeter due to the consistent high contrast between these two layers (Figure 4-5a). The resulting cloud of data points generated a 3D volume of both the femur and the tibia in the image coordinate system (ICS).



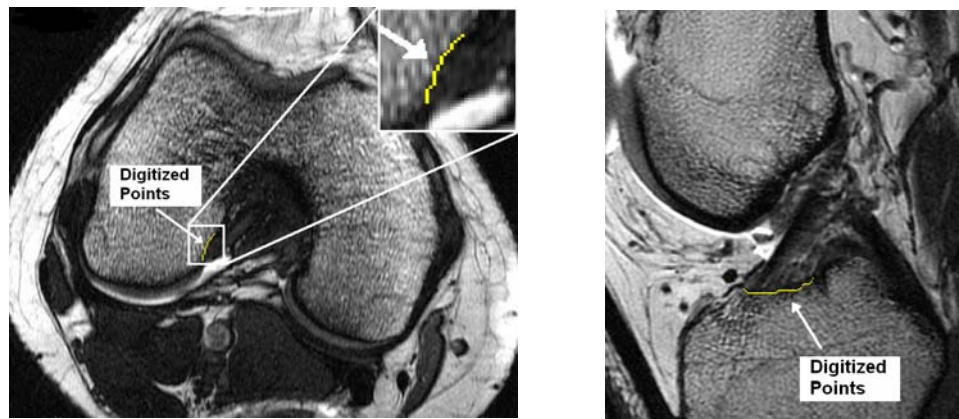
(a)

(b)

Figure 4-5: Image Digitization for (a) LCS and (b) Joint Image Registration

For joint image registration, the surface of the femur and tibia along the condylar contours at the trabecular/cortical bone interface were digitized in high and low resolution sagittal images (Figure 4-5b). Due to the nature of the surface reconstruction algorithm, two digitized points could not be adjacent along the secondary axis (superior/inferior). This digitization process generated a 3D surface cloud of points in the ICS.

For ACL insertion point determination, the edges of the interface of the ACL with bone were digitized in the high resolution image that was perpendicular to the interface. Thus, the femoral insertion was digitized on axial images and the tibial insertion was digitized on sagittal images (Figure 4-6). The joint surfaces at the femoral groove were digitized in both the sagittal and axial views to allow registration from the axial to the sagittal image plane ICS. This process accounts for possible motion of the subject between scans, and is used to transform the femoral ACL insertion point location from the axial to sagittal image plan ICS. All digitized points were output as *.pts files for use in further data processing.



(a) (b)
Figure 4-6: Digitization of ACL insertion point on (a) femur and (b) tibia

4.4.2 Coordinate System Definition

The digitized 3D high resolution femur and tibia volumes were used to define the coordinate systems based on bony geometry. For a right knee, the ICS is oriented with the x-axis positive in the medial direction, y-axis positive in the posterior direction, and z-axis positive in the superior/proximal direction. Both of the local coordinate systems

for the femur (fLCS) and the tibia (tLCS) were oriented based on the convention for the Biomechanics Gait Laboratory at the Heritage Medical Research Building, Calgary, Alberta. The fLCS and tLCS were oriented with the x-axis positive in the inferior/distal direction, y-axis positive in the anterior direction, and z-axis positive in the lateral direction.

4.4.2.1 Femoral Local Coordinate System

The fLCS was calculated with custom Matlab software code (The Mathworks Inc., Natick, USA) based on a technique used previously in the group (Fjeld, 2007). With this method, a least squares cylinder fit is used to approximate the femoral shaft. The longitudinal (x-axis) is taken as the centerline axis of the cylinder. The cylinder fit was found to be sensitive to non-convergence of the Gauss-Newton least squares solution for some datasets. User input is required to define the femoral shaft, long axis and radius of the femoral shaft. An intra-tester repeatability test was done on one day for 10 repetitions of defining the long axis with a cylinder fit. The root mean square (RMS) error of the angle between the z-axis in the ICS and the longitudinal x-axis was found to be 2.03° .

A second technique was developed for definition of the longitudinal x-axis of the bony segments (tibia and femur). An ellipse was fit to each axially oriented slice of data points along the tibial shaft. A centroid of each ellipse was determined, based on minimizing the area enclosed by the ellipse (Figure 4-8a). This procedure resulted in a vertical line of centroids as an initial estimate of the longitudinal axis of the tibia. A 3D least squares

line was fit to these points to fully define the longitudinal axis. The advantage of this technique is that user input is minimized.

An intertester repeatability test was performed as with the cylinder fit defined axis. The RMS error of the estimated angle was 0.30° . Comparing the two methods for longitudinal x-axis determination, the second method had reduced error due to minimized user input, and no issues with solution convergence. Thus, this second technique was chosen to define the longitudinal x-axis of the femur.

The medial/lateral axis (z-axis) was found using a least squares circle fit to the medial and lateral condyles (Figure 4-7) (Fjeld, 2007). A sagittal slice from each of the femoral condyles was selected at the approximate center of the condyle. A line connecting the two center points of the circles was selected as the z-axis. This method was based on previous techniques used to find femoral facet centers (Churchill, et al., 1998; Coughlin, et al., 2003; Freeman and Pinskerova, 2005; Iwaki, et al., 2000). An intratester repeatability test was previously conducted on one day for 10 repetitions of defining the medial/lateral axis. The RMS error of the angle between the x- axis in the ICS and the calculated medial/lateral axis was found to be 0.59° (Fjeld, 2007). The mathematical cross product of the z and x axes was used to calculate the y-axis in the anterior/posterior direction. To ensure orthogonality of the coordinate system axes, the x-axis was redefined as the mathematical cross product of the y and z axes. The coordinate system origin for each segment was defined as the point along the z-axis that had the shortest perpendicular distance to the x-axis, close to the femoral notch.

Repeatability tests were previously conducted on the sensitivity of the fLCS to the user defined estimates for the cylinder fit to the long axis of the femur, the midpoints of the femoral condyles, and the range used for the circle fit to define the medial/lateral z-axis (Fjeld, 2007). Comparisons of RMS error were made between the locations of the fLCS origin in the midsagittal plane. Intra-tester repeatability was done between 2 test sessions on 2 separate days, and was found to be 0.79 ± 0.42 mm. Inter-tester repeatability was 0.85 ± 0.34 mm (Fjeld, 2007). Intra-tester repeatability was done for the current method using an ellipse fit technique for 1 test session on 1 day. The resulting intra-tester repeatability was found to be 0.26 mm in the midsagittal plane, and 0.40 mm in 3D.

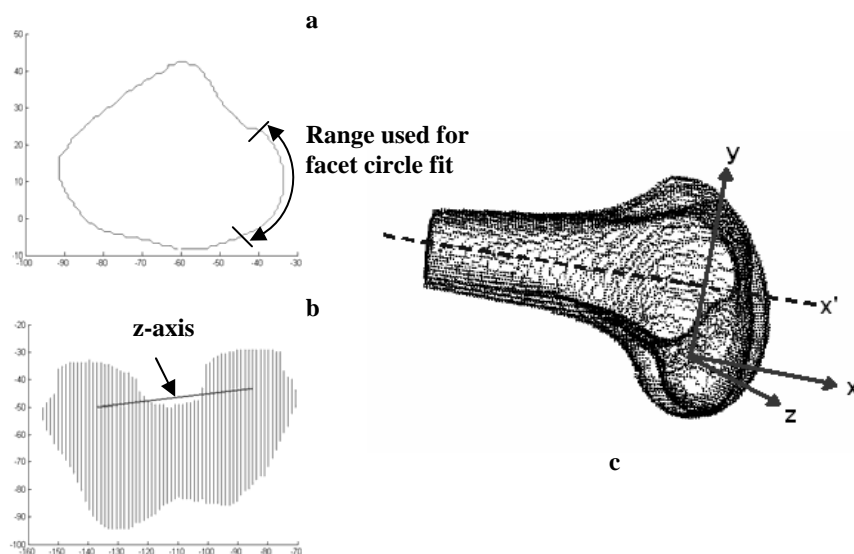


Figure 4-7: fLCS definition: (a) outline of a sagittal slice through a femoral condyle with region selected for facet circle fit, (b) axial view from the distal end of the femur with the resulting z axis through the centres of the facet circles, (c) fLCS displayed within the femur, x' axis shown as longitudinal axis of femur shaft, origin located at projection of x' axis on the z axis used with permission from Fjeld (2007)

4.4.2.2 Tibial Local Coordinate System

The tLCS was defined using a combination of techniques reported in the literature and that were developed for the fLCS method. Compared to the femur, which has well defined geometry for axis definition, the tibia has few identifiable landmarks (Fitzpatrick, et al., 2007). The cylinder fit and the ellipse fit were both considered to define the longitudinal x-axis in the tibial shaft. A cylinder fit was found to be very sensitive to the selection of the user defined tibial shaft length. The same ellipse-fit technique employed for the fLCS x-axis was used for the tLCS x-axis. The intratester repeatability for the axis definition was found to be 3.9° . The greater RMS error for the tibia versus that for the femur longitudinal x-axis, is likely primarily attributed to a shorter length of bone shaft imaged for the tibia.

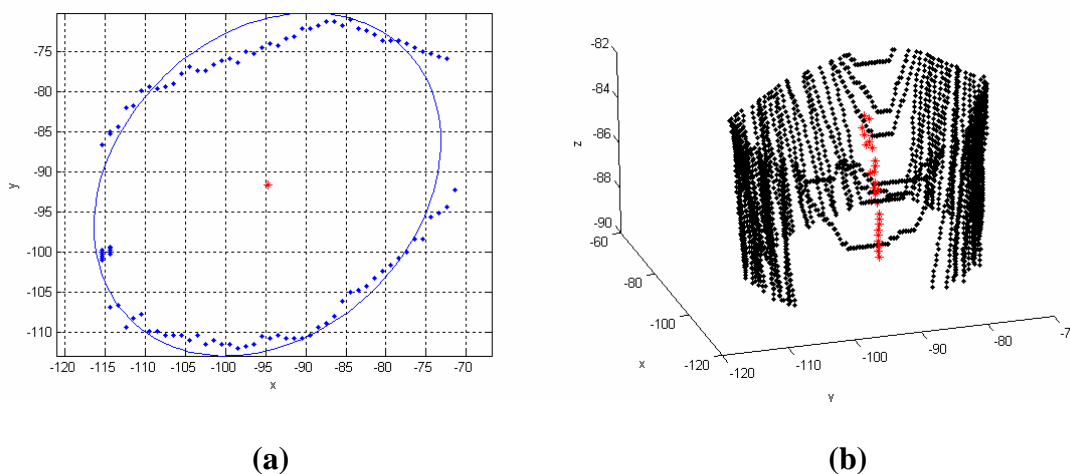
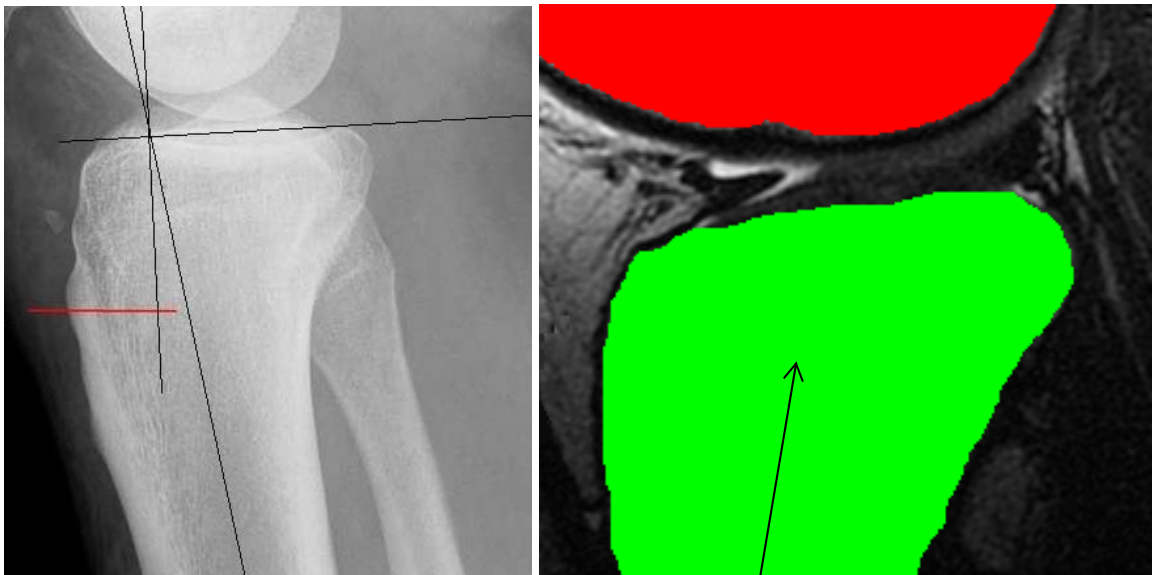


Figure 4-8: (a) Centroid (red) of a slice of the tibial shaft (axial view) based on an elliptical fit resulting in (b) a line of centroids in 3D

Initial calculations revealed that the 30° knee flexion angle (as confirmed with a goniometer) between the tibia and femur long axis is not captured with the ellipse fit technique. This is due to the cut-off point for tibial geometry in the MR image FOVs.

Comparing the MR images to a radiograph, it can be seen that the uppermost tibial geometry will define a long axis that is rotated more anteriorly than the true shaft (Figure 4-9a). Literature methods for proximal tibial coordinate system definitions do not account for this effect (Fitzpatrick, et al., 2007). After construction of the tLCS with the ellipse fit technique, a 30° rotation of the tLCS with respect to the fLCS in the z-y plane of the ICS was used as a correction factor. The 30° adjustment was based on the known knee flexion angle obtained with the goniometer.



(a)

(b)

Figure 4-9: Demonstration of misalignment of long axis based on proximal tibial geometry (a) an exemplary sagittal tibial radiograph (www.fighttimes.com) and (b) an exemplary MR image with either a cylinder fit or ellipse fit

The medial/lateral z-axis was defined using the posterior tibial condylar line (PTCL) (Cubuk, et al., 2000; Fitzpatrick, et al., 2007). The posterior edge of the condyles was defined by the most posterior points of each tibial condyle. To detect these points, a 5th

order polynomial was fit to the axial view of the data set. The most posterior points of the medial and lateral tibial condyles were determined as the local maxima of the 5th order polynomial fit. The line connecting these two points was selected as the z-axis (Figure 4-10a). The y-axis was defined as the mathematical cross product of the z-axis with the x-axis. The z-axis was redefined as the mathematical cross product of the x-axis and the y-axis to ensure coordinate system orthogonality. The coordinate system origin was defined in a similar manner to the fLCS definition, as the point along the x-axis with the shortest perpendicular distance to the z-axis (Figure 4-10b). This approach resulted in an origin positioned at approximately the center and surface of the tibial plateau. Comparisons of RMS error were made between the locations of the tLCS origin, for multiple repetitions of defining the origin in, for both the midsagittal plane projection and the 3D coordinate. Intra-tester repeatability was done for one session and one day for 10 repetitions, and was found to be 0.47 mm in the midsagittal plane and 0.23 mm in 3D.

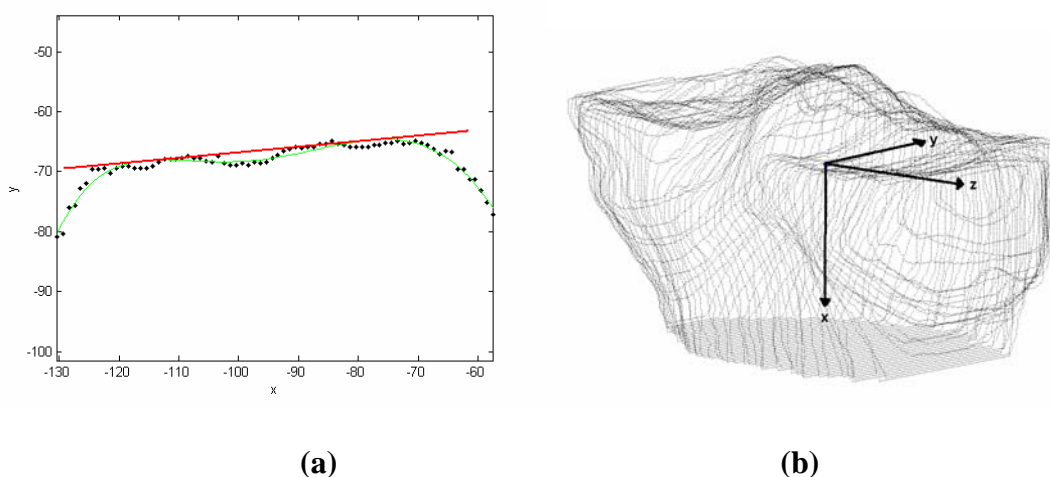


Figure 4-10: (a) Medial/Lateral z-axis definition (red) based on the PTCL using a 5th order polynomial (green) and (b) the tLCS

4.4.3 Surface Reconstruction

A Thin Plate Spline (TPS) algorithm was used to fit a surface to the femoral and tibial cloud of points resulting from digitization of the high and low resolution sagittal images (Figure 4-11). This custom Matlab algorithm (version 7.1, The MathWorks Inc., Natick, USA) has been previously used successfully within our research group (Baker, 2002; Boyd, et al., 1999; Connolly, 2006; Moss, 2001). It was originally developed by Parag Dhar and Dr. Steven Boyd, and further modified by Rita Cheng for use with the Registration software. The application of the TPS to joint surface modelling described in detail by Boyd et al. (1999) is summarized here.

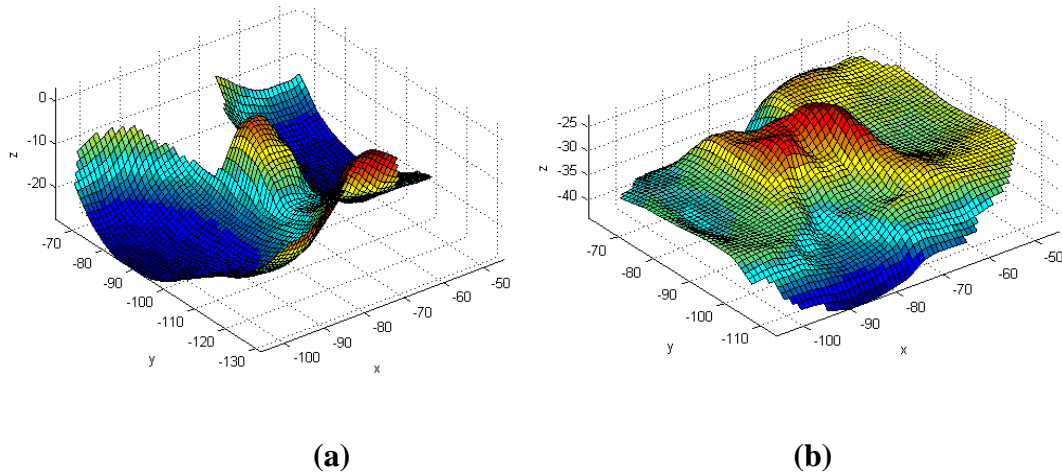


Figure 4-11: TPS Surfaces for high resolution (a) femur and (b) tibia

The TPS deforms an infinite thin plate with bending and without shear to pass through a set of data points such that linearized bending energy is minimized. The bending energy $E(f)$ for a surface $z=f(x,y)$ is given by:

$$E(f) = \iint_{R^2} \left\{ \left[\frac{\partial^2 f}{\partial x^2} \right]^2 + 2 \left[\frac{\partial^2 f}{\partial x \partial y} \right]^2 + \left[\frac{\partial^2 f}{\partial y^2} \right]^2 \right\} dx dy \quad (4.5)$$

where R^2 is the x-y plane, and z describes the deflected height of the surface data points.

Smoothing can be applied to the TPS surface $S(x,y)$

$$S(x, y) = \sum_{i=1}^n c_i f_i(x_i, y_i) + c_{n+1} + c_{n+2}x + c_{n+3}y \quad (4.6)$$

where c_i are constants, and the functions f_i relate the data points to the base surface for n data points. Smoothing is accomplished with a least squares criterion such that the function $J(f)$ (Equation 4.7) is minimized when $f = S$.

$$J(f) = E(f) + \sum_{n=1}^n w_i [f(x_i, y_i) - z_i]^2 \quad (4.7)$$

where w_i are the weights which determine the amount of smoothing. As the value of w_i increases towards infinity, the surface becomes essentially interpolated with minimal smoothing. As w_i decreases towards zero, oversmoothing occurs resulting in reduction to a planar surface. Effects of smoothing were considered for MR imaged porcine specimens in a previous study (Moss, 2001). It was found that smoothing factors between 0.25 and 1.45 showed no significant differences. For this study, a smoothing factor of 0.275 was chosen for the rougher tibial surface, and 0.6 was chosen for the relatively smooth femur (Cheng, 2006).

Applying a TPS surface allows the digitized cloud of points to be resampled into an evenly distributed point set. Computer processing limitations restricted data sets to samples of 4000 points or less. For high resolution data sets, data sets were reduced evenly if they contained more than 4000 points prior to application of the TPS algorithm. High resolution femoral and tibial data were resampled at 1 mm by 1 mm intervals to

homogenize the in-plane and between slice resolutions. Low resolution images were resampled at 3 mm by 1 mm intervals, as a homogenous 3 mm by 3 mm grid would have significantly reduced the data set.

4.4.4 Registration Technique

Registration is a surface matching technique that solves for the transformation parameters needed to match two surfaces. The registration technique used in this project was developed in the Geomatics Department at the University of Calgary (Habib, et al., 2001). It has the benefit over other registration techniques of allowing randomly distributed data sets, different coordinate systems, and a lack of point to point correspondence. This enables data to be collected at different times, with different reference frames, and with different densities of data points (eg: different image resolution). These attributes make this specific registration technique suitable for MR image analysis, where data collection can happen over multiple days or events, using digitized data that yields a cloud of distributed 3D points. This technique has been tested on MR data, specifically for the patella and femur (Cheng, 2006). For registration of femoral image data with a pixel size of 0.6 mm at, the average RMS distance was 0.217 ± 0.035 mm. The technique, detailed in the literature (Cheng, 2006; Habib, et al., 2001), is summarized here.

Primitives are features used to represent a surface dataset. For this registration technique, the first surface (S_1) is defined by points, and the reference surface (S_2) is defined by triangular patches constructed with Delaunay triangulation using Matlab software (The

Mathworks Inc., Natick, USA). A 3D similarity transformation is used to map the two surfaces. This establishes the assumption that the transformation between surfaces is rigid, which is appropriate for registering bone surfaces as was done for this project. A coplanarity condition requires that the volume between a point and corresponding patch be zero (Figure 4-12). This constraint can be mathematically described as a function of the X, Y and Z coordinates of the vertices (p_a, p_b, p_c) of the patch for S_2 (Equation 4.8).

$$V = \begin{vmatrix} X_{q'} & Y_{q'} & Z_{q'} & 1 \\ X_{p_a} & Y_{p_a} & Z_{p_a} & 1 \\ X_{p_b} & Y_{p_b} & Z_{p_b} & 1 \\ X_{p_c} & Y_{p_c} & Z_{p_c} & 1 \end{vmatrix} \quad (4.8)$$

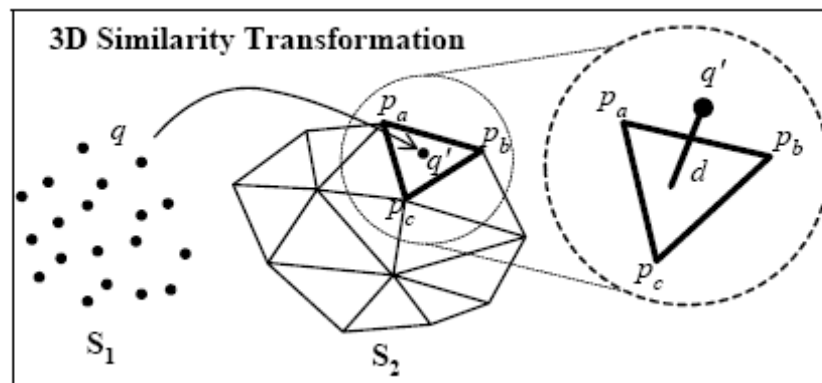


Figure 4-12: ‘Coplanarity condition describes the correspondence between a point in S_1 and a patch in S_2 after performing 3D similarity transformation’ used with permission from Cheng (2006)

The primary output parameter is the transformation function. This describes the relationship between the reference frames of S_1 and S_2 . Seven parameters describe the transformation function: three translations (X_T, Y_T, Z_T), three rotations (ω, ϕ, κ), and a

scaling factor (S). The equation describing the transformation of points from surface 1 (X, Y, Z) to surface 2 (X', Y', Z') is given by:

$$\begin{bmatrix} X' \\ Y' \\ Z' \end{bmatrix} = \begin{bmatrix} X_T \\ Y_T \\ Z_T \end{bmatrix} + S \times R(\omega, \varphi, \kappa) \begin{bmatrix} X \\ Y \\ Z \end{bmatrix} \quad (4.9)$$

For this study, high resolution data was taken as the S_2 surface, and low resolution data was taken as the S_1 surface. The scaling constant S was found to be equal to 1 in all cases. The remaining six output parameters were used to construct a transformation matrix for the femur (T_12hfem) and tibia (T_12htib) at each load level in low resolution image space to the neutral position in high resolution image space. The transformation matrix was used in a series of coordinate transformations (Section 4.5). The distance threshold (between points and patches to identify a match) was set to 0.5 mm. The registration time was approximately 15 minutes per surface using a 3 GHz Pentium 4 processor (Intel, Santa Clara, CA, USA).

4.5 Coordinate Transformations to obtain Gross Joint Displacement

Coordinate transformations are used to determine the relative motion of the femur with respect to the tibia at each load level. A large base of literature exists describing coordinate transformations and their application to biomechanics (Challis, 1995; Soderkvist and Wedin, 1993; Veldpaus, et al., 1988). The primary assumption is that the

segments (femur, tibia) are rigid. The mathematical basis for calculating the transformation matrix between two coordinate systems is briefly summarized here.

The transformation matrix \mathbf{T} between two coordinate systems (CS_1 and CS_2) can be found with a series of calculations based on the work of Soderkvist and Wedin (1993), which was elaborated on by Challis (1995) and implemented in custom Matlab software code (The Mathworks Inc., Natick, USA) (Reinschmidt, 1995). The final position of a point y_i in CS_1 is related to the position of a marker x_i in the CS_2 , the orthogonal rotation matrix \mathbf{R} , the translation vector \mathbf{d} , and error ε in the location of y_i by:

$$\bar{y}_i = R\bar{x}_i + \bar{d} + \varepsilon \quad (4.10)$$

A least squares method can be used to minimize the error. The solution is linear in the translation matrix \mathbf{d} but non-linear in the rotation matrix \mathbf{R} . This is due to the orthogonality condition of \mathbf{R} , where $\mathbf{R}^*\mathbf{R}^T = 1$. Consequently, a singular value decomposition method (SVD) is used to solve for \mathbf{R} and \mathbf{d} , as it is well suited to ill-conditioned problems. The method begins by determining the mean position \bar{x} of three points on the segment (x_1 , x_2 , and x_3) in CS_2 . Similarly, the mean position \bar{y} is determined for CS_1 based on points y_1 , y_2 , y_3 . Matrices \mathbf{A} and \mathbf{B} are defined as:

$$A = [\{x_1 - \bar{x}\} \{x_2 - \bar{x}\} \{x_3 - \bar{x}\}] \quad (4.11)$$

$$B = [\{y_1 - \bar{y}\} \{y_2 - \bar{y}\} \{y_3 - \bar{y}\}] \quad (4.12)$$

The cross dispersion matrix \mathbf{C} is given by $\mathbf{C}=\mathbf{B}\mathbf{A}^T$. The SVD is applied using the Matlab (The Mathworks Inc., Natick, USA) command $[\mathbf{P},\mathbf{T}_o,\mathbf{Q}]=\text{svd}(\mathbf{C})$. It produces a diagonal matrix \mathbf{T}_o of same dimensions as \mathbf{C} with nonnegative diagonal elements in decreasing order. Unitary matrices \mathbf{P} and \mathbf{Q} are given such that $\mathbf{C}=\mathbf{P}*\mathbf{T}_o*\mathbf{Q}$. The rotation matrix \mathbf{R} is determined by $\mathbf{R}=\mathbf{P}\mathbf{Q}^T$. A mathematical check is employed at this stage to ensure that $\det(\mathbf{R})=1$, confirming that \mathbf{R} is a special rather than general orthogonal matrix. Special orthogonal matrices are a closed set that allow a rotation matrix to result from the multiplication of two rotation matrices. The translation vector \mathbf{d} is determined using equation 4.10. Finally, the transformation matrix \mathbf{T} (Equation 4.13) is determined as a combination of the rotation matrix \mathbf{R} and the translation matrix \mathbf{d} :

$$\mathbf{T} = \begin{bmatrix} R_{11} & R_{12} & R_{13} & d_1 \\ R_{21} & R_{22} & R_{23} & d_2 \\ R_{31} & R_{32} & R_{33} & d_3 \\ 0 & 0 & 0 & 1 \end{bmatrix} \quad (4.13)$$

For this study, a series of transformation matrices were required to determine the relative motion between the femur and tibia in the tLCS (Figure 4-13). Transformation matrices for the femur and tibia (T_{l2hfem} and T_{l2htib}) that map the low resolution bone to the high resolution bone in the ICS were found using a registration technique (Section 4.4.4). The coordinate system definition (Section 4.4.2) provided the input required to apply the Soderkvist and Wedin (1993) technique described in Equations 4.10-4.13. The transformation matrix for the femur and tibia ($T_{bonefem}$ and $T_{bonetib}$) were

calculated from the fLCS and tLCS points in the ICS (x_1, x_2, x_3) to the unit vectors

$y_1 = (1,0,0)$, $y_2 = (0,1,0)$, and $y_3 = (0,0,1)$.

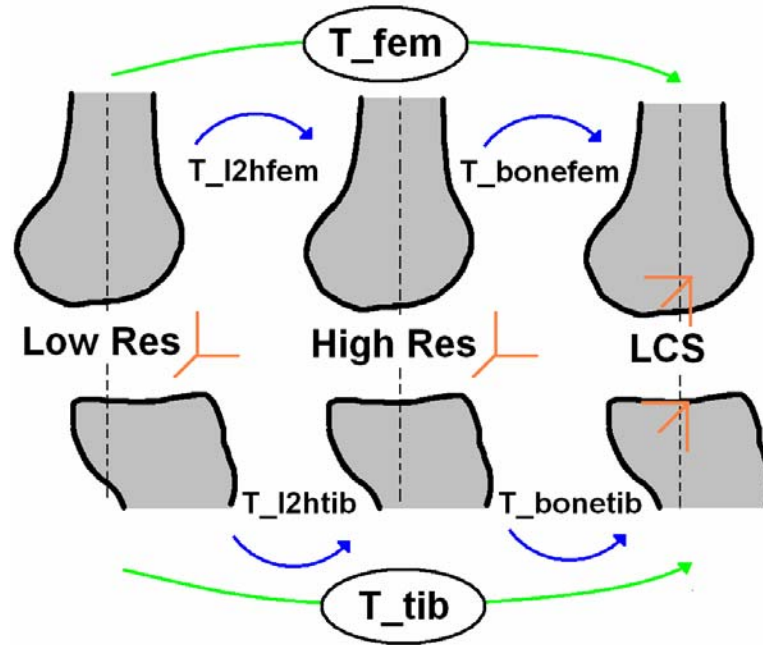


Figure 4-13: Transformation matrices for conversion from low resolution images (applied load) to high resolution images (T_{I2hfem} , T_{I2htib}) to LCS ($T_{bonefem}$, $T_{bonetib}$). Cumulative transformation matrices from low resolution images to LCS (T_{fem} , T_{tib}) are used to obtain relative motion between tibia and femur.

The transformation matrix (T_{rel}) describing the relative motion of the femur with respect to the tibia in low resolution image, described in the tLCS is determined as:

$$T_{rel} = (T_{bonetib} * T_{I2htib}) * (T_{bonefem} * T_{I2hfem})^{-1} \quad (4.14)$$

From the transformation matrix T_{rel} , Cardan angles were chosen to find the joint angles and displacements of the femur with respect to the tibia. The Cardan angle system was selected as it allows the joint motion to be described in anatomically or clinically meaningful directions (Section 2.2). In calculating the transformations, each axis is rotated about once, and is order dependent. Order is typically chosen from the axis about

which the largest angle change will occur, to the smallest (Woltring, 1991). For this study, the angles of rotation were minimal, and the order of rotation was selected as: flexion/extension, internal/external, and ab/adduction (z, x, y). Three rotations and three translations about the tLCS coordinate axes are calculated from the transformation matrix. These values are the main output variables for knee flexion angle, and internal rotation and anterior displacement of the tibia. Ab/adduction angles and translations in the medial/lateral and superior/inferior directions are also output but are not primary outcome measures.

4.5.1 Verification of Transformation Matrices Calculations

A test object was used to ensure that the complex series of transformation matrix calculations were correct. The test object was defined as a rotated cylindrical surface, with a profile described by

$$2 + \cos(t) \tag{4.15}$$

The test object was centered at (0,0,0) to represent the femur in the fLCS and the tibia in the tLCS. To represent the femur in the high resolution ICS, the test object was moved from the (0,0,0) location to a center point at (10,10,0). Similarly, the tibial test object in high resolution ICS was translated to (10,10,-10). To represent the objects in the low resolution ICS, the femoral test object origin was translated to a position of (10,11,0), and the tibial test object was translated by 5 units in the y-direction to (10,15,-10) and then rotated about the z axis by -10° (Figure 4-14). This change in location represents the anterior shift and internal rotation that is typically seen when applying an anterior load to the knee (Logan, et al., 2004b).

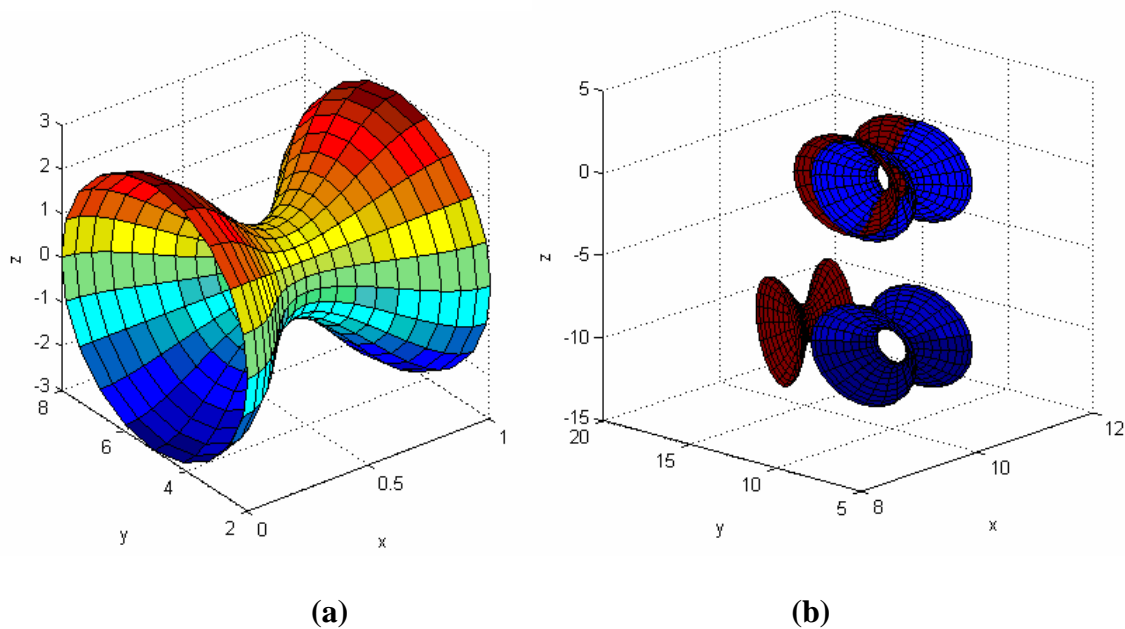


Figure 4-14: (a) Test object as it is (b) shifted (from blue to red) to simulate relative bone displacement and rotation

Transformation matrices were calculated for the femoral and tibial test objects to transform them from 1) the low resolution to high resolution configuration, and 2) the high resolution to LCS configuration. A series of matrix calculations were completed to find the position of the tibia with respect to the femur (Section 4.5). The expected results compared to the calculated results were a y-translation of 4 units versus 3.9132 units, a z-translation of -10 units versus -10.0011 units, and a z-rotation of -10° versus -10.0000° . Based on the excellent agreement between expected and calculated results, it was concluded that the transformation calculations were correct.

4.6 ACL Insertion Point Displacement

Insertion points of the ACL at the tibia and femur were used to estimate the change in length of the ACL resulting from the external force applied to the tibia. This measure

does not account for slack in the tendon, and is intended as a demonstration of the potential outcome measures that MR imaging brings to measures of joint laxity.

Custom Matlab code (The Mathworks Inc., Natick, USA) was developed to calculate the insertion points of the ACL. Sagittal images were used to digitize the interface between tendon and bone at the tibial insertion point. Likewise, axial images were used to digitize the interface at the femoral insertion point. Using these orientations provided an optimal view of the tissue/bone interface. A musculoskeletal radiologist (Dr. Houman Mahalati) was consulted to ensure exact anatomical digitization. Digitization resulted in clouds of 3D points in the ICS (Figure 4-15).

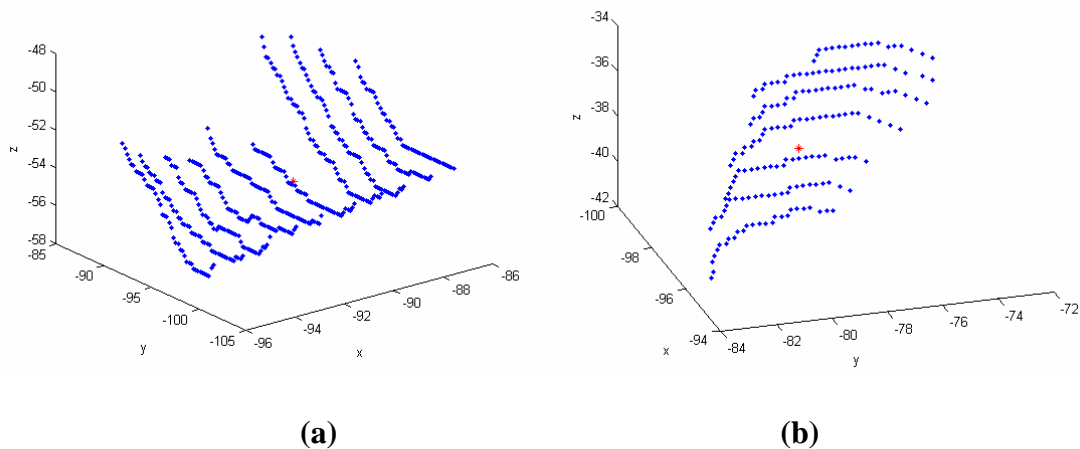


Figure 4-15: Digitized Points for (a) tibial and (b) femoral insertion points with insertion point shown in red

The digitized points were projected to an ICS plane described by the equation

$$n_x x + n_y y + n_z z + C = 0 \quad (4.16)$$

where (n_x, n_y, n_z) is the normal vector of the plane. The digitized points were projected onto the sagittal (y-z) plane for the femoral insertion point, and the axial (x-y) plane for the tibial insertion point. For clarity, the respective projection plane is defined by the plane coordinate system (PCS). The 3D cloud of points was projected into the PCS, resulting in a cloud of 2D points. An ellipse was fit to the 2D data points by minimizing the area enclosed by the ellipse (Figure 4-16). The centroid of this ellipse was transformed from the PCS to the ICS. This point was defined as the insertion point.

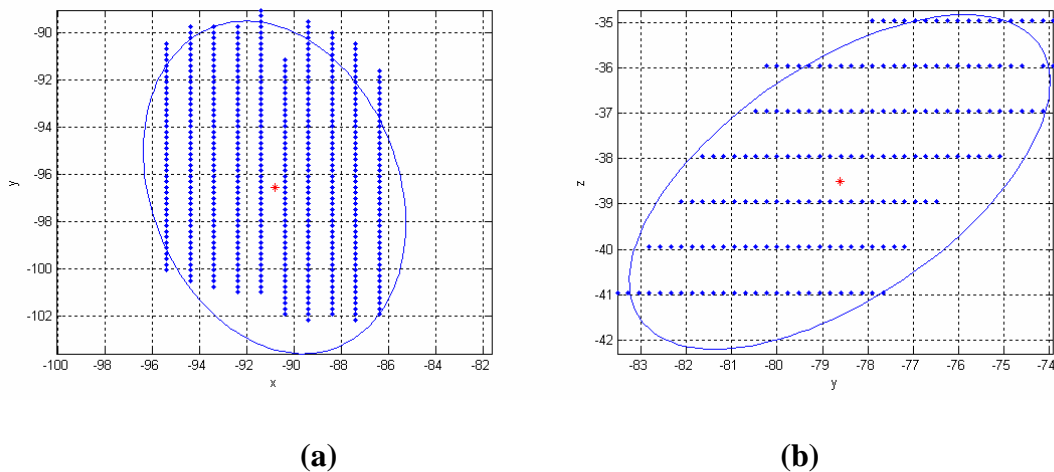


Figure 4-16: Ellipse fit to (a) Tibial and (b) Femoral ACL insertion data points with insertion point shown in red

To account for possible motion between axial and sagittal scans, a registration was done between the femur in the sagittal image and the femur in the axial image. Digitization along the anterior surface of the femur (femoral groove) was done in both orientations to create 3D TPS surfaces that could be registered (Figure 4-17). Parameters for smoothing and re-sampling were equal to those used for the high resolution femoral surfaces in the joint surface TPS. The resulting transformation matrix was applied to the femoral ACL insertion point to transform it into the sagittal ICS. At each load level the ACL length

was calculated as the distance of a line connecting the ACL insertion points using custom Matlab software (The Mathworks Inc., Natick, USA).

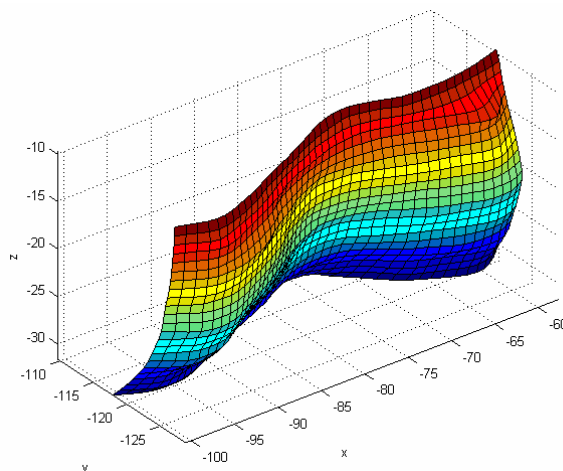


Figure 4-17: TPS Surface of the femoral groove for registration between axial and sagittal high resolution images

4.7 Load Data Processing

Load data were sampled at 0.85 ± 0.03 Hz, and processed with Matlab 7.1 (The Mathworks Inc., Natick, USA). An exemplary plot shows the stepped manner of applied force over time (Figure 3-6).

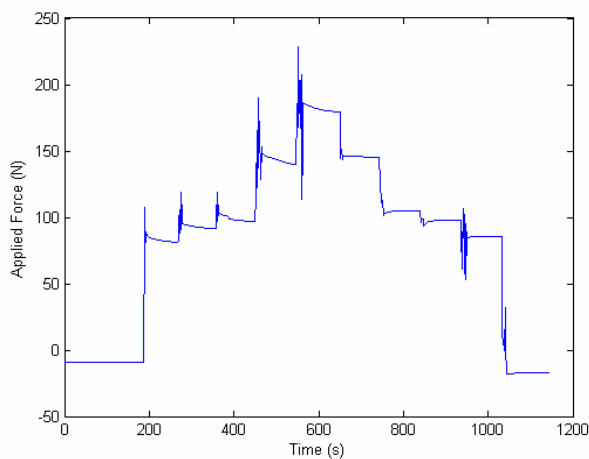


Figure 4-18: Applied force during MR scanning for one subject

The data were not digitally filtered due to the low sampling frequency, which was a result of the LabVIEW 7.1 (National Instruments Corporation, Austin, Texas, USA) program hierarchy that put priority for displaying data rather than recording. An analysis of sample data show that force output followed a normal distribution (Figure 4-19), as the data shown with '+' symbols approaches the dashed line of a true normal distribution. This allows use of data mean and standard deviation to describe the force acting at each level. Data was lost due to a system crash (related to interrupted communication between the DAQ system and the laptop) during testing for subject S04 (all loads except 40 N and 30 N descending) and partially for subject S01 (30 N, 40 N, 50 N, and 89 N ascending). Initial and final loads were recorded on paper for all subjects, and the average of these load values were used for the missing data points.

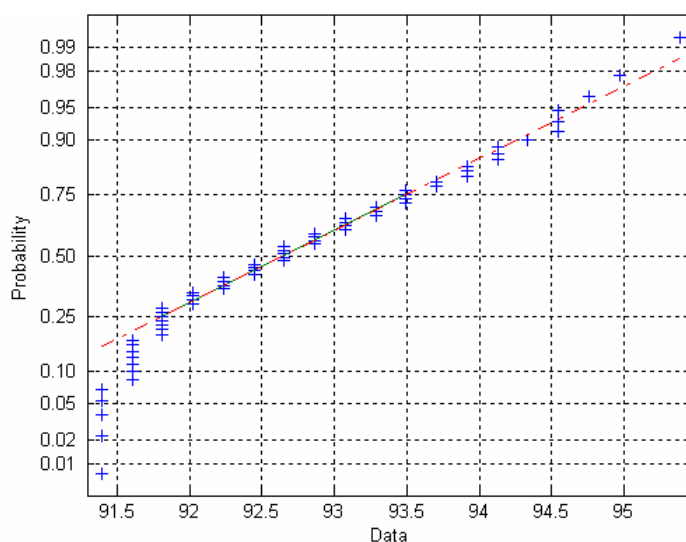


Figure 4-19: Normal Probability Plot for Sample Load Data
 ('+' indicates sample data; '--' indicates true normal distribution)

During testing and data analysis, a stress relaxation phenomenon was noted in the force-time plots. This phenomenon was only present during loading, and not during unloading. Visual comparison to calibration data force-time plots showed that the phenomenon was not seen during calibration tests and therefore was not attributed to hydraulic system behavior. It was not possible to directly measure whether the displacement remained constant during the time that the force was held. However, if the joint was moving during the MR scanning, it could cause motion artifacts, depending on the tissue, type of movement, and the phase-encoding amplitude (Brown and Semelka, 1999). The MR images were reviewed to identify any scans that had visible motion artifacts in comparison to the scan obtained at the reference position.

To quantify the stress relaxation, an exponential curve fit, based on the QLV theory (Section 2.3) and modified for stepped loading, was applied to each force-time curve at each stepped load measured during MR scanning. Previously, additive exponential functions have been used to fit the stress relaxation curve, normalized to peak stress (Abramowitch and Woo, 2004; Thornton, et al., 2001). Two exponential functions with 4-5 constants may be used, yielding two time constants (Thornton, et al., 1997). The first exponential describes the short relaxation time constant and the second describes the long relaxation constant. Due to the short scan time of approximately 1 minute, the stress relaxation curve did not reach equilibrium. For stepped loading, Sarver et al (2003) proposed an alternate form of normalizing the stress relaxation curve. Their technique was used in this study, where the stress (in this case force) axis is normalized to the peak stress, and each stress value is divided by the difference between the peak stress and the

final stress. This removes the strain-dependence that is seen with the typical method, although strain independence is an inherent assumption of the QLV theory.

Consequently, a single exponential was fit (Equation 4.17), using the normalizing method described by Sarver et al (2003):

$$G(t) = Ae^{\frac{-t}{\tau_1}} \quad (4.17)$$

From this model, the time constants were output at each load level for the ascending loads for each subject.

4.8 KT-2000 Testing

Approximately 24 hours before or after the MR imaging session (consistent within subject), subjects were tested with the KT-2000 knee laxity tester. An experienced tester, researcher, and physiotherapist, Dr. Barbara Loitz-Ramage, conducted all of the testing at the Human Performance Lab on the University of Calgary campus in Calgary, Alberta, Canada.



Figure 4-20: KT-2000 Testing

The subject lay supine in slight hip flexion and with a knee flexion angle of approximately 30° (Figure 4-20). The knee had to be flexed adequately to engage the patella in the femoral groove. If the flexion was inadequate, the patella would not provide a stable base from which tibial displacement could be measured. External hip rotation was restricted by a Velcro strap placed mid-thigh. Tibial position was maintained by placing the subject's feet between two vertical supports that prevented the feet from rolling outward. The arthrometer was secured to the anterior tibia with Velcro straps, with a proximal bar contacting the anterior patella surface, the motion axis oriented over the joint line, and the force plunger positioned over the tibial tubercle. With the subject relaxed, a dial on the front of the machine was adjusted to a neutral starting position of the tibia with respect to the patella. The examiner then translated the tibia posteriorly and anteriorly, with a goal of establishing the same neutral starting position with each cycle. This trial also helped the subject to completely relax because it allowed them to become

accustomed to the motion. If the initial starting position changed between cycles, it was likely that the subject was either protecting the joint by contracting the thigh muscles, or the patellar reference pad was moving. Once the starting position was stable, anteriorly and posteriorly directed loads of approximately 133 N were applied through the force handle of the arthrometer for 3 repetitions. The examiner was made aware that the load levels were reached when the sound detector produced a ‘beep’ sound.

4.8.1 Data Processing

KT-2000 force-displacement data were collected at 400 Hz with KT-2000 software. Data were output as excel files and read into a custom Matlab program (The Mathworks Inc., Natick, USA). Data were digitally filtered with a low-pass zero-phase 6th order Butterworth filter at a cut-off frequency of 30 Hz. This cut-off value was found with a power spectrum analysis of both force and displacement data, based on a Fast-Fourier Transform (Figure 4-21).

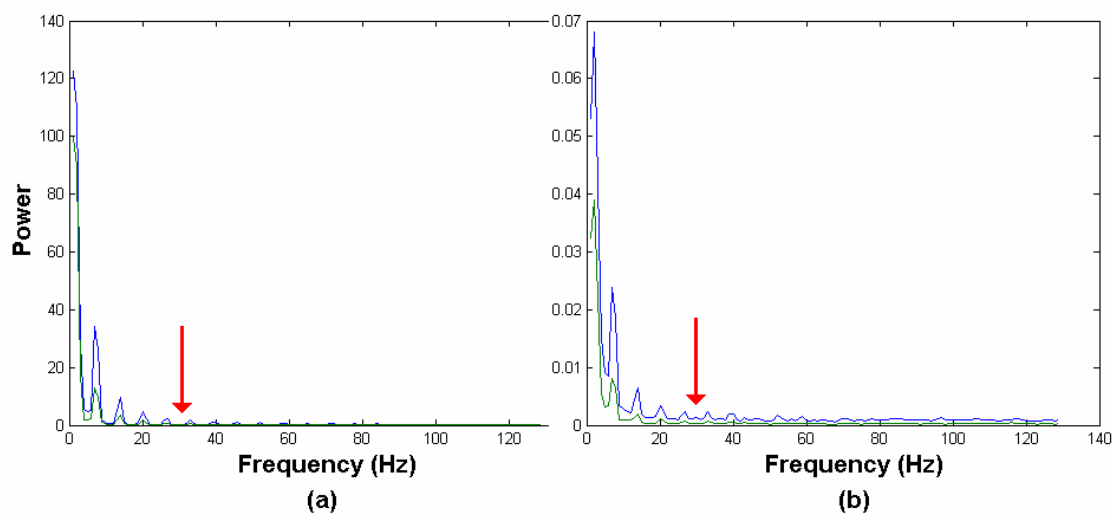


Figure 4-21: Power Spectrum for (a) force and (b) displacement KT-2000 data

Displacement values at force levels corresponding to those used with the KLA (30, 40, 50, 89, and 133 N) were output for all three consecutive trials within a session.

Displacement data was shifted such that the zero initial displacement value corresponded to zero force. One limitation of the KT-2000 was that the sound detector tone indicating that maximum anterior force has been reached did not consistently correspond to 133 N. Consequently, the peak load varied between and within subjects (110 ± 5 N).

For comparisons between KT-2000 and the KLA values, as well as to assess KT-2000 repeatability, the clinical displacement value was output. This is calculated as the displacement on the first ascending curve at 89 N. This is the value that the KT-2000 software outputs to the user. In addition, the compliance index (CI) was calculated as the increase in anterior displacement between 67 N and 89 N on the first ascending curve. The potential for obtaining more information from the force-displacement curve is demonstrated by fitting a 5th order polynomial (Maitland, et al., 1995) and taking the second derivative (change in stiffness) to identify local maxima and minima points along the curve (Figure 4-22). This procedure enables calculation of average stiffness in the 3 main regions of the curve: 1) the initial rise as the weight of the leg is overcome, 2) the middle region as slack is taken up in the quasi-passive joint structures, and 3) the linear region where the onset of primary restraints to anterior displacement occurs (Maitland, et al., 1995). To the knowledge of this author, there are no papers that have used the second derivative to separate the three portions of the force-displacement curve.

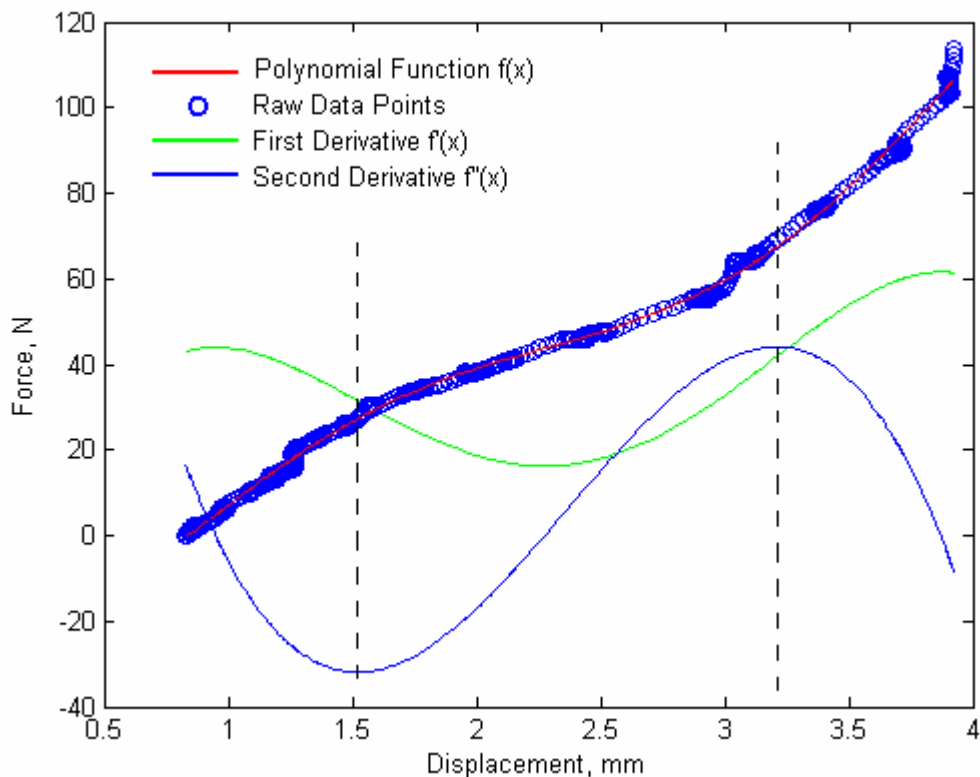


Figure 4-22: Exemplary plot of KT-2000 force-displacement curve including raw data, 5th order polynomial fit, and first (stiffness) and second (change in stiffness) derivatives. Inflection points are indicated with the dashed lines, separating the curve into 3 sections: initial rise, middle, and linear regions.

4.9 Electromyography

Prior to MR testing on a separate day, EMG testing was conducted to ensure that the subjects were not muscle guarding during the passive laxity tests. Subjects wore shorts and were asked not to apply lotion to their legs. Subjects stood and performed an isometric squat and a calf raise to allow the tester to identify and mark the muscle bellies of the vastus medialis, vastus lateralis, rectus femoris, biceps femoris, semitendinosus, medial gastrocnemius, and lateral gastrocnemius. The areas were dry shaven to remove hair, and then swabbed with rubbing alcohol to fully clean the skin surface. When the

surface was dry, silver/silver chloride electrodes (Huggables, ConMed Corporation, NY) were placed over the midline of the muscle belly (Figure 4-23) (DeLuca, 1997).



Figure 4-23: Electrode placement for EMG

EMG was collected for a neutral position that mimicked the subject's position in the KLA, with the knee supported posteriorly by foam padding such that it was flexed at 30° (Figure 4-24).



Figure 4-24: EMG collected at a neutral position outside of the KLA

Maximum voluntary contraction (MVC) signals were collected for the quadriceps, hamstring, and gastrocnemius muscle groups. During the test, verbal encouragement was given to promote MVC exertion. For the quadriceps test, the tester applied pressure to the distal end of the tibia while the subject lay supine. The subject resisted the posterior force, activating the quadriceps to try attempt to extend the leg (Figure 4-25a).



(a)

(b)

Figure 4-25: Maximum voluntary contraction tests for (a) the quadriceps and (b) the hamstring muscle groups

For the hamstring MVC test, the tester applied pressure to the distal end of the tibia in the anterior direction. The subject was prone, with their test leg at approximately 90° of knee flexion. The subject resisted the applied force by attempting to further flex the knee (Figure 4-25b).



Figure 4-26: Maximum voluntary contraction test for the gastrocnemius muscle group

For the gastrocnemius MVC test, the tester applied a downward pressure to the subject's shoulders. The subject was standing with their heels lifted and their knees partially flexed to prevent locking of the knee (Figure 4-26). A five second EMG recording was done for each maximum voluntary contraction test.

The subject was then positioned in the KLA and tested at all load levels for 1 minute durations as in the MR imaging protocol. EMG was collected during load application and during the held load. If an activation signal was visible, indicating that the subject was activating their muscles against the applied load, the load levels were completed as planned. Then the trial was repeated until the subject demonstrated no excited EMG signal from the real time signal output.

4.9.1 Data Processing

EMG signal data for all trials were processed with a custom Matlab program (The Mathworks Inc., Natick, USA). Data were sampled at 1200 Hz. The DC offset was removed, and the data were full wave rectified. For the trials using the KLA, a low pass 4th order Butterworth filter with a cut-off frequency of 50 Hz was used to filter the data in both directions. The cut-off frequency was chosen based on a power spectrum analysis using a Fast Fourier transform (Figure 4-27).

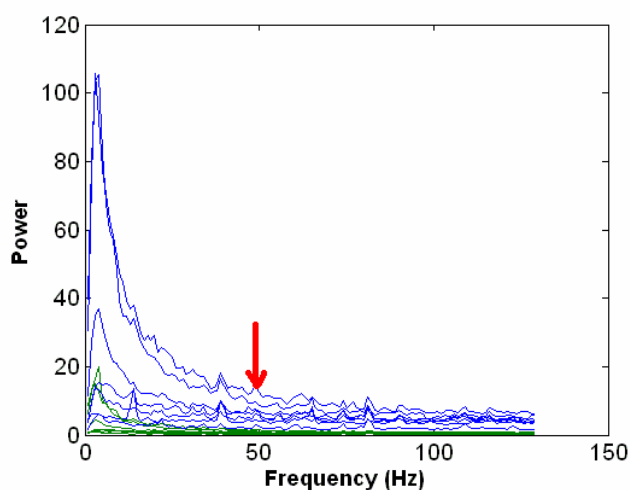


Figure 4-27: Power spectrum for lower limb muscle signals

For each muscle, at each load level the maximum activation as a percentage of the MVC signal was calculated. The RMS of the signal at the neutral position outside of the KLA was subtracted from the RMS of the MVC signals and the loaded test signals. The neutral position file for subject S03 was assumed to have a mean of 0 (no data, including 133 N, 89 N, and 50 N down). Finding the RMS value over the entire MVC trial and the neutral position trial effectively filtered the data.

4.10 Statistics

The main and secondary outcome variables, including joint displacements, rotations, and time constants related to stress relaxation, were statistically evaluated. The hypotheses are addressed with the following comparisons:

H1: The loading apparatus will have repeatable positioning and load application

- Reliability (Cronbach's Alpha) and comparison of values across days (non-parametric Friedman's test) for initial internal rotation angle, initial anterior tibial position, initial ACL insertion point distance, and load application.

H2: Joint and ACL insertion point displacement will be repeatable ($\pm 0.5\text{mm}$) for a given applied load. The force-displacement curves will show increasing displacement with increasing force.

- Comparisons between load levels for anterior tibial position and ACL insertion point distance (Friedman's test and Wilcoxon's signed ranks test)

H3: Force-displacement curves found using novel technique will be less variable and differ from those using the KT-2000.

- Comparison of normalized anterior displacements using a Wilcoxon signed ranks test across methods at each load level
- Cronbach's Alpha for reliability within a method

H4: Subjects will be capable of muscle relaxation in the loading apparatus such that the electromyography (EMG) signal will be less than 5% of manual maximum contraction in all muscles.

- Student t-test to compare EMG data against the required 5% maximum value of signal to maximum voluntary contraction ratio

Due to the small sample size ($n=5$) of this exploratory study, non-parametric tests were used. Care was taken in the interpretation of the statistics due to the small sample size. Comparisons between days and load levels were done with a Friedman's test. A Wilcoxon's signed ranks test was used to compare between methods. Reliability coefficients such as Cronbach's alpha were calculated to identify method reliability. SPSS (Version 13.0, SPSS Inc., Chicago, Illinois, USA) and Excel (Microsoft Office Professional Edition 2003, Microsoft Corporation, Redmond, Washington, USA) were used to compute the statistics.

Chapter Five: Results

5.1 Introduction

The results section presents the findings of this study. In particular, the evaluation of the KLA is quantified for positioning and for the force-displacement results. Reliability of the KLA and KT-2000 are assessed. Variables affecting laxity, including total body water, and muscle activation (via EMG) are presented. Stress relaxation behavior seen during loading is analyzed. For all statistical results, it is important to consider the limitations of statistics when analyzing a small sample size (reliability $n=3$, within day $n=5$). Trends and variability will be considered in the results. Variability may in fact be just as important an indication of the relative success of the KLA design, as a variable may be statistically reliable, but not have acceptable variability (H2).

5.2 Total Body Water

Total body water had low variability for repeated subjects (S02, S03, S05) over the three test sessions. By method, the Watson, Hume-Weyer, Chertow, and physiologic techniques had standard deviations across days of $\pm 0.1-0.5$ L, $\pm 0.2-0.4$ L, $\pm 0.2-0.4$ L, and $\pm 0.2-1.1$ L, respectively (Figure 5-1).

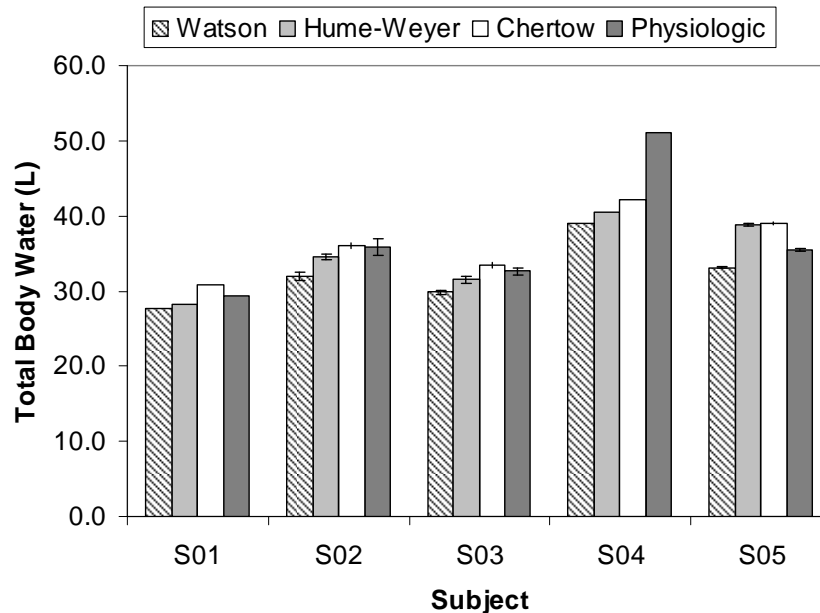


Figure 5-1: Average Total Body Water

5.3 Knee Loading Apparatus

5.3.1 Repeatability of Force Application

The ability to repeatedly apply the same force to the knee on each test day was assessed using Cronbach's alpha (α_c). It is an indication of tester reliability, as the tester controlled the force application. Values range from -1 to 1, where 0 indicates low correlation and 1 indicates high correlation between tests. A value >0.70 indicates significant correlation. A negative reliability coefficient can occur when sampling variability is high with a low sample size. This indicates a low correlation, high sampling variability, or values that have varied in opposite directions.

Significant correlation was found at 40 N, and 50 N ascending, and at 50 N, and 30 N descending, suggesting greater force control at lower loads (Table 5-1).

Table 5-1: Cronbach's Alpha for reliability of force application with the KLA

Anterior Force, N (ascending)				
30	40	50	89	133
0.472	0.767	0.965	0.158	0.622
Anterior Force, N (descending)				
89	50	40	30	0
0.620	0.989	0.643	0.820	-

A non-parametric Friedman's test for comparison of load values across days showed no significant differences ($p > 0.05$). The variability of force for a given test day ranged from ± 0.52 N to ± 6.0 N (Figure 5-2). This represents the variability in achieving the target load (30 N, 40 N, etc), based on the average force calculated over an entire stepped load.

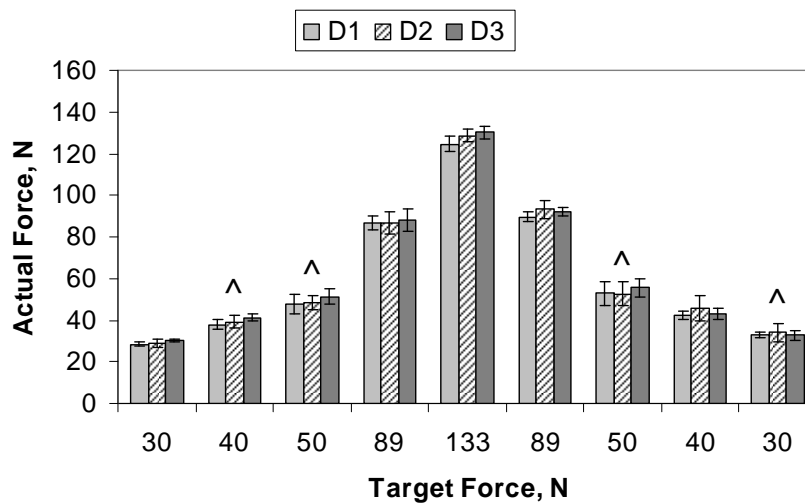


Figure 5-2: Actual force compared to target force using the KLA across days (n=3). ^ indicates significant correlation (high reliability) of loading across days (where D1 = Day 1, D2 = Day 2, and D3 = Day 3)

5.3.2 Repeatability of Positioning

Consistent initial positioning of the subject was a key goal for the KLA design. The efficacy of the KLA to reliably position the subjects was evaluated over the three test days. Cronbach's alpha was calculated for the initial force level (30 N) for internal tibial rotation angle ($\alpha_c = -3.11$), anterior position of the tibia with respect to the femur ($\alpha_c = 0.89$), and initial 3D ACL insertion point distance ($\alpha_c = 0.90$). Statistically significant correlations were found for the initial anterior position and the initial ACL insertion point distance, indicating high reliability (Figure 5-3). The variability in initial anterior position was $\pm 0.4 - 6.4$ mm, and in initial ACL insertion point distance was $\pm 1.0 - 2.3$ mm.

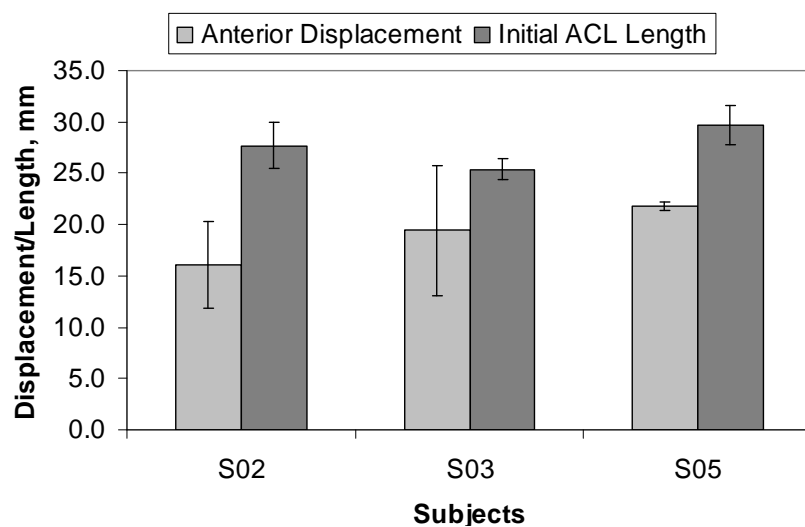


Figure 5-3: Initial anterior position of the tibia with respect to the femur, and ACL insertion point distance, averaged over 3 test days

A potential trend that was noted was a correlation between the initial internal rotation angle, and the initial anterior position of the tibia. A linear fit of initial anterior tibial position against initial internal rotation angle showed a strong proportional relationship for subject S02 ($r^2=0.9734$, Figure 5-4). The other two repeatability subjects (S03, S05) did not have strong linear fits ($r^2=0.595$, $r^2=0.4131$), however the trend for subject S03 was an increase in initial anterior position with an increase in initial internal rotation angle. Subject S05 showed a trend of constant anterior tibial position with increased initial internal rotation angle. This subject had the least variability in the initial internal rotation angle ($3.5^\circ \pm 2.6^\circ$) when compared to the other subjects (S02: $2.3^\circ \pm 5.7^\circ$, S03: $0.3^\circ \pm 5.5^\circ$).

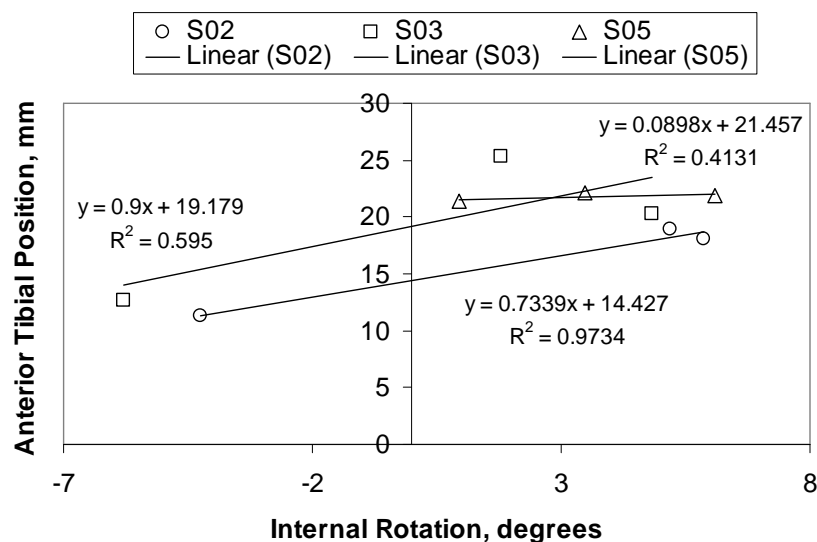


Figure 5-4: Relationship between the initial anterior tibial position and initial internal rotation angle

Within a test session, the variability of the knee flexion angle over loading (ascending and descending, combined) ranged from $\pm 0.48^\circ$ to $\pm 1.71^\circ$ (Figure 5-5).

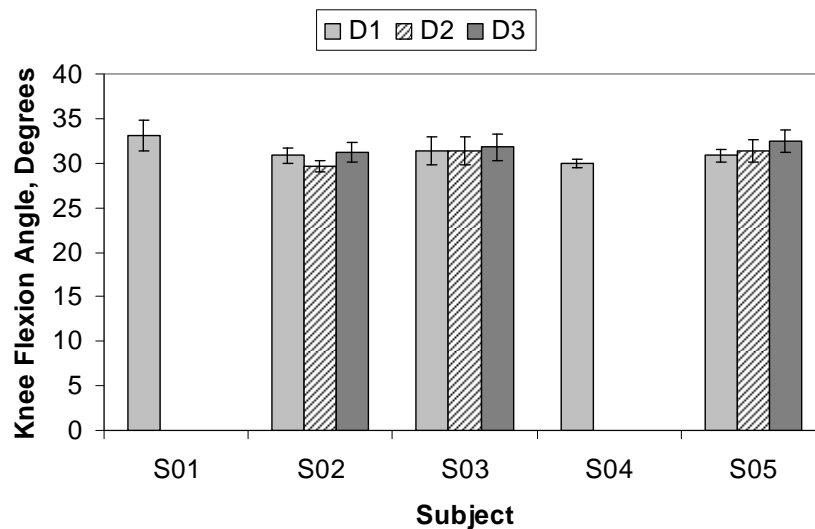


Figure 5-5: Knee flexion angle for all subjects and test days, where D1 = Day 1, D2 = Day 2, and D3 = Day 3

5.3.3 Force-Displacement

Typical force-displacement graphs in the literature show an increasing displacement with increasing force (Daniel, et al., 1985a). The descending portion of the curve exhibits a hysteresis, due to the viscoelastic properties of the knee joint that exhibit an energy release during unloading (Woo, et al., 1999). The force displacement graphs for all subjects show a similar trend of increasing anterior tibial position (Figure 5-6 to Figure 5-10), ACL insertion point distance (Figure 5-11), and internal rotation (Figure 5-12) with increasing force. For a given load, the variability in anterior tibial position ranged from ± 2.6 to 3.3 mm, and the variability of internal rotation angle ranged from $\pm 4.0^\circ$ to 5.3° . For a given load, the average ACL insertion point distance for all subjects ranged from 28.1 ± 2.6 mm to 28.5 ± 2.9 mm, and the largest variability in ACL insertion point distance at a given load was ± 3.2 mm.

Non-parametric Friedman's tests were run for each variable (anterior tibial position, internal rotation angle, or ACL insertion point distance) to assess whether a significant difference in the given variable could be detected between loads (H2). A significant difference was found for anterior tibial position ($p=0.004$) and internal rotation angles ($p=0.01$) across loads. No significant difference ($p>0.05$) was found for ACL insertion point distance across loads.

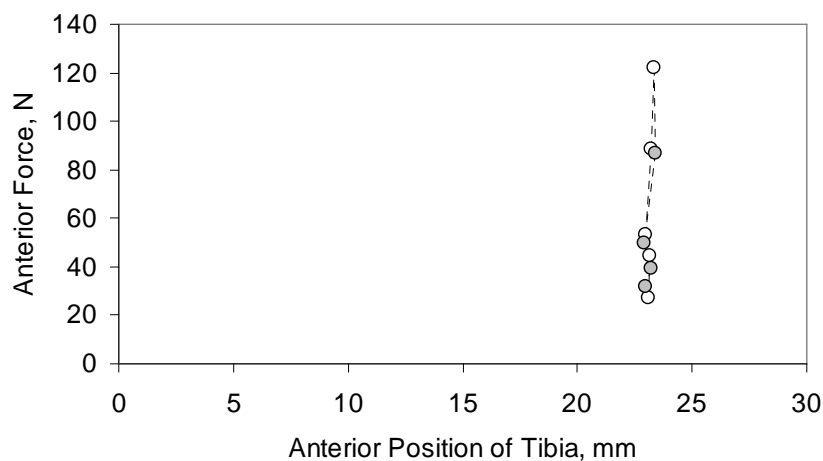


Figure 5-6: KLA Anterior Force-Displacement (S01) showing force ascending (open symbols) and descending (closed symbols)

A Wilcoxon signed ranks test was done for each pair of force-displacement points to determine the load levels at which the anterior tibial position could be distinguished. Based on a sample size of $n=5$, the smallest p -value that can be achieved is 0.063. For this particular analysis, results will be considered significant for $p \leq 0.063$. Displacements at which $p=0.063$ were obtained are shown in Table 5-2 .

Table 5-2: Force Levels at which significant differences in Anterior Tibial Position may be detectable at $p \leq 0.05$ with a sample size of $n > 5$

Ascending		Descending *	
30 N	133 N	30 N	89 N*
40 N	133 N	40 N	89 N*
50 N	89 N	50 N	89 N*
50 N	133 N	50 N	40 N*
89 N	133 N	50 N	30 N*
		89 N	89 N*

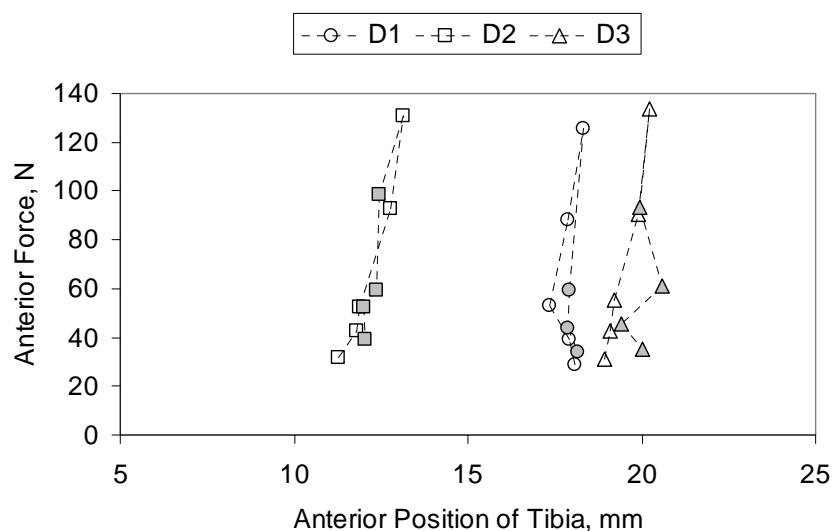


Figure 5-7: KLA Anterior Force-Displacement (S02) showing force ascending (open symbols) and descending (closed symbols) over three test days (D1, D2, D3)

A Wilcoxon signed ranks test was done for each pair of force-internal rotation points to determine the load levels at which the internal rotation angle could be distinguished. As with anterior tibial position, no significant differences were observed at a significance level of $p < 0.05$. Force levels that had significance at $p \leq 0.063$ are listed in Table 5-3.

Table 5-3: Force Levels at which significant differences in Internal Tibial Rotation angle may be detectable at $p < 0.05$ with a sample size of $n > 5$

Ascending		Descending *	
40 N	89 N	40 N	50 N*
40 N	133 N	40 N	40 N*
89 N	133 N	50 N	40 N*

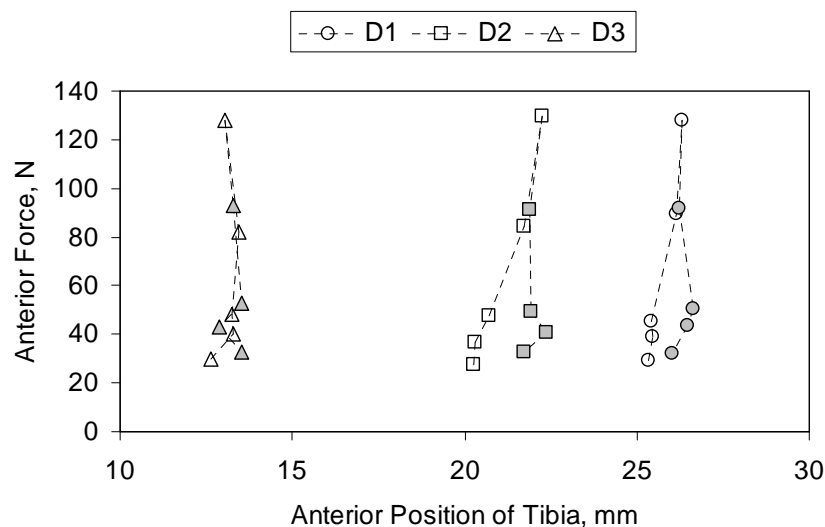


Figure 5-8: KLA Anterior Force-Displacement (S03) showing force ascending (open symbols) and descending (closed symbols) over three test days (D1, D2, D3)

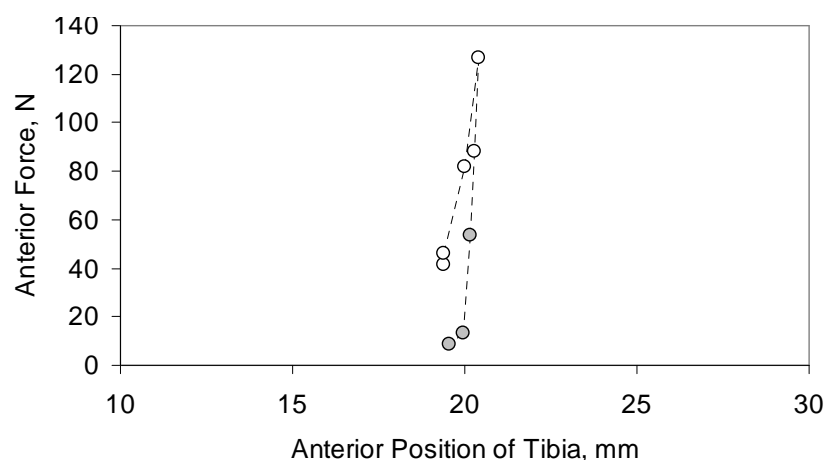


Figure 5-9: KLA Anterior Force-Displacement (S04) showing force ascending (open symbols) and descending (closed symbols)

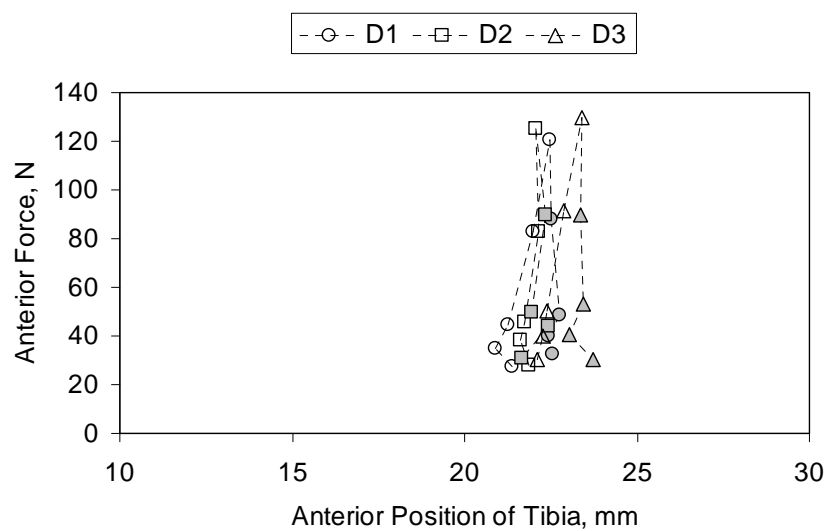


Figure 5-10: KLA Anterior Force-Displacement (S05) showing force ascending (open symbols) and descending (closed symbols) over three test days (D1, D2, D3)

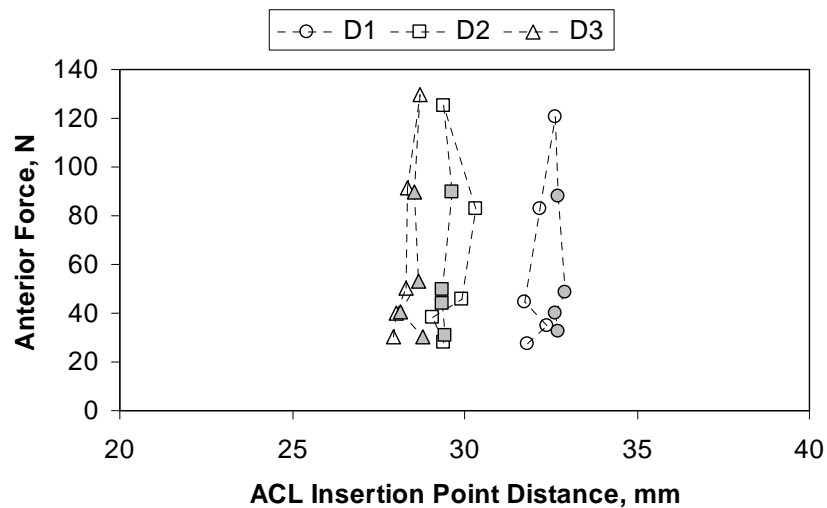


Figure 5-11: Exemplary plot of ACL insertion point distance (S05) across three test days (D1, D2, D3)

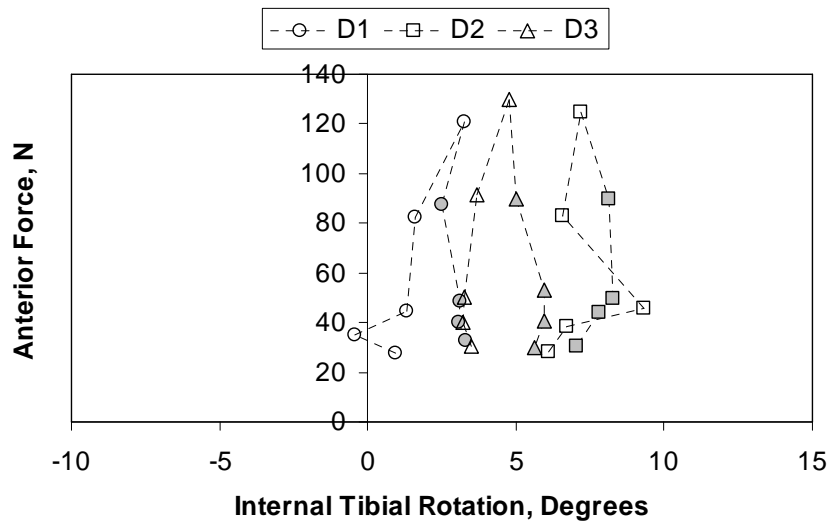


Figure 5-12: Exemplary plot of internal tibial rotation angle (S05) across three test days (D1, D2, D3)

5.3.4 Sources of Error

The registration transformation parameters (X , Y , Z , ω , ϕ , κ) between the high resolution scan and the low resolution scan at the reference position were calculated to determine the error introduced by mapping low to high resolutions scans and possible motion between scans. For the grouped data (both tibia and femur), the transformation parameters were -0.1 ± 1.0 mm, 0.0 ± 1.6 mm, -1.3 ± 1.5 mm, -0.1 ± 0.3 °, 0.0 ± 0.2 °, and 0.2 ± 0.8 ° for X , Y , Z , ω , ϕ , and κ , respectively (Figure 5-13 and Figure 5-14). Subject 5 data from day D3 was not included due to repositioning between high and low resolution scans.

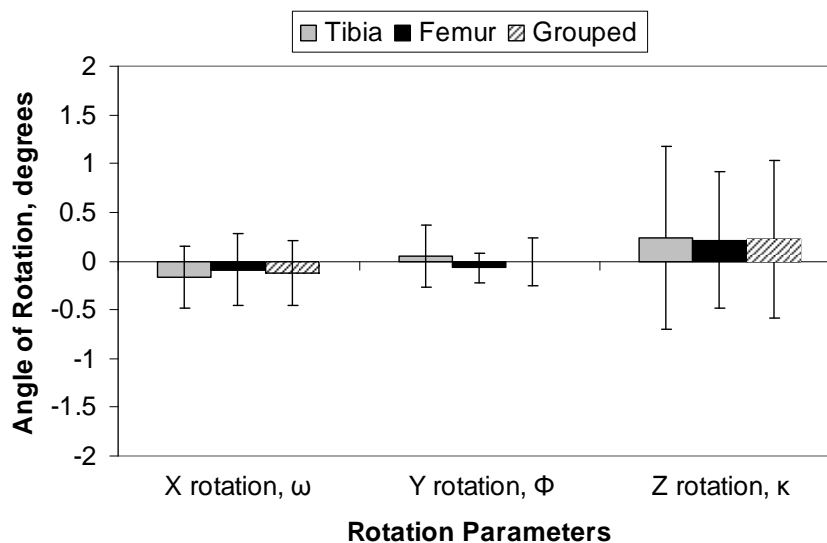


Figure 5-13: Error in rotation parameters due to mapping low to high resolution images and possible subject movement at the reference position

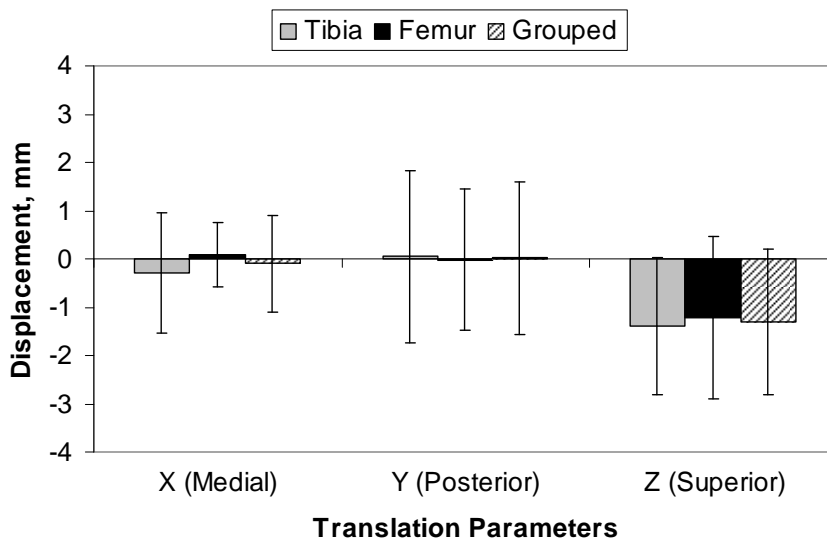


Figure 5-14: Error in translation parameters due to mapping low to high resolution images and possible subject movement at the reference position

The anterior displacement of the joint in the ICS showed evidence of femoral translation. Figure 5-15 shows the typical trend observed for the motion of the tibia and femur in the ICS anterior direction.

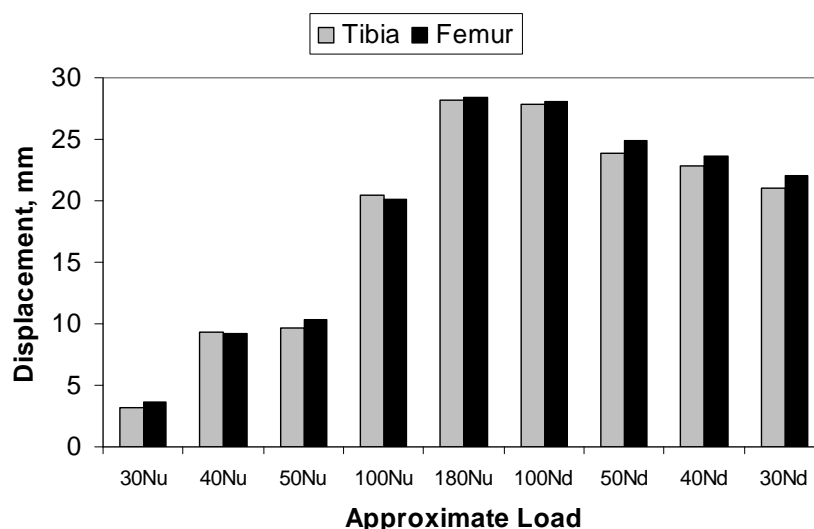


Figure 5-15: Exemplary plot of tibial and femoral translation in the anterior direction of the ICS for S01, normalized to the reference position (Nu refers to ‘Newtons of force on the ascending curve’ and Nd refers to ‘Newtons of force on the descending curve’)

The across day variability of the ACL insertion point locations for both the tibia (Figure 5-16) and the femur (Figure 5-17) were determined. The tibial insertion point showed the most variability in the anterior/posterior (2.74 mm – 4.70 mm) and medial/lateral (1.52 mm – 5.57 mm) directions compared to the superior/inferior direction (0.63 mm – 1.20 mm). The femoral insertion points showed the most variability in the anterior direction (2.00 mm – 2.09 mm) compared to the medial/lateral (0.63 mm – 3.01 mm) and superior/inferior (0.52 mm – 1.79 mm) directions for 2 of 3 subjects. The third subject, S05, showed no clear difference in variability among directions.

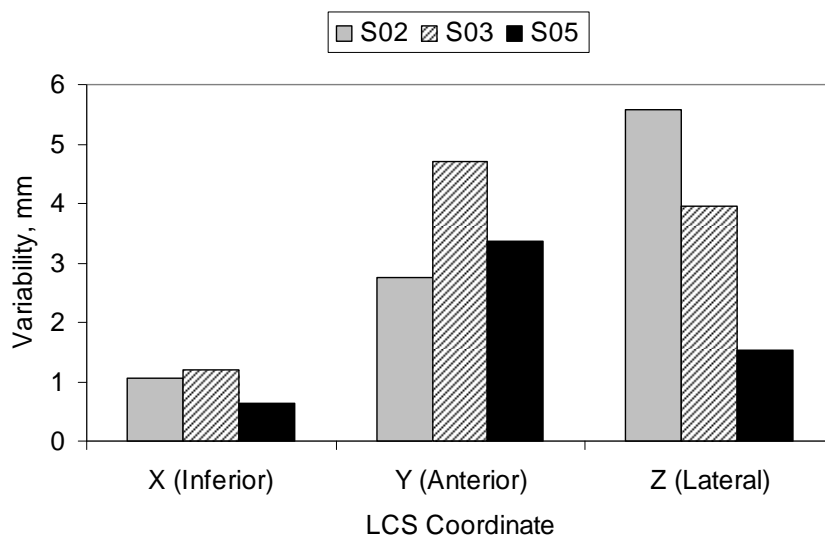


Figure 5-16: Variability of ACL insertion point location for the Tibia in the tLCS

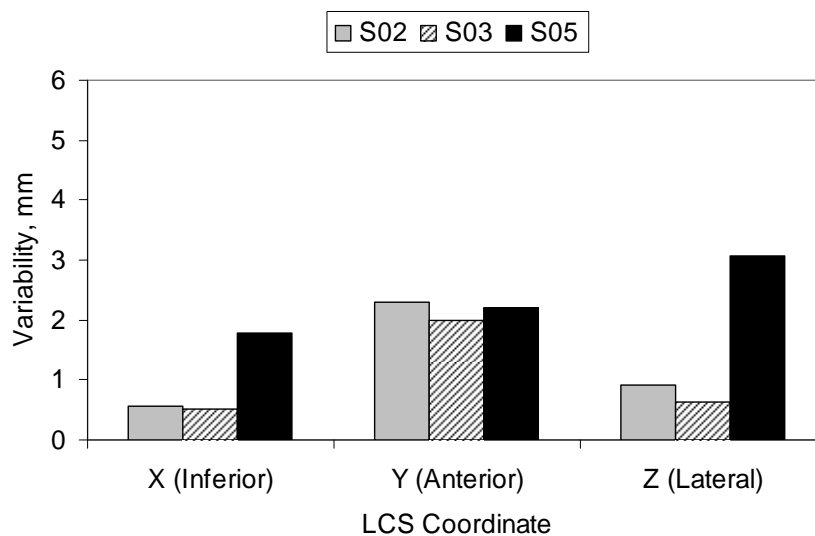


Figure 5-17: Variability of ACL insertion point location for the Femur in the fLCS

Subject movement is also a possible source of error. Although the subjects were trained to relax in EMG testing, some instances of subject movement were noted during MR testing (Table 5-4). This was informally reported by the subjects to be due to falling

asleep or becoming drowsy in the scanner, then waking up in response to the scanner noise, causing a muscle reflex. In the control room, this response was seen as a jump in the force-time curve. The scan was redone if it resulted in blurring of the MR image, based on a qualitative assessment. These force data points were excluded from analysis of stress relaxation. Of approximately 100 loaded MR tests completed, there were six occurrences of subject movement.

Table 5-4: Instances of Movement during MR Scanning

Subject	Day	Load Level	Scan Redone
S01	D1	N/A	N/A
S02	D1	N/A	N/A
	D2	40 N down	No
	D3	40 N down	Yes
S03	D2	40 N up prescan	No
	D3	30 N up	No
	D3	89 N up	No
	D3	89 N down	Yes
	D3	0 N down	Yes

5.4 KT-2000

The KT-2000 force-displacement curves for all subjects are shown in Figure 5-18 to Figure 5-22, inclusive. Although three trials were collected per session, data analysis was performed on the first of three curves, as that is the data used to output values to the clinician. Figure 5-18 also demonstrates the polynomial curve fit that was used to calculate the first and second derivatives of the force-displacement curve. Figure 5-21 highlights the tendency of the force-displacement curve to drift with respect to initial displacement at 0 N over three trials collected during one test session. This supports the selection of the first curve for analysis.

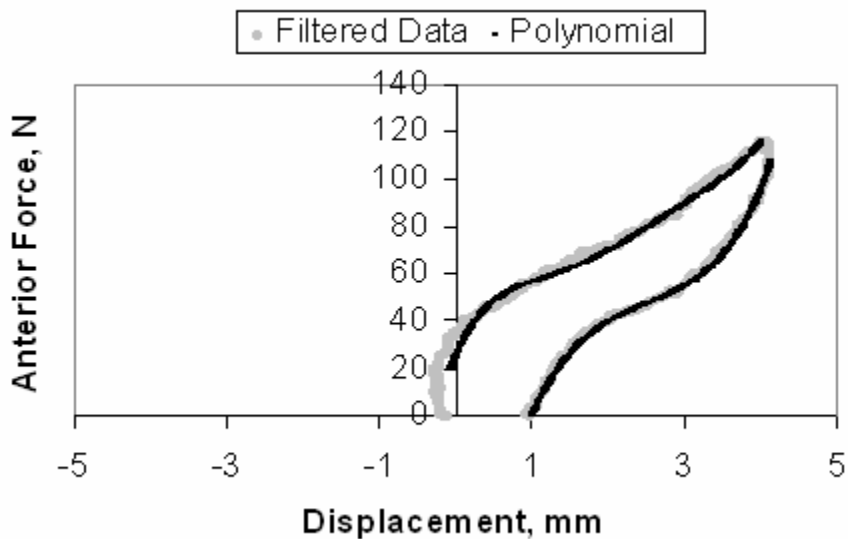


Figure 5-18: KT-2000 Force-Displacement (S01) showing filtered raw data (grey) and the 5th order polynomial fit (black)

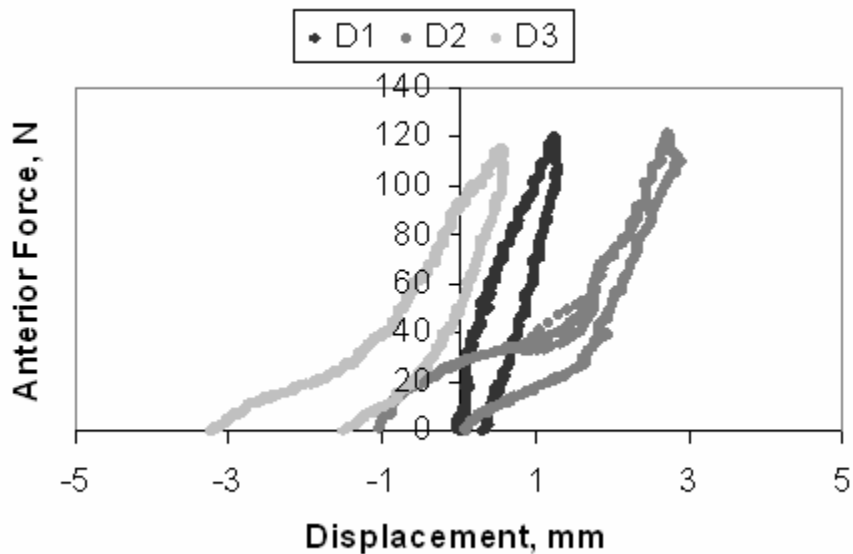


Figure 5-19: KT-2000 Force-Displacement (S02) showing filtered raw data across three days (D1, D2, D3)

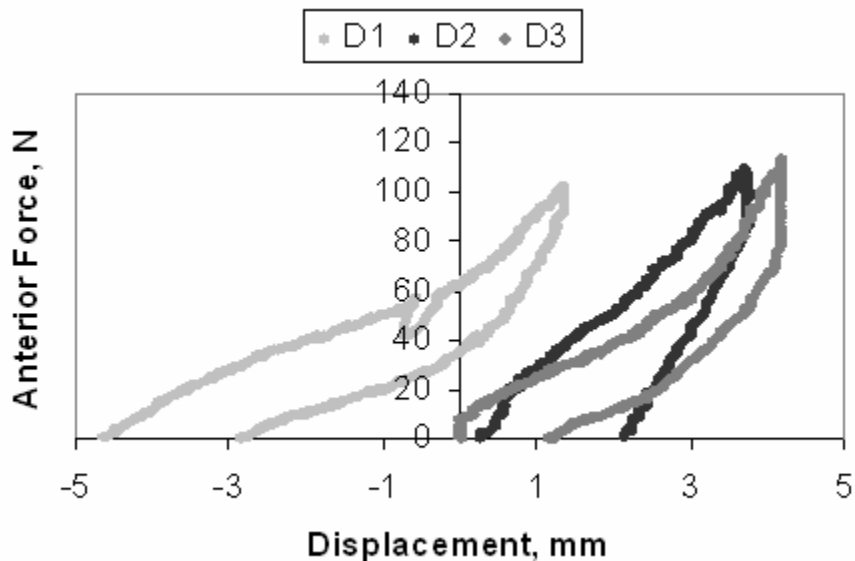


Figure 5-20: KT-2000 Force-Displacement (S03) showing filtered raw data across three days (D1, D2, D3)

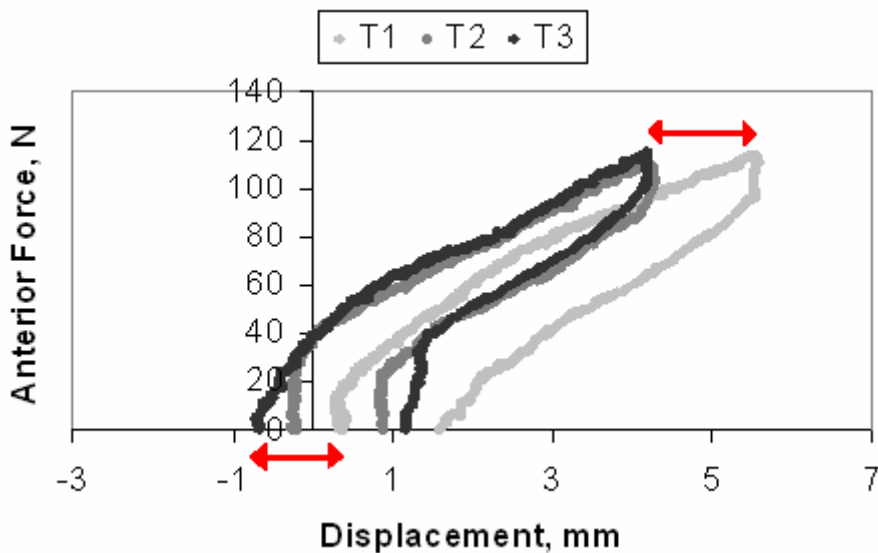


Figure 5-21: KT-2000 Force-Displacement (S04) showing filtered raw data across three trials on one day (T1, T2, T3). A typical shift of data over trials was observed (red). For all subjects, the first full curve (T1) is used to assess KT-2000 data, shifted to 0 mm.

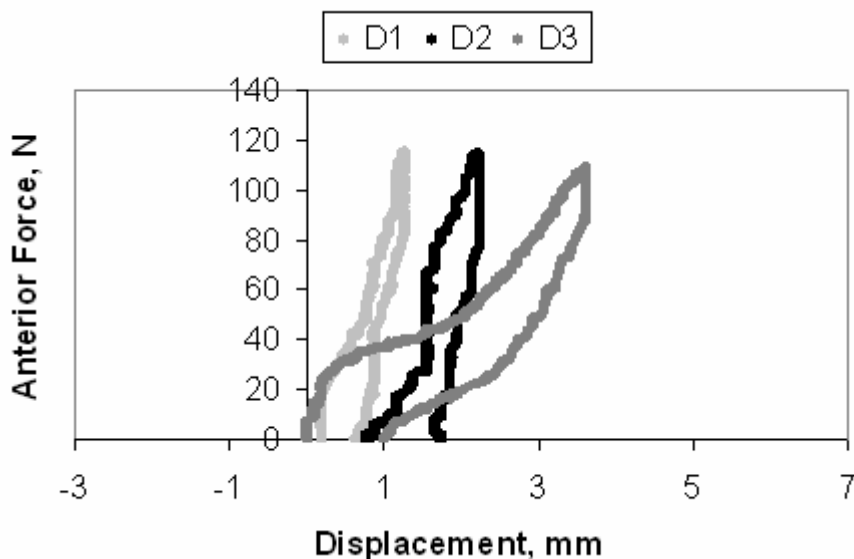


Figure 5-22: KT-2000 Force-Displacement (S05) showing filtered raw data across three days (D1, D2, D3)

To test hypothesis H3, the KT-2000 and KLA values were compared in terms of the displacements at each load level (30 N, 40 N, 50 N, and 89 N ascending and descending) used with the KLA. The 133 N load level was excluded because the KT-2000 did not consistently reach this value (110 ± 5 N). All displacement data was normalized to have an initial displacement of 0 mm to compare the two systems. The KLA force-displacement curve was linearly extrapolated to find the 0 N displacement values for normalization. Four of eleven curves had $r^2 < 0.87$, however, polynomial, exponential, and power curve fits did not improve the quality of fit, and therefore linear extrapolation was used. The first complete curve of the KT-2000 graph was analyzed, as it is used to output values to the clinician. However, the second KT-2000 trials were used for subjects S02 and S03 for days D2 and D1, respectively, because the first curves were incomplete.

Two more analyses were done to assess whether the compliance index or stiffness values for each of the three sections of the curve are more reliable output measures for the KT-2000 (Section 4.8.1).

5.4.1 Displacement

No statistically significant differences were found (all values showed $p > 0.05$) between values found at each load comparing the KT-2000 to the KLA using a non-parametric Wilcoxon signed ranks test (H3). The general trend suggests the KT-2000 displacement value to be larger than the value found with the KLA, however the sample size and variability within individuals limits the statistical comparison.

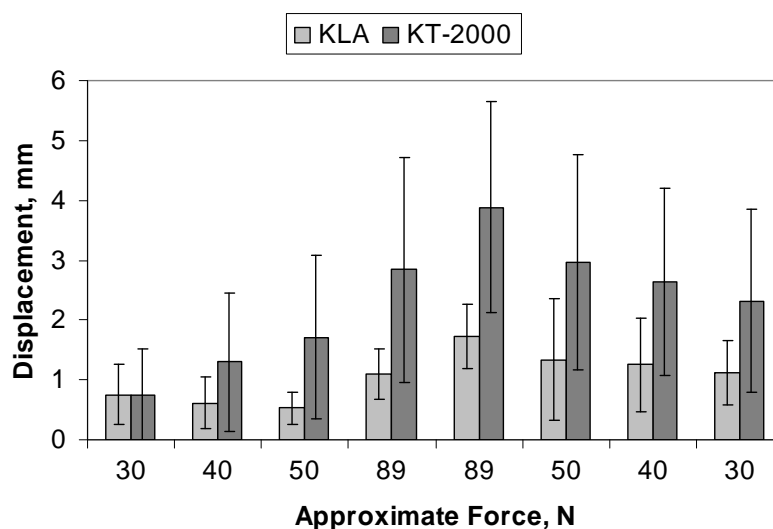


Figure 5-23: Mean displacement at each load level for the KLA and KT-2000 (n=5)

Cronbach's Alpha was calculated for both the KLA (H2) and the KT-2000 as a reliability coefficient by comparing data at each load for the 3 test days (n=3, Table 5-5).

Table 5-5: Cronbach's Alpha Method Reliability for KLA and KT-2000

	Anterior Force, N (ascending)			
Method	30	40	50	89
KLA	-2.492	-0.051	0.015	0.358
KT-2000	0.575	0.408	0.572	0.732
	Anterior Force, N (descending)			
	89	50	40	30
KLA	-1.565	0.196	0.612	-0.948
KT-2000	0.73	0.744	0.719	0.704

Reliability for the KT-2000 using Cronbach's Alpha was >0.70 at five of eight load levels (forces levels past 89 N ascending). In particular, at 89 N ascending, the clinical value of anterior displacement, the reliability was 0.732. The average variability of KT-2000 displacement was 1.47 mm (range 0.49 mm – 1.88 mm). There was no significant correlation between days for the reliability of the KLA method. The average variability of KLA displacement was 0.58 mm (range 0.26 mm – 1.01 mm), a third of the magnitude of variability seen with the KT-2000 (H2, H3).

5.4.2 Compliance Index

The compliance index (anterior displacement from 67 N to 89 N) is another common output measure of the KT-2000 (Figure 5-24). The compliance index for these five subjects ranged from 0.34 mm to 1.36 mm. The reliability of this measure was not significant at 0.661 using Cronbach's Alpha (described in Section 5.3.1). The average variability of this measure was 0.13 mm (range 0.11 mm – 0.15 mm).

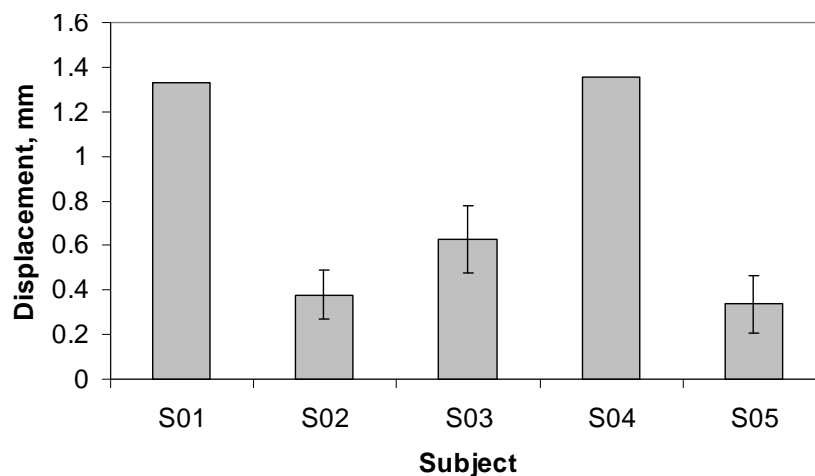


Figure 5-24: KT-2000 Compliance Index

5.4.3 Stiffness

The average stiffness at each of the three portions of the KT curve (initial rise, middle, and linear) were computed. All 2 or 3 curves completed per test session were analyzed for all subjects and across all days. The purpose was to evaluate whether the technique was able to separate the curve for the majority of the KT-2000 data. Of 33 possible curves, 24 curves were successfully separated into three regions. The average slopes of each of the three regions for the first curves (for consistency, or second curves when first curves could not be divided into three regions: S02 D1) were compared using a non-parametric Friedman's test across days (n=3, Figure 5-25). No significant difference was detected ($p > 0.05$).

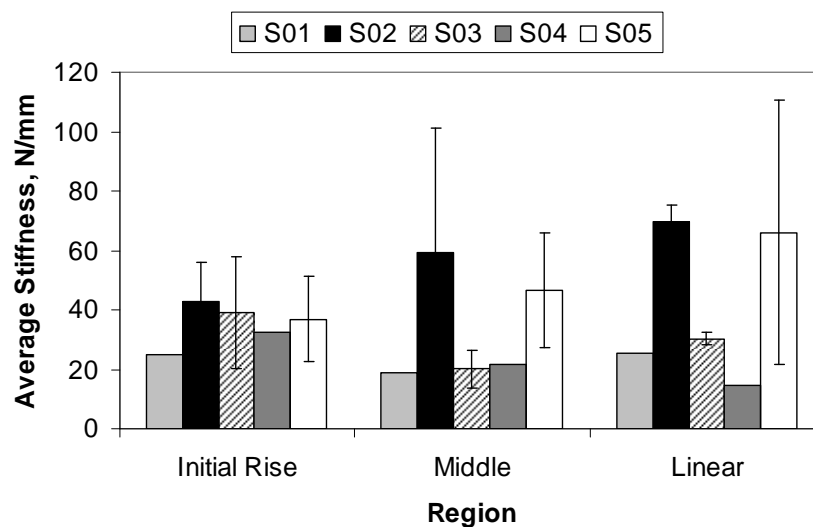


Figure 5-25: KT-2000 average Stiffness for the three regions of the force-displacement curve

In addition, a Friedman's test across the three regions was conducted, to determine whether a difference in slopes by region could be detected ($n=5$). No significant difference was detected ($p>0.05$). The variability in stiffness for subjects S02, S03, and S05 (tested across three days) was ± 13.5 to 18.9 N/mm for the initial rise, ± 6.5 to 41.8 N/mm for the middle region, and ± 2.1 to 44.5 N/mm for the linear region.

5.5 Electromyography

Muscle activation under loading in the KLA was measured outside of the MR Scanner prior to testing (H4). Muscle groups included the quadriceps (VM, VL, RF), the hamstrings (BF, ST), and the gastrocnemius (GM, GL).

5.5.1 Maximum Signal

A series of one-tailed paired t-tests were completed to assess whether the maximum EMG signal as % of MVC while loaded (both load ramp up and sustained loading) was less or greater than 5% (n=5). Data was compared for a given muscle at each load level ($\alpha = 0.05$). The majority of values (maximum EMG signal as % of MVC) were significantly less than 5% with the exception of the VM (0 N, 50 N ascending), VL (40 N, 50N, 133N ascending, 89 N, ramp down to 50 N, 40 N, 30 N, and 0 N descending), RF (40 N descending), BF (133 N ascending, 50 N descending), ST (ramp down to 89 N, 89 N, 50 N descending), GL (0 N, 30 N, 40 N, ramp up to 89 N, 89 N, ramp up to 133 N ascending, ramp down to 50 N, 40 N, 30 N, 0 N), and GM (all values except ramp up to 50 N, ramp down to 89 N, and ramp down to 30 N). At these loads, no statistical difference was found between the mean and 5%. No values were statistically greater than 5%. The key finding is that there does not appear to be a loading effect on muscle guarding, and that across subjects, no significant muscle activity was detected. Considering the limitations of statistical tests with an n=5 sample size, outliers should be pointed out for individual subjects. Data across loads was averaged, and plots for maximum EMG signal as % of MVC are shown for each subject across muscles (Figure 5-26).

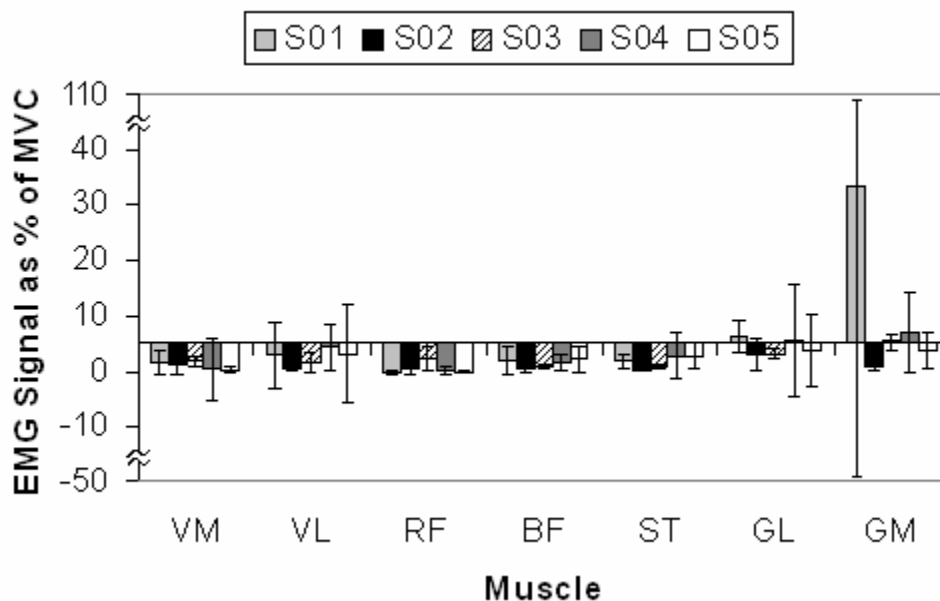


Figure 5-26: EMG signal as % of MVC for all muscles (VM, VL, RF, BF, ST, GL, GM) for all subjects (n=5). The X-axis crosses the Y-axis at 5%

A large EMG signal as % of MVC was observed for the GM in subject S01. The muscle activity occurred during load ramp up to 133 N (220% ascending) and ramp down to 0 N (347% descending). The fact that the values are >100% suggests that the technique for obtaining the MVC for the gastrocnemius may not have yielded the true MVC in all cases. Figure 5-26 also indicates subject specific EMG signals between 5% to 30% of MVC were seen but typically did not represent the average. The exception to this was for subjects S01 and S04 for the gastrocnemius (GL and GM), with an average maximum signal > 5%. This could indicate a trend of gastrocnemius contraction, or reflect the low MVC values for this muscle group.

5.5.2 Average Signal

The average signal over the load ramp up and sustained loading was also assessed. Data was compared for a given muscle at each load level ($\alpha = 0.05$) with a paired, one-sided t test. At all load levels, the EMG signal as a % of MVC was significantly less than 5%, with the exception of the GM at the ramp down to 0 N (descending) where no significant difference was detected (ie: neither significantly greater or less than 5%). The value that was an outlier at this load was for subject S01. The average signal over this trial was $41\% \pm 75\%$. This result suggests that for subject S01, muscle guarding was sustained during ramp down to 0 N. For all other subjects, muscle guarding was not sustained over the trial at any load level.

5.6 Stress Relaxation

Evidence of stress relaxation was observed in the force-time plots recorded while stepped loading was applied. The input force was modulated by the tester to reach the target force, and then a valve was closed. From this point, the output force degraded exponentially in a classic stress relaxation curve. The exponential fit (Equation 4.17) was $r^2=0.98 \pm 0.01$, and yielded at time constant τ_1 . An exemplary plot shows the reduced relaxation function $G(t)$ found for one subject at one force level (Figure 5-30).

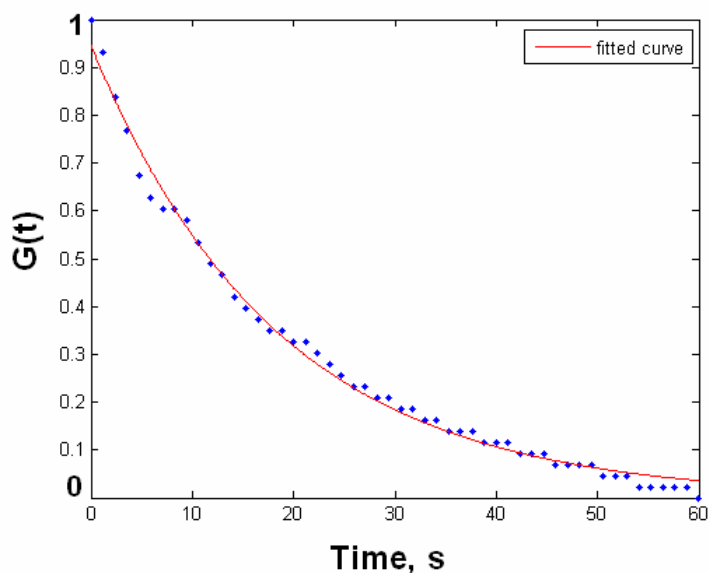


Figure 5-27: Exemplary Stress Relaxation Curve showing $G(t)$ (fitted curve, red) and the raw data (blue)

To accommodate the stepped loading (Section 4.7), the $G(t)$ function was normalized over a 0-1 range ($G(0)=1$, $G(t=t_{\max})=0$) rather than just to peak force ($G(0)=1$). This normalization purposefully removes the effect that the previous stepped loading will have on the subsequent curve. A plot of the time constants against anterior force shows no correlation between the two variables. However, without normalization, the variability of force over a given 1 minute interval of stepped loading showed a general, although weak, trend (linear $r^2=0.5422$) of increasing variability with ascending load (Figure 5-29). The variability in force over 1 minute ranged from ± 0.70 to ± 5.50 N. The length of time that a force was held was 78.8 ± 11.0 s.

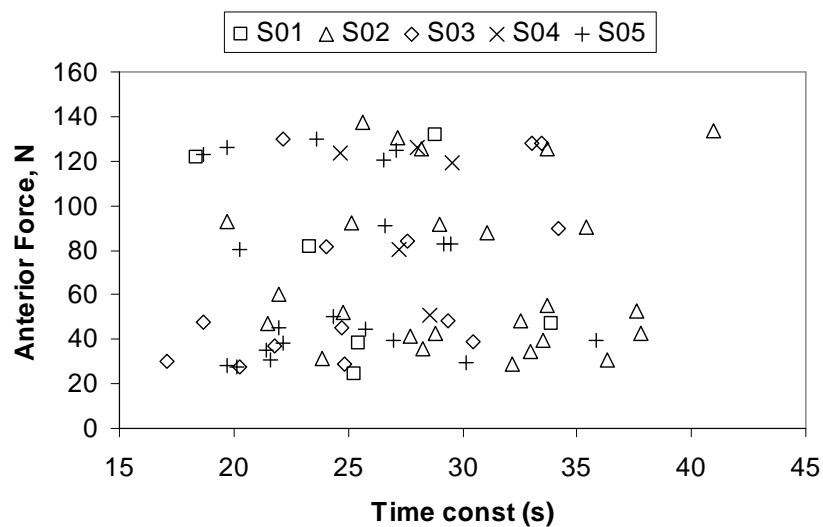


Figure 5-28: Distribution of time constants indicates no correlation with anterior force

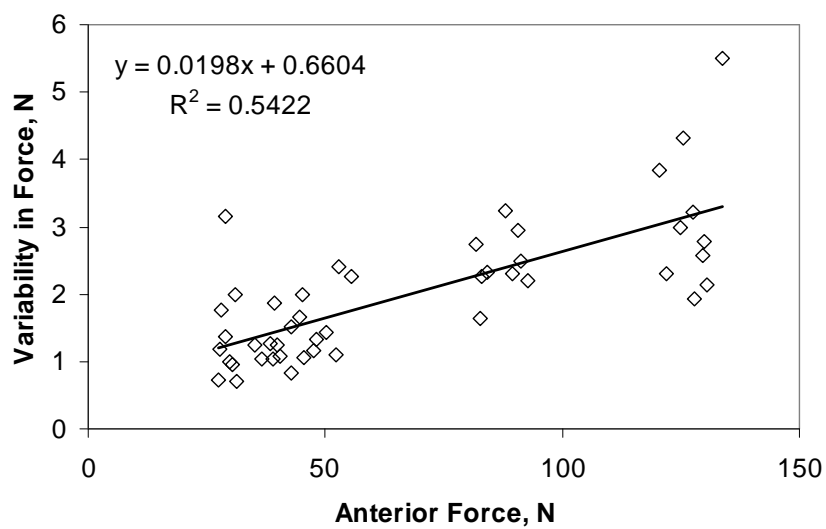


Figure 5-29: Variability in force over 1 minute scan length shows a general increase with anterior force during ascending loading

The average time constants for all subjects during MR testing are shown (Figure 5-30). Subjects S04 and S01 show data from the EMG session (due to system crash during MR data collection, Section 4.7); therefore a constant displacement could not be confirmed indirectly from MR images for those subjects. MR images were reviewed, and no evidence of motion artifacts were seen.

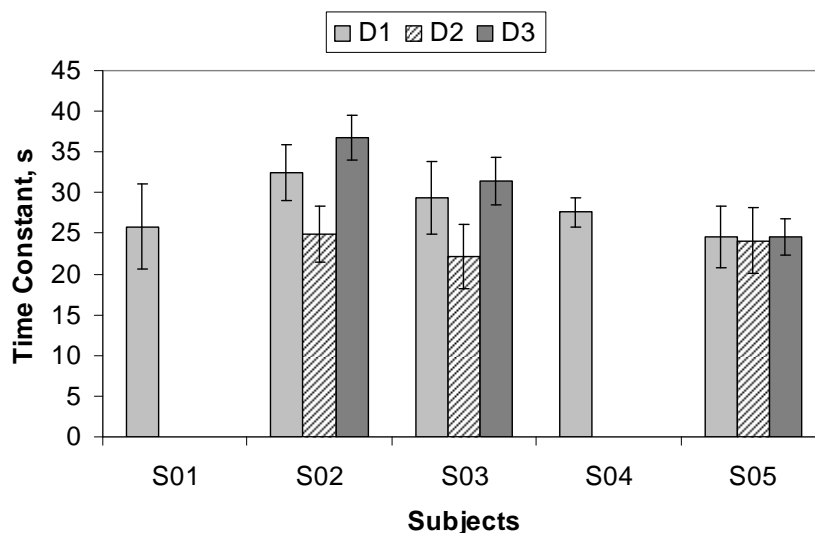


Figure 5-30: Stress relaxation time constants for all subjects across days (D1, D2, D3)

A non-parametric Friedman's test was done for the time constants of repeatability subjects. It was found that there was a significant difference in time constants between days ($p=0.028$). Wilcoxon signed ranks tests were used to discern which day the differences were found. Significance was not reached for these tests, but suggested that the Friedman's test was detecting differences between D1 and D2, and D2 and D3 ($p=0.125$). The average time constant for all normal subjects on day D1 was 28.3 ± 2.9 s. The range of variability seen within a subject and within a day was ± 1.8 to ± 4.7 s.

Chapter Six: Discussion and Future Work

The long term research goal is to advance understanding of the relationships between joint mechanics and joint health, and between joint structure and dynamic joint function. To better understand how the quasi-passive structures of the knee joint play a role in joint function, the mechanical properties of the joint and soft tissues must be precisely quantified. This study presents a novel technique to quantify non-invasive, *in-vivo* knee joint laxity. Laxity is defined as the anterior displacement of the knee joint under an external load. Applying an anterior external force to the tibia primarily tests the ACL, a main supporting ligament of the knee that opposes anterior tibial translation and internal rotation. In this study, a loading apparatus, the KLA, was designed to position the limb and apply the anterior force while obtaining MR images of the knee joint. The following hypothesis were tested to evaluate the KLA:

Hypotheses: The novel MR-based measure of laxity and incorporated knee model will be tested on normal subjects through the following hypotheses:

H1: The loading apparatus will have repeatable positioning and load application

H2: Joint and ACL insertion point displacement will be repeatable (± 0.5 mm) for a given applied load. The force-displacement curves will show increasing displacement with increasing force.

H3: Force-displacement curves found using novel technique will be less variable and differ from those using the KT-2000.

H4: Subjects will be capable of muscle relaxation in the loading apparatus such that the electromyography (EMG) signal will be less than 5% of manual maximum contraction in all muscles.

The KLA was designed and evaluated as defined in the following specific aims:

Specific Aim 1: Design an MR compatible loading apparatus that applies an anterior load to the knee (H1).

Specific Aim 2: Apply a registration technique to MR images to observe 3D joint motion and change in ACL insertion point location (H2).

Specific Aim 3: Measure *in-vivo* joint response (displacement and time-dependent phenomena) to applied stepped forces. (H2, H4).

Specific Aim 4: Investigate repeatability of force-displacement curves in normal subjects (n=3) over 3 trials (H2, H3).

Specific Aim 5: Use EMG to evaluate the ability of subjects to avoid muscle activation during knee joint loading (H4).

6.1 KLA Design

The design of the KLA (Chapter Three), an MR compatible device constructed from wood, plastic, and brass, satisfied Specific Aim 1. The KLA attempts to improve over other laxity measurement devices by reducing the system dependence on the tester. The KT-2000, for example, requires the tester to position the subject with a moveable thigh support and foot brace. Obtaining a consistent limb position, and ultimately a repeatable measure of joint laxity is highly dependent on the ability of the specific tester (Huber, et

al., 1997). The magnitude and direction of the force is also applied by the tester through the force handle. Although the tester pulls primarily in the anterior direction, out of plane forces could be applied inconsistently. These characteristics are likely the main contributors to the low inter-tester repeatability that has been documented in the literature (Huber, et al., 1997).

6.1.1 KLA Subject Positioning

When designing the KLA, providing consistent loading and positioning (DC6, DC7) was a critical factor as reflected in the first hypothesis (H1). To assess the consistency of subject position in the KLA, three main variables describing the initial tibial position were assessed: anterior position, internal rotation angle, and initial ACL insertion point distance. The results indicate that the initial anterior tibial position and initial ACL insertion point distance were reliable for the KLA ($\alpha_c = 0.89$ and 0.90 , respectively), but had variability across days of $\pm 0.4 - 6.4$ mm and $\pm 1.0 - 2.3$ mm, respectively. This variability is within the order of magnitude of the difference in position and length observed across the entire force-displacement curve. This indicates that although Cronbach's alpha indicated a reliable variable, it did not reflect a low variability. Reliability coefficients should be interpreted not only within the standard threshold ($\alpha_c > 0.70$) indicating a reliable measure, but also within the variability of the data.

Initial internal tibial rotation angle was not reliable ($\alpha_c = -3.11$). Interestingly, the data suggested a possible positive linear relationship between initial internal rotation angle and initial anterior position. This was observed strongly for subject S02 ($r^2 = 0.97$) but

less so for subject S03 ($r^2=0.60$). Subject S05 showed a trend of constant anterior tibial position with increasing initial internal rotation angle ($r^2=0.41$). This subject showed the least variability in initial internal rotation angle ($\pm 2.6^\circ$) compared to subjects S02 ($\pm 5.7^\circ$) and S03 ($\pm 5.5^\circ$). The literature supports this possible positive relationship between internal rotation and anterior tibial translation. In a study by Logan et al (2004b) tibiofemoral contact patterns in MR imaging were investigated for knees tested with the clinical Lachman knee laxity test. For normal subjects, an increase in internal tibial rotation (seen as an increased translation of the lateral tibiofemoral contact point in relation to the medial contact point) was coupled with an increase in anterior tibia translation.

Multiple studies have investigated tibiofemoral contact patterns in MR imaging with increasing knee flexion (Scarvell, et al., 2004; Shefelbine, et al., 2006; Wretenberg, et al., 2002). Increased internal tibial rotation was observed with increased flexion angles for all studies at 0 to 30° of knee flexion. In this current study, knee flexion angle varied by $\pm 0.48^\circ$ to $\pm 1.71^\circ$ over the course of a complete test. Wretenberg et al (2002) found that the tibia rotated internally by 1.7° between 0° and 30° of knee flexion. Simplifying this to a linear relationship between knee flexion angle and tibial rotation, the effect of the knee flexion angle variability observed with the KLA would affect internal tibial rotation in the order of $\pm 0.03^\circ$ to 0.10° . Even accounting for the fact that cartilage contact points tend to have less anterior excursion than bony geometry (DeFrate, et al., 2004), a fourfold increase of the estimate for the KLA knee angle variability effect is $\pm 0.1^\circ$ to 0.4° . Using this logic, we can indirectly conclude that the KLA was effective in maintaining a

relatively constant knee flexion angle during loading, such that internal tibial rotation was not greatly affected.

A limitation of the test method was the assumption that the initial knee angle was 30° , based on the goniometer measurement. Future studies should capture a longer portion (more distal) of the tibial shaft by increasing the FOV of the knee joint with respect to the tibia. This will ensure that the initial knee flexion angle can be obtained from bony geometry and not a goniometer, which has less accuracy (Jagodzinski, et al., 2000). The optimal solution would not reduce image resolution to gain the additional geometry. To do so, two options are available. First, a second scan of the more distal portion of the tibia could be taken and registered to the first scan in the reference position.

Alternatively, the number of phase or frequency encoding steps in the k matrix can be increased as the FOV is increased, such that pixel resolution is maintained. From this study the efficacy of the KLA to reliably position the subject at an initial knee joint angle of 30° , can only be assessed within the error of the goniometer [$3.92 \pm 1.41^\circ$ (Jagodzinski, et al., 2000)]. Based on the estimate from Wretenburg (2002), and accounting for the findings in Defrate (2004), the error in the initial knee angle could have affected the internal tibial rotation angle by $\pm 0.6^\circ$ to 1.2° . With respect to initial internal rotation angle, knee angle, and anterior tibial position, the variability in the initial limb position should be addressed in future studies. Initial limb position has been identified as a limitation of the current KLA test method.

An additional source of positioning error was femoral translation (Section 5.3.4). The femur was constrained to allow relative anterior tibial translation at a constant knee angle. A balance was struck when securing the femur, to reduce possible motion but to ensure comfort, circulation, and a slack patellar tendon. In the global ICS coordinate system, the femur translated anteriorly to a maximum of 2.8 cm from the reference position. The variability in knee joint angle may be reduced by minimizing this effect in future design iterations for the KLA. The technique employed in the KLA design was an overall distribution of the force with a stiff wrap. Conceivably, a thigh restraint that increases the force distribution of the thigh strap may allow higher pressures (and thus more constrained positioning) to be applied to the femur without sacrificing subject comfort.

Based on the study results, the second design iteration of the KLA should aim to reduce the variability of the initial limb position (with respect to internal tibial rotation angle and anterior tibial position). One possible way to achieve this is to develop a real time limb positioning feedback system. If the techniques used to define the joint surfaces (digitization, TPS, registration, and coordinate system transformations) are automated, they could be implemented by inputting a low resolution MR scan taken at the beginning of a test session. Real time feedback would allow the tester to adjust the tibia to a standardized initial limb position, and confirm the accuracy of this position with a second iteration. Additional features could be added to the KLA to assist with this, such as a foot constraint that would rotate about the long axis of the tibia and be secured in position.

6.1.2 Force Application

Normal subjects were tested at nine load levels (30 N, 40 N, 50 N, 89 N, 133 N ascending and descending). When testing with the KLA, the ability to reach a target force value repeatedly is important because the KLA tests at discrete force levels rather than a continuous force curve (eg: KT-2000). The original concept for the KLA data analysis was to fit a curve to the data points and to interpolate data for direct comparisons at equal force levels. However, it was found that linear curve fitting was only successful, based on r-squared values of greater than 0.87, in seven of eleven KLA force-displacement curves. As design iterations progress in future work on the KLA, curve fitting may prove to be a valuable technique for interpolating between force-displacement data. As seen for the KT-2000 data analysis, fitting a 5th degree polynomial to the force-displacement curve allowed derivatives to be calculated (stiffness and change in stiffness) without amplifying noise effects by differentiating the filtered data (Section 4.8.1). If the goal is to construct a single force displacement plot for a single subject, then reliability of force application is not a concern. Rather, ensuring a well distributed selection of test force levels will allow a force-displacement curve to be constructed. For comparisons between subjects or populations, equal force values will be important if a curve fit is not possible. A reliable curve fit would allow the comparison of interpolated values.

Another possible limitation of this study was the force model assumption at the hinge of the KLA. The force model assumes (based on calibration tests) that the horizontal (F_x) and vertical (F_y) forces at the hinge are proportional. The scope of this study was such that this assumption was not explicitly tested beyond the values calculated during

calibration. Future studies should evaluate the validity of this assumption. Possible methods include an instrumented joint specimen or test object that will allow the forces and moments at the joint end to be measured. A back-calculation can be done to solve for F_x and F_y , resulting in a plot of the F_x/F_y ratio at different external loads. A comparison of the assumption to measured values may result in improved accuracy in applying target loads.

In general, results showed that lower loads were more reliable. The non-parametric Friedman's test was unable to detect differences for a given load value over three test days, although the limitations of the statistical methods were noted given the small sample size ($n=3$). The variability seen in the force (based on an average force calculated for a given stepped load) was ± 0.52 N to ± 6.0 N. This variability is different than the variability in force over the one minute scan duration, which was ± 0.70 to ± 5.50 N. Qualitatively, it was more difficult for the tester to achieve the target load at higher loads than at lower loads. At high loads, when the tester pushed the piston, an initially high load would rapidly drop before the valve could be fully closed. This was due to difficulty holding a high load constant with the piston in one hand, and turning the valve with the other. When the valve was closed, the force data would slowly degrade over time. A clear edge could be detected in the force-time plots where the valve went from opened to closed. All analyses of force data were done from the point where the valve was closed.

Ideally, testing at a target force would be highly reliable at all load levels. The logical way to achieve this is to remove tester influence on force control. A design improvement

would be an automated motorized feedback system (Robu, 2007) that would adjust the piston position, thereby controlling system pressure. The feedback mechanism would be the real-time voltage from the pressure transducer, calibrated to the target force, designed to reach a desired target force within a specified threshold. A non-automated system was designed in a separate parallel MR study (Robu, et al., 2007), that used a crank system to modulate the hydraulics. Future studies could, as a minimum, apply this mechanism to better control force input.

6.2 Three Dimensional Joint Motion and ACL Insertion Point Distance

MR Imaging was used to quantify the gross joint displacement and ACL insertion point displacement. Specific Aim 2 was accomplished by successfully applying a registration technique (Cheng, 2006; Habib, et al., 2001) to observe the gross joint motion and ACL insertion point distance across load levels. This registration technique was previously applied to MR images by Cheng (2006) for the patella and the femoral bone along the articulating surfaces. The current study extended this application to include the tibial plateau to quantify the relative motion between the femur and the tibia in 3D. The primary advantage of using a registration technique is that a high resolution image can be taken of the knee in a fixed reference position. The high resolution detailed bony geometry is used to define coordinate axes, and the low resolution images are used during loading. Generally, an increase in image resolution causes an increase in the length of the scan time. For a measurement of laxity, the scan time should be minimized to reduce the effect of stress relaxation (Section 6.3.2). The registration technique enables low resolution scans to be used at the loaded conditions, thereby reducing scan time while

achieving high position accuracy. The registration technique has been shown to match joint surfaces with 1/3 of a pixel size (0.2 mm), and with an absolute registration accuracy of 1 pixel (0.54 mm) (Cheng, 2006). In the current study, a comparison was made between the high resolution and low resolution transformation parameters (X, Y, Z, ω , ϕ , κ) at the reference position. For the grouped data (both tibia and femur, excluding subject S05), the transformation parameters were -0.1 ± 1.0 mm, 0.0 ± 1.6 mm, -1.3 ± 1.5 mm, -0.1 ± 0.3 °, 0.0 ± 0.2 °, and 0.2 ± 0.8 ° for X, Y, Z, ω , ϕ , and κ , respectively. This represents the combined error introduced from the registration technique, digitization, and TPS, combined with possible minor subject movement in the MR scanner. Overall, these findings strongly support the notion that the registration technique provides an extremely accurate and quantifiable approach for working with MR images of different resolutions.

The high resolution images are used to define embedded coordinate systems in the tibia and femur. This is an important element of the methodology, as a measure of anterior tibial translation has been shown to be sensitive to the joint coordinate system definition, yielding average differences of 4.2 mm (Beardsley, et al., 2007). However, Beardsley, et al. (2007) defined coordinate systems by identifying bony geometry in lateral radiographs. The intertester repeatability was 1.8 to 3.3 mm for location of an anatomical point. In the current study, tester input is minimized by only requiring the selection of the data to be used to define the axis of the tibia and femur, the sagittal slices used, and the initial guesses for circle fit points for the flexion facet centers. In comparison to Beardsley, et al. (2007) the variability in the origin point location for this study ranged

from 0.26-0.47 mm for intra-tester repeatability, and in a study from our research group (Fjeld, 2007), inter-tester repeatability was 0.79 ± 0.42 mm.

Kinematic crosstalk can occur when solving for joint rotations if the defined coordinate system is not oriented parallel to the true axis of rotation (Ramsey and Wretenberg, 1999). In this study, the ability of the tester to consistently define the coordinate system was assessed (Section 4.4.2). Variability in axis definition was 0.3° for the femoral long axis and 3.69° for the tibial long axis. The tibial long axis variability could be reduced in future studies by imaging a longer portion of the tibial shaft. The variability in the origin point location ranged from 0.26 to 0.47 mm. The ability to repeatedly locate the LCS origin appears to be improved by removing tester dependence, which propagates to reduce translation errors associated with variability in coordinate system origin definition. The existence of kinematic crosstalk is potentially a limitation of this study.

In future work, the registration technique could be particularly useful if the KLA is used with cine phase-contrast MR Imaging, or fluoroscopy (DeFrate, et al., 2004; Sheehan and Rebmann, 2003). In the literature, techniques have been used to match static MR images to fluoroscopic images collected during dynamic tasks (DeFrate, et al., 2004). With these systems, the KLA could be used to administer a continuous knee laxity test (similar to the rate of anterior displacement observed with the KT-2000). This would have the benefit of reducing a stress relaxation effect, allowing a continuous force-displacement curve to be captured. However to clarify, the current study cannot delineate whether a stepped-loading laxity test (eg: KLA) results in different laxity values compared to a continuous

laxity test (eg: KT-2000), due to small sample size (Section 6.3). In addition, if a difference could be detected, it would be difficult to delineate the cause, be it loading method (continuous versus stepped) or uncontrolled variables leading to error with the KT-2000 (eg: out of plane force application or initial limb position).

6.2.1 Joint Displacement

Specific Aim 3 was achieved by applying the KLA design and method to a group of normal subjects (n=5). Specific Aim 4 was achieved by conducting repeated tests, on three subjects over three days (monthly). Total body water was shown to vary minimally, at most by 1.1 L for a given subject. However, it is not known at this time how variations in total body water filter through to affect the joint and ligaments. Challenges remain in accounting for a variety of variables that may affect laxity outcomes, such as inflammation, particularly in pathologic subjects where complex biological responses may be present. Force-displacement curves were constructed from the anterior tibial position, obtained from the 3D joint position of the femur relative to the tibia. The force-displacement graphs for all subjects appeared to have a trend of increasing anterior tibial position with increasing load. This was the expected result, based on typical force-displacement curves (Section 2.6.1.1). In the literature, force-displacement curves exhibit an increasing displacement with increasing force (Daniel, et al., 1985a). The descending portion of the curve exhibits a hysteresis, due to the viscoelastic properties of the knee joint that exhibit an energy release during unloading (Woo, et al., 1999). Laxity values in normals for the right knee with the KT-2000 at 89N were found to be 5.5 ± 1.8 mm (Daniel, et al., 1985a).

In the current study, a significant difference was found when comparing anterior tibial position at different loads. When individual paired tests were applied to delineate which loads show significant differences, no significant differences were found. This was due to the small sample size, as a number of p values were $p=0.063$ for samples where all values in load 1 had a rank of 1 and all values in load 2 had a rank of 2. Thus, $p=0.063$ was the smallest achievable p value for $n=5$. The discussion includes the displacement and rotation values that had a significance of $p=0.063$, however, the reader should remain aware of the statistical limitations.

For anterior tibial position, the results suggest a trend showing differences in displacements between the low loads (30 N, 40 N, 50 N) and high loads (89 N, 133 N) can be detected on the ascending portion of the curve. Furthermore, results suggest that displacements at 89 N and 133 N can be differentiated, but displacements at the low loads cannot. Along the descending curve the displacements can be detected when compared to the ascending portion of the curve, with the exception of displacements at 133 N. This result reflects the hysteresis trend observed in the force-displacement curves. The knee joint is viscoelastic and as such will dissipate energy when released after stretching (Woo, et al., 1999). This is seen as a hysteresis in the force-displacement curve. The KLA successfully loaded the joint such that this behavior was captured in the force-displacement curves.

Considering individual test subjects, subject S05 exhibited the most repeatable curves across three test days, based on the plots shown in Section 5.3.3. This may be linked to

the initial position, discussed in Section 6.1.1, which was most consistent for subject S05. This result supports the concept that obtaining a consistent initial limb position, especially with respect to internal tibial rotation angle, is a key element for consistent laxity testing.

A significant difference was also found between internal rotation angles at different loads. Force-internal tibial rotation plots showed a general trend of increased rotation with increased loading. Statistically, no differences could be detected between loads for $p < 0.063$ when conducting paired Wilcoxon rank tests. At $p = 0.063$, only rotations at 40 N could be detected as different from rotations at 89 N and 133 N (ascending), and 40 N and 50 N (descending). Additionally, rotations could be differentiated at 89 N and 133 N (ascending), and at 50 N compared to 40 N (descending). Internal rotations were too variable ($\pm 4.0^\circ$ to 5.3°), with the exception of 40 N, for differences to be seen between the rotation angle at the low loads and 133 N. Internal rotations were also undetectable amongst the low loads. These results further support the importance of a consistent initial limb position.

This study has provided pilot data that allows a power calculation to determine the number of subjects required to detect changes within ± 0.5 mm (H2) across a sample population of normal subjects. Based on the sample standard deviation of ± 2.8 mm at $\alpha = 0.05$, the required sample size is 124. Conducting a study of this size would enable characterization of normal force-displacement behavior of the knee joint. Subject groups could be compared to the normal population, which would add value in distinguishing the

differences between them. The value of 0.5 mm as a desired accuracy is that it allows clinically relevant laxity differences to be deciphered. A side to side difference of 3 mm of laxity at 89 N is generally considered indicative of ACL disruption (Daniel, et al., 1985b). An ACL deficient group would be on the high end of the spectrum of laxity, representing the maximum anterior tibial translation that would likely be tested. A gold standard device should be, as a minimum, an order of magnitude smaller than the difference looked for, which would be between 0.1 and 0.5 mm.

6.2.2 ACL insertion

The ability to gain additional information from joint geometry, such as 3D ACL insertion point distance, is a key feature of the novel KLA measure of joint laxity. The use of MR imaging allows definition of soft tissue geometry. The ACL is the main structure that resists anterior tibial displacement and internal tibial rotation (Butler, et al., 1980). Consequently, it is of interest to quantify the behavior of the ACL, the primary structure being evaluated, under anterior loading *in-vivo*.

A main contribution of this study is the application of existing concepts for estimating ACL length (Sheehan and Rebmann, 2003) to assess laxity at a ligament specific level non-invasively. To our knowledge, no studies have looked at *in-vivo* ACL displacement or strain of the knee while undergoing an anterior knee laxity test. Previous studies have used MR imaging to evaluate the Lachman test (Logan, et al., 2004b) but did not go beyond the level of anterior displacement, measured in the ICS from one sagittal image. A study by Sheehan and Rebmann (2003) looked at ACL strain at varied knee angles

with a technique that included measuring the distance between insertion points. Finally, multiple studies have measured ACL strain invasively with devices such as the Differential Variable Reluctance Transducer and the Arthroscopic Strain Analyzer (Cha, et al., 2000; Fleming and Beynnon, 2004).

Fleming and Beynnon (2004) published a review article on strain measurements, and highlighted some limitations of measuring ACL insertion points from MR images, particularly in reference to the study done by Sheehan and Rebmann (2003). First, anatomical landmarks must be properly identified and these landmarks must be consistent over the range of motion tested. In the current study, the application of the registration technique allows consistent landmark detection over the range of motion, as the ACL insertion points were only defined once in the reference high resolution image. Second, Fleming and Beynnon (2004) identify that the ACL is assumed to remain straight and does not wrap around bone (eg: roof of the femoral notch) as the knee flexes, and does not interact with the PCL. That same assumption was made for the current study. However, as the range of joint motion is small, error introduced with this assumption is likely small. This assumption could be tested in future work by digitizing the ACL, PCL, and bone, and looking for possible geometric interference between the three.

The average ACL length estimation, based on ACL insertion point distance at 30 N, ranged from 28.1 ± 2.6 mm to 28.5 ± 2.9 mm. Comparable values were reported in a study by Cha et al. (2000), where the average ACL length in 59 subjects, measured during surgery, was found to be 27.23 ± 4.40 mm. Variation amongst normal subjects in femoral and tibial insertion points varies in the anterior/posterior direction by an order of

1.1 mm and 1.6 mm, respectively (Colombet, et al., 2006). The variability associated with identifying the ACL insertion points was assessed. The tibial insertion point was identified in the sagittal MR slices, and showed highest variability (range: 1.52 to 4.70 mm) in the anterior/posterior and medial/lateral directions compared to the superior/inferior direction (0.63 to 1.20 mm). This indicates that the most variable components of the insertion points are in the directions where the edges of the insertion points are defined. Specifically, the medial/lateral edge is chosen based on where the ligament appears to fade out of the sagittal slices, which are spaced 1 mm apart. The anterior/posterior length is defined by the digitization to the edge of the insertion point, which is challenging on the posterior side. Along this edge, the image is not as clearly defined between the tendon and the cortical bone, both appearing as black in the images.

Based on anatomical studies, the tibial ACL insertion is typically 10 to 14 mm posterior to the anterior tibial border, extending to the medial and lateral tibial spine. The insertion area can be triangular or oval, with diameters ranging between 10 to 13 mm and 15 to 19 mm in the frontal and sagittal plane, respectively (Petersen and Zantop, 2006). The femoral insertion is 2 to 3 mm from the femoral articular cartilage, oval, and has been found to have a mean length of 18 mm and width of 11 mm (Petersen and Zantop, 2006). In this study, the femoral ACL insertion point revealed less variability than the tibial insertion point when located on the same three repeatability subjects over three test sessions. The largest variability (2.00 to 2.09 mm) was observed for two of three subjects in the anterior/posterior direction. As with the anterior/posterior direction in the tibial insertion point digitization, the edges faded into the cortical bone, and were difficult to

clearly identify in comparison to the other directions. In the worst case scenario, with errors of (± 1.2 mm, ± 4.7 mm, ± 5.6 mm) in the tibial insertion point and (± 1.8 mm, ± 2.3 mm, ± 3.1 mm) in the femoral insertion point, the ACL insertion point distance could change by 11.7 mm. This situation was not seen for a given subject, but shows the sensitivity of the ACL insertion point distance (estimate for ACL length) with the current method used to identify insertion points. To ensure the ACL insertion point distance does not vary by more than 0.5 mm, the insertion points must be identified within 0.14 mm in each direction.

This variability is likely primarily responsible for the finding of no significant differences for the force-ACL insertion point distance curves, for distances compared between load levels. The KLA method holds promise as a method to delve down to the ligament level for quantifying laxity, but the variability of the method used to identify ACL insertion points must be reduced. A study by Aalbersberg, et al. (2005b) outlined a method for determining tendon direction by fitting a spline to the centroids of the cross sections of the ACL from MR images. In future studies, this technique could be applied to the KLA method to determine the length of the ACL from the soft tissue geometry. This may be an improvement on the ACL insertion point technique used in the current study, and could test the assumption that the ACL remains straight. Fleming, et al. (2004) noted that a method is required for determining the slack-taught transition of the ACL for *in-vivo* measures of strain. The proposed technique could also potentially be used to determine the slack-taught transition of the ACL, and to identify where it occurs on the force-displacement curve for both ACL and gross anterior tibial translation.

The ACL resists internal rotation and anterior translation (Butler, et al., 1980). The ACL is comprised of two bundles: the AM and PL bands. Towards full extension, the PL band is tight while the AM band is moderately lax (Petersen and Zantop, 2006). A study by Zantop et al. (2007) showed that at 30° of flexion, transection of the PL bundle resulted in a significantly greater anterior translation under a 134 N anterior tibial load when compared to the intact joint. No significant difference was found with transection of the AM band. Their results suggested that the PL bundle may be important in restraining anterior tibial loads at lower flexion angles. Based on this knowledge, future studies with the KLA may gain further insights by considering the contributions of the two bands of the ACL separately.

A measure of ACL laxity would be highly beneficial to improve understanding of ligament mechanical properties *in-vivo*. For example, in populations with ACL reconstructed knees where the graft is stretching out over time, the graft laxity could be evaluated at time points to intervene before significant damage or instability occurs. JHS populations could be assessed to evaluate whether their ACL laxity is significantly different from the normal population. It is speculated that the force-displacement curve in the JHS population would tend to show the most differences from normal in the linear region. This is the region of the curve where the ACL is fully engaged in resisting the applied force. This reduced stiffness could possibly be less than seen in normals, but greater than seen in ACL deficient subjects, who lack the structure altogether. These few examples demonstrate how much understanding could be gained by assessing laxity at the ligament level, and across various subject populations.

6.3 Comparison to a Clinical Arthrometer

In this study, a series of comparisons were conducted between the KLA and the most widely used clinical arthrometer, the KT-2000. One of the goals of the KLA design and method is to produce a 'gold standard tool' against which systems like the KT-2000 can be assessed. Until the KLA is shown to be highly accurate, a topic not explored in this study, the KLA and KT-2000 can only be compared as two different methods.

To test hypothesis H3, the KT-2000 and KLA displacements were compared at each load level, excluding 133 N. A limitation of the KT-2000 was revealed when the device indicated that it had reached 133 N when, in fact, the average peak load recorded was 110 ± 5 N. Both KLA and KT-2000 data were normalized to an initial displacement of 0 mm. No statistical differences were found between the two methods. However, an observed trend suggested that a larger sample size may show that the KT-2000 displacements were larger than the KLA displacements. A few studies have explored the KT-2000 and how it compares to 'gold standard' techniques such as RSA (Fleming, et al., 2002; Isberg, et al., 2006). As mentioned in Chapter Two, RSA is a very accurate method for describing bone movement (Karrholm, 1989), but has the disadvantages of not including soft tissue structures, and exposing the subjects to radiation. Isberg, et al. (2006) showed, for the intact contralateral limb of 22 ACL deficient subjects, that the KT-1000 significantly overestimated the RSA laxity value (8.0 mm compared to 3.1 mm). A study by Fleming, et al. (2002) showed that the KT-1000 laxity measure (from 90 to 130 N) overestimated laxity in 15 ACL reconstructed knees compared to RSA (11.4

± 3.0 mm compared to 6.9 ± 3.0 mm). The trends observed in the current study are in agreement with and strongly support the values reported in the literature.

The reliability coefficients (Cronbach's Alpha) indicated that the KT-2000 was a more reliable device than the KLA, showing reliability >0.7 for five of eight load levels tested, at the high loads and for the descending loads. This result supports the selection of higher load values (eg: 89 N) to assess laxity with the KT-2000, as is done in the literature (Daniel, et al., 1985a). However, the KLA showed less variability than the KT-2000, with an average of ± 0.58 mm compared to ± 1.47 mm, respectively. As discussed earlier (Section 6.1.1), a reliable outcome based on Cronbach's Alpha may not correlate to a level of acceptable variability. The variability observed for the KT-2000 in this study is high considering that an equivalent level of variability in the measurement of the contralateral knee laxity could result in a clinically relevant indication of an ACL tear in a normal knee. The variability observed for the KLA was within the magnitude of the target variability of ± 0.50 mm, and is considered a success at this prototype design stage.

Some of the variability observed with the KT-2000 may be explained by the challenges seen in initial limb position with the KLA (Section 6.1.1). The positioning frame of the KLA is designed to remove some of the dependence on tester ability to properly position the subject. In this controlled environment, variability was still seen for initial limb position. It is hypothesized that the KT-2000 method also suffers from this variability, which may account for the variation seen in the force-displacement curves.

Two additional measurements, the compliance index and average stiffness three regions of the force-displacement curve, were assessed with the KT-2000 but not compared to the KLA. The purpose was to evaluate whether measures other than displacement are more reliable for the KT-2000. The compliance index had a Cronbach's Alpha reliability coefficient of 0.66, which is less than the reliability seen for displacement at five of eight force levels. In the literature, the value of the compliance index is seen as an indicator of ACL disruption (Daniel, et al., 1985a). A compliance index >1 mm (indicating ACL disruption) in 53 ACL deficient knee was found to be detectable in 79% of the cases (Highgenboten, et al., 1992). The specificity was $>90\%$ in asymptomatic subjects. Compliance index values seen in the five normal subjects of the current study (0.34 to 1.36 mm) were within the range of compliance index values seen in 338 normal subjects (0.9 ± 0.32 mm) (Daniel, et al., 1985a). The results of the current study do not support or refute the literature values. The results suggest (within the limitations of statistical power) that displacements at loads past 89 N ascending may be more reliable than the compliance index.

The stiffness measures for the three main portions of the force-displacement curve (initial rise, middle, and linear) were not statistically different between days or across regions. The small sample size is a limitation for this assessment. However, variability was high across all 3 regions, ranging from ± 13.5 to 18.9 N/mm for the initial rise, ± 6.5 to 41.8 N/mm for the middle region, and ± 2.1 to 44.5 N/mm for the linear region. No patterns were seen in terms of higher stiffness for the linear region. The linear region was expected to have higher stiffness values, as it is the region that represents the resistance

of the ACL during loading (Maitland, et al., 1995). From these results, it appears that measuring an average stiffness over the regions of the KT-2000 curve does not prove to be more reliable than other measures. It also highlights the low reliability of the KT-2000 to quantify stiffness over a region.

One benefit of the KT-2000 over the KLA is the reduced test time, which is a few minutes compared to a half of an hour. This is primarily due to the continuous loading used with the KT-2000, rather than a stepped and held loading used with the KLA. However, the KLA was designed with the flexibility to provide either stepped or continuous loading, the latter being potentially more amenable to a clinical setting. A real-time imaging modality could be used, and would be the only required adjustment to the test setup. The force application could be administered continuously rather than with stepped loading. The KLA has potential for clinical use because of this flexibility to vary the loading regime. As well, the MR compatibility of the device allows soft tissue geometry to be obtained, a feature that the KT-2000 does not have. Certainly the KLA is currently at a prototype stage; however clinical applications should be kept in mind as the design iterations progress.

Future work should aim to quantify the accuracy of the KLA. This study has provided an initial assessment of the KLA measure of joint laxity, specifically to quantify the reliability of the method in a small population of normal subjects. A study using a cadaveric or porcine limb could be done to compare the KLA measure of laxity found using MR imaging against an accurately digitized and rendered surface using a 3D spatial

digitizer such as the FaroArm (FARO Technologies Inc., Lake Mary, Florida, USA) at the same load level. Force transducers in the ligaments could also be used to validate a lumped parameter model, allowing the force-displacement curve to be constructed for the ACL.

6.3.1 Muscle Guarding

Specific Aim 5 was achieved by testing five subjects in the KLA outside of the MR Scanner, 2 to 5 days prior to MR scanning. A key assumption was that the environment of the laboratory where EMG was collected would be comparable to the MR scanner environment. However differences do exist, including increased noise level and a more enclosed space in the MR scanner. A limitation of the EMG testing is that these variables were not controlled for. However, all other test protocol was duplicated.

Across subjects, no statistical difference was observed for muscle activity, for either maximum EMG signal or average EMG signal as a % of MVC. There was no effect of load level on muscle activity. When individual subjects were considered, the gastrocnemius was the muscle group that saw the most EMG signals with > 5% of MVC. Subject S01 reached EMG signals > 100% MVC, which suggested that the method for obtaining the gastrocnemius group MVC may not have resulted in a true MVC. During testing, the gastrocnemius was the most difficult muscle group for which to obtain an MVC.

Taking into consideration that the GM MVC was likely submaximal, the observation that subject S01 showed a high average signal of approximately 42% of MVC for the GM during the ramp down to 0 N at the end of the trial was likely still important. This is an interesting result, as the hamstring and quadriceps groups tend to be the focus of muscles contributing to resistance of anterior tibial translation (Iversen, et al., 1989). Iversen, et al. (1989) assessed the effect of voluntary hamstring contraction on anterior tibial translation in ACL deficient subjects and found that anterior tibial translation was significantly reduced. Hamstring contraction may be more prevalent in other groups such as ACL deficient subjects (Branch, et al., 1989). ACL deficient subjects show a coping mechanism of increased hamstring activation during dynamic activity (Branch, et al., 1989). Muscle contributions to joint laxity measures should continue to be monitored, particularly as new subject groups with a variety of pathologies are tested (eg: ACL deficient, JHS).

The ideal condition where no muscle guarding occurs was reflected across the group of subjects. Subject S01 is an example of how muscle guarding can still occur, despite training the subject to relax. As mentioned, there was not a statistical trend across load levels. However, the maximal contractions seen in subject S01 occurred during two ramp down trials. It would be interesting to test whether there may be more muscle guarding during a continuous test like the KT-2000 where all of the loading is dynamic (ie: a ramp up or down) in comparison to stepped loading used with the KLA. No studies were found that measured and reported EMG during a KT-2000 test. A study by Feller, et al. (2000) used EMG feedback to encourage hamstring relaxation, but found that this did not

significantly change the laxity measures for a subject. However, no EMG values were output to discern whether the subject was significantly contracting during the ‘no feedback’ trials. EMG feedback is an interesting concept as a non-invasive way to reduce muscle guarding. Unfortunately, this technique cannot currently be applied in an MR scanner.

Although muscle guarding cannot be eliminated as a possibility, it was shown that the majority of subjects were able to stay relaxed, particularly over the entire loaded time. Studies have shown that anterior laxity values are greater for subjects under anaesthetics than when conscious (Highgenboten, et al., 1992). A study comparing the KLA to the KT-2000 for subjects under anaesthesia may be an important study to complete in the future. In general, anaesthetics are not a practical method to ensure subject relaxation, particularly in a clinical setting where many patients must be seen and evaluated. However, it remains the only sure method of measuring truly passive knee joint laxity.

Subjects must continue to be encouraged to fully relax for the entire test session.

Palpation of the patellar tendon at the beginning of testing, a technique used with the KT-2000, is an additional measure taken in this study to ensure that the quadriceps muscles were relaxed. A training session, such as the one done for this study, where EMG was measured may be useful to identify subjects or patients who will have difficulty relaxing. In this study, earplugs were used in an effort to dampen the noise of the MR Scanner for both comfort and to prevent a jerk reaction to the noise. However, future studies may want to increase the amount of coaching to ‘remain alert but relaxed’ communicated to

the subject through the speaker system from the control room. As a knee model is developed (eg: lumped parameter), muscle forces may be taken into account and tested virtually for their effect on knee joint laxity.

6.3.2 Stress Relaxation

A stress relaxation phenomenon was observed during load application. The KLA method uses an input of initial force, and then allows the hydraulic system to maintain equilibrium. Due to the viscoelastic nature of the knee joint, a decrease in force over time occurs when the joint is held at a constant displacement. Stress relaxation is classically defined as a decrease in stress over time while holding strain constant. In this study, force and displacement are not normalized to stress and strain. Doing so has proven to be extremely challenging in ligament mechanics, due to varied cross sectional area, and difficulty defining zero strain length (Fleming, et al., 1994; Goodship and Birch, 2005). It is unknown currently whether the knee joint is stress or strain modulated. Consequently, both stress relaxation and creep effects are quantified when mechanically testing ligaments (Thornton, et al., 1997). MR imaging is particularly amenable to a stress relaxation test because a clear image requires a constant position in space over the image duration. Viewing the MR images was the indirect way that displacement was confirmed to be relatively constant within a given force level application in this study.

Brown and Semelka (1999) describe motion artifacts in MR imaging. They occur due to tissue movement during the data acquisition period. The appearance of the motion itself depends upon the type of motion and the measurement. Typically, signals are detected

from tissue multiple times during a scan. Sensitivity to motion depends on the phase-encoding amplitude. Motion during measurements with high amplitude positive or negative phase encoding gradient results in minimal artifacts (edges of k space, edge definition), as opposed to low amplitude phase encoding gradient producing substantial artifacts (center of k space, image contrast). In-plane motion tends to produce a more global artifact. A variable motion tends to produce ghost images that appear as a smearing through the image compared to a constant motion where an offset and fewer ghost images are produced (eg: respiration). These factors suggest that motion due to the knee joint slowly displacing in the anterior/posterior direction over time would tend to produce artifacts that are global and offset and somewhat blurred. MR images for all subjects were reviewed, and no evidence of motion artifacts was seen.

To the authors' knowledge, no studies have been done to measure *in-vivo* stress relaxation in the human knee joint. A study by Duong et al. (2001) measured stress relaxation in the ankle joint by applying a set dorsiflexion angle for 20 minutes to 8 normal subjects, and continuously measuring the resulting torque. The KLA may have application to quantify not just joint laxity, but also *in-vivo* viscoelastic joint behavior. The current study set out to capture viscoelastic behavior as it occurred within the laxity test setup. It was expected that some form of joint stress relaxation would occur, however scan times were minimized to reduce this effect.

Stress relaxation was observed on the ascending curve only of the force-time curves.

This is thought to be a result of stretching the joint as the load increased, resulting in an

equilibrium for the descending curve. An exponential function was fit to the normalized force-time curve to describe the time constant at each loaded joint position. The average time constant for all subjects on day D1 was 28.3 ± 2.9 s. The range of variability seen within a subject and within a day was ± 1.8 to ± 4.7 s. A statistically significant between day effect was found for the repeatability subjects. It can be speculated that the differences between days may be attributed to the variability in the length of time that each load was held (78.8 ± 11.0 s). Sarver et al (2003) noted that unrelaxed stress will have a cumulative effect during an incremental test. Since the stress relaxation curves showed that equilibrium was not reached (only fitting to one exponential rather than a summation of two), the cumulative stress affect may have been important. Future studies should look at the impact of the loading regime (force levels, load time, load ramp up time) on the time constants, and develop a standard protocol for measuring stress relaxation.

Future studies could look at applying the KLA to measure stress relaxation as a primary goal. Tests could be conducted outside of the MR scanner, and over longer periods to capture the second portion of the stress relaxation curve. It would be very interesting to measure stress relaxation across different subject groups, such as JHS and ACL deficient. It is conceivable that differences could be detected in the stress relaxation behavior (eg: time constant) of the whole joint between subject populations. In future studies that use the KLA to investigate *in-vivo* stress relaxation, the time at which relaxation is stopped should be chosen carefully. A key validation would be to ensure that the joint

displacement is held constant. This could be confirmed with fluoroscopy, or possibly an external measure such as a displacement transducer.

6.4 Summary and Future Work

The novel KLA design is a new contribution to the field of biomechanics, specifically for quantifying knee joint laxity. Although multiple knee laxity measurement devices exist (Daniel, et al., 1985a; Highgenboten, et al., 1989; Muellner, et al., 2001), none have combined a controlled positioning and loading device with MR imaging. This new device will allow investigations of joint laxity at the ligament level, relative bone motion, and cartilage contact patterns. Furthermore, it holds promise as a tool to quantify *in-vivo* stress relaxation behavior of the knee joint.

A main contribution of this study was the application of techniques to quantify ligament laxity. Although the technique used to identify ACL insertion points was unsuccessful, important insights have been gained about the requirements for a robust measure of ACL length. The KLA itself is a novel method and contribution, as it combines MR imaging with controlled external loading and positioning to measure knee joint laxity. Tests done to assess the reliability of a variety of measures associated with the KLA, particularly initial joint position, have contributed a better understanding of the relative success of the KLA at this design stage. Future work can build off of these insights to produce a gold standard tool for quantifying passive knee joint properties, including joint laxity and viscoelasticity. For the first time, stress relaxation has been documented *in-vivo* in normal human subjects.

To summarize the future work identified for the KLA design and implementation, six key recommendations have been identified:

- 1) Standardize the initial limb positioning by developing a real-time feedback system that allows the tester to finely adjust the tibial position.
- 2) Apply the manual crank system (Robu, et al., 2007) to better control force application. In the long term, a device to automatically modulate force would further improve the quality and ease of use (DC10) of the hydraulic system.
- 3) Test the assumption that $F_x \propto F_y$ for the hinge of the KLA. Test methods could include instrumented joint specimens or test object to compare model force against measured force.
- 4) Model the knee joint with lumped parameter techniques to bring the joint laxity model to the next level of complexity. This will allow construction of force-displacement curves for individual ligaments, particularly the ACL
- 5) Apply highly accurate techniques for identifying the ACL insertion points to quantify ACL laxity.

- 6) Explore the potential of the KLA as a measure of *in-vivo* knee joint stress relaxation by testing across different subject groups and for longer durations to capture the full stress relaxation curve as it reaches equilibrium.

This study aimed to design and evaluate a novel measure of *in-vivo* joint laxity. The purpose was to gain a better understanding of the mechanical properties of quasi-passive joint structures. In the long term, an improved understanding of the contributions of quasi-passive joint structures to dynamic joint stability may be achieved if laxity is reliably and accurately quantified. Anterior laxity, in particular, is a measure of the integrity of the ACL, a primary quasi-passive ligament of the knee. The KLA was designed to apply an anterior load to the knee to test the ACL. The design phase showed that the KLA successfully met key design criteria.

A key focus of future studies should be the standardization of initial limb position, and extending the knee joint model to a lumped parameter approach. This will allow further insights into ligament specific laxity. Validation of the KLA method in terms of accuracy would evaluate whether the method can be used as a 'gold standard' against current clinical laxity tools. The KLA shows promise as an accurate and reliable tool for measuring *in-vivo* joint laxity and viscoelastic behavior.

References

- Aalbersberg, S., Kingma, I., Blankevoort, L., van Dieen, J.H., 2005a. Co-contraction during static and dynamic knee extensions in ACL deficient subjects. *Journal of Electromyography and Kinesiology* 15, 349-357.
- Aalbersberg, S., Kingma, I., Ronsky, J.L., Frayne, R., van Dieen, J.H., 2005b. Orientation of tendons in vivo with active and passive knee muscles. *Journal of Biomechanics* 38, 1780-1788.
- Abramowitch, S.D., Woo, S.L., 2004. An improved method to analyze the stress relaxation of ligaments following a finite ramp time based on the quasi-linear viscoelastic theory. *J Biomech Eng* 126, 92-97.
- Acasuso Diaz, M., Collantes Estevez, E., Sanchez Guijo, P., 1993. Joint hyperlaxity and musculoligamentous lesions: study of a population of homogeneous age, sex and physical exertion. *Br J Rheumatol* 32, 120-122.
- Aircast, 2007. Rolimeter by Aircast. In. <http://www.rolimeter.com/> [10/10/07].
- Al-Rawi, Z.S., Al-Aszawi, A.J., Al-Chalabi, T., 1985. Joint mobility among university students in Iraq. *Br J Rheumatol* 24, 326-331.
- Almekinders, L.C., Pandarinath, R., Rahusen, F.T., 2004. Knee stability following anterior cruciate ligament rupture and surgery. The contribution of irreducible tibial subluxation. *J Bone Joint Surg Am* 86-A, 983-987.
- Andersen, H.N., Jorgensen, U., 1998. The immediate postoperative kinematic state after anterior cruciate ligament reconstruction with increasing peroperative tension. *Knee Surg Sports Traumatol Arthrosc* 6 Suppl 1, S62-69.
- Anderson, A.F., Lipscomb, A.B., 1989. Preoperative instrumented testing of anterior and posterior knee laxity. *Am J Sports Med* 17, 387-392.
- Anderson, A.F., Snyder, R.B., Federspiel, C.F., Lipscomb, A.B., 1992. Instrumented evaluation of knee laxity: a comparison of five arthrometers. *Am J Sports Med* 20, 135-140.
- Arendt, E.A., Agel, J., Dick, R., 1999. Anterior Cruciate Ligament Injury Patterns Among Collegiate Men and Women. *J Athl Train* 34, 86-92.
- Baker, S.N., 2002. In-vivo quantification of patellofemoral joint contact force using a mathematical model. University of Calgary, Calgary
- Baum, J., Larsson, L.G., 2000. Hypermobility syndrome--new diagnostic criteria. *J Rheumatol* 27, 1585-1586.

- Beardsley, C.L., Paller, D.J., Peura, G.D., Brattbakk, B., Beynnon, B.D., 2007. The effect of coordinate system choice and segment reference on RSA-based knee translation measures. *J Biomech* 40, 1417-1422.
- Belanger, M.J., Moore, D.C., Crisco, J.J., 3rd, Fadale, P.D., Hulstyn, M.J., Ehrlich, M.G., 2004. Knee laxity does not vary with the menstrual cycle, before or after exercise. *Am J Sports Med* 32, 1150-1157.
- Boyd, S.K., Ronsky, J.L., Lichti, D.D., Salkauskas, K., Chapman, M.A., 1999. Joint surface modeling with thin-plate splines.[erratum appears in *J Biomech Eng* 2000 Feb;122(1):104 Note: Salkauskas D [corrected to Salkauskas K]]. *J Biomech Eng* 121, 525-532.
- Branch, T.P., Hunter, R., Donath, M., 1989. Dynamic EMG analysis of anterior cruciate deficient legs with and without bracing during cutting. *Am J Sports Med* 17, 35-41.
- Bray, R., Salo, P., Lo, I., Ackermann, P., Rattner, J., Hart, D.A., 2005. Normal Ligament Structure, Physiology and Function. *Sports Medicine and Arthroscopy Review* 13, 127-135.
- Bridges, A.J., Smith, E., Reid, J., 1992. Joint hypermobility in adults referred to rheumatology clinics. *Ann Rheum Dis* 51, 793-796.
- Brown, M.A., Semelka, R.C. (Eds.), 1999. *MRI: Basic Principles and Applications*. Wiley-Liss, Inc., New York, NY.
- Butler, D.L., Noyes, F.R., Grood, E.S., 1980. Ligamentous restraints to anterior-posterior drawer in the human knee. A biomechanical study. *J Bone Joint Surg Am* 62, 259-270.
- Cannon, W.D., 2002. Use of Arthrometers to Assess Knee Laxity and Outcomes. *Sports Medicine and Arthroscopy Review* 10, 191-200.
- Cha, H.S., Lee, S.H., Ryu, S.J., 2000. The Measurement of the Strain of the Anterior Cruciate Ligament. In 22nd Annual EMBS International Conference, July 23-28. Chicago, IL.
- Challis, J.H., 1995. A procedure for determining rigid body transformation parameters. *J Biomech* 28, 733-737.
- Chandrashekar, N., Slauterbeck, J., Hashemi, J., 2005. Sex-based differences in the anthropometric characteristics of the anterior cruciate ligament and its relation to intercondylar notch geometry: a cadaveric study. *Am J Sports Med* 33, 1492-1498.
- Cheng, R.W.T., 2006. Registration for the In-Vivo Studies of Osteoarthritis based on Magnetic Resonance Imaging. University of Calgary, Calgary.

- Cheng, R.W.T., Frayne, R., Ronsky, J.L., Habib, A.F., 2005. Matching strategy for co-registration of surfaces acquired by magnetic resonance imaging. In Geoscience and Remote Sensing Symposium, IGARSS '05. Proceedings 2005 IEEE International.
- Chertow, G.M., Lazarus, J.M., Lew, N.L., Ma, L., Lowrie, E.G., 1997. Development of a population-specific regression equation to estimate total body water in hemodialysis patients. *Kidney Int* 51, 1578-1582.
- Chimich, D., Shrive, N., Frank, C., Marchuk, L., Bray, R., 1992. Water content alters viscoelastic behaviour of the normal adolescent rabbit medial collateral ligament. *J Biomech* 25, 831-837.
- Churchill, D.L., Incavo, S.J., Johnson, C.C., Beynnon, B.D., 1998. The transepicondylar axis approximates the optimal flexion axis of the knee. *Clin Orthop Relat Res*, 111-118.
- Colombet, P., Robinson, J., Christel, P., Franceschi, J.P., Djian, P., Bellier, G., Sbihi, A., 2006. Morphology of anterior cruciate ligament attachments for anatomic reconstruction: a cadaveric dissection and radiographic study. *Arthroscopy* 22, 984-992.
- Connolly, K.D., 2006. In-vivo Characterization of Patellar Tracking in Normal and PFPS. University of Calgary, Calgary.
- Coughlin, K.M., Incavo, S.J., Churchill, D.L., Beynnon, B.D., 2003. Tibial axis and patellar position relative to the femoral epicondylar axis during squatting. *J Arthroplasty* 18, 1048-1055.
- Cram, J.R., 2003. The history of surface electromyography. *Appl Psychophysiol Biofeedback* 28, 81-91.
- Cubuk, S.M., Sindel, M., Karaali, K., Arslan, G., Akyildiz, F., Ozkan, O., 2000. Tibial Tubercle Position and Patellar Height as Indicators of Malalignment in Women with Anterior Knee Pain. *Clinical Anatomy* 13, 199-203.
- Daniel, D.M., Malcom, L.L., Losse, G., Stone, M.L., Sachs, R., Burks, R., 1985a. Instrumented measurement of anterior laxity of the knee. *Journal of Bone and Joint Surgery* 67A, 720-726.
- Daniel, D.M., Stone, M.L., 1990. Instrumented measurement of knee motion. Raven, New York.
- Daniel, D.M., Stone, M.L., Sachs, R., Malcom, L., 1985b. Instrumented measurement of anterior knee laxity in patients with acute anterior cruciate ligament disruption. *Am J Sports Med* 13, 401-407.
- Darcy, S.P., Kilger, R.H., Woo, S.L., Debski, R.E., 2006. Estimation of ACL forces by reproducing knee kinematics between sets of knees: A novel non-invasive methodology. *J Biomech* 39, 2371-2377.

- Davis, I., Ireland, M.L., Hanaki, S., 2007. ACL injuries--the gender bias. *J Orthop Sports Phys Ther* 37, A2-7.
- DeFrate, L.E., Sun, H., Gill, T.J., Rubash, H.E., Guoan, L., 2004. In Vivo Tibiofemoral Contact Analysis Using 3D MRI-based Knee Models. *Journal of Biomechanics* 37, 1499-1504.
- Deie, M., Sakamaki, Y., Sumen, Y., Urabe, Y., Ikuta, Y., 2002. Anterior knee laxity in young women varies with their menstrual cycle. *Int Orthop* 26, 154-156.
- DeLuca, C.J., 1997. The Use of Surface Electromyography in Biomechanics. *Journal of Applied Biomechanics* 13, 135-163.
- Derrington, M.C., Smith, G., 1987. A review of studies of anaesthetic risk, morbidity and mortality. *Br J Anaesth* 59, 815-833.
- Doorenbosch, C.A., Joosten, A., Harlaar, J., 2005. Calibration of EMG to force for knee muscles is applicable with submaximal voluntary contractions. *J Electromyogr Kinesiol* 15, 429-435.
- Dragoo, J.L., Lee, R.S., Benhaim, P., Finerman, G.A., Hame, S.L., 2003. Relaxin receptors in the human female anterior cruciate ligament. *Am J Sports Med* 31, 577-584.
- Duong, B., Low, M., Moseley, A.M., Lee, R.Y., Herbert, R.D., 2001. Time course of stress relaxation and recovery in human ankles. *Clin Biomech (Bristol, Avon)* 16, 601-607.
- Eastlack, M.E., Axe, M.J., Snyder-Mackler, L., 1999. Laxity, instability, and functional outcome after ACL injury: copers versus noncopers. *Med Sci Sports Exerc* 31, 210-215.
- Eisenbeiss, C., Welzel, J., Schmeller, W., 1998. The influence of female sex hormones on skin thickness: evaluation using 20 MHz sonography. *Br J Dermatol* 139, 462-467.
- Ejerhed, L., Kartus, J., Sernert, N., Kohler, K., Karlsson, J., 2003. Patellar tendon or semitendinosus tendon autografts for anterior cruciate ligament reconstruction? A prospective randomized study with a two-year follow-up. *Am J Sports Med* 31, 19-25.
- Feller, J., Hoser, C., Webster, K., 2000. EMG biofeedback assisted KT-1000 evaluation of anterior tibial displacement. *Knee Surg Sports Traumatol Arthrosc* 8, 132-136.
- Fitzcharles, M.A., 2000. Is hypermobility a factor in fibromyalgia? *J Rheumatol* 27, 1587-1589.
- Fitzpatrick, C., FitzPatrick, D., Auger, D., Lee, J., 2007. A tibial-based coordinate system for three-dimensional data. *Knee* 14, 133-137.

- Fjeld, I.R., 2007. In-Vivo Dynamic Joint Stability Quantified in Intact and ACL Deficient Knees. University of Calgary Calgary.
- Fleming, B.C., Beynnon, B.D., 2004. In Vivo Measurement of Ligament/Tendon Strains and Forces: A Review. *Annals of Biomedical Engineering* 32, 318-328.
- Fleming, B.C., Beynnon, B.D., Tohyama, H., Johnson, R.J., Nichols, C.E., Renstrom, P., Pope, M.H., 1994. Determination of a zero strain reference for the anteromedial band of the anterior cruciate ligament. *J Orthop Res* 12, 789-795.
- Fleming, B.C., Brattbakk, B., Peura, G.D., Badger, G.J., Beynnon, B.D., 2002. Measurement of anterior-posterior knee laxity: a comparison of three techniques. *J Orthop Res* 20, 421-426.
- Freeman, M.A., Pinskerova, V., 2005. The movement of the normal tibio-femoral joint. *J Biomech* 38, 197-208.
- Frey, M., Riener, R., Michas, C., Regenfelder, F., Burgkart, R., 2006. Elastic properties of an intact and ACL-ruptured knee joint: measurement, mathematical modelling, and haptic rendering. *J Biomech* 39, 1371-1382.
- Fung, Y.C., Perrone, N., Anliker, M. (Eds.), 1972. "Stress Strain History Relations of Soft Tissues in Simple Elongation", in *Biomechanics: Its Foundations and Objectives*. PrenticeHall, Englewood Cliffs, NJ.
- Gold, G.E., Besier, T.F., Draper, C.E., Asakawa, D.S., Delp, S.L., Beaupre, G.S., 2004. Weight-bearing MRI of patellofemoral joint cartilage contact area. *J Magn Reson Imaging* 20, 526-530.
- Goodship, A.E., Birch, H.L., 2005. Cross sectional area measurement of tendon and ligament in vitro: a simple, rapid, non-destructive technique. *J Biomech* 38, 605-608.
- Grathwohl, K.W., 2007. Anesthesiology. *J Trauma* 62, S105-106.
- Gray, H., 1918. *Anatomy of the human body* 20th ed. In: Lewis, W.H. (Ed.). Philadelphia: Lea & Febiger, 1918; Bartleby.com, 2000. www.bartelby.com/107/. [02/05/07].
- Gupta, S., Hawker, G.A., Laporte, A., Croxford, R., Coyte, P.C., 2005. The economic burden of disabling hip and knee osteoarthritis (OA) from the perspective of individuals living with this condition. *Rheumatology (Oxford)* 44, 1531-1537.
- Habib, A.F., Lee, Y.R., Morgan, M., 2001. Surface Matching and Change Detection using a Modified Hough Transformation for Robust Parameter Estimation. *Photogrammetric Record* 17, 303-315.

- Hakim, A., Grahame, R., 2003. Joint Hypermobility. *Best Practice & Research Clinical Rheumatology* 17, 989-1004.
- Hargreaves, B.A., Vasanawala, S.S., Nayak, K.S., Hu, B.S., Nishimura, D.G., 2003. Fat-suppressed steady-state free precession imaging using phase detection. *Magn Reson Med* 50, 210-213.
- Haut, T.L., Haut, R.C., 1997. The state of tissue hydration determines the strain-rate-sensitive stiffness of human patellar tendon. *J Biomech* 30, 79-81.
- Herrington, L., Wrapson, C., Matthews, M., Matthews, H., 2005. Anterior cruciate ligament reconstruction, hamstring versus bone-patella tendon-bone grafts: a systematic literature review of outcome from surgery. *Knee* 12, 41-50.
- Herzog, W., Binding, P., 1999. Mathematically indeterminate systems. In: Nigg, B.M., Herzog, W. (Eds.), *Biomechanics of the Musculo-skeletal System*. John Wiley & Sons Ltd, West Sussex, England, pp. 533-545.
- Herzog, W., Leonard, T.R., 1996. Soleus forces and soleus force potential during unrestrained cat locomotion. *J Biomech* 29, 271-279.
- Highgenboten, C.L., Jackson, A., Meske, N.B., 1989. Genucom, KT-1000, and Stryker knee laxity measuring device comparisons. *American Journal of Sports Medicine* 17, 743-746.
- Highgenboten, C.L., Jackson, A.W., Jansson, K.A., Meske, N.B., 1992. KT-1000 arthrometer: conscious and unconscious test results using 15, 20, and 30 pounds of force. *Am J Sports Med* 20, 450-454.
- Himmelfarb, J., Evanson, J., Hakim, R.M., Freedman, S., Shyr, Y., Ikizler, T.A., 2002. Urea volume of distribution exceeds total body water in patients with acute renal failure. *Kidney Int* 61, 317-323.
- Hingorani, R.V., Provenzano, P.P., Lakes, R.S., Escarcega, A., Vanderby, R., Jr., 2004. Nonlinear viscoelasticity in rabbit medial collateral ligament. *Ann Biomed Eng* 32, 306-312.
- Hsu, W.H., Fisk, J.A., Yamamoto, Y., Debski, R.E., Woo, S.L., 2006. Differences in torsional joint stiffness of the knee between genders: a human cadaveric study. *Am J Sports Med* 34, 765-770.
- Huber, F.E., Irrgang, J.J., Harner, C., Lephart, S., 1997. Intratester and intertester reliability of the KT-1000 arthrometer in the assessment of posterior laxity of the knee. *Am J Sports Med* 25, 479-485.
- Hume, R., Weyers, E., 1971. Relationship between total body water and surface area in normal and obese subjects. *J Clin Pathol* 24, 234-238.

Isberg, J., Faxen, E., Brandsson, S., Eriksson, B.I., Karrholm, J., Karlsson, J., 2006. KT-1000 records smaller side-to-side differences than radiostereometric analysis before and after an ACL reconstruction. *Knee Surg Sports Traumatol Arthrosc* 14, 529-535.

Iversen, B.F., Sturup, J., Jacobsen, K., Andersen, J., 1989. Implications of muscular defense in testing for the anterior drawer sign in the knee. A stress radiographic investigation. *Am J Sports Med* 17, 409-413.

Iwaki, H., Pinskerova, V., Freeman, M.A., 2000. Tibiofemoral movement 1: the shapes and relative movements of the femur and tibia in the unloaded cadaver knee. *J Bone Joint Surg Br* 82, 1189-1195.

Jagodzinski, M., Kleemann, V., Angele, P., Schonhaar, V., Iselborn, K.W., Mall, G., Nerlich, M., 2000. Experimental and clinical assessment of the accuracy of knee extension measurement techniques. *Knee Surg Sports Traumatol Arthrosc* 8, 329-336.

Johnson, J.C., 2006. Quantification of In-Vivo Knee Joint and Ligament Stiffness Characteristics. In Proceedings of the 3rd Annual Schulich School of Engineering Graduate Student Research Conference. University of Calgary, Calgary, Alberta, May 1-2 (Oral Presentation).

Jorn, L.P., Friden, T., Ryd, L., Lindstrand, A., 1998. Simultaneous measurements of sagittal knee laxity with an external device and radiostereometric analysis. *J Bone Joint Surg Br* 80, 169-172.

Jozsa, L., Kannus, P. (Ed.) 1997. *Human Tendons - Anatomy, Physiology, and Pathology*. Human Kinetics Publishers

Karrholm, J., 1989. Roentgen stereophotogrammetry. Review of orthopedic applications. *Acta Orthop Scand* 60, 491-503.

Kupper, J.C., Loitz-Ramage, B., Corr, D.T., Hart, D.A., Ronsky, J.L., 2007a. Measuring knee joint laxity: a review of applicable models and the need for new approaches to minimize variability. *Clin Biomech (Bristol, Avon)* 22, 1-13.

Kupper, J.C., Ronsky, J.L., Frayne, R., Loitz-Ramage, B., Hart, D.A., 2007b. A Novel Measure of In-Vivo Knee Joint Laxity. In Proceedings of the ASME Summer Bioengineering Conference. Keystone Resort and Conference Center, Keystone, Colorado, June 20-24 (Poster Presentation).

Kupper, J.C., Ronsky, J.L., Frayne, R., Robu, I., Hart, D.A., 2006a. A Novel Measure of Knee Joint Laxity. In Proceedings of the Canadian Arthritis Network's Annual Scientific Conference. The Fairmont Winnipeg, Winnipeg, Manitoba, Nov 30 - Dec 2 (Poster Presentation).

Kupper, J.C., Ronsky, J.L., Frayne, R., Robu, I., Hart, D.A., 2006b. A Novel Measure of Knee Joint Laxity. In Proceedings of the Canadian Arthritis Network's Satellite Program Workshop: Update on the Osteoarthritis Strategic Research Initiative - Advancing the OA Agenda. The Fairmont Winnipeg, Winnipeg, Manitoba, Nov 29 - 30 (Poster Presentation).

Lanczos, C. (Ed.) 1956. Applied Analysis. PrenticeHall, Englewood Cliffs, NJ.

Landry, S.C., McKean, K.A., Hubley-Kozey, C.L., Stanish, W.D., Deluzio, K.J., 2007. Neuromuscular and lower limb biomechanical differences exist between male and female elite adolescent soccer players during an unanticipated run and crosscut maneuver. *Am J Sports Med* 35, 1901-1911.

Lewkonja, R.M., 1993. The biological and Clinical Consequences of Articular Hypermobility. *Journal of Rheumatology* 20, 220-222.

Liu, S.H., al-Shaikh, R., Panossian, V., Yang, R.S., Nelson, S.D., Soleiman, N., Finerman, G.A., Lane, J.M., 1996. Primary immunolocalization of estrogen and progesterone target cells in the human anterior cruciate ligament. *J Orthop Res* 14, 526-533.

Logan, M.C., Dunstan, E., Robinson, J., Williams, A., Gedroyc, W., Freeman, M., 2004a. Tibiofemoral Kinematics of the Anterior Cruciate Ligament (ACL)-Deficient Weightbearing, Living Knee Employing Vertical Access Open "Interventional" Multiple Resonance Imaging. *American Journal of Sports Medicine* 32, 720-726.

Logan, M.C., Williams, A., Lavelle, J., Gedroyc, W., Freeman, M., 2004b. What Really Happens During the Lachman Test? A Dynamic MRI Analysis of Tibiofemoral Motion. *American Journal of Sports Medicine* 32, 369-375.

Lohmander, L.S., Englund, P.M., Dahl, L.L., Roos, E.M., 2007. The long-term consequence of anterior cruciate ligament and meniscus injuries: osteoarthritis. *Am J Sports Med* 35, 1756-1769.

Maffulli, N., 1998. Laxity versus instability. *Orthopedics* 21, 837, 842.

Maitland, M.E., Bell, G.D., Mohtadi, N.G., Herzog, W., 1995. Quantitative analysis of anterior cruciate ligament instability. *Clin Biomech (Bristol, Avon)* 10, 93-97.

Malanga, G.A., Andrus, S., Nadler, S.F., McLean, J., 2003. Physical examination of the knee: a review of the original test description and scientific validity of common orthopedic tests. *Arch Phys Med Rehabil* 84, 592-603.

Martineau, P.A., Al-Jassir, F., Lenczner, E., Burman, M.L., 2004. Effect of the oral contraceptive pill on ligamentous laxity. *Clin J Sport Med* 14, 281-286.

- MEDmetric-Corporation, 2007. MEDmetric Product Pricelist. In. <http://www.medmetric.com/price.htm> [10/10/07].
- Merletti, R., Rainoldi, A., Farina, D., 2001. Surface electromyography for noninvasive characterization of muscle. *Exerc Sport Sci Rev* 29, 20-25.
- Moglo, K.E., Shirazi-Adl, A., 2003. Biomechanics of passive knee joint in drawer: load transmission in intact and ACL-deficient joints. *Knee* 10, 265-276.
- Moller-Nielsen, J., Hammar, M., 1989. Women's soccer injuries in relation to the menstrual cycle and oral contraceptive use. *Med Sci Sports Exerc* 21, 126-129.
- Moss, R., 2001. Characterization of joint cartilage deformation using magnetic resonance imaging. University of Calgary, Calgary
- Moul, J.L., 1998. Differences in Selected Predictors of Anterior Cruciate Ligament Tears Between Male and Female NCAA Division I Collegiate Basketball Players. *J Athl Train* 33, 118-121.
- Muellner, T., Bugge, W., Johansen, S., Holtan, C., Engebretsen, L., 2001. Inter- and intratester comparison of the Rolimeter knee tester: effect of tester's experience and the examination technique. *Knee Surg Sports Traumatol Arthrosc* 9, 302-306.
- Myrer, J.W., Schulthies, S.S., Fellingham, G.W., 1996. Relative and absolute reliability of the KT-2000 arthrometer for uninjured knees. Testing at 67, 89, 134, and 178 N and manual maximum forces. *Am J Sports Med* 24, 104-108.
- Netti, P., D'Amore, A., Ronca, D., Ambrosio, L., Nicolais, L., 1996. Structure-mechanical properties relationship of natural tendons and ligaments. *Journal of Materials Science: Materials in Medicine* 7, 525-530.
- Nigg, B.M., 1999. Measuring Techniques: Force. In: Nigg, B.M., Herzog, W. (Eds.), *Biomechanics of the Musculo-skeletal System*. John Wiley & Sons Ltd, West Sussex, England, pp. 355-375.
- Pandy, M.G., Shelburne, K.B., 1998. Theoretical analysis of ligament and extensor-mechanism function in the ACL-deficient knee. *Clin Biomech (Bristol, Avon)* 13, 98-111.
- Papandreou, M.G., Antonogiannakis, E., Karabalis, C., Karliaftis, K., 2005. Inter-rater reliability of Rolimeter measurements between anterior cruciate ligament injured and normal contra lateral knees. *Knee Surg Sports Traumatol Arthrosc* 13, 592-597.
- Patel, R.R., Hurwitz, D.E., Bush-Joseph, C.A., Bach, B.R., Jr., Andriacchi, T.P., 2003. Comparison of clinical and dynamic knee function in patients with anterior cruciate ligament deficiency. *Am J Sports Med* 31, 68-74.

- Pearsall, A.T., Pyevich, M., Draganich, L.F., Larkin, J.J., Reider, B., 1996. In vitro study of knee stability after posterior cruciate ligament reconstruction. *Clin Orthop Relat Res*, 264-271.
- Petersen, W., Zantop, T., 2006. Anatomy of the Anterior Cruciate Ligament with Regard to its Two Bundles. *Clin Orthop Relat Res* 454, 35-47.
- Picano, E., 2004. Sustainability of medical imaging. *Bmj* 328, 578-580.
- Provenzano, P., Lakes, R., Keenan, T., Vanderby, R., Jr., 2001. Nonlinear ligament viscoelasticity. *Ann Biomed Eng* 29, 908-914.
- Purslow, P.P., Wess, T.J., Hukins, D.W., 1998. Collagen orientation and molecular spacing during creep and stress-relaxation in soft connective tissues. *J Exp Biol* 201, 135-142.
- Ralphs, J.R., Benjamin, M., 1994. The joint capsule: structure, composition, ageing and disease. *J Anat* 184(3), 503-509.
- Ramsey, D.K., Wretenberg, P.F., 1999. Biomechanics of the knee: methodological considerations in the in vivo kinematic analysis of the tibiofemoral and patellofemoral joint. *Clin Biomech (Bristol, Avon)* 14, 595-611.
- Reinschmidt, C., 1995. *soder.m. In.*, Calgary.
- Robu, I., 2005. Improved Loading Apparatus for Knee Imaging Using Magnetic Resonance. In, 6th Alberta Biomedical Engineering Conference. The Banff Center, Banff, Alberta, Oct 21 - 23.
- Robu, I., 2007. Personal Communication (verbal) re: Motorized KLA Hydraulic System. In: Kupper, J.C. (Ed.). Calgary.
- Robu, I., Ronsky, J.L., Frayne, R., Habib, A.F., 2007. Assessment of a Novel Technique for In-Vivo Investigation of Joint Cartilage Deformation Characteristics. In ASME 2007 Summer Bioengineering Conference. Keystone Resort & Conference Center, Keystone, Colorado.
- Ronsky, J.L., 1994. In-vivo quantification of patellofemoral joint contact characteristics. University of Calgary, Calgary, Alberta, Canada.
- Rozzi, S.L., Lephart, S.M., Gear, W.S., Fu, F.H., 1999. Knee joint laxity and neuromuscular characteristics of male and female soccer and basketball players. *Am J Sports Med* 27, 312-319.
- Rudy, T.W., Sakane, M., Debski, R.E., Woo, S.L., 2000. The effect of the point of application of anterior tibial loads on human knee kinematics. *J Biomech* 33, 1147-1152.

- Sakane, M., Livesay, G.A., Fox, R.J., Rudy, T.W., Runco, T.J., Woo, S.L., 1999. Relative contribution of the ACL, MCL, and bony contact to the anterior stability of the knee. *Knee Surg Sports Traumatol Arthrosc* 7, 93-97.
- Sarver, J.J., Robinson, P.S., Elliott, D.M., 2003. Methods for quasi-linear viscoelastic modeling of soft tissue: application to incremental stress-relaxation experiments. *J Biomech Eng* 125, 754-758.
- Scarvell, J.M., Smith, P.N., Refshauge, K.M., Galloway, H.R., Woods, K.R., 2004. Evaluation of a Method to Map Tibiofemoral Contact Points in the Normal Knee using MRI. *Journal of Orthopaedic Research* 22, 788-793.
- Schultz, R.A., Miller, D.C., Kerr, C.S., Micheli, L., 1984. Mechanoreceptors in human cruciate ligaments. A histological study. *J Bone Joint Surg Am* 66, 1072-1076.
- Selvik, G., 1989. Roentgen stereophotogrammetry. A method for the study of the kinematics of the skeletal system. *Acta Orthop Scand Suppl* 232, 1-51.
- Sernert, N., Kartus, J., Kohler, K., Ejerhed, L., Karlsson, J., 2001. Evaluation of the reproducibility of the KT-1000 arthrometer. *Scand J Med Sci Sports* 11, 120-125.
- Shahar, R., Banks-Sills, L., 2004. A quasi-static three-dimensional, mathematical, three-body segment model of the canine knee. *J Biomech* 37, 1849-1859.
- Sheehan, F.T., Rebmann, A., 2003. Non-invasive, in vivo measures of anterior cruciate ligament strains. In 49th Annual Meeting of the Orthopaedic Research Society. New Orleans, Louisiana.
- Shelfbine, S.J., Ma, C.B., Lee, K.Y., Schrupf, M.A., Patel, P., Safran, M.R., Slavinsky, J.P., Majumdar, S., 2006. MRI analysis of in vivo meniscal and tibiofemoral kinematics in ACL-deficient and normal knees. *Journal of Orthopaedic Research* 24, 1208-1217.
- Shultz, S.J., Gansneder, B.M., Sander, T.C., Kirk, S.E., Perrin, D.H., 2006. Absolute serum hormone levels predict the magnitude of change in anterior knee laxity across the menstrual cycle. *J Orthop Res* 24, 124-131.
- Shultz, S.J., Kirk, S.E., Johnson, M.L., Sander, T.C., Perrin, D.H., 2004. Relationship between sex hormones and anterior knee laxity across the menstrual cycle. *Med Sci Sports Exerc* 36, 1165-1174.
- Slauterbeck, J., Clevenger, C., Lundberg, W., Burchfield, D.M., 1999. Estrogen level alters the failure load of the rabbit anterior cruciate ligament. *J Orthop Res* 17, 405-408.
- Slauterbeck, J.R., Fuzie, S.F., Smith, M.P., Clark, R.J., Xu, K., Starch, D.W., Hardy, D.M., 2002. The Menstrual Cycle, Sex Hormones, and Anterior Cruciate Ligament Injury. *J Athl Train* 37, 275-278.

- Snyder-Mackler, L., Fitzgerald, G.K., Bartolozzi, A.R., 3rd, Ciccotti, M.G., 1997. The relationship between passive joint laxity and functional outcome after anterior cruciate ligament injury. *Am J Sports Med* 25, 191-195.
- Soderkvist, I., Wedin, P.A., 1993. Determining the movements of the skeleton using well-configured markers. *J Biomech* 26, 1473-1477.
- Staubli, H.U., Noesberger, B., Jakob, R.P., 1992. Stressradiography of the knee. Cruciate ligament function studied in 138 patients. *Acta Orthop Scand Suppl* 249, 1-27.
- Stratford, P., Miseferi, D., Ogilvie, R., Binkley, J., Wuori, J., 1991. Assessing the Responsiveness of Five KT1000 Knee Arthrometer Measures used to Evaluate Anterior Laxity at the Knee Joint. *Clinical Journal fo Sport Medicine* 1, 225-228.
- Thornton, G.M., Oliynyk, A., Frank, C.B., Shrive, N.G., 1997. Ligament creep cannot be predicted from stress relaxation at low stress: a biomechanical study of the rabbit medial collateral ligament. *J Orthop Res* 15, 652-656.
- Thornton, G.M., Shrive, N.G., Frank, C.B., 2001. Altering ligament water content affects ligament pre-stress and creep behaviour. *J Orthop Res* 19, 845-851.
- Uhorchak, J.M., Scoville, C.R., Williams, G.N., Arciero, R.A., St Pierre, P., Taylor, D.C., 2003. Risk factors associated with noncontact injury of the anterior cruciate ligament: a prospective four-year evaluation of 859 West Point cadets. *Am J Sports Med* 31, 831-842.
- Un, B.S., Beynnon, B.D., Churchill, D.L., Haugh, L.D., Risberg, M.A., Fleming, B.C., 2001. A new device to measure knee laxity during weightbearing and non-weightbearing conditions. *J Orthop Res* 19, 1185-1191.
- Unknown, 2007. illustration, body planes <http://training.seer.cancer.gov>. In, Surveillance Epidemiology and End Resuls Program. Atlanta, Georgia.
- Veldpaus, F.E., Woltring, H.J., Dortmans, L.J., 1988. A least-squares algorithm for the equiform transformation from spatial marker co-ordinates. *J Biomech* 21, 45-54.
- Wacker, F.K., Hillenbrand, C., Elgort, D.R., Zhang, S., Duerk, J.L., Lewin, J.S., 2005. MR imaging-guided percutaneous angioplasty and stent placement in a swine model comparison of open- and closed-bore scanners. *Acad Radiol* 12, 1085-1088.
- Watson, P.E., Watson, I.D., Batt, R.D., 1980. Total body water volumes for adult males and females estimated from simple anthropometric measurements. *Am J Clin Nutr* 33, 27-39.
- Williams, B.A., Kentor, M.L., Williams, J.P., Figallo, C.M., Sigl, J.C., Anders, J.W., Bear, T.C., Tullock, W.C., Bennett, C.H., Harner, C.D., Fu, F.H., 2000. Process analysis

in outpatient knee surgery: effects of regional and general anesthesia on anesthesia-controlled time. *Anesthesiology* 93, 529-538.

Winter, D. (Ed.) 1990. *Biomechanics and Motor Control of Human Movement*. Wiley-Interscience.

Wojtys, E.M., Huston, L.J., Boynton, M.D., Spindler, K.P., Lindenfeld, T.N., 2002. The effect of the menstrual cycle on anterior cruciate ligament injuries in women as determined by hormone levels. *Am J Sports Med* 30, 182-188.

Woltring, H.J., 1991. Representation and calculation of 3-D joint movement. *Human Movement Science* 101, 603-616.

Woo, S.L., 1982. Mechanical properties of tendons and ligaments. I. Quasi-static and nonlinear viscoelastic properties. *Biorheology* 19, 385-396.

Woo, S.L., Debski, R.E., Withrow, J.D., Janaushek, M.A., 1999. *Biomechanics of Knee Ligaments*. American Journal of Sports Medicine 27, 533-543.

Wretenberg, P., Ramsey, D.K., Nemeth, G., 2002. Tibiofemoral contact points relative to flexion angle measured with MRI. *Clin Biomech (Bristol, Avon)* 17, 477-485.

Zantop, T., Herbort, M., Raschke, M.J., Fu, F.H., Petersen, W., 2007. The role of the anteromedial and posterolateral bundles of the anterior cruciate ligament in anterior tibial translation and internal rotation. *Am J Sports Med* 35, 223-227.

Zazulak, B.T., Paterno, M., Myer, G.D., Romani, W.A., Hewett, T.E., 2006. The effects of the menstrual cycle on anterior knee laxity: a systematic review. *Sports Med* 36, 847-862.

Zimny, M.L., Wink, C.S., 1991. Neuroreceptors in the Tissues of the Knee Joint. *Journal of Electromyography and Kinesiology* 1, 148-157.

APPENDIX A: KÜPPER ET AL 2006

A.1. Publisher's Permission to Include Publication in Thesis

From: Jones, Jennifer (ELS-OXF) [J.Jones@elsevier.co.uk]
Sent: Thursday, May 31, 2007 4:51 AM
To: johnsojc@ucalgary.ca
Subject: RE: Obtain Permission

Dear Jessica C Kupper

We hereby grant you permission to reprint the material detailed below at no charge in your thesis subject to the following conditions:

1. If any part of the material to be used (for example, figures) has appeared in our publication with credit or acknowledgement to another source, permission must also be sought from that source. If such permission is not obtained then that material may not be included in your publication/copies.

2. Suitable acknowledgment to the source must be made, either as a footnote or in a reference list at the end of your publication, as follows:

"This article was published in Publication title, Vol number, Author(s), Title of article, Page Nos, Copyright Elsevier (or appropriate Society name) (Year)."

3. Your thesis may be submitted to your institution in either print or electronic form.

4. Reproduction of this material is confined to the purpose for which permission is hereby given.

5. This permission is granted for non-exclusive world English rights only. For other languages please reapply separately for each one required. Permission excludes use in an electronic form other than submission. Should you have a specific electronic project in mind please reapply for permission

6. This includes permission for the Library and Archives of Canada to supply single copies, on demand, of the complete thesis. Should your thesis be published commercially, please reapply for permission.

Yours sincerely

Jennifer Jones
Rights Assistant

Your future requests will be handled more quickly if you complete the online form at www.elsevier.com/permissions

Elsevier Limited, a company registered in England and Wales with company number 1982084, whose registered office is The Boulevard, Langford Lane, Kidlington, Oxford, OX5 1GB, United Kingdom.

-----Original Message-----

From: johnsojc@ucalgary.ca [mailto:johnsojc@ucalgary.ca]
Sent: 17 May 2007 20:51
To: Rights and Permissions (ELS)
Subject: Obtain Permission

This Email was sent from the Elsevier Corporate Web Site and is related to Obtain Permission form:

Product: Customer Support
Component: Obtain Permission
Web server: http://www.elsevier.com
IP address: 10.10.24.148
Client: Mozilla/4.0 (compatible; MSIE 6.0; Windows NT 5.1; SV1; InfoPath.1; .NET CLR 1.1.4322)

Invoked from:
http://www.elsevier.com/wps/find/obtainpermissionform.cws_home?isSubmitted=yes&navigateXmlFileName=/store/prod_webcache_act/framework_support/obtainpermission.xml

Request From:
Ms. Jessica C. Kupper
University of Calgary
#310, 3111-34th Ave NW
T2L 0Y2
Calgary
Canada

Contact Details:
Telephone: 403-220-4687
Fax:
Email Address: johnsojc@ucalgary.ca

To use the following material:
ISSN/ISBN: 0268-0033
Title: Clinical Biomechanics
Author(s): Kupper J, Loitz-Ramage B, Corr D, Hart D, Ronsky J
Volume: 22
Issue: 1
Year: 2007
Pages: 1 - 13
Article title: Measuring knee joint laxity: A review of applic...

How much of the requested material is to be used:
The entire article

Are you the author: Yes
Author at institute: Yes

How/where will the requested material be used: [how_used]

Details:

I would like to include the article "Measuring knee joint laxity: a review of applicable models and the need for new approaches to minimize variability" in my masters thesis. According to the thesis guidelines at the University of Calgary, I must rework the paper into my thesis, in this case into my intro, literature review, and methods sections. Additionally, I will have an appendix with the original paper, and a list of contributions from my co-authors to help delineate my contribution. Finally I must have permission from the publisher and permission from my coauthors.

Additional Info: This review paper is based on the literature review that I did for my graduate work, and is an important part of my thesis.
- end -

For further info regarding this automatic email, please contact:
WEB APPLICATIONS TEAM (esweb.admin@elsevier.co.uk)
This email is from Elsevier Limited, a company registered in England and Wales with company number 1982084, whose registered office is The Boulevard, Langford Lane, Kidlington, Oxford, OX5 1GB, United Kingdom.

A.2. Co-Authors' Permission to Include Publication in Thesis

From: Janet Ronsky [mailto:jlronsky@ucalgary.ca]
Sent: Tuesday, January 08, 2008 8:55 AM
To: Jessica Kupper

Jess:

Thanks, and yes you certainly have my permission to use the laxity paper review in the published thesis.

Janet.

From: Barbara Ramage [Barbara.Ramage@calgaryhealthregion.ca]
Sent: Tuesday, July 03, 2007 4:51 PM
To: Jessica Kupper
Cc: 'David Hart'; Janet Ronsky; corrd@rpi.edu

I give my permission to use the article for your thesis. No problem.
Barbara

From: David T. Corr [corrd@rpi.edu]
Sent: Tuesday, July 03, 2007 6:41 PM
To: Jessica Kupper

Of course, please use it to the fullest extent. Good luck in writing your thesis.

Cheers,
-D

From: David Hart [hartd@ucalgary.ca]
Sent: Tuesday, July 03, 2007 6:51 PM
To: Jessica Küpper
Hi Jessica,

You have my permission to use the review for your thesis.

Dave Hart

Jessica Küpper wrote:

Co-Authors,

I would like to include our article "Measuring knee joint laxity: a review of applicable models and the need for new approaches to minimize variability" (Clin Biomech, 2007) in my masters thesis. According to the thesis guidelines at the University of Calgary, I must rework the paper into my thesis, in this case into my intro, literature review, and methods sections. Additionally, I will have an appendix with the original paper, and a list of contributions from my co-authors to help delineate my contribution. Finally I must have permission from the publisher (which I have just received) and permission from my coauthors. If you could send a quick reply to this email indicating whether I may have your permission, I believe that would meet the requirements.

Thanks very much,
Jessica Küpper

A.3. Breakdown of Contributions by Section

1. Kupper, Loitz-Ramage, Hart
2. Kupper, Loitz-Ramage, Ronsky
3. Kupper, Ronsky,
4. Kupper, Corr, Ronsky
5. Kupper, Loitz-Ramage, Corr, Hart

A.4. Küpper, J.C., Loitz-Ramage, B., Corr, D.T., Hart, D.A., Ronsky, J.L.

Measuring Knee Joint Laxity: A Review of Applicable Models and the need for New Approaches to Minimize Variability. Clinical Biomechanics, 22(1):1-13, 2007



Review

Measuring knee joint laxity: A review of applicable models and the need for new approaches to minimize variability

J.C. Küpper^a, B. Loitz-Ramage^b, D.T. Corr^b, D.A. Hart^{c,*}, J.L. Ronsky^{a,b}

^a Department of Mechanical and Manufacturing Engineering, University of Calgary, Calgary, AB, Canada

^b McCaig Centre for Joint Injury and Arthritis Research, 3330 Hospital Dr. NW, Calgary, AB, Canada T2N 4N1

^c Departments of Surgery, Microbiology and Infectious Diseases, and Medicine, University of Calgary, Calgary, AB, Canada

Received 10 March 2006; accepted 21 August 2006

Abstract

Knee joint laxity can result from soft tissue injury, such as a ligament tear, or from genetic factors such as joint hypermobility syndrome and various forms of Ehlers–Danlos Syndrome. The location of a subject's passive knee laxity along a continuous spectrum is dependent on the mechanical properties of the existing structures, and the increased motion that often follows joint injury. At a threshold along the spectrum, a patient will be at risk for joint instability and further injury to joint structures. Links between instability and laxity may be better understood if laxity can be reliably and accurately quantified. Current measures of laxity have not been compared to a 'gold standard' in all cases, and when they have, were found to overestimate the laxity values. This is attributed to soft tissue deformation. Consequently, a noninvasive measure of laxity with improved accuracy and repeatability would be useful clinically and in the research sector. In this review, current clinical measures of laxity are critiqued, criteria for a measure of laxity are identified, and three theoretical models of knee laxity are outlined. These include contact, lumped parameter, and finite element models, with emphasis on applicability, strengths, and limitations of each. The long term goal is to develop a model and method able to differentiate subjects along a spectrum of laxity, and understand the functional implications of altered joint integrity. This would allow careful scrutiny of clinical interventions aimed at improving joint health and provide a valuable research tool to study joint injury, healing, and degeneration. © 2006 Elsevier Ltd. All rights reserved.

Keywords: Stiffness; Ligament force; Magnetic resonance imaging; Contact; Lumped parameter; Finite element

1. Introduction

In biomechanical terms, passive laxity is a measure of joint movement within the constraints of ligaments, capsule, and cartilage (Cross, 1996) when an external force is applied to the joint during a state of muscular relaxation. Laxity depends on the shape of the involved bony surfaces, the mechanical behavior of the joint's soft tissue structures, such as the joint capsule and ligaments, and contributions from other supporting structures, such as menisci, that may improve the bony fit between relatively incongruent joint surfaces. Theoretically, laxity can be measured at any joint,

although some joints are inherently very stable, such as the sacroiliac joints between the two halves of the pelvis and the centrally located sacrum. In these cases, laxity is not typically assessed by quantifying the motion of the joint, but by whether passive motion produces pain or other symptoms. The human shoulder is a good example of a lax joint that relies entirely upon ligaments for passive stability because the capsule is very loose and the bony anatomy provides minimal contributions to joint stability. In this case, the benefit of having a lax joint is a considerable increase in the total range of joint motion, allowing humans to reach overhead with relative ease. Therefore, a measure of laxity must be interpreted contextually, including the function of the joint (weightbearing support vs. functional reach or grasping).

* Corresponding author.

E-mail address: hartd@ucalgary.ca (D.A. Hart).

Increased joint laxity can result from a local soft tissue injury such as a ligament tear or from genetic factors such as joint hypermobility syndrome and the various forms of Ehlers–Danlos Syndrome. Excessive joint laxity predisposes the joint to instability including recurrent dislocations and subluxations, and low grade inflammatory arthritis (Lewkonja, 1993). However, the link between instability and laxity is not fully understood (Maffulli, 1998; Patel et al., 2003). Knee joint laxity is of particular interest, and has been studied extensively, in part, due to the high incidence of knee injuries, knee joint pain, and degeneration that account for substantial morbidity, functional loss, and health care expenditures.

The knee joint exhibits a wide spectrum of laxity, from inherently stable joints at one end, to excessively lax joints at the other. The causes of abnormal laxity are numerous and complex. Individuals with high joint laxity, such as those with Anterior Cruciate Ligament (ACL) tears, are more likely to incur subsequent knee injuries. Interestingly, even the normal, uninjured population displays a wide range of knee laxity. For example, young, fit military recruits, who are otherwise healthy, have exhibited laxity at the high end of the spectrum, without any prior injury or existing pathology (Uhorchak et al., 2003). This normal range of laxity is further complicated in sexually mature females where, at least in a subpopulation of them, changes in joint laxity have been reported to occur during the menstrual cycle (Deie et al., 2002; Shultz et al., 2004, 2006; Wojtys et al., 2002). However, this point is still controversial (Belanger et al., 2004), and it is not clear if there are biologically different populations, or subtle differences in methodology that are confounding the findings.

In the ACL deficient knee (ACLD), laxity values lie at the far end of the spectrum. ACLD subjects are often subdivided into copers, who functionally adjust to the injury, and noncopers, who experience increased instability, including recurrent subluxations (Eastlack et al., 1999). Noncopers are often candidates for ACL reconstruction (ACLR), where the torn ligament is commonly replaced by either the central third of the patellar tendon or the gracilis/semitendinosus tendon (Herrington et al., 2005). After reconstruction, laxity is reduced but the joint does not return to normal function (Almekinders et al., 2004; Ejerhed et al., 2003).

Another factor that affects joint laxity is an individual's genetic predisposition for pathologies such as Marfan's syndrome, Ehlers–Danlos syndrome, and joint hypermobility syndrome. This latter disorder appears to affect connective tissue matrix proteins, thereby altering the mechanical properties of the soft tissues and creating an inherent joint laxity (Hakim and Grahame, 2003). The majority of individuals with joint hypermobility syndrome are female (Acasuso-Diaz et al., 1993; Baum and Larsson, 2000; Bridges et al., 1992), and the incidence has been reported to vary from 5% of the Caucasian population to ~30% of females of Middle Eastern descent (Al-Rawi et al., 1985; Bridges et al., 1992; Fitzcharles, 2000). These

subjects are more lax than normal, and are unique from an injured population because the musculoskeletal laxity is something they have matured with rather than having to adjust to a sudden change in joint laxity following an acute injury. Those with joint hypermobility syndrome are also unique because the laxity may not be restricted to a particular joint. Some patients with joint hypermobility syndrome demonstrate laxity throughout all joints, while others may experience laxity in only upper extremity or only lower extremity joints.

It is important to distinguish *passive* laxity, which is measured during a state of muscle relaxation, from *functional* or *active* laxity, which describes the joint motion that occurs during functional activities. In the latter, the forces applied through the joint arise from muscle contraction or external loads related to movement, such as inertial or ground reaction forces. This distinction is clinically important because some patients with passive laxity do not demonstrate functional laxity (Snyder-Mackler et al., 1997). Muscle contraction or co-contraction (Aalbersberg et al., 2005a) that is well-timed and of an appropriate magnitude may play a role in controlling dynamic joint function by preventing excessive joint laxity from limiting function or increasing joint injury risk. Regardless of the underlying cause or number of affected joints, at a certain threshold along the spectrum a patient will be at risk for joint injury because of instability. The link between instability and laxity may be further understood if laxity can be reliably and accurately quantified.

The objective of this review is to critique the current clinical measures of laxity, identify the criteria for a measure of laxity, and outline three potential theoretical models of knee laxity. The long term goal is to develop a model and method that can be used to differentiate subjects along the laxity spectrum, and understand the functional implications of altered joint integrity.

2. Current measures of joint laxity

Traditionally, passive tests have been used to assess knee laxity in patients. These measures include the Lachman test, the anterior/posterior drawer test, the pivot shift test, the quadriceps active test, and the varus/valgus stress test (Malanga et al., 2003). The primary structures being tested are the ACL, posterior cruciate ligament (PCL), and medial and lateral collateral ligaments (MCL, LCL). These clinical measures can be effective for an experienced physician, and have been useful for determining treatment protocol. However, they do not allow for quantitative comparison between subjects or testers since the results are qualitative and primarily used for diagnosis (Malanga et al., 2003). These clinical measures are not sufficient for understanding the impact of the injuries or genetic pathologies.

In response to this need, instrumented devices such as the KT-2000 arthrometer (<http://www.medmetric.com>, MedMetric, San Diego, CA, USA), the Genucom Knee

Analysis System (<http://www.faro.com/>, Faro Medical Technologies, Champlain, NY, USA), the Rolimeter (<http://www.rolimeter.com>, Aircast, Summit, NJ, USA), and the Stryker Ligament Tester (<http://www.stryker.com>, Stryker, Kalamazoo, MI, USA) were developed to quantify laxity. These devices use displacement transducers and/or digitized bony landmark positions to measure tibial translation with respect to the patella under an applied load.

The devices that have been and are currently used to measure joint laxity include traditional and alternative systems. Traditionally, the KT-2000 arthrometer, the Genucom Knee Analysis System, the Rolimeter, and the Stryker Ligament Tester have been used in research and clinical settings. Each system has features that have set the standard for measuring knee laxity. Cannon (2002) noted that arthrometers allow experienced clinicians to detect injuries that would have been missed otherwise. Alternate systems, such as planar stress radiography, Roentgen Stereophotogrammetric Analysis RSA, and magnetic resonance imaging (MRI), have been primarily employed in research to obtain more accurate measures of displacement under a known applied force or task.

2.1. Traditional measurement systems

The most commonly used arthrometer in both biomechanical research and clinics is the KT-2000, which measures anterior–posterior knee laxity during the drawer test. The subject lies supine in slight hip flexion and with a knee flexion angle between 20° and 35° (Fig. 1a). The knee must be flexed adequately to engage the patella in the femoral groove. If the flexion is inadequate, the patella will not provide a stable base from which tibial displacement can be measured. External hip rotation is restricted by a Velcro strap placed midthigh and tibial position is maintained by placing the subject's feet between two vertical supports that prevent the feet from rolling outward. The arthrometer is secured to the anterior tibia with Velcro straps, with a proximal bar contacting the anterior patella surface, the motion axis oriented over the joint line, and the force plunger positioned over the tibial tubercle. With the subject relaxed, a dial on the front of the machine is adjusted to a neutral starting position of the tibia with respect to the patella. The examiner then passively translates the tibia posteriorly and anteriorly, with a goal of establishing the same neutral starting position with each cycle. This trial also helps the subject to completely relax because it allows them to become accustomed to the motion. If the initial starting position changes between cycles, it is likely that the subject is either protecting the joint by contracting the thigh muscles, or the patellar reference pad is moving. If the starting position is stable, anteriorly and posteriorly directed passive loads of 67N and 178N (Myrer et al., 1996) are then applied through the force handle of the arthrometer.

The Genucom is also used to measure anterior–posterior knee laxity, however, it is also capable of measuring

a ACL Assessment: Quadriceps Active Test at 30°

Purpose: To Measure tibial displacement with a quadriceps muscle contraction

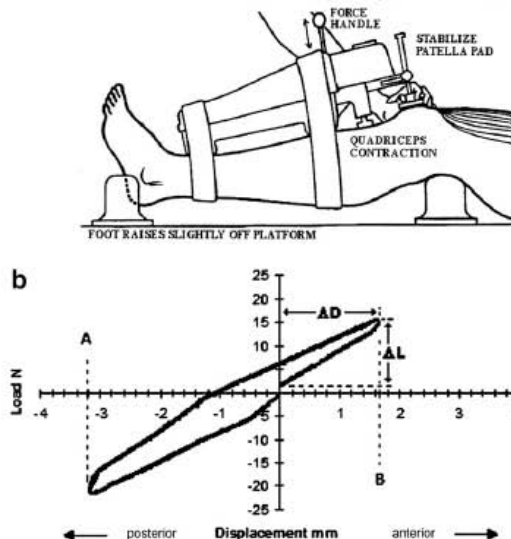


Fig. 1. (a) Positioning of subject for testing with the KT-2000 arthrometer. Modified from "Quadriceps active test at 30° " reprinted with permission from MEDMetric Inc. (b) A typical force–displacement curve resulting from testing with the KT-2000 arthrometer; "A" and "B" denote peak posterior and anterior displacement respectively. The compliance index for the anterior drawer test is calculated as $\Delta L/\Delta D$.

motion in several planes simultaneously (Cannon, 2002). This includes measuring varus–valgus, pivot shift, and recurvatum (Highgenboten et al., 1989). The testing procedure for measuring anterior–posterior knee laxity with this device, as summarized here, was originally described in Highgenboten et al. (1989). The Genucom system includes a computer that is used to record the subject's data file. The subject is positioned with the knee flexed to 20° . The thigh is secured with restraints, and an electrogoniometer is attached to the thigh and shank. Anatomical landmarks including the tibial tubercle, tibial crest, medial and lateral femoral condyles, and the patella are marked and digitized, and used to obtain a coordinate system and record the relative displacement at the knee joint, and the distance between markers is documented. Consequently, this system is sensitive to soft tissue motion as with any markers, although this effect is minimized by locating them on bony landmarks. To account for motion within the Genucom, a soft tissue compensation test can be performed in three planes while maintaining the same distance between the markers. Furthermore, as with the KT-2000, the patella should be engaged in the femoral groove. The anterior–posterior drawer test is completed at the system's required force magnitude of 21 lbs (93.45 N). Data is collected continuously at a rate of 8 Hz (Andersen and Jorgensen, 1998), and is stored electronically.

The Rolimeter is used to measure anterior–posterior laxity for Lachman, anterior drawer, and ‘step off’ tests. The subject is positioned supine, with knees flexed to 25° for the Lachman test, 80° for the anterior drawer test, and an unspecified angle for the ‘step off’ test. The knee is supported by a pillow for the Lachman test. Unlike the KT-2000, the only specification for foot position is for the anterior drawer test, where the tester sits on the subject’s foot. A proximal convex pad rests over the patella, and a distal pad is fixed to the tibia with a rubber strap (Papandreou et al., 2005). The two pads are connected a few inches above the limb by a calibrated steel bar. The stylus is an additional arm that projects down from the steel bar onto the tibial tuberosity. As described in Muellner et al. (2001), the patella can either be stabilized with the thumb, or with the technique used for the KT-1000. Similarly for the KT-2000, the quadriceps muscles must be relaxed. The knee is preconditioned with three applications of a posterior force to the tibia. The tester must ensure that the stylus foot is in contact with the tibial tuberosity, and the white indicator, a movable plastic ring, is against the adjustment knob. The white indicator displaces when the tibia is manually pulled anteriorly. The displacement is measured in increments of 2 mm. For both the Lachman and anterior drawer tests, a manual maximum anterior force is applied three times, and the three maximal anterior translations are measured and averaged. For the ‘step off’ or side-to-side difference test, the Rolimeter is calibrated by applying it to the injured leg while applying a posterior force, ensuring that the stylus is in contact with the tibial tuberosity. It is then applied to the uninjured leg, and the side to side difference can be recorded. The benefit of the Rolimeter is that it is small, portable, and autoclavable. However, it neither records data nor tests at a variety of force levels. Furthermore, the displacements are measured at the endpoint of tibial motion with relatively low resolution (± 2 mm).

The Stryker Ligament Tester has a patient positioning seat, force applicator, and a displacement transducer. Like both the KT-2000 and the Rolimeter, this device uses the patella and the tibial tuberosity as reference points to measure displacement. One disadvantage of using the patella as a reference point is that it is not firmly attached to the femur, and therefore must be well-seated in the femoral groove to reduce the relative motion. Unlike the Genucom, which can account for out of plane motion, the Stryker Ligament Tester assumes that there is only anterior–posterior displacement. As Cannon (2002) describes, the ankle is secured with a strap, and the flexion angle is set between 0° and 90°, although 25°–30° is typical. The calibrated ruler is positioned horizontally, and the proximal tibial bracket is placed on the tibial tubercle. The distal bracket is positioned above the ankle, with an external rotation to align it with the tibia. Three straps secure the device at the proximal and distal ends of the tibia, and at the thigh just above the patella. The measuring gauge is positioned over the patella with the button at the midpoint. The patient leans back and relaxes while the examiner stabilizes the thigh

with their non dominant hand, and applies a load with the force applicator, which is positioned over the crest of the tibia for a posterior load and behind the proximal calf for an anterior load. The resulting displacement at the endpoint of tibial displacement is measured to the nearest 0.5 mm.

For the arthrometers that are capable of measuring continuously during the anterior–posterior drawer test, including the KT-2000 and the Genucom, force and displacement of the tibial sensor are recorded throughout the posterior and anterior motions, and can result in a plot as seen in Fig. 1b. Traditionally, laxity is measured from these cycles as the peak displacement with respect to the starting zero point at a given load. A compliance index (Daniel et al., 1985) is also computed from the force–displacement curve as the slope of a line connecting the points corresponding to zero displacement and the peak anterior or posterior displacement. Both knees of the subject are tested and an interlimb difference is computed. Interlimb differences normalize the subject’s involved knee to the uninjured, thereby accounting for the subject’s specific, total body laxity. Moreover, this value can also be obtained by arthrometers that only measure the displacement at the endpoint of tibial motion, including the Rolimeter and the Stryker Ligament Tester. An interlimb peak displacement difference greater than 3 mm is considered indicative of anterior cruciate ligament insufficiency.

Additional work has been done by Maitland et al. (1995) to quantify the nonlinear force–displacement curve by taking the first (stiffness) and second (change in stiffness) derivatives. These values differ from the compliance index by calculating the instantaneous slope at each discrete point along the force–displacement curve, giving true stiffness, rather than an average slope based on initial and peak displacements, which does not characterize the entire curve. By accounting for the entire nonlinear response, this method is able to identify significant material behaviors that could not be appreciated by an average linear stiffness. Quantifying the entire force–displacement curve highlights an increasing slope as the ACL works to restrain the knee after tibial weight is overcome. In this study, the authors showed that low values of stiffness and change in stiffness were typical for ACLD subjects in the upper region of the force–displacement curve, where the ACL is believed to be the primary restraint. In comparison, control subjects showed higher stiffness and change in stiffness over this range. These results highlight the value in quantifying stiffness along the curve, as individual sections of the curve (toe region, linear portion, upper region) can be analyzed and used to differentiate injured from control populations. It is particularly important to quantify the low load behavior during the toe region of the force–displacement curve as it spans the normal operating range of the knee.

The relative use of these arthrometers has changed over time. The KT-2000 system continues to be the most popular device for measuring joint laxity, while other units such as the Genucom seem to be used less frequently in recent

years based on literature reports. This conclusion is highlighted in Fig. 2, which shows the number of papers per year in which each type of arthrometer is referenced. Searches were done using the National Center for Biotechnology Information PubMed database (from 1966 to June 2006) using the search terms “KT 1000” or “KT-1000” or “KT 2000” or “KT-2000”, “Genucom”, “Stryker Ligament Tester” or “Stryker Knee Laxity Tester” or “Stryker Laxity Tester”, and “Rolimeter”. There are many possible reasons why the KT-2000 appears to be the preferred laxity measurement system. Some factors could include cost, availability, or the suitability of the system to the application. Complex systems that allow a greater range of measurements such as the Genucom may be better suited to a research environment, however, using the KT-2000 in a research study allows for comparison of data to a large body of published work. The KT-2000 is smaller and thus more easily portable than the Genucom, making it amenable to the clinical setting. The Rolimeter and the Stryker Ligament Tester are also small lightweight systems, making them easily transportable and straightforward to use. However, the KT-2000 has a digital output rather than analog, and so can generate real-time force–displacement graphs. It seems that the KT-2000 may fit a niche due to the balance of convenience and simplicity with descriptive output measures.

One limitation of the majority of these devices is that they only measure translational displacement, which is assumed to be solely in the anterior/posterior direction, thereby neglecting the entire range of laxity as the knee moves with six degrees of freedom. It has been shown that passive laxity tests with the KT-2000 do not correlate to functional outcome after ACL injury (Snyder-Mackler et al., 1997). A number of studies have been conducted to assess the accuracy and reliability of these devices (Anderson and Lipscomb, 1989; Anderson et al., 1992; Cannon, 2002; Highgenboten et al., 1989; Huber et al., 1997; Papandreou et al., 2005). The results are summarized in Table I. Most of these studies rely on comparisons between arthrometers or repeatability studies for validation, rather than determining accuracy with respect to a ‘gold standard’

measurement device. It is important to note that the importance of studying accuracy is to determine how closely an arthrometer can measure the correct value. Conversely, repeatability describes how closely a device can obtain the same value over multiple measurements, regardless of whether this value is correct or not.

It has been found that, in general, there is variability between testers (Cannon, 2002). The KT-1000, for example, had an intertester reliability of ± 2.95 mm and ± 3.74 mm for posterior and anterior translation, respectively (Huber et al., 1997). Given that a right-left difference of 3 mm or more is taken as an indication of increased laxity (Cannon, 2002), poor intertester reliability may result in false negative tests because the difference between examiners is greater than the patient’s interlimb difference. Highgenboten et al. (1989) compared the KT-1000, Genucom, and Stryker Ligament Tester devices. They found that the Genucom produced significantly higher anterior laxity values than the other devices, showing that the results are specific to each device. These studies have shown that although the current laxity devices have made methodological advances for quantifying laxity, poor inter-tester reliability continues to plague current devices. A few studies have been done to determine the accuracy of arthrometers. In the study done by Jorn et al. (1998), the Stryker Ligament Tester was compared to RSA, and found to overestimate anterior tibial translation, which was attributed to soft tissue displacement. Thus, there is clearly a need for both a measure of laxity that is less variable and improved methodology for clinical assessment of joint laxity in a defined manner. This is of particular importance to understanding the mechanisms involved with, and the efficacy of, interventions developed to negate the impact of excessive or variable laxity on joint function and minimize risk for loss of joint health.

2.2. Alternate measurement systems

Various techniques other than displacement transducers have been used to measure tibial motion, including planar stress radiography, RSA, and MRI. These imaging techniques have shown promise in measuring displacement, especially as the quality of images improves with technology. Images of the knee can also be reconstructed or quantified in three dimensions, thereby allowing calculation of the entire tibial displacement, rather than simply in the anterior–posterior direction.

Planar stress radiography uses a series of lateral radiographs to quantify the displacement of the tibial condyles with respect to the femoral condyles (Fleming et al., 2002). It is noninvasive, with a reproducibility of ± 0.5 mm (Stäubli et al., 1992). RSA measures motion in three dimensions by spatial reconstruction of tantalum beads implanted into the cortices of the bones of interest, with reported translational and rotational accuracies of 10–250 μ m and 0.03° – 0.6° respectively (Kärrholm, 1989; Selvik, 1989). Although this technique provides the most

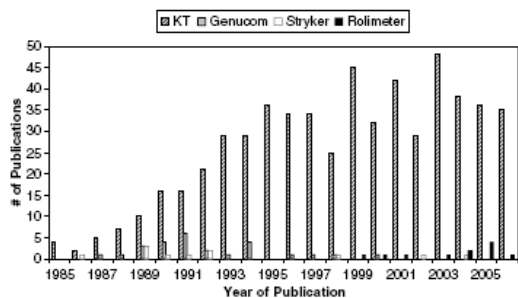


Fig. 2. Number of publications per year that include the KT-1000/2000, Genucom, Stryker Ligament Tester, or Rolimeter arthrometers from 1985 to 2006.

Table 1
Accuracy and repeatability of current laxity devices

Device	Repeatability/reliability	References
KT-1000 or KT-2000	Anterior: ± 3.99 mm, ± 3.89 mm, ± 3.74 mm ^a	Huber et al. (1997)
	Posterior: ± 2.95 mm, ± 2.53 mm, ± 3.27 mm	
	Anterior: 0.87 ^b	Highgenboten et al. (1989)
	Posterior: 0.79	
	0%, 82% ^c	Anderson et al. (1992)
	0%, 75% ^c	Anderson and Lipscomb (1989)
Genucom	Anterior: 0.96 ^b	Highgenboten et al. (1989)
	Posterior: 0.86	
	23%, 76% ^c	Anderson et al. (1992)
	10%, 70% ^c	Anderson and Lipscomb (1989)
Rolimeter	Anterior between three testers:	Papandreou et al. (2005)
	$r(P1 \text{ vs. } P2) = 0.96$	
	$r(P1 \text{ vs. } P3) = 0.55$	
	$r(P2 \text{ vs. } P3) = 0.57$	
Stryker ligament tester	Anterior: 0.74 ^b	Highgenboten et al. (1989)
	Posterior: 0.87	
	Anterior/posterior: 0.83	Jorn et al. (1998)
	0%, 82% ^c	Anderson et al. (1992)
	10%, 75% ^c	Anderson and Lipscomb (1989)
	4.4 mm, 8.0 mm ^d	Jorn et al. (1998)

^a 95% CI for novice, experienced, and intertester respectively.

^b r value.

^c Percentage of 50 subjects diagnosed with false positives for ACL deficiency, percentage of 50 subjects diagnosed with true positives for ACL deficiency.

^d Mean difference from known value at 90 N and 180 N respectively.

accurate measure of laxity, the implantation of tantalum beads is highly invasive, and thus, cannot be readily applied to every subject group. Despite the benefits of both planar stress radiography and RSA, a major drawback to each is that patient exposure to radiation is required. The current standard for the recommended use of radiation is to minimize subject exposure, based on the understanding that any dose of radiation can have harmful effects (Picano, 2004). Furthermore, while radiography provides very clear images of bone, it does not image soft tissues well. This is an important limitation, as the majority of the passive restraints of the knee are soft tissues. Thus, a very clear view of joint laxity can be gained through bone-bone displacement, however, the behaviors of joint's soft tissues cannot be well observed, and thus the underlying reasons for the laxity may not be appreciated.

MRI imaging shows promise as a noninvasive, accurate modality for measuring displacement. Our group has applied methods from Geomatics engineering to improve surface registration of MRI images, and have obtained results with an average normal distance (a measure of how well two superimposed or registered images fit together) of 0.201 mm (Cheng et al., 2005). Employing imaging techniques to measure laxity would provide an improvement over knee arthrometer measurements because arthrometers require that the patella be well seated in the femoral groove to obtain an indication of the position of the femur relative to the tibia, while imaging modalities allow the direct measurement of the femoral position. Additionally, the detailed geometry attained with imaging

techniques allows for additional measures to be made. For example, the location of the tibiofemoral cartilage contact area can be found as an alternative measure of relative position, or the change in length of the ACL can be quantified. MRI has the additional benefit over other imaging modalities of being able to visualize soft tissues without requiring the subjects to be exposed to radiation. Thus, the entire joint, including the soft tissue structures, can be imaged in a radiation-free, non-invasive fashion. The best image quality can be achieved with a closed bore MRI compared to open bore or dynamic MRI. Closed bore MRI is also more widely available and is appropriate for the positioning typically used to measure knee joint laxity. However, closed bore MRI limits the range of motion that can be tested because of bore hole constraints, and requires the patient to lie supine.

3. Criteria for a measure of joint laxity

A measure of laxity must be applicable to a wide range of pathological and physiological conditions, including normal (normal males and hormonally cycling females), ACLD, ACLR, and joint hypermobility syndrome. Experimental protocols and theoretical models must therefore be designed to account for these conditions, and appreciate their differences among various patient populations. Daniel and Stone (1990) identified six variables upon which a measure of laxity will depend: measurement system, initial joint position, motion constraints of the test system, applied force, muscle activity, and passive motion constraints. All

of these variables must be controlled or accounted for if laxity is to be accurately and precisely measured. The measure of laxity should also be accessible, *in vivo*, noninvasive, safe, accurate, and repeatable to be applied successfully to either a clinical or research population.

3.1. Joint position, applied force, and motion constraints

Laxity has typically been assessed statically with the subject lying supine and the knee flexed at angles between full extension and 90° of flexion (Malanga et al., 2003). Anterior translation is most commonly assessed at a flexion angle of 30°, since this angle is believed to represent the slack-taut transition for the ACL (Sheehan and Rebmman, 2003). A limitation of testing in a supine position is that physiological loads of the knee cannot be obtained. To overcome this limitation a method was developed in which the subject can either apply a load (10%–15% of maximum) to a foot pedal or to resist a plantar force applied to the foot (Ronsky, 1994). This increases the patello-femoral contact area, confirming that external or resistive loading does affect knee contact mechanics (Gold et al., 2004; Ronsky, 1994). The external force must be applied uniformly to the tibia to ensure that the displacement is solely in the anterior direction. Laxity measures appear to be sensitive to the location of a point load because of the resulting internal/external moment applied to the tibia (Rudy et al., 2000). Forces are typically applied in the anterior–posterior direction, although some studies of laxity apply a torque to the tibia and measure torsional joint stiffness (Hsu et al., 2006). The wide ranging methods used to measure laxity underscore the need for a systematic and universally accepted definition of joint laxity and a similarly accepted technique for applying the necessary loads. Before undertaking comprehensive studies of interventions aimed at influencing joint laxity, researchers and clinicians must adapt similar language and measuring tools to allow comparison between laboratories and across disciplines.

3.2. Muscle activity

In measurements of laxity, methods are typically employed to minimize or exclude muscular contributions, such as quadriceps palpation to reduce muscle guarding during the anterior drawer test, and the administration of anaesthetics to induce muscle relaxation (Sernert et al., 2001). Alternatively, muscle forces can be included in laxity measurements; however, they must be accurately quantified. Muscle force can be measured directly, although these techniques are invasive, and typically reserved for animal models (Herzog and Leonard, 1996). This has led to the inclusion of noninvasive measures of muscular contributions, such as electromyography (EMG). Although EMG has been used to measure muscle force (Doorenbosch et al., 2005), it is a highly controversial method. Nigg (1999) notes that while there is a qualitative relation between muscle force and EMG signal, quantifying that

relationship is affected by a number of variables. Firstly, electrodes must be mounted properly to achieve a clear signal. Secondly, an electromechanical delay exists between the onset of the EMG signal and the actual force production of the muscle. Although the delay can be quantified, it may be variable throughout the contraction due to the viscoelasticity in the muscle–tendon unit. Isometric quadriceps contraction as seen in laxity testing is the optimal case for relating EMG to muscle force because a one to one relationship exists, and electromechanical delay will not change the result because there is no time dependence. However, deep muscle force cannot be measured from surface EMG, and thus the muscle force contribution will be restricted to that of the superficial muscles. Therefore, using EMG to measure muscle force should be approached with caution. The strength of this method is in obtaining relative force contributions rather than absolute measures of muscle force. If EMG is used in a theoretical knee model, the model should be tested for sensitivity to muscle force.

4. Theoretical models

A theoretical model of joint laxity requires a set of measurable inputs, outputs, and known constraints regardless of the modeling method chosen. The inputs can include the magnitude and direction of the applied force, knee flexion angle, detailed *in vivo* knee geometry before and after load application, limb mass, and constraint of all degrees of freedom of the femur. Additional inputs that could be measured include muscle force via EMG, and ground reaction force at the foot using a force transducer. The desired output of a theoretical model is a measure of joint laxity. Laxity can be viewed as the compliance of the joint, which is the reciprocal of joint stiffness. Therefore, an increase in joint compliance (laxity) will appear as a proportional decrease in joint stiffness. Stiffness is related to the passive structures of the knee joint, which in turn are related to the joint function. As a result, stiffness has been identified as a promising measure to study knee joint laxity (Maitland et al., 1995). If forces in the internal structures are plotted against their respective displacements, the stiffness of each structure can be determined as the slope of its force–displacement curve. Likewise, stiffness of the joint as a whole can be found from its displacement under an applied load. Stiffness provides a measure well-suited to quantify the behavior of the joint and internal structures because it describes the resistance of a body to applied forces.

Extensive literature exists that describes theoretical knee modeling, and consequently only a portion of this literature could be reviewed. Applicable knee models can be grouped into three main categories: contact, lumped parameter, and finite element models. The following discusses these categories of theoretical modeling, highlighting many of the advantages and limitations of each method.

4.1. Contact models

Contact models use contact points or areas between cartilage layers or bone position to describe tibial translation with respect to the femur in the direction of applied force. A proximity algorithm is often used to determine the points of contact. This method is well-suited to a gross measure of laxity, since displacement of the whole joint can be quantified based on anatomical landmarks. However, the specific points of contact considered and how displacement of those points is quantified influence the findings and must be considered when interpreting the data.

DeFrate et al. (2004) measured tibial displacement as the perpendicular distance from a line, connecting the mid-points of the medial and lateral tibial plateaus to the contact point. The contact point was defined in two ways: the centroid of the area formed by the overlap of the tibial and femoral cartilage, and the shortest distance between the tibia and femur, perpendicular to the tibial plateau. Their results showed a difference between the two contact point methods, highlighting the importance of cartilage geometry over bony geometry in determining contact points (DeFrate et al., 2004).

Other landmarks have been used to define anterior–posterior motion in the sagittal plane. Logan et al. (2004a,b) used the technique developed by Iwaki et al. (2000) in which the distance between the flexion facet center (the center of the posterior circular surfaces of the femoral condyles) and a line from the ipsilateral posterior tibial cortex is measured. Scarvell et al. (2004), note that the position of the femoral condylar centers can be more applicable to total knee arthroplasty prosthesis design because malalignment of the rotation axis may affect prosthesis fixation. The distance between the center of the tibiofemoral contact area and the posterior tibial cortex was also calculated. This choice was supported by the concept that these contact patterns describe motion that may affect articular cartilage degradation. Displacement in three dimensions was considered by Wretenberg et al. (2002) for contact areas on the medial and lateral condyles. They identified the most anterior, posterior, medial, and lateral contact point coordinates. These four points determined a contact area, from which the centroid points in all three planes were found. The benefit of considering a three dimensional measure is that it may provide more information about complex motion at the tibiofemoral interface than a simple two dimensional measure.

In a contact model, the magnitude and direction of the applied forces, limb position, and opposing muscle forces are assumed to be consistent between tests and across subjects. However, in practice, while applied forces and positioning can be controlled by the tester, some variability is introduced by the muscle forces acting on the knee. Furthermore, the relative contribution of the involved muscles may differ between patient populations. For example, slight subjects may exhibit different muscular activation strategies than trained individuals with welldeveloped mus-

culature, such as athletes. This is particularly important since athletes comprise a large portion of the ACL-injured population for whom laxity measures may be most relevant. Therefore, it is critical to control muscle activation levels when applying contact models, to minimize variability and improve the accuracy of comparisons across and within subject populations. One manner in which variability can be reduced is to employ a muscle palpation method, such as that used in KT-2000 tests, to ensure that the subject is fully relaxed. As a result, the subject is maintained in a state of muscular relaxation, and the variability incurred by muscle activation will be minimized, or avoided entirely.

Theoretical models are driven by the clinical purpose or research questions being asked. To understand the link between laxity and dynamic function, contact models may be advantageous because they provide a measure of whole joint laxity. Laxity measured at the whole joint level may be more clinically relevant since, theoretically, two individual joints may have identical whole joint laxity regardless of differences in the dimensions or mechanical properties of the internal structures. Furthermore, a measure of joint laxity describes how the joint performs as a whole, in physiologic conditions. Since contact models quantify relative joint position, they offer the theoretical model that most closely parallels current clinical laxity tests with potentially improved accuracy because displacement measurements are taken from accurate images of internal structures rather than external landmarks. Another benefit of contact models is that, in general, the model will not change among various subject populations. This is because the output measurements do not rely upon the material properties of the soft tissue, or the existence of specific structures other than the femur, tibia, and cartilage. For example, the model measurements do not depend on the existence of the ACL, and consequently, identical input and output variables are required when applying this model to a control population as for an ACLD population.

If the researcher or clinician desires to understand the underlying mechanisms of joint laxity, specifically within well-defined subject groups, a contact model will not be sufficient. Since the model does not include knowledge of the internal soft tissue structures, it is unable to appreciate their contributions to whole joint mechanics. The clinical importance of identifying how individual soft tissue structures affect the whole joint motion is an improved understanding of the underlying mechanisms of laxity. For example, comparing the stiffness of soft tissue structures in a normal knee to those in a knee with an MCL tear may aid in interpreting how and why the gross joint motion and functional ability of the patient differs from normal. Furthermore, if muscles are activated during a laxity test, these forces and their effects could be included to ensure consistency across tests. To account for these soft tissue effects, a specific lumped parameter model may be employed.

4.2. Lumped parameter models

Lumped parameter models use simple geometric shapes to characterize the arrangement of the underlying structures (e.g. muscles, tendons, and ligaments). The joint is modeled as a system of simplified geometries or mechanical constructs (e.g. two-force member). The combined behavior of these elements produces a model that displays similar mechanical behavior to the joint. These models provide an appropriate model of joint laxity provided the goal is to determine a gross value of stiffness for each soft tissue element that is individually included. Tendons and ligaments are assumed to behave as two force members. Therefore, lumped parameter models typically assume that all tendon and ligament fibers are the same length, and shorten the same amount. Two dimensional geometrical arrangements are often assumed to simplify the model, although three dimensional models have been constructed (Shahar and Banks-Sills, 2004).

The underlying assumptions of a lumped parameter model have a direct impact on the resulting measure of laxity. The knee joint represents an indeterminate system where the number of unknown internal forces is greater than the available equations describing the system (Herzog and Binding, 1999) (Fig. 3). The available equations include the four equations of static equilibrium (sum of forces and moments is zero), and the compatibility of deformations. These can be written for both the tibiofemoral and patel-

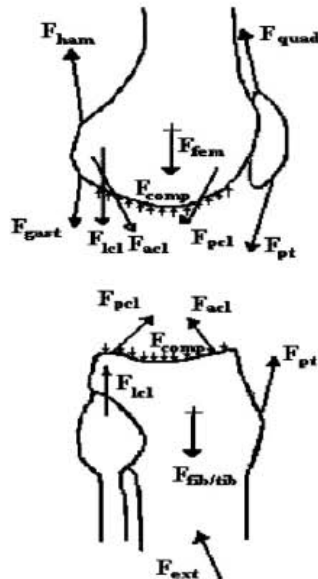


Fig. 3. Exemplary free body diagram of the knee joint including external (ext) forces, forces due to compression (comp), muscle force [gastrocnemius (gast), hamstring (ham), quadriceps femoris (quad)], femoral mass (fem), tibial and fibular mass (tib/fib), and forces through the anterior cruciate ligament (acl), posterior cruciate ligament (pcl), lateral collateral ligament (lcl), and patellar tendon (pt).

lofemoral joints. The unknown internal forces include the forces in the ACL, PCL, LCL, MCL, patellar tendon, capsule, contacting cartilage, menisci, and muscle forces (either passive or active). The modeler must then make the indeterminate system solvable. One solution method reduces the number of unknowns and/or increases the number of equations. The limitation of this approach is that relevant information about the contribution of a structure may be lost due to the simplification. Optimization is an alternative solution to the distribution problem that overcomes this issue. The system may be optimized to minimize a variable such as metabolic cost, total muscle force, or total muscle stress. These optimization techniques assume that the human body regulates forces in this manner, which is unlikely to be the true physiological mechanism. The clinical impact is that the model being used to treat and assess may be based on faulty assumptions. This could affect the accuracy of the outcome measures, and provide the clinician with incorrect values. Any or all of these methods may be employed to obtain a solvable model.

Lumped parameter models have been applied in a variety of ways to solve for the internal forces in the knee. Shahar and Banks-Sills (2004) included the femur, tibia, and patella, the hip joint reaction force, ground reaction force, muscle forces acting on the femur, and the collateral and cruciate ligaments of the knee in a three dimensional quasi-static model of the canine knee joint. They neglected hind limb weight, menisci, friction between joint surfaces, extensibility of the patellar ligament, and out of sagittal plane rotation of the patella. This model was applied to a simulated slow walk to observe ligament forces during stance phase in both an intact knee and a knee with a ruptured cruciate ligament, illustrating how a lumped parameter model can be developed to solve for ligament forces during a task and altered to consider other scenarios such as the effect of removing a structure.

Some studies consider various methods for determining the lines of actions of the force bearing structures (Aalbersberg et al., 2005b; Lu and O'Connor, 1996) or the muscle moment arms (Arnold et al., 2000). These types of studies often address parameter accuracy, and model sensitivity to each parameter (Tououngi et al., 1997). This is an important step in the modeling process. The model output accuracy is highly dependent on the accuracy and relative weighting of the input values. If an input value is physiologically variable, difficult to measure accurately, or can be measured in a variety of ways, it is crucial to test the sensitivity of the model to that input. Sensitivity is indicated by the amount of change in the output as a result of a change in the input. Each researcher must determine what level of sensitivity is acceptable given the specific application of the model.

Lumped parameter models allow ligament and tendon forces to be estimated *in vivo*. This class of model is quite flexible because it can be as simple models as a four bar linkage, or complex enough to include additional structures such as the joint capsule (Pandy and Shelburne, 1998). This

flexibility could be quite valuable clinically, as the model is adjustable to consider subjects who have an incomplete or lost structure. The complexity of the model is determined by its purpose. A lumped parameter model would theoretically be equally applicable to a model where the joint laxity is due to ACL loss compared to whole joint laxity as seen with joint hypermobility syndrome, as no assumptions are made with respect to material properties. The ACLD model would simply require one less unknown ligament force, and thus one less two-force member in the model. A model of knee joint laxity may help to determine how the muscle forces and the passive forces of the major supporting structures contribute to the overall joint stiffness.

The lumped parameter model has the potential to add more information to the clinician's assessment of laxity. This is achieved by identifying the mechanical contributions of individual soft tissue structures. These could be used to assess the mechanism of abnormal joint laxity and thus help to identify the appropriate treatment. Furthermore, coping strategies may be better understood if muscle forces and stiffness are determined. Lumped parameter models may provide a balance between increasing the understanding of how the soft tissue structures affect subject specific knee laxity and providing a level of detail that is appropriate for clinical application.

Nevertheless, the lumped parameter model can be quite sensitive to the assumptions that are made. As more structures are included, more constraints and assumptions must be included to solve for the system. Furthermore, not all structures can be simply represented as a two force member, such as the capsule or the cartilage. To gain insight into the mechanical behavior of individual structures based on *in situ* knee geometry rather than assuming idealized geometrical shapes, a finite element model can be used.

4.3. Finite element models

The finite element (FE) method is a modeling technique (numerical method) that discretizes a continuum into simple shapes called finite elements. Engineering concepts, including but not limited to beam theory, dynamics theory, or heat transfer theory, and constraints are applied to the elements to solve for the mechanical behavior of the entire structure. The advantage of an FE model is that complex three-dimensional geometry may be considered and the mechanical contributions of the individual structures can be included. Stress and displacement solutions can be found for the entire structure at each discrete point. This is a more detailed result than a lumped parameter model, and may potentially reveal localized weak points in the components that comprise the structure. Furthermore, the ability to apply static, dynamic, and thermal analyses to a complex geometry makes the FE method well suited to biomechanical problems.

FE models have been applied to solve the indeterminate system of the knee (Bendjaballah et al., 1998; Li et al., 2002; Moglo and Shirazi-Adl, 2003). That is, since the

model accounts for the mechanical contributions of the soft tissue structures individually, it allows tests (simulations) to be conducted in which tissue parameters are altered in a controlled manner. FE models can investigate the sensitivity of joint function to the mechanics of the supporting structures, providing a unique experimental avenue that cannot be carried out *in vivo*. These models can be employed to study the contributions of the musculature and passive tissue structures to knee joint function, such as the effect of quadriceps force when the ACL is removed, or partially torn (Li et al., 2002), the effect of passive tissue structure removal (Bendjaballah et al., 1998; Moglo and Shirazi-Adl, 2003), or reduced ligament stiffness on joint function (Li et al., 2002).

Modeling at this structural level allows FE models to appreciate the contributions of individual soft tissue structures to overall joint mechanics, as well as the sensitivity of the joint's function (e.g. range of motion, laxity) to changes in the individual soft tissue structures. However, since joint behavior is determined by the combined mechanical contributions of the substructure, the accuracy of FE models is only as good as the geometric representations and the material properties used to describe the soft tissue structures. One such mechanical property is Young's Modulus, which quantifies a material's ability to resist forces independent of geometry. It is not suited to a gross measure of laxity because there is no clear way to describe cross sectional area or a reference length for the entire knee joint, necessary quantities in the measurement of stress and strain. Young's Modulus could be used to describe each of the internal structures of the knee, such as the ACL, PCL, MCL, and LCL. However, difficulties arise in quantifying stress and strain because they vary along the length and throughout the tissue cross section (Fleming and Beynon, 2004). These properties are often obtained experimentally with cadaveric tissue (Quapp and Weiss, 1998). This may be a source of error for models of joint hypermobility syndrome, for example, in which connective tissue mechanical behavior differs from that of normal subjects. FE models must converge to a repeatable solution regardless of how many finite elements the model is divided into (referred to as mesh size), thereby requiring time and computer memory to handle refined meshes in complex models that cannot take advantage of symmetry and other model simplifications. The model is only as relevant as the material properties and geometric representation of the included structures. More importantly, FE modeling has a complexity that may not be appropriate for the level of detail required from a model of laxity. However, further work must be done to identify the necessary modeling detail required to differentiate between groups across the spectrum of laxity.

4.4. Theoretical modelling summary

A theoretical model of knee joint laxity can be as broad as a gross measure of displacement under a translational

force or as specific as the complex three dimensional displacement or stress distribution of each structure within the joint. The main concern with any theoretical model is to determine whether it will provide information that cannot otherwise be obtained. The benefit of a gross model of laxity is that the displacement measurement does not require knowledge of the mechanics of the internal joint structures. Since a gross model describes joint laxity with a single measure, it may be easier to make comparisons between subjects. Additionally, a gross measure may be easier to correlate to other subject variables like dynamic function or stability because it characterizes the behavior of the joint as a whole. However, if the relative contributions of the soft tissue structures to overall joint laxity is desired, a different modeling technique must be employed. It could be valuable to further describe differences between subjects by quantifying the laxity of each internal structure and identifying how those individual structures contribute to the increased laxity of the entire knee joint. This information would require more in-depth modeling, such as lumped parameter or finite element. The advantage is that it could lead to improved clinical techniques (therapy or surgery), or further understanding regarding the underlying mechanisms of joint laxity.

5. Summary

There is a decisive gap between engineering models and clinical measures of laxity. One reason for this gap may be the disparity between clinical and engineering goals. For example, the clinician may be interested in the effect of acquired knowledge on treatment protocol, while the engineer may focus on measurement techniques such as accurately calculating the strain in the ACL. This review highlights the need for collaboration and the development of models that are appropriate for the desired level of detail. Integration of the two may require such developments as increased accessibility to MRI; however the primary hurdle is to fully validate an appropriate model and measurement technique. The lack of a clinical 'gold standard' measure of joint laxity leaves an open avenue for clinicians and engineers to move forward. The challenge is to develop an experimental and theoretical method that provides insight into the mechanics of the many structures of the knee, while maintaining safety, ease of use, and clear data interpretation that is necessary for clinical evaluation.

Joint laxity is usually measured as anterior tibial translation under a known applied load, giving a gross measure of joint laxity. Only a few studies have used gold standards, such as RSA, to validate the existing arthrometers that are often used to quantify joint laxity in a clinical setting. In the paper by Jorn et al. (1998), arthrometers were found to overestimate anterior tibial translation, which was attributed to soft tissue deformation. Otherwise, validations have been based on relative performance between arthrometers, or on repeatability. In a clinical setting, arthrometers are often used exclusively as a diagnostic tool.

This may help to explain why the definition of quantified joint laxity and its relation to stability remain unclear.

Models, by nature, are driven by the questions being asked, which tends to lead toward more specialized rather than generalized models. Models are available to consider the joint at varying levels of detail, including contact models for a gross measure of joint laxity, lumped parameter models for further information about the contributions of the tissue structures that comprise the joint, and FE models for more detailed analysis of stress and strain in those structures, often based on experimental data. The modeling techniques described in this article are currently used to address a wide variety of research questions. Focusing on these proven techniques when building theoretical models of joint laxity could help to bridge the gap to clinical assessment.

The benefit of incorporating an engineering model into a clinical laxity assessment is that it could improve the way that laxity is measured and interpreted. Currently, the primary clinical concern is to identify injured versus non injured, and to determine the change in laxity before and after treatment such as pre- and post-ACL reconstruction. However, there is also potential to develop a diagnostic tool that provides further detail and is anatomically patient specific. For example, an internal image of the knee could be combined with a knee laxity test and a resultant model with predictive capabilities such as stiffness of key ligaments or contact forces. These measures could then be used to help to identify candidates for ligament reconstruction or other treatments, determine an optimal tensioning force for a replacement ACL, simulate surgical results, identify the root cause of the laxity, or develop and evaluate clinical interventions such as exercise programs. The development of theoretical models that accurately represent joint behavior, as well as its supporting structures, in combination with more precise and repeatable clinical assessment of joint laxity, should lead to an improved understanding of joint laxity and the factors associated with acute injury and genetic pathologies that affect joint stability.

Acknowledgements

The authors gratefully acknowledge the financial support of the National Sciences and Engineering Research Council of Canada (NSERC), Alberta Ingenuity Fund (AIF), Ernst and Young Fellowship in Joint Injury and Arthritis Research, and the Institute of Gender and Health of the Canadian Institutes of Health Research (CIHR).

References

- Aalbersberg, S., Kingma, I., Blankevoort, L., van Dieën, J.H., 2005a. Co-contraction during static and dynamic knee extensions in ACL deficient subjects. *J. Electromyogr. Kinesiol.* 15, 349–357.
- Aalbersberg, S., Kingma, I., Ronsky, J.L., Frayne, R., van Dieën, J.H., 2005b. Orientation of tendons in vivo with active and passive knee muscles. *J. Biomech.* 38 (9), 1780–1788.

- Acasuso-Diaz, M., Collantes-Estevez, E., Sanchez-Guijo, P., 1993. Joint hypermobility and musculoligamentous lesions: study of a population of homogeneous age, sex, and physical exertion. *Br. J. Rheumatol.* 32, 120–122.
- Almekinders, L.C., Pandarinath, R., Rahusen, F.T., 2004. Knee stability following anterior cruciate ligament rupture and surgery. *J. Bone Joint Surg.* 86A (5), 983–987.
- Al-Rawi, Z.S., Al-Aszawi, A.J., Al-Chalabi, T., 1985. Joint mobility among university students in Iraq. *Br. J. Rheumatol.* 24, 326–331.
- Andersen, H.N., Jorgensen, U., 1998. The immediate postoperative kinematic state after anterior cruciate ligament reconstruction with increasing peroperative tension. *Knee Surg., Sports Traumatol., Arthrosc.* 6 (Suppl 1), S62–S69.
- Anderson, A.F., Lipscomb, A.B., 1989. Preoperative instrumented testing of anterior and posterior knee laxity. *Am. J. Sports Med.* 17 (3), 387–392.
- Anderson, A.F., Snyder, R.B., Federspiel, C.F., Lipscomb, A.B., 1992. Instrumented evaluation of knee laxity: a comparison of five arthrometers. *Am. J. Sports Med.* 20 (2), 135–140.
- Arnold, A.S., Salinas, S., Asakawa, D.J., Delp, S.L., 2000. Accuracy of muscle moment arms estimated from MRI-based musculoskeletal models of the lower extremity. *Comp. Aided Surg.* 5, 108–119.
- Baum, J., Larsson, L.-G., 2000. Hypermobility syndrome- new diagnostic criteria. *J. Rheumatol.* 27, 1586–1587.
- Belanger, M.J., Moore, D.C., Crisco, J.J., Fadale, P.D., Hulstyn, M.J., Ehrlich, M.G., 2004. Knee laxity does not vary with the menstrual cycle, before or after exercise. *Am. J. Sports Med.* 32 (5), 1150–1157.
- Bendjaballah, M.Z., Shirazi-Adl, A., Zukor, D.J., 1998. Biomechanical response of the passive human knee joint under anterior–posterior forces. *Clin. Biomech.* 13, 625–633.
- Bridges, A.J., Smith, E., Reid, J., 1992. Joint hypermobility in adults referred to rheumatology clinics. *Ann. Rheum. Dis.* 51, 793–796.
- Cannon, W.D., 2002. Use of arthrometers to assess knee laxity and outcomes. *Sports Med. Arthro. Rev.* 10, 191–200.
- Cheng, R.W.T., Fraymne, R., Ronsky, J.L., Habib, A.F., 2005. Matching strategy for co-registration of surfaces acquired by magnetic resonance imaging. In: *International Geoscience and Remote Sensing Symposium*, July 25–29, Seoul, Korea. Presentation.
- Cross, M., 1996. Clinical terminology for describing knee instability. *Sports Med. Arthrosc. Rev.* 4, 313–318.
- Daniel, D.M., Stone, M.L., 1990. Instrumented measurement of knee motion. In: Daniel, D.M., Akeson, W.H., O'Connor, J.J. (Eds.), *Knee Ligaments: Structure, Function, Injury, and Repair*. Raven, New York, pp. 421–426.
- Daniel, D.M., Malcom, L.L., Losse, G., Stone, M.L., Sachs, R., Burks, R., 1985. Instrumented measurement of anterior laxity of the knee. *J. Bone Joint Surg.* 67A (5), 720–726.
- DeFrate, L.E., Sun, H., Gill, T.J., Rubash, H.E., Li, G., 2004. In vivo tibiofemoral contact analysis using 3D MRI-based knee models. *J. Biomech.* 37, 1499–1504.
- Deie, M., Sakamaki, Y., Sumen, Y., Urabe, Y., Ikuta, Y., 2002. Anterior knee laxity in young women varies with their menstrual cycle. *Int. Orthop.* 26 (3), 154–156.
- Doorenbosch, C.A.M., Joosten, A., Harlaar, J., 2005. Calibration of EMG to force for knee muscles is applicable with submaximal voluntary contractions. *J. Electromyogr. Kinesiol.* 15 (4), 429–435.
- Eastlack, M.E., Axe, M.J., Snyder-Mackler, L., 1999. Laxity, instability, and functional outcome after ACL injury: copers versus noncopers. *Med. Sci. Sports Exerc.* 31 (2), 210–215.
- Ejerhed, L., Kartus, J., Sernert, N., Kohler, K., Karlsson, J., 2003. Patellar tendon or semitendinosus tendon autografts for anterior cruciate ligament reconstruction? A prospective randomized study with a two-year follow-up. *Am. J. Sports Med.* 31 (1), 19–25.
- Fitzcharles, M.A., 2000. Is hypermobility a factor in fibromyalgia? *J. Rheumatol.* 27, 1587–1589.
- Fleming, B.C., Beynon, B.D., 2004. In vivo measurement of ligament/tendon strains and forces: a review. *Ann. Biomed. Eng.* 32 (3), 318–328.
- Fleming, B.C., Brattbakk, B., Peura, G.D., Badger, G.J., Beynon, B.D., 2002. Measurement of anterior–posterior knee laxity: a comparison of three techniques. *J. Orthop. Res.* 20, 421–426.
- Gold, G.E., Besier, T.F., Draper, C.E., Asakawa, D.S., Delp, S.L., Beaupre, G.S., 2004. Weightbearing MRI of patellofemoral joint cartilage contact area. *J. Mag. Res. Imag.* 20, 526–530.
- Hakim, A., Grahame, R., 2003. Joint hypermobility. *Best Prac. Res. Clin. Rheum.* 17 (6), 989–1004.
- Herrington, L., Wrapson, C., Matthews, M., Matthews, H., 2005. Anterior cruciate ligament reconstruction, hamstring versus bone-patella tendon-bone grafts: a systematic literature review of outcome from surgery. *The Knee* 12, 41–50.
- Herzog, W., Binding, P., 1999. Mathematically indeterminate systems. In: Nigg, B.M., Herzog, W. (Eds.), *Biomechanics of the Musculo-skeletal System*, second ed. John Wiley & Sons Ltd, West Sussex, England, pp. 533–545.
- Herzog, W., Leonard, T.R., 1996. Soleus forces and soleus force potential during unrestrained cat locomotion. *J. Biomech.* 29 (3), 271–279.
- Highgenboten, C.L., Jackson, A., Meske, N.B., 1989. Genucom, KT-1000, and Stryker knee laxity measuring device comparisons. Device reproducibility and interdevice comparison in asymptomatic subjects. *Am. J. Sports Med.* 17 (6), 743–746.
- Hsu, W.H., Fisk, J.A., Yamamoto, Y., Debski, R.E., Woo, S.L., 2006. Differences in torsional joint stiffness of the knee between genders: a human cadaveric study. *Am. J. Sports Med.* 34 (5), 765–770.
- Huber, F.E., Irrgang, J.J., Harner, C., Lephart, S., 1997. Intratester and intertester reliability of the KT-1000 arthrometer in the assessment of posterior laxity of the knee. *Am. J. Sports Med.* 25 (4), 479–485.
- Iwaki, H., Pinskerova, V., Freeman, M.A.R., 2000. Tibiofemoral movement I: the shapes and relative movements of the femur and tibia in the unloaded cadaveric knee. *J. Bone Joint Surg. Br.* 82B, 1189–1195.
- Jorn, L.P., Fridén, T., Ryd, L., Lindstrand, A., 1998. Simultaneous measurements of sagittal knee laxity with an external device and radiostereometric analysis. *J. Bone Joint Surg.* 80B (1), 169–172.
- Kärrholm, J., 1989. Roentgen stereophotogrammetry: review of orthopaedic applications. *Acta. Orthop. Scand.* 60, 491–503.
- Lewkonja, R.M., 1993. The biology and clinical consequences of articular hypermobility. *J. Rheum.* 20, 220–222.
- Li, G., Suggs, J., Gill, T., 2002. The effect of anterior cruciate ligament injury on knee joint function under a simulated muscle load: a three-dimensional computational simulation. *Ann. Biomed. Eng.* 30, 713–720.
- Logan, M., Dunstan, E., Robinson, J., Williams, A., Gedroyc, W., Freeman, M., 2004a. Tibiofemoral kinematics of the anterior cruciate ligament (ACL)-deficient weightbearing, living knee employing vertical access open 'interventional' multiple resonance imaging. *Am. J. Sport Med.* 32 (3), 720–726.
- Logan, M.C., Williams, A., Lavelle, J., Gedroyc, W., Freeman, M., 2004b. What really happens during the Lachman test? A dynamic MRI analysis of tibiofemoral motion. *Am. J. Sports Med.* 32 (2), 369–375.
- Lu, T.-W., O'Connor, J.J., 1996. Lines of action and moment arms of the major force-bearing structures crossing the human knee joint: comparison between theory and experiment. *J. Anat.* 189, 575–585.
- Maffulli, N., 1998. Laxity versus instability. *Orthop.* 21 (8), 837–842.
- Maitland, M.E., Bell, G.D., Mohtadi, N.G.H., Herzog, W., 1995. Quantitative analysis of anterior cruciate ligament instability. *Clin. Biomech.* 10 (2), 93–97.
- Malanga, G.A., Andrus, S., Nadler, S.F., McLean, J., 2003. Physical examination of the knee: a review of the original test description and scientific validity of common orthopedic tests. *Arch. Phys. Med. Rehabil.* 84, 592–603.
- Moglo, K.E., Shirazi-Adl, A., 2003. Biomechanics of passive knee joint in drawer: load transmission in intact and ACL-deficient joints. *The Knee* 10, 265–276.

- Muellner, T., Bugge, W., Johansen, S., Holtan, C., Engebretsen, L., 2001. Inter- and intratester comparison of the Rolimeter knee tester: effect of tester's experience and the examination technique. *Knee Surg. Sports Traumatol. Arthrosc.* 9, 302–306.
- Myrer, J.W., Schulthies, S.S., Fellingham, G.W., 1996. Relative and absolute reliability of the KT-2000 arthrometer for uninjured knees. Testing at 67, 89, 134, and 178 N and manual maximum forces. *Am. J. Sports Med.* 24 (1), 104–108.
- Nigg, B.M., 1999. Measuring techniques: force. In: Nigg, B.M., Herzog, W. (Eds.), *Biomechanics of the Musculo-skeletal System*, second ed. John Wiley & Sons, Ltd, West Sussex, England, pp. 355–375.
- Pandy, M.G., Shelburne, K.B., 1998. Theoretical analysis of ligament and extensor-mechanism function in the ACL-deficient knee. *Clin. Biomech.* 13 (2), 98–111.
- Papandreou, M.G., Antonogiannakis, E., Karabalis, C., Karliafitis, K., 2005. Inter-rater reliability of rolimeter measurements between anterior cruciate ligament injured and normal contralateral knees. *Knee Surg. Sports Traumatol. Arthrosc.* 13, 592–597.
- Patel, R.R., Hurwitz, D.E., Bush-Joseph, C.A., Bach, B.R., Andriacchi, T.P., 2003. Comparison of clinical and dynamic knee function in patients with anterior cruciate ligament deficiency. *Am. J. Sports Med.* 31 (1), 68–74.
- Picano, E., 2004. Sustainability of medical imaging. *BMJ* 328, 578–580.
- Quapp, K.M., Weiss, J.A., 1998. Material characterization of human medial collateral ligament. *J. Biomech. Eng.* 120 (6), 757–763.
- Ronsky, J.L., 1994. In-vivo quantification of patellofemoral joint contact characteristics. Ph.D. Dissertation, University of Calgary, Calgary, Canada.
- Rudy, T.W., Sakane, M., Debski, R.E., Woo, S.L.-Y., 2000. The effect of the point of application of anterior tibial loads on human knee kinematics. *J. Biomech.* 33, 1147–1152.
- Scarvell, J.M., Smith, P.N., Refshauge, K.M., Galloway, H.R., Woods, K.R., 2004. Evaluation of a method to map tibiofemoral contact points in the normal knee using MRI. *J. Orthop. Res.* 22, 788–793.
- Schultz, S.J., Gansneder, B.M., Sander, T.C., Kirk, S.E., Perrin, D.H., 2006. Absolute serum hormone levels predict the magnitude of change in anterior knee laxity across the menstrual cycle. *J. Orthop. Res.* 24, 124–131.
- Selvik, G., 1989. Roentgen stereophotogrammetry. A method for the study of the kinematics of the skeletal system. *Acta. Orthop. Scand.* 60 (Suppl 232), 1–51.
- Semert, N., Kartus, J., Kohler, K., Ejerhed, L., Karlsson, J., 2001. Evaluation of the reproducibility of the KT-1000 arthrometer. *Scand. J. Med. Sci. Sports* 11 (2), 120–125.
- Shahar, R., Banks-Sills, L., 2004. A quasi-static three-dimensional, mathematical, three-body segment model of the canine knee. *J. Biomech.* 37, 1849–1859.
- Sheehan, F.T., Rebmann, A., 2003. Non-Invasive, in vivo measures of anterior cruciate ligament strains. 49th Annual Meeting of the Orthopaedic Research Society, Transactions, vol.1 28, Paper #0240, New Orleans, Louisiana.
- Shultz, S.J., Kirk, S.E., Johnson, M.L., Sander, T.C., Perrin, D.H., 2004. Relationship between sex hormones and anterior knee laxity across the menstrual cycle. *Med. Sci. Sports Exerc.* 36 (7), 1165–1174.
- Snyder-Mackler, L., Fitzgerald, G.K., Bartolozzi, A.R., Ciccotti, M.G., 1997. The relationship between passive joint laxity and functional outcome after anterior cruciate ligament injury. *Am. J. Sports Med.* 25 (2), 191–195.
- Stäubli, H.U., Noesberger, B., Jakob, R.P., 1992. Stress radiography of the knee: cruciate ligament function studied in 138 patients. *Acta. Orthop. Scand.* 63 (Suppl 249), 1–27.
- Toutoungi, D.E., Zavatsky, A.B., O'Connor, J.J., 1997. Parameter sensitivity of a mathematical model of the anterior cruciate ligament. *Proc. Instn. Mech. Engrs.* 211, 235–246.
- Uhorchak, J.M., Scoville, C.R., Williams, G.N., Arciero, R.A., St. Pierre, P., Taylor, D.C., 2003. Risk factors associated with noncontact injury of the anterior cruciate ligament: a prospective four-year evaluation of 859 West Point cadets. *Am. J. Sports Med.* 31, 831–842.
- Wojtyś, E.M., Huston, L.J., Boynton, M.D., Spindler, K.P., Lindenfeld, T.N., 2002. The effect of the menstrual cycle on anterior cruciate ligament injuries in women as determined by hormone levels. *Am. J. Sports Med.* 30, 182–188.
- Wretenberg, P., Ramsey, D.K., Nemeth, G., 2002. Tibiofemoral contact points relative to flexion angle measured with MRI. *Clin. Biomech.* 17 (6), 477–485.

APPENDIX B: ETHICS



FACULTY OF MEDICINE | UNIVERSITY OF CALGARY

2005-03-10

Dr. D. Stefanyshyn
Human Performance Laboratory
Faculty of Kinesiology
University of Calgary
Calgary, Alberta

OFFICE OF MEDICAL BIOETHICS

Room 93, Heritage Medical Research Bldg
3330 Hospital Drive NW
Calgary, AB, Canada T2N 4N1
Telephone: (403) 220-7990
Fax: (403) 283-8524
Email: omb@ucalgary.ca

Dear Dr. Stefanyshyn:

RE: Relationship Between Joint Laxity and Hormonal Status in Healthy Females and females with Benign Joint Hypermobility Syndrome

Grant-ID: 18200

PhD Student: Park, Sang-Kyoon

The above-named research project, including the study protocol, the revised consent form (version dated January 20, 2005), the 3T MR Research Consent Form (version rev.2, dated March 2003), the study poster, and the Benign Joint Hypermobility Syndrome Syndrome 2004 Questionnaire, has been granted ethical approval by the Conjoint Health Research Ethics Board (CHREB) of the Faculties of Medicine, Nursing and Kinesiology, University of Calgary, and the Affiliated Teaching Institutions. The Board conforms to the Tri-Council Guidelines, ICH Guidelines and amendments to regulations of the Food and Drug Act re clinical trials, including membership and requirements for a quorum.

You and your co-investigators are not members of the CHREB and did not participate in review or voting on this study.

Please note that this approval is subject to the following conditions:

- (1) appropriate procedures for consent for access to identified health information has been approved,
- (2) a copy of the informed consent form must have been given to each research subject, if required for this study;
- (3) a Progress Report must be submitted by 2006-03-10, containing the following information:
 - i) the number of subjects recruited;
 - ii) a description of any protocol modification;
 - iii) any unusual and/or severe complications, adverse events or unanticipated problems involving risks to subjects or others, withdrawal of subjects from the research, or complaints about the research;
 - iv) a summary of any recent literature, findings, or other relevant information, especially information about risks associated with the research;
 - v) a copy of the current informed consent form;
 - vi) the expected date of termination of this project.
- (4) a Final Report must be submitted at the termination of the project.

Please accept the Board's best wishes for success in your research.

Yours sincerely,
Christopher J. Doig, MD, MSc, FRCPC

Chair, Conjoint Health Research Ethics Board

CJD/km

c.c. Adult Research Committee Dr. W.L. Veale (information) Research Services Sang-Kyoon Park (PhD Student)
Office of Information & Privacy Commissioner



FACULTY OF | UNIVERSITY OF
MEDICINE | CALGARY

March 16, 2007

Dr. D. Stephanyshyn
 Faculty of Kinesiology, KNB 203B
 University of Calgary
 Calgary
 Alberta

OFFICE OF MEDICAL BIOETHICS

Room 93, Heritage Medical Research Bldg
 3330 Hospital Drive NW
 Calgary, AB, Canada T2N 4N1
 Telephone: (403) 220-7990
 Fax: (403) 283-8524
 Email: omb@ucalgary.ca

Dear Dr. Stephanyshyn:

Re: Relationship Between Joint Laxity and Hormonal Status in Healthy Females and Females with Benign Joint Hypermobility Syndrome

Grant ID: 18200

Your request to modify the above named research protocol and has been reviewed and approved.

I am pleased to advise you that it is permissible for you to use the revised protocol adding Ms. Jessica Kupper to the study as a co-investigator and approval is hereby given of the addendum to the study relating to the validation of the joint laxity testing device in female subjects, based on the information contained in your correspondence of March 1 and emailed correspondence dated March 5, 2007.

A progress report concerning this study is required annually, from the date of the original approval 2005-03-10. The report should contain information concerning:

- (i) the number of subjects recruited;
- (ii) a description of any protocol modification;
- (iii) any unusual and/or severe complications, adverse events or unanticipated problems involving risks to subjects or others, withdrawal of subjects from the research, or complaints about the research;
- (iv) a summary of any recent literature, finding, or other relevant information, especially information about risks associated with the research;
- (v) a copy of the current informed consent form;
- (vi) the expected date of termination of this project;

Thank you for the attention which I know you will bring to these matters.

Yours sincerely,

Glenys Godlovitch, BA(Hons) LLB, PhD.
 Chair, Conjoint Health Research Ethics Board
 GG/eb

c.c. Adult Research Committee S.K. Park Ms. Jessica Kupper



Human Performance Laboratory
 Faculty of Kinesiology
 2500 University Drive N.W.
 Calgary, AB T2N 1N4
 Telephone: (403) 220-8637
 Fax: (403) 284-3553

Subject Consent Form

TITLE: Relationship between joint laxity and hormonal status in healthy females and females with benign joint hypermobility syndrome.

SPONSOR: CIHR

INVESTIGATORS: Dr. Darren Stefanyshyn, Sang-Kyoon Park, Dr. David Hart, Dr. Janet Ronsky, Dr. Susan Barr, Dr. Raylene Reimer, Dr. Karl Riabowol

This consent form is only part of the process of informed consent. It should give you the basic idea of what the research is about and what your participation will involve. If you would like more detail about something mentioned here, or information not included here, please ask. Take the time to read this carefully and to understand any accompanying information. You will receive a copy of this form.

BACKGROUND

Females are more likely to incur injuries to the ACL or the shoulder than males engaged in a similar athletic activity. In some reports, this increased risk is non-randomly associated with different phases of the menstrual cycle. As the majority of these knee injuries are the result of non-contact events, investigators have started to examine methods to modify training and running/cutting style to overcome this apparent risk. However, while there is an increased risk in females compared to males, the increased risk is such that most female athletes still do not incur ACL injuries. The finding that knee laxity can vary in many females during different phases of the menstrual cycle implies that a subset of individuals are affected by the hormonal fluctuations more or less than others. Therefore, a subset of females may be at higher risk than others due to hormonal impact on genetic factors, which are indicative of risk for other conditions later in life. Thus, assessment of the association between passive knee laxity and dynamic joint function changes (quantified by Biomechanical Analysis) and hormonal status may identify a subpopulation of females that should be the target of specific interventions to maintain joint health across their lifespan.

You have been asked to participate (as one of approximately 100 subjects) in this study because you have either been diagnosed with benign joint hypermobility syndrome (bJHS) or because you have no lower extremity injuries and you will serve as a control subject. Your participation will involve 4 testing sessions lasting between approximately 2- 3 hours. In addition you may be asked to repeat the data collection one year later to establish reliability of the measures.

WHAT IS THE PURPOSE OF THE STUDY?

The purpose of this study is to assess the correlation between variation in joint laxity and hormonal status during the menstrual cycle in a population of fit young females and females with benign joint hypermobility syndrome (bJHS). The goal of this research is to identify why females are at greater risk of developing joint injuries while participating in athletic activities.

WHAT WOULD I HAVE TO DO?

Hormone Levels Testing

The first measurements will be taken during the beginning of the menstrual phase, when estrogen levels are expected to be low. The second data collection will occur approximately 7 days later based on the ovulation predictor kit results. The third data collection will occur 7 days following the peak estrogen surge. The final data collection will occur at the beginning of the next menstrual phase (approximately 7 days later).

At the initial visit, the study will be explained to you by the study coordinator. In addition, the study coordinator and you will discuss your menstrual history, and you will have a chance to explore all of the testing apparatus. If you are not using oral contraceptives, you will be asked to use an ovulation predictor kit to help determine the appropriate days for testing. This involves dipping a test stick into a cup of urine or holding the test stick in the urine stream. If you are not using oral contraceptives then you will also be asked to have your blood drawn each day of testing at the Exercise Physiology Laboratory (Human Performance Laboratory), Faculty of Kinesiology at the University of Calgary, which will then be tested for estrogen levels.

The study involves participating in a series of experiments 4 different times during different phases of your menstrual cycle. The following is an outline of what will happen at each visit.

Blood samples will be taken by qualified individuals with subsequent hormone level analysis performed by Calgary Laboratory Services. In order to ensure blood samples are taken during the estrogen surge immediately prior to ovulation, an outline of the menstrual phases will be constructed based on the length of your previous menstrual cycle, the expected phase length, and information obtained from the ovulation kit. This portion of the test will take approximately 30 minutes.

Knee Joint Laxity Measurement

Next knee joint laxity will be measured by a qualified individual using a KT-2000 arthrometer. Knee joint laxity will be assessed by attaching a small apparatus to your lower leg, manually pulling the lower leg forward relative to the thigh with a force of 30 pounds, and measuring the amount of displacement within the knee. This portion of the measurements will take approximately 30 minutes.

Motion Analysis Data Collection

Next you will complete a motion analysis test and will perform approximately 10 trials for different conditions: 1) walking, 2) running straight ahead, 3) a V-Cut, 4) a C-Cut, 5) running & stopping, 6) jumping & landing. Reflective markers will be affixed to your legs and waist with medical glue or adhesive tape and markers will also be attached to your shoes. Laboratory video cameras will only record the motion of these markers and are not capable of recording standard video images. In addition,

Electromyography (EMG) electrodes will be taped to the skin overlaying muscles under investigation, after the contact area has been cleaned of hair, dead skin and sweat. These electrodes will record the changes in the muscular activity over the course of the testing. This portion of the experiment will take approximately 90 minutes.

MR Imaging

Following these tests, you may be asked to participate in part of on-going studies by Dr. Janet Ronsky involving magnetic resonance imaging (MRI).

You will have MR images obtained of your knee joint structures under loading conditions similar to the KT-2000, for the three time points (day 7 (follicular phase), day 14 (ovulation phase) and day 21 (luteal phase)) in your menstrual cycle. You will be requested to attend a MRI training session at the University of Calgary Health Science Center lasting approximately 1 hour. The purpose of this training session is to familiarize you with the set-up that will be used during the MR scans and to determine the level of force that can be comfortably maintained for approximately 4 minutes. Following successful training, you will complete various MRI scans conducted at the Seaman Family MR Research Centre. This will be on a separate day from the training session. The total time involved to complete the MRI study is approximately 1.5 hours. There are no reproductive risks associated with this MR imaging.

Will you participate in follow up study? Please check one of the boxes below

- Yes, I am willing to participate in following study.
 No, I am not willing to participate in following study.

MR imaging has been requested to be performed on you using the 3 Tesla (T) MR imaging machine housed in the Seaman Family Magnetic Resonance (MR) Research Centre.

This machine differs from the more common 1.5 T MR scanners in that the strength of the magnetic field is twice as large. The 3 T MR machine is an experimental unit however most components of the device have received approval from the Health Protection Branch of Canada and from the Food and Drug Administration of the United States. Some of the software and hardware used in this study, while developed according to widely accepted safety practices, has not been approved.

There are no known long-term effects from MR imaging at 1.5 T or 3 T. This study, however, carries a remote risk of injury for which you will be carefully screened and monitored. The attached screening form is used to identify any potential exclusions to 3 T MR imaging. MR imaging can provide a safe and noninvasive way of obtaining diagnostic information about the structure and function of the body. In addition, the information obtained during your examination may be helpful in establishing diagnosis, defining extent of disease, as well as planning and monitoring therapy in future patients.

Signing this form indicates that you agree to participate in the 3 T MR research program however, participation is voluntary and you are free to withdraw at any time. Withdrawing from the procedure will not affect your care - the care you receive will not be affected whether or not you choose to participate in this imaging study.

Images obtained may be used for publication or presentation to scientific or medical imaging industry audiences. Data will be stored in the Seaman Family MR Research Centre. Confidentiality will be maintained in any transmittal of information by way of database, publication or presentation. There are no financial inducements to the investigators to have you participate in this research.

Should you require further information, please ask to speak to the Principal Investigator or the Director

of the High Field Program. All these individuals may be reached at 403 944 1800.

WHAT ARE THE RISKS?

There should be no ill effects from your participation in these tests. There are minimal risks or discomforts as the study involves activity only slightly more strenuous than normal walking, therefore you may feel muscle fatigue. Blood samples and knee joint laxity test will be carried out according to routine procedure by an experienced technician. You will be given opportunity to rest during the testing sessions, if necessary. There are no guaranteed benefits to you personally for your participation in this study.

WILL I BENEFIT IF I TAKE PART?

You will be participating in a study that will provide new information insight about why females are at greater risk of developing joint injuries while participating in athletic activities as compared to males.

DO I HAVE TO PARTICIPATE?

You still have all your legal rights. Nothing said here in any way alters your right to recover damages. Participation in this study is voluntary and you reserve the right to withdraw at any time without prejudice.

WILL MY RECORDS BE KEPT PRIVATE?

All information collected in this study will remain absolutely confidential. Only those directly involved in the study will have access to information gained. Any report of the findings will be published in a manner that in no way identifies you as a subject. In addition, the University of Calgary Conjoint Health Research Ethics Board will have access to the records.

IF I SUFFER A RESEARCH-RELATED INJURY, WILL I BE COMPENSATED?

In the event that you suffer injury as a result of participating in this research, no compensation will be provided for you by the University of Calgary, CHIR, Calgary Health Region, the researchers, or anyone else directly involved in this project.

SIGNATURES

Your signature on this form indicates that you have understood to your satisfaction the information regarding your participation in the research project and agree to participate as a subject. In no way does this waive your legal rights nor release the investigators, or involved institutions from their legal and professional responsibilities. You are free to withdraw from the study at any time without jeopardizing your health care. If you have further questions concerning matters related to this research, please contact:

Dr. Darren Stefanyshyn (403) 220-8637

Or

Sang-Kyoon Park (403) 220-3853

If you have any questions concerning your rights as a possible participant in this research, please contact Pat Evans, Associate Director, Internal Awards, Research Services, University of Calgary, at 220-3782.

_____	_____
Participant's Name	Signature and Date
_____	_____
Investigator/Delegate's Name	Signature and Date
_____	_____
Witness' Name	Signature and Date

The University of Calgary Conjoint Health Research Ethics Board has approved this research study.

A signed copy of this consent form has been given to you to keep for your records and reference.



**Mechanical and Manufacturing Engineering
MEB 512**

Telephone: 403 220 8134/8620/4327
Fax: 403 282 8406
Email: jlrnsky@ucalgary.ca

January 25th, 2007

Dr. Glenys Godlovitch, Chair of CHREB
Office of Medical Bioethics
3330 Hospital Dr. NW
HMRB Rm G93
Calgary, Alberta
T2N 4N1

Grant ID: 18200
PI: Dr. Darren Stefanyshyn

RE: Request for Modification to Previously Approved Protocol, "Relationship between joint laxity and hormonal status in healthy females and females with benign joint hypermobility syndrome"

Dear Dr. Godlovitch:

Due to difficulties with availability of the MRI scanner from the initially proposed resources, we are asking for approval to extend our subject criteria to include subjects who are taking hormone based therapies. As such, we would like to ask the subjects specifically whether they are on any hormone therapy, including contraceptives, and the name, strength, and dosage form of the drug that they are taking. By comparing subjects who are on comparable controlled hormone therapies, we will be able to account for hormone effects, while allowing advanced booking of the MRI since their cycles are known in advance.

We are also asking approval of an additional recruitment poster, included with this letter. There have been no changes to the attached subject consent form. Please contact me if you have any questions.

Best regards,

Janet L. Ronsky, PhD PEng
Professor, Mechanical and Manufacturing Engineering
Canada Research Chair in Biomedical Engineering



**Mechanical and Manufacturing Engineering
MEB 512**

Telephone: 403 220 8134/8620/4327
Fax: 403 282 8406
Email: jlrnsky@ucalgary.ca

March 1, 2007

Dr. Glenys Godlovitch, Chair of CHREB
Office of Medical Bioethics
3330 Hospital Dr. NW
HMRB Rm G93
Calgary, Alberta
T2N 4N1

Grant ID: 18200
PI: Dr. Darren Stefanyshyn

**RE: Request for Modification to Co-investigator list for Previously Approved Protocol,
"Relationship between joint laxity and hormonal status in healthy females and females with
benign joint hypermobility syndrome"**

Dear Dr. Godlovitch:

We would like to add master's student Jessica Küpper to the list of co-investigators on this study. In addition, based on discussions with staff at the office of medical bioethics, the other co-investigators (Dr. Barbara Loitz-Ramage, Dr. Janet Ronsky, Dr. David Hart, and Dr. Susan Barr) are listed in the original file but not in your computer database. We would like to have those co-investigators added to the database if possible.

Thank you very much, and please contact me if you have any questions.

Best regards,

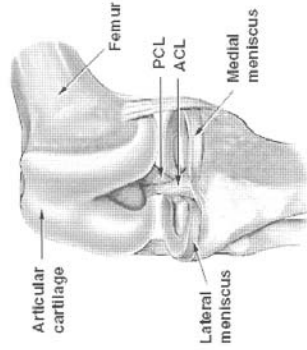
Janet L. Ronsky, PhD PEng
Professor, Mechanical and Manufacturing Engineering
Canada Research Chair in Biomedical Engineering

Would you like an MRI of your knee?

We are looking for subjects who have **no history of knee injury**. The purpose of this study is to evaluate a new way to measure knee joint stiffness.

The following **criteria** must be met to qualify for the study:

- Female, Age: 19 to 35 years
- No history of knee injury
- No surgical repair of ACL
- No related lower limb injuries, like a fracture
- Participate in regular exercise (2-5 times per week)
- Currently using oral contraceptives or hormone therapies



© 1998 Nucleus Communications, Inc. - Atlanta
www.nucleustrc.com

After an initial screening to confirm all inclusion criteria are met, **subjects will be asked to:**

- Have their knee joint stiffness and muscle activation measured
- Undergo magnetic resonance (MR) scan to image the knee

For more information or if you would be interested in participating in the study, please contact:

Jessica Küpper
University of Calgary
Human Performance Lab
Phone: 220-4687
E-mail: johnsojc@ucalgary.ca

Jessica Küpper
#220-4687
johnsojc@ucalgary.ca